Phosphorylation events surrounding the DNA damage response in *Saccharomyces cerevisiae*

Inauguraldissertation

zur

Erlangung der Würde eines Doktors der Philosophie

vorgelegt der

Philosophisch-Naturwissenschaftlichen Fakultät
der Universität Basel

von

Thomas Andreas Schleker

aus Deutschland

Basel, im Jahre 2007

Genehmigt von der Philosophisch-Naturwissenschaftlichen Fakultät

auf Antrag von

Prof. Dr. Susan Gasser (Referat)

Prof. Dr. Primo Schär (Korreferat)

Basel, den 16.10.2007

Prof. Dr Hans-Peter Hauri

Dekan der Philosophisch Naturwissenschaftlichen Fakultät der

Universität Basel

Ich erkläre, dass ich die Dissertation “Phosphorylation events surrounding the DNA damage response in *Saccharomyces cerevisiae* ” nur mit der darin angegebenen Hilfe verfasst und bei keiner anderen Universität und keiner anderen Fakultät der Universität Basel eingereicht habe.

Thomas Schleker

Basel, September 2007

Meinen Eltern

Acknowledgements

My biggest thanks go to Prof. Dr. Susan Gasser for giving me the opportunity to do my PhD studies in her laboratory, for training me, for very helpful suggestions, and for guiding me throughout my project, but also for leaving me freedom to bring in my own ideas. Thanks also for communicating a great passion for science!

I thank Prof. Dr. Primo Schär for taking over the role of co-referee for this thesis, for spending a lot of time on discussions, and for very helpful suggestions. In this context, I would also like to thank my other committee members Dr. Dirk Schübeler and Prof. Dr. Maria Pia Longhese for their time, and for many helpful suggestions. Many thanks to Prof. Longhese for her big effort to join my committee meeting in Basel.

Many thanks go to Dr. Kenji Shimada, who spent a lot of his time introducing me to yeast work and offered many helpful suggestions throughout these years, and who also helped with the Rad53 project. Many thanks equally to Dr. Haico Van Attikum, who suggested some crucial experiments and with whom I had many helpful discussions, and who helped with the γH2A project.

I would like to thank Véronique Kalck for performing IF and microscopy experiments, and for her great enthusiasm about this project! I would like to thank Ragna Sack. The determination of phosphorylation sites by MS was a breakthrough for this project! Thanks also for spending a lot of time explaining the results.
Many thanks to all members of the Gasser lab for scientific advice, a good attitude towards sharing tools and reagents and for a good working atmosphere with nice non-scientific discussions as well. I would like to thank Dr. Jennifer Cobb for introducing me to ChIP, and I also acknowledge discussions about the outline of chapter 1.5. I would like to thank Dr. Monika Tsai-Pflugfelder for helpful suggestions and for making the plasmids with the Rad53 domains available. Thanks to Dr. Brietta Pike for helpful suggestions and for being interested in continuing one of my projects. I would like to thank my lab neighbors and members of the DNA-damage minigroup Dr. Lotte Bjergbaek, Dr. Olivier Fritsch, Anna-Maria Friedel as well as my neighbors in the FMI office for many helpful suggestions and for letting me spread out from time to time.

Many thanks to all the members of the FMI facilities; to Franz Fischer for peptide synthesis; to Dr. Susanne Schenk for the production of monoclonal antibodies; to Dr. Patrick Schwab, Thierry Laroche, and Dr. Aaron Ponti for imaging support; and to Hubertus Köhler for help with FACS analysis. Thanks to the Bonner, Durocher, Gilson, and other laboratories all around the world for providing us with important research tools. Thanks to colleagues of the Gasser lab and to Sara Oakeley for proofreading my thesis. Thanks also go to many members of the Friedrich Miescher Institute in Basel and the Department of Molecular Biology in Geneva for providing helpful discussions and scientific education in seminars, helpful suggestions, and a good working atmosphere.
Many thanks go finally to my family and friends for their support throughout this time.

Thomas Schleker

Summary

Protein phosphorylation mediated by checkpoint kinases is crucial for the cellular response to DNA damage. The sensor kinases Mec1 and Tel1 initiate the checkpoint signaling cascade by directly activating the checkpoint effector kinase Rad53. This checkpoint pathway, however, is responsive to normal endogenous replication as well. As a result an S-phase specific threshold for Rad53 activation exists, which allows cells to tolerate endogenous damage-like structures.

Here we show that Rad53 itself is phosphorylated in a cell-cycle dependent manner independent of DNA damage signaling (Chapter 2). We propose that this is part of the cell-cycle regulated sensitivity of Rad53 to activation. This phosphorylation occurs in G2/M, persists until S phase onset and depends on both the polo-like kinase, Cdc5, and the cyclin-dependent kinase, Cdc28. These cell-cycle dependent phosphorylation events are located in the C-terminal part of Rad53. Serines 774 and 789 were shown to be phosphorylated by mass spectrometry. Mutation of these sites eliminated the cell-cycle dependent phosphorylation of Rad53 and partially impaired the activation of Rad53 in response to minor amounts of DNA damage in G2/M. This led to more rapid checkpoint adaptation in response to irreparable DNA damage. Thus, cell-cycle dependent phosphorylation in the C-terminal part of Rad53 enhances Rad53 activation in response to DNA double strand breaks (DSBs).

Mec1 and Tel1 initiate a response to DNA damage independently of Rad53. The phosphorylation of histone H2A at serine 129 (γH2A) at DSBs by Mec1 and Tel1 has an important role in mediating DNA repair. This study shows that the occurrence of γH2A is not limited to DSBs, but also occurs at stalled replication forks (Chapter 3). Using chromatin immunoprecipitation high γH2A levels were monitored at hydroxyurea-stalled replication forks and depended nearly exclusively upon Mec1 kinase activity. Furthermore our study showed that γH2A not only occurs at damaged chromatin but in regions of normally replicating chromatin and near telomeres (Chapter 4). High levels of γH2A could be monitored both in the rDNA of normally growing yeast cells and at telomeres. Here γH2A depended mainly on Tel1 and γH2A levels increased during S phase and during the elongation of critically short telomeres. We also provide evidence that γH2A contributes to telomeric anchoring in S phase yeast cells in addition to the yKu and Sir4 anchoring pathways.

Contents

Table of Contents

Table of Figures

CHAPTER 4:

Table of Tables

CHAPTER 1

CHAPTER 2

CHAPTER 4

List of Abbreviations

2D	Two dimensional
4-NQO	4-nitroquinoline 1-oxide
5-FOA	5-Fluoroorotic acid
9-1-1	Rad9-Rad1-Hus1
A	Alanine
Aa	Amino acid
Ala	Alanine
ARS	Autonomous replicating sequence
ATM	Ataxia telangiectasia mutated
ATP	Adenosinetriphosphate
ATR	Ataxia telangiectasia and Rad3 related
BrdU	Bromodeoxyuridine
BSA	Bovine serum albumin
CDK	Cyclin-dependent kinase
ChIP	Chromatin immunoprecipitation
CHX	Cycloheximide
CIP	Calf intestinal phophatase
CK2	Casein kinase 2
CPT	Camptothecin
DAPI	4',6-Diamidino-2-phenylindole
DMSO	dimethyl sulfoxide
DNA	deoxyribonucleic acid
dNTP	deoxyribonukleotide
DSB	double strand break
DTAF	dichlorotriazinylaminofluorescein
DTT	dithiothreitol
E	glutamic acid
E2F1	E2F transcription factor 1
ELISA	Enzyme linked immunosorbent assay
ESI	Electrospray ionisation
Exp.	Exponential(ly)
FACS	Fluorescence activated cell sorting
FHA	Forkhead associated
G1 phase	Gap 1 phase
G2 phase	Gap 2 phase
GFP	Green fluorescent protein
GINS	Go, Ichi, Nii, and San (five, one, two, and three in Japanese),
Glu	Glutamic acid
GST	Glutathione-S-transferase
H2A	Histone 2a
HA	Hemagglutinin
HIR	Histone regulation
HML	Hidden MAT left
HMR	Hidden MAT right
HO-endonuclease	Homothallic switching endonuclease
HPLC	High performance liquid chromatography
HR	Homologous recombination
HRP	Horseradish peroxidase
HU	Hydroxyurea
IDA	Information-dependent acquisition
IF	Immunofluorescence
IP	Immunoprecipitation
IPTG	Isopropyl-ß-D-thiogalaktopyranosid
K	Lysine
Kb	Kilobase
LC	Liquid chromatography

M phase	Mitotic phase
Mab	Monoclonal antibody
MAT	Mating type (locus)
MCM	Minichromosome maintenance
mec1	Mitosis entry checkpoint mutant 1
MMS	Methylmethanesulfonate
MRN	Mre11, Rad50, Nbs1
MRX	Mre11, Rad50, Xrs2
MS	Mass spectroscopy
MSMS	Tandem mass spectrometry
Na-PP1	Naphthylpyrazolopyrimidine analog number 9
NaPPi	Sodium pyrophosphate
NHEJ	Non-homologous end joining
Noc	Nocodazole
ORF	Open reading frame
PCNA	Proliferating cell nuclear antigen
PCR	Polymerase chain reaction
Pfu	*Pyrococcus furiosus*
PI3K	Phosphoinositide-3 kinase
PMSF	Phenylmethylsulfonylfluorid
Pol	Polymerase
PP2C	Protein phosphatase 2c
Q	Glutamine
qPCR	Quantitative PCR
rad53	Radiation sensitive mutant 53
rDNA	Ribosomal DNA
RFA	Replication factor A
RFB	Replication fork barrier
RFC	Replication factor C
RNAi	RNA interference
RNR	Ribonucleotide reductase
RPA	Replication protein A
S	Serine
S phase	Synthesis phase
SC	Synthetic complete
SD	Standard deviation
SDS-PAGE	Sodium dodecyl sulfate polyacrylamide gel electrophoresis
Ser	Serine
SIR	Silent information regulator
ssDNA	Single-stranded DNA
SUMO	Small ubiquitin-related modifier
T	Threonine
TCA	Trichloroacetic acid
Tel	Telomere
tel1	Telomere maintenance mutant 1
TERT	Telomerase Reverse Transcriptases
T-loop	Telomere loop
TLS	Translesion synthesis
TPE	Telomere position effect
Tris	Tris(hydroxymethyl)-aminomethan
tRNA	Transfer RNA
UV	Ultraviolet
WT	Wildtype
YP(A)D	Yeast extract peptone (adenine) dextrose

Chapter 1

Introduction

1.1 Cell cycle and cell cycle checkpoints

Eukaryotic cell-cycle research was pioneered by work in the budding yeast *Saccharomyces cerevisiae*. Leland Hartwell and coworkers isolated temperature-sensitive *cdc* (cell-division cycle) mutants, which cause cell cycle arrest with a uniform morphology corresponding to the mutants termination point (Hartwell et al., 1970). Genetic analysis of these mutant strains led to a model, where *START* (where the *cdc28*-1 mutant arrests) and cytokinesis mark the beginning and end of the cell cycle and encompass a temporal sequence of single cellular events in two pathways, replication and budding (Hartwell et al., 1974).

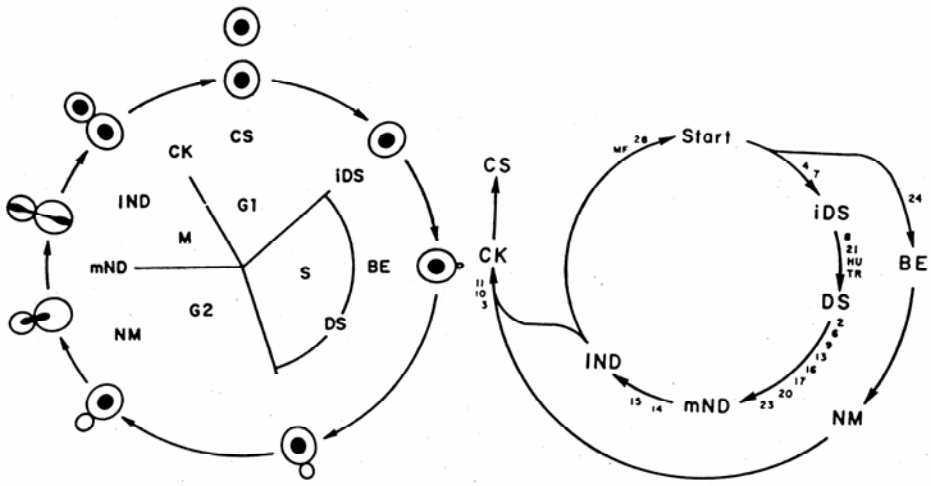

Fig. 1. The sequence of events in the cell division cycle of yeast: *iDS*, initiation of DNA synthesis; *BE*, bud emergence; *DS*, DNA synthesis; *NM*, nuclear migration; *mND*, medial nuclear division; *lND*, late nuclear division; *CK*, cytokinesis; *CS*, cell separation. Other abbreviations: *G1*, time interval between previous cytokinesis and initiation of DNA synthesis; *S*, period of DNA synthesis; *G2*, time between DNA synthesis and onset of mitosis: and *M*, the period of mitosis.

Fig. 3. The circuitry of the yeast cell cycle. Events connected by an arrow are proposed to be related such that the distal event is dependent for its occurrence upon the prior completion of the proximal event. The abbreviations are the same as in Fig. 1. Numbers refer to *cdc* genes that are required for progress from one event to the next; *HU* and *TR* refer to the DNA synthesis inhibitors hydroxyurea and trenimon, respectively; *MF* refers to the mating factor, α factor.

Figure 1.1: The sequence of events in the cell-division cycle of yeast and the circuitry of the yeast cell cycle (from Hartwell et al., 1974)**.**

Cdc28 is the single cyclin-dependent kinase (CDK) in budding yeast, a serine-threonine kinase which, as the name suggests, is activated by association with multiple cyclins. CDK can initiate different cell-cycle events, characterized by passage of the G1/S and the G2/M boundaries, regulated through intrinsic substrate specificity as well as undulating expression of the cyclins during the cell cycle

(Bloom and Cross, 2007; Mendenhall and Hodge, 1998). A unidirectional propagation through the cell cycle is mediated by the co-ordinated action of protein phosphorylation by CDK and ubiquitin-mediated protein degradation by the proteasome. In the case of G1/S transition this implies degradation of Sic1 and during mitosis, degradation of anaphase inhibitors and mitotic cyclins (Deshaies, 1997; Pagano, 1997).

Checkpoints are built-in surveillance systems over the cell cycle and are conserved throughout eukaryotic evolution (Elledge, 1996). They monitor the completion of crucial cell-cycle events and stop cell-cycle progression if those events are not occurring according to plan (Hartwell and Weinert, 1989). The first checkpoint gene was once again discovered in *Saccharomyces cerevisiae*. A yeast mutant for the *RAD9* (Radiation sensitive) gene was shown to arrest in the G2 phase of the cell cycle in response to ionizing radiation in all phases of the cell cycle (Weinert and Hartwell, 1988), as well as DNA damage resulting from incomplete replication (Hartwell and Weinert, 1989). Interestingly, according to the definition by Hartwell and Weinert, Rad9 is one of the few "real" checkpoint genes, since it promotes cell-cycle arrest and facilitates repair, but does not carry out a cell cycle or repair function by itself (Weinert and Hartwell, 1988). Instead, this is an additional function of other important checkpoint genes (see examples in Section 1.5.2).

The best characterized checkpoints monitor genomic stability. Besides checkpoints monitoring DNA damage and replication problems (see Section 1.2), the mitotic checkpoint monitors as spindle checkpoint the fidelity of chromosome segregation as well as, in a different branch, correct cytokinesis (Kops et al., 2005; Musacchio and Salmon, 2007; Smith et al., 2002). Recently, checkpoints monitoring yeast cell morphogenesis (checking correct cell wall synthesis, cell size, and bud formation) have been identified (Kellogg, 2003; Lew, 2003; Suzuki et al., 2004). Yeast morphogenesis and replication act in parallel pathways of the cell cycle control (see Figure 1.1). It is therefore surprising to note that cross-talk between both pathways has been observed and, indeed, the replication checkpoint has been shown to modulate the morphogenesis checkpoint (Enserink et al., 2006). The same replication checkpoint can influence the mitotic checkpoint and inhibit mitotic division as well, when replication is incomplete (Sanchez et al., 1999). Checkpoints can therefore generate a comprehensive response, including both progress and timing of the cell cycle.

1.2 An overview of DNA-damage checkpoints and the replication checkpoint

The DNA-damage checkpoint pathway inhibits cell-cycle progression during all cell-cycle stages in response to DNA damage (Nyberg et al., 2002). This damage results from the effect of exogenous mutagens, such as UV light, ionizing irradiation, or chemical compounds. If not repaired by continuously active repair pathways, these mutagenes will lead to base mutations or DNA double-strand breaks (DSBs; Sancar et al., 2004). Different kinds of lesions also require different repair pathways, and, similarly, they are differentially recognized by the DNA-damage checkpoint. The components of the DNA-damage, as well as replication, checkpoint pathways (see below) are conserved between *Saccharomyces cerevisiae*, *Schizosaccharomyces pombe*, and human cells (Elledge, 1996). The cellular response to DSBs, one of the most deleterious lesions, is conserved and therefore well characterized. Progression into mitosis with DSBs in a chromosome would lead to chromosome loss and would therefore be disastrous. In this context, it is not surprising that the most stringent checkpoint acts at the G2/M boundary and can be activated by a single DSB (Sandell and Zakian, 1993; Toczyski et al., 1997). The components of the DNA-damage checkpoint build signal transduction pathways in response to DSBs and replication problems, and can be classified as sensors, adaptors, and effectors (see Table 1.1).

Function	***Saccharomyces cerevisiae***	***Homo sapiens***	***Schizosaccharomyces pombe***
Signal	RFA (RFA1-3)	**RPA**	**RPA**
Sensor (RFC-like complex)	Rad24 (+RFC)	Rad17 (+RFC)	Rad17 (+RFC)
Sensor (PCNA-like complexes)	Ddc1/Rad17/Mec3	**Rad9/Rad1/Hus1**	**Rad9/Rad1/Hus1**
Sensor (MRX/MRN)	Mre11, Rad50, Xrs2	Mre11, Rad50, Nbs1	Rad32, Rad50, Nbs1
Sensor (signaling kinase)	Mec1/Ddc2	ATR/ATRIP	Rad3/Rad26
Sensor (signaling kinase)	Tel1	ATM	Tel1
Fork associated (sensor?)	Dpb11*	**TopBP1***	Cut5*
Fork associated (sensor?)	Polε*	Polε*	Polε*
Fork associated (sensor?)	Sgs1*	BLM*	Rqh1*
Fork associated (mediator?)	Tof1*	?	Swi1*
Mediator	Mrc1*	Claspin*	Mrc1*
Mediator	Rad9	Mdc1/BRCA1/53BP1?	Crb2
Effector (signaling kinase)	Rad53	Chk2	Cds1
Effector (signaling kinase)	Chk1	Chk1	Chk1

Table 1.1: Selection of important checkpoint proteins/complexes and their orthologues or proteins with analog function.
Proteins with their specific or main function in the S phase checkpoint are indicated by *. Protein names are marked in bold if the name of the homologous protein is also used in budding yeast.

Most of the proteins involved are also necessary for the activation of the G1/S, the intra-S, or the G2/M checkpoints (Nyberg et al., 2002).

As Hunter stated in 1995, "Protein phosphorylation is a major currency of signal transduction pathways" (Hunter, 1995). Similarly, kinases are also essential and are central elements of DNA-damage signaling pathways (McGowan and Russell, 2004; Zhou and Bartek, 2004). During checkpoint recovery after successful repair or adaptation in the case of an irreparable situation, dephosphorylation is essential (Harrison and Haber, 2006). Crucial components in sensing and activating downstream checkpoint targets are the PI3K-like kinases Mec1 and Tel1, which are homologues of the human ATR/ATM kinases (see Figure 1.2).

Mec1 is known to act, together with its cofactor Ddc2, as a sensor and activator of the crucial checkpoint kinases Chk1 and Rad53 (human CHK2-homolog) through phosphorylation (Melo and Toczyski, 2002). Mec1 forms a complex with Ddc2, and Ddc2 is essential for the checkpoint function of Mec1 (Paciotti et al., 2000; Rouse and Jackson, 2000; Wakayama et al., 2001) as well as for targeting it to sites of DNA damage (Rouse and Jackson, 2002). The checkpoint signal sensed by Mec1/Ddc2 is single-stranded DNA coated with RPA (Zou and Elledge, 2003). DNA damage is also sensed by Rad24, which is an RFC1-homolog that forms an RFC-like complex with Rfc2-5, and acts as a "clamp loader" to load the yeast 9-1-1 PCNA-like "checkpoint sliding clamp" (Rad17, Ddc1, and Mec3; Majka and Burgers, 2004).

Both Mec1/Ddc2 and Rad24-RFC can be independently loaded on damaged chromatin, but both are required for full checkpoint activation (Kondo et al., 2001; Melo et al., 2001). It has recently been shown that the 9-1-1 checkpoint clamp directly interacts with Mec1 and enhances its activation (Majka et al., 2006), showing once again that Mec1 is the central sensor kinase initiating the checkpoint signaling pathway (Carr, 1997). Another pathway which senses DNA damage involves the MRX complex (Mre11, Rad50, and Xrs2) and a second PI3-like kinase Tel1. While the loss of Tel1 is less debilitating for the damage checkpoint, in the absence of Mec1 and in S-phase cells, Tel1 can activate the downstream target Rad53, as well as increase Mec1 activity (Clerici et al., 2004; Mantiero et al., 2007).

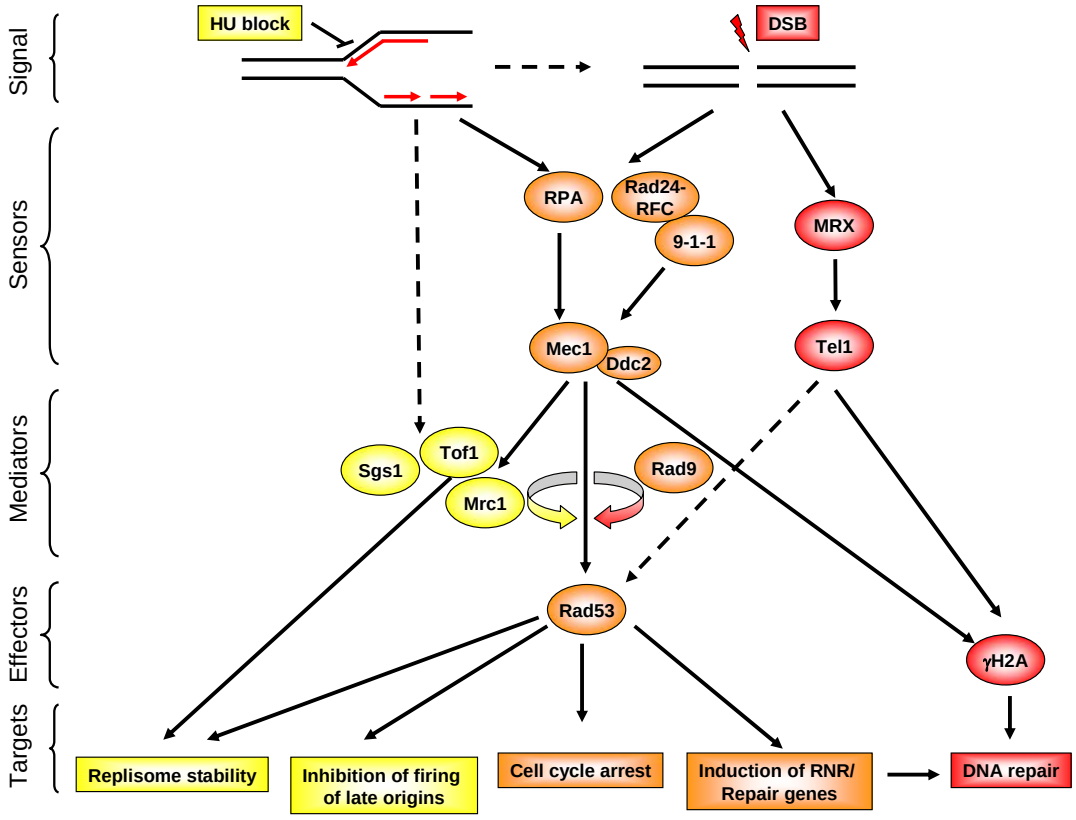

Figure 1.2: The DNA-damage and replication checkpoint in *Saccharomyces cerevisiae.*

This figure illustrates the signaling cascade triggered in response to stalled replication forks (yellow), double-strand breaks (red), and the central signaling cascade in response to both genotoxic insults (orange). Important components of this central signaling pathway are the sensory kinase Mec1, which is recruited to single-stranded DNA via RPA and is also activated by Rad24-RFC and the 9-1-1 complex. Mec1 activates the central effector kinase Rad53, and this activation is mediated specifically either by Mrc1 (replication checkpoint) or Rad9 (DNA-damage checkpoint). The phosphorylation of histone H2A at serine 129 (γH2A) is a target of the checkpoint response branching out upstream of Rad53. In this case, Mec1 and Tel1 are effector kinases.

The adaptor protein Rad9 functions by transmitting and amplifying the DNA-damage signal and enhancing activation of Chk1 and Rad53 (Sanchez et al., 1999). Rad9 itself is also activated by Mec1-mediated phosphorylation (Emili, 1998). Activated Rad9 binds Rad53 and seems to link Mec1 to Rad53 and to facilitate autophosphorylation of Rad53 *in trans*, thus amplifying the checkpoint signal (Gilbert et al., 2001; Schwartz et al., 2002; Sweeney et al., 2005). Figure 1.3 shows the current model for activation of the effector kinase Rad53.

In short, Rad53 itself is as effector kinase and, in the same way as its human homolog Chk2 (Ahn et al., 2004; Nevanlinna and Bartek, 2006), a central player in the DNA-damage checkpoint pathway in mediating downstream checkpoint responses which, due to its specific protein structure (containing two FHA-signaling domains), seems to have obtained the capacity to mediate the integration of checkpoint signals from both

the DNA-damage and the replication checkpoints (Pike et al., 2003; Schwartz et al., 2003; Shimada et al., 2002). Rad53 will be thoroughly introduced in Chapter 2.

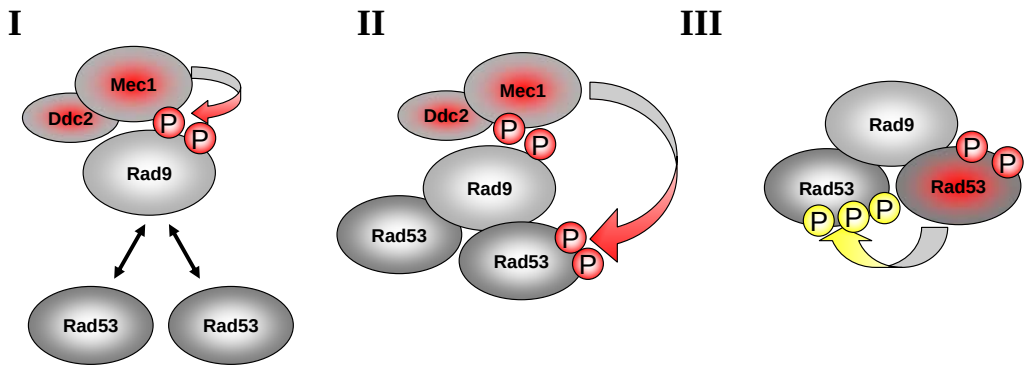

Figure 1.3: Model for the role of adaptor proteins in Rad53 activation.

I. Mec1/Tel1 phosphorylation of Rad9 generates a phosphoepitope, which is recognized and bound by the Rad53 FHA domains. II. The Rad9-Rad53 interaction recruits Rad53 proteins to the site of lesion. Mec1 can now directly phosphorylate Rad53. III. Docking of more than one Rad53 protein onto one phosphorylated Rad9 protein facilitates Rad53 in-trans autophosphorylation through increasing the local concentration. There is biochemical evidence supporting a function of Rad9 in step II as well as step III. The replication checkpoint protein Mrc1 is thought to mediate the checkpoint signal in a similar way (Pellicioli and Foiani, 2005; Sweeney et al., 2005; Toh and Lowndes, 2003).

The DNA-damage checkpoint signaling pathway presented above also occurs in S phase and, indeed, DSBs can be created in an S-phase specific manner by methylmethanesulfonate (MMS), a DNA-alkylating agent (Tercero et al. 2003), activating the so-called "intra-S-phase checkpoint". This pathway is, however, supplemented by a second pathway, which leads to activation of Rad53. A DNA-damage-like signal originating from stalled replication forks in response to hydroxyurea (HU) is detected by sensor proteins that are also involved in the normal replication process (e.g. DNA polymerase ε, Dpb11, and Sgs1) and act locally at the replication forks. Stalled replication forks lead to activation of Rad53 via the 9-1-1 complex, as well as through the adaptor protein Mrc1 (Cobb et al., 2003; Frei and Gasser, 2000; Katou et al., 2003; Osborn and Elledge, 2003; Tercero et al., 2003; Wang and Elledge, 2002). The DNA-damage branch and the replication checkpoint branch of the intra-S-phase checkpoint are often simultaneously activated (Bjergbaek et al., 2005; Longhese et al., 2003). Yet the maintenance of fork integrity appears to be the most important task of the intra-S checkpoint response (Tourriere and Pasero, 2007). This aspect is covered more completely in Section 1.5.

1.3 Downstream targets of checkpoint kinases

The task of a checkpoint has to be considered in the context of a given cell-cycle stage. The G2/M checkpoint must avoid deleterious segregation of DNA damage (particularly of DSBs) in mitosis (Harrison and Haber, 2006), while the intra-S phase checkpoint must not only block the next cell-cycle transition (S to M), but must also stabilize the replisome (Tourriere and Pasero, 2007). Not only do the downstream targets differ, but some functions do not even involve the effector kinases Rad53 and Chk1. Instead, they may target other enzymes, such as has been shown for Mrc1, which maintains fork stability independently of its function in mediating Rad53 activation (Osborn and Elledge, 2003).

Besides promoting cell-cycle arrest and stabilizing replication forks, the checkpoint pathway facilitates and induces DNA repair mechanisms (Harrison and Haber, 2006; Nyberg et al., 2002). The best-characterized case is the induction of ribonucleotide reductase, leading to higher dNTP pools by Dun1 (Elledge et al., 1993). Interestingly, suppression of lethality of both *mec1* and *rad53* mutant strains stems from higher basal activation of Dun1, which is important for the inactivation of Sml1 (a negative regulator of ribonucleotide reductase) and which normally depends on both Mec1 and Rad53 (Zhao et al., 2001; Zhao et al., 1998; Zhao and Rothstein, 2002). This is one example where Mec1 functions are mediated by Rad53. There are many more uncharacterized targets of this global checkpoint signal transduction cascade. A recent study identified *in vivo* targets of Mec1 and Rad53 using proteomics (Smolka et al., 2007). The same study showed that several checkpoint targets are activated by Mec1 and Tel1 directly, and do not involve Rad53. One well-known example of such a checkpoint response is the phopshorylation of serine 129 of histone H2A (γH2A, in mammals the histone variant H2AX is modified to make γH2AX, see Figure 1.2). γH2A is, so far, the best-characterized histone modification induced by DNA damage, but an increasing number of other covalent histone modifications (including phosphorylation, ubiquitylation, and acetylation) on core histones H2A, H2B, H3, and H4 have recently been associated with cellular DNA-damage responses (Downs et al., 2007; van Attikum and Gasser, 2005). γH2A will be introduced in detail in Chapters 3 and 4. In brief, γH2A serves two roles. First, it is important for amplifying the checkpoint response in mammalian cells via recruitment of the checkpoint mediator Mdc1 (Su, 2006) and maintaining high checkpoint activity in yeast (Keogh et al.,

2006), Second, it is needed for the recruitment of both the INO80 and SWR1 chromatin remodeling complexes, as well as cohesins, to DSBs. These promote efficient repair of this particular lesion by HR or error-prone NHEJ (Morrison et al., 2004; Strom et al., 2004; Unal et al., 2004; Van Attikum et al., 2007; van Attikum et al., 2004). These are examples of the pleiotropic response induced by the activated DNA-damage checkpoint, which demonstrate that the checkpoint is interlocked with DNA repair in a multi-faceted way.

1.4 Telomeres and the DNA-damage response

Telomeres protect the free ends of chromosome arms, which might otherwise resemble DSBs and activate the checkpoint response (Viscardi et al., 2005). Budding yeast telomeres (see Figure 1.4) contain a nucleosome-free, ~300 bp long $TG_{1\text{-}3}$ repeat which ends in a single-stranded 3' overhang (Dionne and Wellinger, 1996; Wright et al., 1992). $TG_{1\text{-}3}$ repeats are bound by the protein Rap1, and the single-stranded overhang by Cdc13 (Viscardi et al., 2005). Rap1 was found to be a nucleation site for SIR-protein recruitment (Cockell et al., 1995; Moretti et al., 1994). SIR complexes spread into sub-telomeric chromatin and make it a heterochromatic and transcriptionally repressed domain (Gasser and Cockell, 2001). Telomeres also influence the organization of chromatin in the nucleus, as they are clustered into nuclear foci that are anchored at the nuclear periphery (Klein et al., 1992; Palladino et al., 1993b).

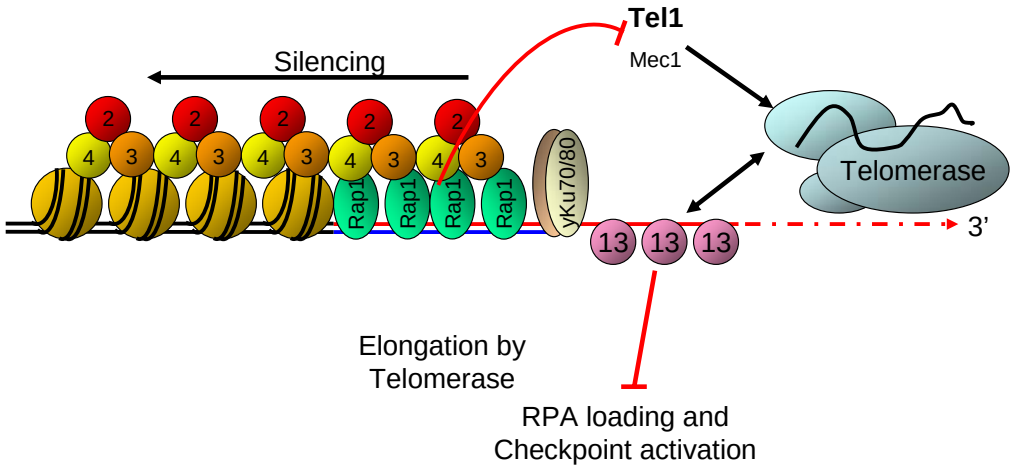

Figure 1.4: Structural components of the yeast telomere, and the main factors regulating telomere elongation by telomerase.

The G-rich strand is shown in red, the C-rich strand in blue. $TG_{1\text{-}3}$ repeats are bound by Rap1 and the single-stranded overhang by Cdc13. Tel1 activates telomerase indirectly once the $TG_{1\text{-}3}$ repeat stretch gets shorter and the inhibiting effect of bound Rap1 is abolished. Telomerase elongates the G-rich single-stranded overhang, which is then a template for primase and the normal replisome for synthesis of the complementary strand (Blackburn, 2001; Dubrana et al., 2001; Viscardi et al., 2005).

Telomeres get shorter each time the chromosome undergoes replication (Lingner et al., 1995; Lundblad and Szostak, 1989; Lustig and Petes, 1986). To counterbalance this effect, telomeres require a specific enzyme, called telomerase, which contains an

RNA subunit that serves as a template to allow elongation of the TG_{1-3} repeat (Hug and Lingner, 2006; Teixeira and Gilson, 2005). The maintenance of an equilibrium length of the TG_{1-3} repeat is ensured by a protein-counting mechanism that senses the number of Rap1 proteins bound to the double-stranded TG_{1-3} repeats. This signal, which is Tel1-dependent, negatively regulates telomerase (Marcand et al., 1997). Telomerase is also positively regulated by the two checkpoint kinases Mec1 and Tel1, as well as Cdc13, a protein that binds to the single-stranded TG_{1-3} overhang (Evans and Lundblad, 1999; Taggart et al., 2002; Tseng et al., 2006). Telomerase is inactive in the absence of Tel1 and Mec1, and yeast cells undergo cellular senescence (Ritchie et al., 1999). The telomeric presence of checkpoint kinases has puzzled researchers in the DNA-damage checkpoint field. Why are structures that look more or less like DSBs not recognized as such, but nonetheless require checkpoint kinases to maintain their structure?

One basic principle of telomere structure is that it is protected from activating the checkpoint response. Cdc13, and not RPA, covers the single-stranded telomeric overhang in budding yeast. Loss of Cdc13 induces rapid end resection and permanent checkpoint arrest (Viscardi et al., 2005). Thus Cdc13 is important for preventing a checkpoint response. In mammalian cells, a more complex protein machinery called shelterin fulfills the same function (Verdun and Karlseder, 2007). In addition to Mec1 and Tel1, an ever-increasing number of checkpoint and repair proteins are found at telomeres (Gasser, 2000; Lydall, 2003; Verdun and Karlseder, 2007; Viscardi et al., 2005), and the question therefore remains as to exactly how a checkpoint response is avoided under normal growth.

1.5 Excursus:
Damaged forks in yeast: A survey on checkpoint mechanisms, replication fork stability, repair mechanisms and chromatin

1.5.1 Summary

During S phase DNA is both synthesized and repaired, and in S phase checkpoint mechanisms are integrated into normal ongoing replication. This makes the generation of an independent surveillance system almost impossible. Recently it became clear that damage during replication requires an integration of checkpoint response with replication itself and other cellular pathways, such as replication pausing, recombination and translesion synthesis (Lambert et al., 2007; Moldovan et al., 2007; Tourriere and Pasero, 2007). Indeed, the outcome of a genotoxic event in S phase depends largely upon whether or not the replisome can be maintained in a stable structure when it hits the lesion. This chapter will focus upon recent advances in our understanding of the proteins that contribute to the replication checkpoint and the maintenance of fork integrity. Recent reports suggest that histone modifications and chromatin remodeling complexes are also involved into this process.

1.5.2 Replication checkpoint activation: What is the signal for checkpoint activation

The S phase checkpoint does not block progression into the following cell-cycle stage like the G1/S and G2/M checkpoints, but has to deal with the more complicated tasks of maintaining replication integrity by stabilizing components of the replisome (Cobb et al., 2003; Cobb et al., 2005; Katou et al., 2003; Osborn and Elledge, 2003), preventing the firing of late origins (Santocanale and Diffley, 1998; Shirahige et al., 1998) and preventing spindle elongation. This last point is a function of the S-phase checkpoint in mitosis, called the S to M checkpoint. Failure to assemble the spindle or impaired mitotic CDK function cause the replication checkpoint-induced mitotic arrest (Krishnan et al., 2004). It is particularly relevant for the response to DNA damage and replication problems in S phase to understand the function of different drugs on checkpoint and repair mechanisms. In human cells, some drugs only provoke

a checkpoint response when the damage encounters a moving replication fork. For instance HU was shown to be replication fork-dependent, but progression independent, while MMS is independent of both. On the other hand, Adozelesin, another alkylating agent, required both fork presence and progression (Liu et al., 2003). The response to DNA damaging drugs differs widely, as does the genome wide requirements for resistance. This allows one to define drug-specific gene-clusters (Brown et al., 2006; Lee et al., 2005b). Mass spectrometric analysis of Rad53 phosphorylation in response to DNA damage induced by the drugs 4-NQO and MMS, has revealed drug-specific patterns of Rad53 phosphorylation (Smolka et al., 2005; Sweeney et al., 2005). Another drug extensively used in chemotherapy is Camptothecin (CPT), which traps topoisomerase I in a covalent complex with DNA. Once the trapped transient cleavage complex is hit by the replisome, a lesion occurs (Pommier, 2006). Repair of this lesion, which is a checkpoint-blind DSB, requires a specific subset of proteins, including Tof1 and γH2A (Redon et al., 2006; Redon et al., 2003). When a replication fork hits a site of DNA damage such as an alkylated base or an abasic site, either the fork collapses and leaves behind a DSB, or components of the replication checkpoint promote errorprone translesion synthesis (TLS), errorfree bypass synthesis, or the replisome is stabilized allowing lesion repair (Tourriere and Pasero, 2007). Another specific threat for cells are stalled replication forks, which can be induced experimentally by inhibiting ribonucleotide reductase by HU, which leads to fork stalling via depletion of cellular dNTP pools (Yarbro, 1992). Stalled replication fork structures resemble naturally paused replication forks, yet do elict a checkpoint response (Tourriere and Pasero, 2007). The replication checkpoint pathway prevents replication fork collapse in this specific situation. It does not, however, conform to the narrow definition of a checkpoint pathway as an independent surveillance system (Hartwell and Weinert, 1989). Because many replication checkpoint proteins are involved in the replication process itself (see section 1.5.3), the replication checkpoint is not strictly an independent surveillance system. It is also important to remember that cells are not equally sensitive to DNA damaging agents throughout the cell cycle. Some agents are more harmful at different cell cycle stages, and in particular there is a higher threshold for checkpoint activation during S phase (Shimada et al., 2002). Because some checkpoint mutants show different sensitivities to different drugs, we propose that a balanced action of multiple pathways is involved.

1.5.3 Replication, repair and checkpoint activation: Overlapping structures, complexes and mechanisms

Replication and repair mechanisms share a number of key factors. One important component is the single strand binding protein RPA, which besides its crucial role of protecting single-stranded parts of the replicating double helix, is important for DNA repair (Aboussekhra et al., 1995; He et al., 1995) Indeed, RPA is a required signal for checkpoint activation (Zou and Elledge, 2003). It is not known if the large stretches of ssDNA that arise during replication are distinct from those in damaged DNA. However an increase in the single stranded stretches from ~ 220 bp for a normal unchallenged replication fork to around 300 bp in case of an HU-stalled fork is able to activate the checkpoint kinase Rad53 (Sogo et al., 2002). Therefore it is most likely the amount of single stranded DNA bound by RPA that determines activation of the replication checkpoint (Tourriere and Pasero, 2007).

Another key component of normal replication that is also important for DNA repair and checkpoint activation is the sliding clamp PCNA. PCNA forms a trimeric ring around the double helix, and is loaded onto DNA by replication factor C (RFC), a heteropentameric complex formed by the proteins Rfc1 to Rfc5 (Majka and Burgers, 2004). PCNA promotes polymerase δ or ε processivity and orchestrates various processes related to replication, repair and chromatin assembly (Moldovan et al., 2007). In addition a PCNA homolog called the 9-1-1-complex (Rad9, Rad1 and Ddc1) is dedicated to DNA repair and checkpoint activation (Parrilla-Castellar et al., 2004). Whereas PCNA is loaded during the initiation of DNA replication by the Rfc1-RFC complex, 9-1-1 is loaded by a related, checkpoint-specific complex, the Rad24-RFC. Two additional RFC-like complexes are Elg1-RFC and Ctf18-RFC (Majka and Burgers, 2004). How the functions of these four loading complexes are coordinated is not yet completely understood. However, Rad24-RFC is primarily important for checkpoint activation, the complex containing Ctf18 is important for sister chromatid cohesion, and the Elg1 complex has a role in DNA repair. The fact that the mutants show additive defects after treatment of yeast cells with DNA damage argues that they also share overlapping functions.

In the case of PCNA different functions are regulated by ubiquitylation and sumoylation through the *RAD6* postreplicative repair pathway (Hoege et al., 2002). Interestingly both modifications are positioned at K164 of the PCNA monomer, and

Rad6 and Rad18 mediated PCNA-mono-ubiquitylation displaces the replicative polymerases Polδ and Polε for TLS polymerases (Lehmann et al., 2007; Moldovan et al., 2007). TLS polymerases belong to the Y-family of DNA polymerases, which have a high error rate, yet are able to synthesize DNA across an abasic site or over other lesions (Fleck and Schär, 2004). Not only translesion synthesis, but also error free bypass is mediated by PCNA ubiquitylation. K63-linked multi-ubiquitilation occurs again at K164 of PCNA, depending upon *RAD5,UBC13* and *MMS2* (Hoege et al., 2002). This poly-ubiquitilation induces error free DNA repair either by replication restart or template switching mechanisms (Moldovan et al., 2007).

In contrast to the ubiquitin pathway, SUMO-modification of PCNA influences the ability of the fork to overcome problems during normal replication. It also stimulates spontaneous mutagenesis by Polζ (Hoege et al., 2002; Stelter and Ulrich, 2003). SUMO-modification occurs at K127 and K164 of the PCNA monomer. Thus for K164 modification SUMO and ubiquitin may compete. This competition may influence the choice of the PCNA-mediated repair pathway (Moldovan et al., 2007; Ulrich, 2005).

Sumoylation of PCNA was also observed during an unperturbed S phase and was shown to recruit the anti-recombinogenic helicase Srs2 (Papouli et al., 2005; Pfander et al., 2005). Homologous recombination is important for repair of DSBs (Dudas and Chovanec, 2004) and recombination-based fork restart mechanisms are essential in situations of replication fork collapse (Lambert et al., 2007; Wyman and Kanaar, 2006). However, recombination at replication forks must be repressed if there is no DSB or collapse. It was shown that in absence of Sgs1 damaged replication forks undergo recombination (Liberi et al., 2005) and that at DSBs both Sgs1 and Srs2 suppress crossing-over during repair by homologous recombination (Ira et al., 2003). By inhibiting recombination at replication forks these helicases favor error-free bypass and translesion synthesis (Barbour and Xiao, 2003). The sumoylation of PCNA requires the E3 SUMO-ligase Siz1, while the E3 SUMO-ligase Mms21 acts on PCNA, Sgs1 and Srs2 to suppress recombination at replication forks (Branzei et al., 2006). Although Sgs1 was not yet shown to be directly sumoylated by Mms21, sumoylation is important for Sgs1 and Srs2 function at stalled replication forks. Accordingly in fission yeast Meister et al. showed that replication and recombination are temporally separated by the replication checkpoint, to avoid aberrant strand exchange events and pathogenic replication fork structures (Meister et al., 2005).

Interestingly, PCNA also controls sister chromatid cohesion in S phase cells by interaction with Eco1. This function is inhibited by sumoylating PCNA (Moldovan et al., 2006). In this context it is interesting to note that sister chromatid cohesion and the loading of additional cohesins are important both for postreplicative and DSB repair (Strom and Sjogren, 2005; Strom et al., 2007). In fission yeast the cohesin-like proteins Smc5 and Smc6 have been shown to be required for the repair of collapsed replication forks by homologous replication (Ampatzidou et al., 2006). It is proposed that recombination may become necessary when other repair pathways fail. For example, it was shown that phosphorylation of Rad55, most likely by Mec1 or Rad53, which is a factor supporting the formation of Rad51 filaments is required for the efficient recovery of MMS-induced DNA damage (Herzberg et al., 2006). Furthermore, genetic data argue that DNA damage checkpoints may favor the *RAD6* mediated postreplicative repair pathways of error-free lesion bypass and TLS (Barbour et al., 2006). In fission yeast phosphorylation of Rad9 (part of the PCNA-like 9-1-1 complex) by the ATR/Mec1 homologous kinase Rad3 seems to favor error-free repair via the *Rhp6 (Sc RAD6)* pathway, rather than recombination. How also checkpoints influence the choice of fork-associated repair pathways appears very complex and it is likely that it will be influenced by the molecular nature of the lesion at the stalled or damaged replication fork.

How are the various modifications of PCNA triggered? It was recently shown by using *Xenopus* egg extracts, that PCNA mono-ubiquitylation requires replisome uncoupling from the MCM helicase (Chang et al., 2006). Interestingly, activation of ATR via the Aphidicolin-induced replication checkpoint requires also uncoupling of the MCM helicase and polymerase activities (Byun et al., 2005). Again using *Xenopus* egg extracts MacDougall et al. showed that primed ssDNA is sufficient for ATR activation, with the amount of ssDNA determining the strength of the checkpoint response. ssDNA is most likely a common checkpoint activating structure that results from many different types of damage (MacDougall et al., 2007). It therefore seems that the molecular structures that induce fork associated repair via TLS and DNA-damage checkpoint activation share partially overlapping mechanisms and are interconnected.

1.5.4 Acting at the fork: Checkpoint components and their role in the maintenance of replication fork stability

Many proteins which are involved in the replication checkpoint cascade have an important function during an unchallenged S phase e.g. Mrc1 (Osborn and Elledge, 2003). Even though many of the checkpoint signaling components move with the replication fork, the replication checkpoint is not activated most of the time. Replication checkpoint components thus initiate a global checkpoint response, as well as acting locally at replication forks to allow adequate resumption of DNA synthesis after recovery from stress. The sensor kinase Mec1 and the effector kinase Rad53 are key players in the DNA damage checkpoint. Other sensor components, e.g. Rad24-RFC, are only involved if replication forks collapse and may be a substrate for the damage checkpoint pathway (Bjergbaek et al., 2005). At stalled but not broken replication forks, Rad24-RFC is replaced by Sgs1 for checkpoint kinase activation (Frei and Gasser, 2000).

Checkpoint activation itself involves the phosphorylation and autocatalytic activation of Rad53. Rather than the adaptor protein Rad9, the replication fork component Mrc1 acts as a mediator of the activating signal at stalled forks (Alcasabas et al., 2001). Indeed, Mrc1 in budding yeast was shown to interact with Rad53 (Smolka et al., 2006). This adaptor function is conserved in the fission yeast homolog Mrc1 (Tanaka and Russell, 2001) and in the human homolog Claspin (Kumagai and Dunphy, 2000). In fission yeast, the interaction of the FHA domain of Cds1 (Rad53) with Mrc1, which itself if modified by Rad3 (Mec1), allows Cds1 recruitment to stalled forks. This allows Rad3 to activate Cds1, which is followed by autophosphorylation of Cds1. Interestingly, fission yeast Mrc1 directly interacts with DNA through a helix-loop-helix motif, a sequence that is conserved in human and budding yeast homologues. This region is important for Mrc1 function in the replication checkpoint. Mutation of this interaction domain renders cells sensitive to HU (Zhao and Russell, 2004). Human Claspin was also shown to bind with high affinity to branched replication-fork like DNA structures (Sar et al., 2004).

Both Tof1 and Mrc1 are components of the replisome complex, which also includes the MCM helicase, the initiation and elongation factor Cdc45, and GINS, a complex of the proteins Sld5, Psf1, Psf2 and Psf3, which is required to couple the MCM helicase to the other components of the replisome (Gambus et al., 2006; Katou et al.,

2003; Labib and Gambus, 2007). In fission yeast, specific mutations in MCM or in Cdc45 suppress the HU sensitivity of *mrc1* mutants (Nitani et al., 2006), suggesting that Mrc1 may bridge between these replication factors. The functions of Mrc1 in checkpoint activation and in replisome stability can be separated genetically. The checkpoint deficient $mrc1^{AQ}$ mutant strain, which is lacking its Mec1-phosphorylation sites and therefore its interface for Rad53 activation in response to replication stalling, has no defect during normal replication and progresses unperturbed through S phase (Osborn and Elledge, 2003). Surprisingly the direct fork-stabilizing function of Mrc1 seems to be more important than the checkpoint response function (Tercero et al., 2003).

Results from Robert and coworkers showed that Mrc1 promotes Srs2 recruitment to sumoylated PCNA, thereby helping to inhibit the formation of homologous recombination intermediates at stalled replication forks (Robert et al., 2006). This inhibition of homologous recombination acts in parallel to Sgs1, which resolves such intermediates (Robert et al., 2006). Polymerase stability (Polε) is reduced in the recombination-deficient *rad51* mutant and in cells lacking Sgs1 and these effects are not additive (Bjergbaek et al., 2005). In contrast Sgs1 and Mrc1 act synergisitcally to stabilize polymerases at stalled replication forks. This supports the model that Sgs1 and Srs2/Mrc1 act on parallel pathways to maintain fork stability (Bjergbaek et al., 2005). This may account for the synthetic lethality observed between *sgs1* and *srs2* (Lee et al., 1999). The fact that *mrc1 sgs1* double mutant strains are viable argues that Sgs1 and Srs2 have other activities as well (Bjergbaek et al., 2005).

The functions of Mrc1 and Tof1 seem somewhat similar (Zegerman and Diffley, 2003) and therefore a more careful analysis of overlapping versus specific functions of both proteins became necessary. Two studies addressed this question on the molecular level by using a combination of single-molecule analysis (DNA combing) and 2D gels and Chromatin Immunoprecipitation (Tourriere et al., 2005; Szyjka et al., 2005). Tourriere and coworkers showed that both Mrc1 and Tof1 are required for normal fork progression. Single molecule analysis of BrdU incorporation showed that the replication fork moves more slowly in both mutants independent of their checkpoint function, resulting in a prolonged S phase. Nonetheless, there are functional differences between the two proteins as well. Natural fork pausing in the rDNA depends on Tof1, but not Mrc1, thus Mrc1 is a *bona fide* adaptor of the replication checkpoint while Tof1 is not (Tourriere et al., 2005). Szyjka and

colleagues also demonstrated that replication forks progress more slowly in a *mrc1* mutant than in a wildtype strain. They also showed that this is independent of Mrc1 checkpoint function, since the *mrc1*^{AQ} mutant has a normal fork progression rate (Szyjka et al., 2005). These results further suggest that Mrc1 is not absolutely required for the resolution of paused replication forks. This is in contradiction to results published by Bjergbaek et al. (Bjergbaek et al., 2005) who showed a partial loss of DNA Polε at forks on HU in a *mrc1*Δ strain.

Further distinctions between the function of Mrc1 in checkpoint activation and in normal replication arose from an analysis of the genetic relationship between Mrc1 and Rrm3. Rrm3 is a helicase that helps replication forks advance through protein complexes (Szyjka et al., 2005). Replication forks are known to pause transiently at sites where non-nucleosomal proteins are bound tightly to the DNA strand. There are probably more than 1000 pausing sites in the budding yeast genome (Ivessa et al., 2003). Repair of stalled replication forks in *rrm3* cells was shown to depend on Mrc1 for viability (Ivessa et al., 2003). Szyjka et al. then showed that the checkpoint function of Mrc1 does not participate in replication fork pausing and resolution even in a double mutant with *rrm3.* In contrast, *mrc1 rrm3* double mutants are lethal. They propose that Rrm3 is required to resolve replication fork defects resulting from deletion of Mrc1`s function in normal replication (Szyjka et al., 2005). Calzada et al. (2005) then asked whether Mrc1 and Tof1 are important for maintaining replisome integrity at normally occurring pausing sites such as the replication fork barrier (RFB) in the rDNA (Calzada et al., 2005; Lambert et al., 2007; Tourriere and Pasero, 2007). By integrating a pair of RFB sequences between the two efficient and early firing origins, *ARS305* and *ARS306,* it was possible to block forks in a Fob1-dependent manner. By chromatin immunoprecipitation the authors showed that pausing does not lead to disassembly of the replisome since the fork associated MCM-complex, Cdc45, GINS, the DNA polymerases α and ε and also Mrc1 and Tof1 stay associated. Indeed, Mrc1 and Tof1 were needed to maintain replication fork integrity after fork stalling (Calzada et al., 2005). The authors then addressed the question of how these proteins would influence fork pausing. Intriguingly fork pausing was shown to depend on Tof1, but not Mrc1. Density-transfer assays also argue that Tof1 but not Mrc1 mediates fork pausing, although they also observe that Mrc1 is crucial for a normal fork progression rate (Hodgson et al., 2007).

An important role for Tof1 in fork pausing was also shown for the fission yeast homolog Swi1 (Dalgaard and Klar, 2000; Krings and Bastia, 2004) which argues that the proteins and mechanisms required for replication are fairly conserved. Interestingly, a partner of Swi1, Swi3, also affects fork pausing and its *S. cerevisiae* homologue, Csm3, interacts with Tof1 (Ito et al., 2001). Both Tof1 and Csm3 play a role in sister chromatid cohesion (Mayer et al., 2004). A clear role of fork associated Tof1 in cohesion is not yet established, but this may involve histone modifications, which are discussed in the next section.

We note that the helicase Rrm3 is also recruited to paused replication forks and is probably needed to unwind the RFB to allow fork progression over this barrier. In contrast to the situation at HU-stalled forks pausing and recovery at natural pausing sites does not require the checkpoint kinases Mec1 or Rad53, nor is recombination involved (Calzada et al., 2005; Ivessa et al., 2003). Importantly, it was shown that paused forks at endogenous pausing sites in the rDNA are regulated in a similar manner (Calzada et al., 2005). The Tof1/Csm3 complex but not Mrc1 seems to counteract the function of Rrm3 at RFBs and maybe also at places, where replication collides with transcription (Mohanty et al., 2006).

Taken together it is clear that the proteins Mrc1 and Tof1 are implicated both in maintaining fork stability through multiple pathways, as well as being required for normal fork progression. Only Tof1, but not Mrc1, plays a role at natural pause sites. On the other hand, Tof1 plays a minor role in the replication checkpoint, while Mrc1 is an essential adaptor for Rad53 activation in response to HU. Mrc1 also promotes fork recovery in a Rad53-independent manner by maintaining replisome integrity after HU-induced replication fork stalling. These two proteins exemplify a general theme arguing that different lesions (HU-stalled fork) or lesion-like structures (paused fork) are detected differently and trigger distinct molecular responses.

1.5.5 The role of the chromatin environment in maintaining genomic stability in response to stalled replication forks

DNA replication in eukaryotic cells does not occur on a naked double helix but instead the template is wrapped around nucleosomes. The expected overall structure at this stage of the cell cycle resembles the 30nm fiber (Bystricky et al., 2005; Tremethick, 2007). Therefore, it was expected that factors involved in nucleosome

deposition and in chromatin remodeling would interfere and modulate the activation of the replication checkpoint or the fate of stalled or collapsed replication forks.
Although the assembly of histone variants can occur in a replication-independent manner, the assembly of the bulk of nucleosomes is coupled to replication (Henikoff and Ahmad, 2005). Chromatin Assembly factor 1 (CAF1) deposits histones directly at the replication fork. CAF1 recruitment is mediated by its interaction with PCNA. Loss of the essential function of CAF1 in proliferating human cells creates spontaneous DNA damage and defects in S phase. Consistently, a dominant negative mutant of CAF1 induces an S-phase arrest through an intact checkpoint pathway. This shows that defects in chromatin assembly can lead to a DNA damage signal (Ye et al., 2003).

In budding yeast *caf1* mutants show no severe phenotype, since there exists a parallel pathway of nucleosome assembly involving Hir proteins. These were originally described as repressors of histone gene transcription after activation of the replication checkpoint. In addition the histone chaperone Asf1 functions during replication and shows synthetic defects with CAF1 (Gunjan et al., 2005; Kats et al., 2006). Several reports link the function of Hir proteins, histone gene transcription, and heterochromatic silencing with the protein Asf1 (Green et al., 2005; Krawitz et al., 2002; Sharp et al., 2001; Sharp et al., 2005; Sutton et al., 2001). Asf1 is important for genomic stability since *asf1* mutant cells are sensitive to MMS as well as HU, and arrest at the G2/M checkpoint after release from an acute HU block (Tyler et al., 1999). Interestingly Rad53 forms a complex with Asf1, which is resolved after checkpoint activation. The overexpression of Asf1 can suppress the temperature sensitivity of *mrc1 rad53* double mutants and the HU sensitivity of *rad53* mutants, suggesting that one major function of Rad53 is to regulate chromatin assembly (Emili et al., 2001; Hu et al., 2001). Additionally Rad53 regulates histone protein levels in a kinase-dependent surveillance mechanism. Consistently, *rad53* mutants are extremely sensitive to histone overexpression (Gunjan and Verreault, 2003). Budding yeast Asf1 can be functionally replaced through human and Drosophila orthologs for its role in suppressing replicational stress or DNA damage (Tamburini et al., 2005). Since these orthologs are not interacting with Rad53 this opens the question whether the Asf1-Rad53 interaction is important for maintaining genomic stability.
Sharp et al. now provide evidence that the function of the Asf1-Hir-protein complex in chromatin-mediated silencing is regulated by the checkpoint kinases Mec1 and

Dun1. The authors propose that Mec1 promotes the dissociation of the inactive Rad53-Asf1 complex towards an active Asf1-Hir complex formation, while the Rad53 target Dun1 has the opposite role (Sharp et al., 2005). On the other hand, progression through S phase is also impaired in *asf1* mutants because the loss of *ASF1* activates the DNA damage checkpoint, causing cells to accumulate at G2/M-phase. Spontaneous DNA damage resulting from impaired replication correlates with an elevated rate of Ddc2-damage foci formation. This in turn leads to a higher rate of genomic instability than would normally occur. This harmful situation can be further aggravated by either compromising the checkpoint by a *rad53* mutant by impairing recombination (i. e. *rad52* deletion) or by changing the epigenetic chromatin environment. This was achieved with the *h2a*^{S129*} double mutant, as discussed below (Ramey et al., 2004). Similar observations were made in another study, which showed that *asf1* mutant yeast cells have a delayed S phase progression and increased Ddc2 foci formation (Kats et al., 2006). There is also an increased Rad53 phosphorylation in *asf1* mutant cells. The authors argue that normal S phase progression in *asf1* mutant cells requires replication checkpoint proteins and that defects in Asf1 lead to unstable replication forks, which then are stabilized by checkpoint proteins to avoid fork collapse. Furthermore *asf1* mutant cells are sensitive to MMS and show a slow growth phenotype on HU.

A recent report of Franco and coauthors lends further insight into the molecular role of Asf1. The authors show that the replication defect of *asf1* mutant cells is strongly aggravated by a cold sensitive *rfc1*-1 mutation, leading to incomplete replication and growth defects. This effect is due to a specific interaction with Asf1 since mutants of Caf1 and Hir-complex proteins did not show these phenotypes. This suggests a direct role for Asf1 at the replisome, and indeed Asf1 is required for replication in the presence of a low dose of MMS. Finally it was also shown that by HU stalled replication forks are unstable in *asf1* mutant cells (Franco et al., 2005). Although Asf1 binds directly to the RFC complex, the amount of RFC, PCNA and Polε decreases in *asf1* mutants. In contrast, Polα is enriched at stalled replication forks in the same alleles. The authors suggest that Asf1 maintains the elongation machinery at stalled replication forks. In mutants that uncouple MCM helicase from the replisome or deregulate the polymerase switch, Polα levels increase. Thus, Franco et al. show nicely that besides its functions for histone deposition and regulation of histone gene

transcription, Asf1 affects genomic stability also in a more direct manner, by acting at the replisome itself.

The findings in yeast cells are likely to be valid in higher eukaryotes as well, since yeast *asf1* mutants can be complemented by homologues of higher eukaryotes. Depletion of *ASF1* function in higher organisms is even more deleterious than in yeast. Specifically, RNAi mediated knockdown of *Drosophila ASF1* leads to accumulation of cells with replication foci and causes a defect in DNA replication monitored as reduced BrdU incorporation. Consistently, dASF1 colocalizes with MCM2-7 by immunofluorescence throughout S phase (Schulz and Tyler, 2006). Asf1 depletion in chicken DT40 cells resulted in accumulation of cells in S phase with decreased DNA replication and finally leading to cell death (Sanematsu et al., 2006) These authors also report impaired nucleosome assembly and increased nuclease sensitivity. In addition to the functions discussed above, a recent report links Asf1 to histone H3 acetylation at lysine 56 (Recht et al., 2006).

1.5.6 A role of histone modifications at stalled and collapsed replication forks?

Specific histone modifications are important for the cellular response to DNA damage (Downs et al., 2007; van Attikum and Gasser, 2005). Here I will focus on those modifications with a potential role in the response to stalled or damaged replication fork structures.

The occurrence of histone H3 acetylation at lysine 56 was discovered at the same time by three different groups (Masumoto et al., 2005; Ozdemir et al., 2005; Xu et al., 2005) and its *in vivo* presence was confirmed soon thereafter by mass spectrometry (Hyland et al., 2005). Xu and coworkers discovered that K56 acetylation impairs the contact of DNA with the globular domain of H3. Its presence is important for recruitment of the SWI/SNF remodeling complex and for histone gene transcription. Masumoto et al. and Ozdemir et al. then showed that mutant strains lacking the acetylation of K56 are very sensitive to HU, UV irradiation, as well as DNA breaks induced by CPT and Bleomycin. Whereas Ozdemir and coworkers observed equal abundance of this modification throughout the cell cycle (Ozdemir et al. 2005), Masumoto and coauthors showed that H3K56 acetylation is most abundant on newly synthesized H3 and that modified H3 was incorporated into chromatin during replication (Masumoto et al., 2005; Ozdemir et al., 2005). This was later confirmed by

two independent studies (Driscoll et al., 2007; Maas et al., 2006): K56 acetylation occurs only during S phase and disappears in G2. The modification was shown to occur adjacent to replication coupled DSBs, and to be abundant in chromatin immunoprecipitations for topoisomerase I, when bound to broken DNA ends. Though the acetylation normally disappeared in G2, in cells with DNA breaks the modification is maintained in a manner dependent on DNA damage signaling by Rad9 (Masumoto et al., 2005). Finally it was show that the acetylation of H3-K56 is important for histone DNA interactions. Nucleosomes bearing the H3 K56Q mutation were hypersensitive to micrococcal nuclease digestion, because the plasmid supercoiling was decreased. This argues that acetylation opens up chromatin by weakening histone DNA interactions. The open chromatin environment seems to be beneficial for the repair of replication coupled DSBs (Masumoto et al., 2005).

Using a genetic approach Recht et al. showed that mutants for H3-K56 acetylation have similar DNA damage phenotypes as *asf1,* and that *asf1* and K56 ^{ac} mutants act in the same genetic pathway. Acetylation of H3-K56 is lost in *asf1* mutants, but not in cells lacking the CAF1 or HIR complexes. Moreover the loss of K56 acetylation correlates with the DNA damage sensitivity of *asf1* alleles. The site of interaction between Asf1 and the C-terminus of H3 was correlated with damage sensitive *asf1* mutations, whereas the sites of interaction between Asf1 and Hir proteins were not. Finally, the *asf1* mutants that showed intermediate levels of K56 acetylation also showed intermediate sensitivity to DNA damaging drugs, while mutants that abolished K56 acetylation were highly sensitive to DNA damage. This correlation led the authors to conclude that Asf1 acts primarily through H3-K56^{ac} to maintain genomic stability (Recht et al., 2006). If this were true the acetylation mimicking H3-K56Q mutation should complement an *asf1* mutant phenotype. Indeed, HU sensitivity and the slow growth phenotype of *asf1* mutant cells was substantially suppressed in this mutant, yet H3-K56Q cells still were slightly hypersensitivity to HU. This suggested that deacetylation might also be important for genomic stability (Recht et al., 2006). The deacetylases that remove H3-K56^{ac} are two Sir2 homologues, Hst3 and Hst4. They act in the G2 phase of the cell cycle. Both, the deacetylation of H3-K56 during normal unchallenged cell-cycle progression, as well as downregulation of the deacetylase in response to checkpoint activation to maintain H3-K56 acetylation, are important for genome stability (Celic et al., 2006; Maas et al., 2006).

The acetyltransferase responsible for H3-K56 modification was identified as Rtt109 this year (Collins et al., 2007; Driscoll et al., 2007; Han et al., 2007a). *rtt109* mutants lose H3-K56 acetylation and show increased sensitivity to the genotoxic drugs creating DNA damage in S phase: HU, MMS, CPT and Phleomycin. Furthermore they show an S-phase specific increase in spontaneous chromosome breaks as monitored by Rad52 foci formation (Driscoll et al., 2007; Han et al., 2007a). Driscoll et al. furthermore showed that *RTT109* deletion suppresses the temperature sensitive growth defect of *hst3 hst4* mutant strains. By assaying the superhelical density of a 2μ plasmid they found increased supercoiling in the *rtt109* mutant, like that found in the *asf1* mutants. They propose that Asf1 stimulates the *in vitro* acetyltransferase activity of Rtt109 for histone H3-K56 acetylation. This suggests that these proteins may act together in one pathway to regulate chromatin structure and genomic stability (Driscoll et al., 2007). This was confirmed by a genetic interaction map that places H3-K56 acetylation in one epistasis group with *RTT101, MMS1, MMS22, RTT109* and *ASF1*. The first three genes *(RTT101, MMS1, MMS2)* are members of a ubiquitin ligase complex and deletion of these genes suppresses the growth defect induced by hyperacetylation of H3-K56. This suggests that the ubiquitin-ligase complex involving *RTT101* acts downstream of H3-K56 acetylation (Collins et al., 2007). The authors suggest, based on genetic interaction data, that the Rtt101 ubiquitin ligase complex-mediated ubiquitylation may target components of the replication checkpoint (Mrc1, Tof1, Csm3) as well as cohesion factors (Dcc1, Ctf4, Ctf8, Ctf18) for degradation through the proteasome to promote replication fork progression (Collins et al., 2007). In the meanwhile it was shown that H3-K56 acetylation was stimulated when Rtt109 forms an active complex with either Asf1 or another histone chaperone Vps75. Only the Rtt109/Asf1 complex was found to be important for resistance to genotoxic stress (Tsubota et al., 2007). The binding of histones H3 and H4 to Asf1 is required for efficient acetylation of H3-K56 (Adkins et al., 2007), and recently also the structure of Asf1 bound to H3 was solved. Intriguingly, point mutations in H3 that perturb the histone/Asf1 interface decrease levels of H3-K56 *in vivo* and show a corresponding phenotypic defect (Agez et al., 2007).

Importantly H3-K56 acetylation seems to be crucial for the maintenance of replication fork stability, since replication fork association of three replisome components Polε, PCNA and Rfc3 at two early firing origins *ARS607* and *ARS305* was reduced to background levels by Chromatin Immunoprecipitation after release of *rtt109 or*

H3K56R mutant cells into HU (Han et al., 2007b). Therefore H3-K56 acetylation may also explain many of the replication functions associated with Asf1. It is the first example of a histone modification that affects genomic maintenance during an unperturbed S phase, as well as in response to fork associated DNA damage.

Interestingly, this modification behaves differently than other modifications. The most well known marker of DNA breaks is γH2AX (in yeast γH2A), namely phosphorylation of $H2A^{S129}$ (Fillingham et al., 2006; Foster and Downs, 2005; Lowndes and Toh, 2005). This phosphorylation occurs in the absence of Rad9 and is maintained in this mutant for longer times than the acetylation of H3K56, indicating the persistence of DNA breaks. Yet a report from Redon and coworkers showed that $H2A^{S129}$ phosphorylation acts in a parallel pathway to *RAD9* (Redon et al., 2003), and a recent report of the same laboratory suggests that it might work in the same pathway as Tof1 to overcome replication coupled DNA damage induced by CPT (Redon et al., 2006).

In human cells the induction of DNA damage during S-phase by UV, MMS and other drugs, leads to phosphorylation of H2AX and formation of γH2AX foci. These foci are thought to be associated with DSBs created by replication fork movement through a lesion. γH2AX foci are also formed by HU treatment, which leads to stalled replication forks, but also creates DSBs at a fraction of these replication forks; therefore these foci are widely also seen as DSB associated H2AX phosphorylation (Takahashi and Ohnishi, 2005). Nonetheless, γH2AX does not associate exclusively with DSBs, since phosphorylation of H2AX at DSBs depends mainly on ATM kinase, and H2AX in response to replicational stress created by HU-treatment is modified in an ATR-dependent manner (Ward and Chen, 2001). There is clear molecular evidence that the mechanism of γH2A phosphorylation in response to HU might be different from that at DSBs (Cobb et al., 2005). In budding yeast $H2A^{S129}$ phosphorylation at DSBs depends on both Tel1 and Mec1 (van Attikum and Gasser, 2005), whereas at HU-stalled replication forks it depends on Mec1 alone. This result confirmes earlier studies in human cells. It is likely that the enrichment of H2A phosphorylation at early firing origins after HU treatment is not only associated with DSBs, but with stalled fork damage itself. Whereas H2A phosphorylation occurs over 50 kb surrounding a DSB, it is exclusively fork-associated after HU treatment. Mec1 and not Tel1 is associated with the replication fork providing a means to modify H2A (Cobb et al., 2005). This study did not provide evidence for a functional role for H2A

phosphorylation in replication fork maintenance, although it will be very interesting if such a role can be uncovered. Initial evidence comes from Redon et al. (Redon et al., 2006), who showed that Tof1 and Csm3 function in the same pathway and downstream of γH2A, yet both acted in parallel to pathways involving Mrc1 or Rad9 activation in response to topoisomerase I/CPT induced DNA damage.

Under normal replication conditions both topoisomerase I and II are essential to counteract tortional stress generated by helicase mediated DNA unwinding as well as sister chromatid entanglement, and the absence of both proteins leads to Rad53 activation (Bermejo et al., 2007). In contrast to damage induced by absence of topoisomerase I, damage created by hitting a topoisomerase-cleavage complex seems to be checkpoint blind (Redon et al., 2003). Endogenous DNA damage during replication of the rDNA repeats is also checkpoint blind, since cells progress without arrest at the G2/M boundary into mitosis (Torres-Rosell et al., 2007). Delayed rDNA replication occurs in *smc5* or *smc6* mutants (which form a complex related to Cohesin) and Smc5 and Smc6 were shown to be recruited to DSBs as well as to collapsed replication forks (Lindroos et al., 2006; Torres-Rosell et al., 2005). The CPT-sensitivity of $h2a^{S129*}$ mutant cells (Redon et al., 2003), as well as the phosphorylation of H2A (γH2A) at stalled replication forks (Cobb et al., 2005) and the occurence of γH2A in rDNA repeats during S phase (Schleker et al. unpublished, see Chapter 4), together with the genetic linkage of Tof1/Csm3 to sister chromatid cohesion (Redon et al., 2006), argues that γH2A may have an important role in mediating sister chromatid cohesion at stalled replication forks. Indeed γH2A is required for cohesin loading at DSBs (Strom and Sjogren, 2005). γH2A should therefore be particularly important in situations that induce fork collapse and break induced replication (Kraus et al., 2001).

Besides histone H3 acetylation mediated by GCN5 also acetylation of histone H4 (dependent on the NuA4 complex) was shown to be important during replication. Choy and Kron could show that the viable *yng2* mutation leads to enhanced sensitivity to DNA damage created in S phase by using HU, CPT or MMS or by compromising replication by using *cdc8* or *cdc9* mutations (Choy and Kron, 2002). This DNA damage created persistence of the intra-S-phase checkpoint by affecting the efficiency of DNA repair. Further the synthetic lethality between *gcn5* and *yng2* mutations points on partially overlapping and important roles for histone H3 and H4 acetylation during DNA replication.

Besides acetylation, other histone modifications have been linked to the DNA damage response in S phase. Notably, ubiquitylation of histone H2B on lysine 123 by Rad6 is required for Rad53 activation in response to UV and MMS, as well as for the corresponding cell cycle arrest mediated by the G1 and the G1/S checkpoint pathways (Giannattasio et al., 2005). The authors show that this function is specific for the E2 ubiquitin conjugating enzyme Rad6 and does not involve Rad5 or the E3 ubiquitin ligase Rad18, but requires the E3 enzyme Bre1. Rad6/Bre1 acts also by inducing a further posttranslational modification, namely methylation of lysine 79 on histone H3, which is mediated by Dot1. The authors herewith could extend a previous finding by (Ng et al., 2002) showing that the ubiquitination of H2B by Rad6 is required for methylation of H3-K79 by Dot1 on a function for checkpoint activation in S phase. The authors finally showed that if additionally H3-K4 methylation by Set1 is compromised, the corresponding double mutant strain shows a further aggravated defect in the G1/S checkpoint induced by UV treatment (Giannattasio et al., 2005).
Giannattasio and colleagues have explored further modifications: the methylation of H3K79, which is also important for the activation of the effector kinase Rad53. Both, Bre1 and Dot1 seem not to be required for Mec1 activation, since both Ddc1 (9-1-1 complex) and Ddc2 (regulatory subunit of Mec1–kinase) are phosphorylated as in wildtype cells (Giannattasio et al., 2005). This suggests that both modifications do not affect DNA damage signal perception per se. But phosphorylation of Rad9 is strongly reduced. Wysocki et al. (MCB, 2005) enriched these findings by showing that *dot1* mutant cells are deficient for Rad9 phosphorylation and Rad53 activation by γ-irradiation in cells arrested in G1 but not in G2/M. They also showed by chromatin immunoprecipitation that the recruitment of Rad9 to DSBs in G1 and also in G2 is dependent on Dot1. This argues that even the classical DNA damage checkpoint pathway monitoring DSBs is differently regulated during the cell cycle and that this regulation depends to some degree on chromatin modifications. Additionally the authors provided novel insight into the molecular mechanisms of action of these chromatin modifications, since they could complement the requirement for Dot1 in the intra-S phase checkpoint, by transforming with a Ddc2-Rad53 fusion protein. This allowed them to overcome the need for Rad9 as an adaptor in checkpoint signaling, thus suggesting a role for the structural connection between H3-K79 methylation and Rad9. It was furthermore shown that the human protein 53BP1, a Rad9 homologue, binds histone H3 methylated on Lys 79, and that the corresponding conserved

residues in a domain called Tudor domain were also required for recruitment of 53BP1 to DSBs (Huyen et al., 2004). Wysocki et al. next mutated a conserved residue in the binding pocket of Rad9, and obtained phenotypes resembling the defect of a *dot1* mutant strain in G1- and intra-S-phase checkpoint. However they did not affect G2 checkpoint signaling (Wysocki et al., 2005). This argues that the docking of Rad9 onto chromatin does depend on this conserved Tudor domain (Grenon et al., 2007). But does H3-K79 methylation primarily affect the DSB-associated checkpoint function? Analysis of epistasis of the *dot1* mutation with *rad9* in backgrounds that impair several repair pathways suggested that Dot1 and H3 K76 methylation function in base excision repair, homologous recombination and error-free lesion bypass (Bostelman et al., 2007).

These novel reports implicating histone modifications in S phase checkpoint signaling suggest that different modifications are important for maintaining genomic stability during replication. They may define an epigenetic code analogous or partially homologous to that postulated previously for transcription (Jenuwein and Allis, 2001). The epigenetic damage marks may be differently required and have a different read-out regarding genomic stability for the same damage in different cell cycle stages or for different kinds of lesions. Potential links might be made between differential functional clusters, as checkpoint activation, fork stability and postreplicative repair.

1.5.7 A perspective: Chromatin remodeling and maintenance of replication fork structure

Chromatin remodeling complexes of the Swi/Snf family e.g. SWR1 and INO80 have been shown to be important for the repair of DSBs (Bao and Shen, 2007). It was recently shown that the INO80 chromatin remodeling complex localizes to DSBs and is important for repair, and that this localization depends upon phosphorylation of $H2A^{S129}$ (van Attikum and Gasser, 2005), which as described in the previous section was also shown to be localized at stalled replication forks.

It is tempting to speculate that the INO80 complex is also recruited to stalled replication forks, even more because mutants of the INO80 complex have been shown to be very sensitive to HU (Shen et al., 2000; van Attikum et al., 2004). Other data points to a more direct role for chromatin remodelers of the SWI/SNF family - e. g. INO80 and SWR1 chromatin remodeling complexes- in DNA replication (Falbo and

Shen, 2006) It will be interesting to understand to which extent chromatin remodeling is required for origin firing and progression of unperturbed replication or for replication in the presence of damage.

The remodeler SWR1 is also clearly linked to DNA replication and maintenance of replication fork structure. SWR1 was shown to be required for deposition of the histone H2A variant Htz1 into chromatin and a recent report now showed that *htz1* mutants were delayed for DNA replication and cell cycle progression (Dhillon et al., 2006). Furthermore in the same study a *htz1* mutation showed genetic interactions with replication genes like *orc2*-1 and required the replication checkpoint (shown by genetic interactions with *mrc1*-1, *rad53*-1 and *pol2*-11) for survival. This suggests a potential role of chromatin remodeling in the maintenance of proper replication fork structure, similar to that discussed earlier for chromatin assembly by Asf1.

Further support for a functional link between replication and chromatin maintenance pathways was provided by (Pan et al., 2006). This study analysed the DNA integrity network of budding yeast by functionally clustering single genes into modules based upon their synthetic fitness or lethality defects. Based upon 4956 interactions with 74 query genes in total interactions between 875 genes were found. The authors could define multi-component modules contributing to DNA integrity in yeast. These are DNA replication, oxidative stress response, DNA repair, checkpoint signaling and chromatin structure maintenance. More specifically, genetic interactions between DNA replication genes, *DIA2*, *POL32* and *RAD27*, the absence of which creates endogenous DNA damage, and three functional clusters contributing to chromatin structure maintenance, were found. These defined the functions of chromatin assembly (represented by *CAF1*, the HIR module and *ASF1*), a module linked to histone acetylation (with *YAF9*, *EAF3*, *EAF5* and *VID21*), and chromatin remodeling with components such as the INO80 and SWR1 complexes, and the histone H2A variant *HTZ1*. This study provided genome-wide evidence linking replication, chromatin assembly, histone modification, and remodeling to the maintenance of genetic stability. Hopefully the molecular mechanisms through which chromatin remodeling contributes to this will be uncovered soon.

The Ies4 subunit of the INO80 complex was recently shown to be a direct target for Mec1/Tel1 phosphorylation in response to DNA damage. The Mec1-induced phosphorylation of Ise4 was shown through a phosphomimicking mutant to increase the phosphorylation state of Rad53. Consistently, cell cycle arrest in response to

MMS was enhanced and cells were hypersensitive to MMS and HU. The phospho-deficient mutant instead shows sensitivity to DNA damage in the absence of Tof1, leading to a very pronounced defect on viability in the double mutant. γH2A levels and its interaction with INO80 were however not changed (Morrison et al., 2007). This genetic interaction with Tof1 supports the idea that the INO80 complex fulfills a critical function during checkpoint activation and repair in S phase. Morrison and coworkers propose that Mec1 and Tel1 regulates INO80 via two pathways. According to this model, Mec1/Tel1 mediated phosphorylation of H2A would recruit the INO80 complex to pursue mainly a function in DNA repair, whereas phosphorylation of the Ies4 subunit would lead to checkpoint modulation in concert with Tof1 (Morrison et al., 2007). It would be important to determine in future studies, if the INO80 complex also helps maintain replication fork stability at stalled replication forks or natural pausing sites, as Tof1 does. A first indication that INO80 indeed might act at the replication fork, comes from results showing that *arp8* mutants (a subunit of the INO80 complex) have a defective in sister chromatid cohesion and are very sensitive to benomyl (Ogiwara et al., 2007). The authors further argue that the INO80 complex might be involved in establishment of sister chromatid cohesion together with PCNA and Ctf18. Future studies are expected to link remodeler-mediated chromatin dynamics with the stabilisation of replication forks in response to genotoxic lesions or to pause sites in an unperturbed S phase.

1.6 Aim of this thesis

Protein phosphorylation as a post-translational modification has a dominant role as a molecular signal for regulating cell-cycle transitions as well as for activating the DNA-damage checkpoint signaling pathway. This checkpoint pathway depends crucially upon the activity of kinases.

The aim of this thesis is to contribute to our knowledge of the role of phosphorylation for DNA-damage signaling by analyzing two specific phosphorylation events, one found in the DNA-damage sensing part of the signaling cascade, the other targeting a downstream effector of the checkpoint signaling cascade.

Upstream components of the checkpoint pathway, the sensor kinases Mec1 and Tel1, have a prime function in initiating the checkpoint signaling cascade by directly activating the checkpoint effector kinase Rad53, which then phosphorylates target proteins. These in turn mediate cell-cycle arrest and induce repair genes. At the source of the signaling cascade, checkpoint responses differ in a cell-cycle dependent manner, such that a higher threshold for damage is needed to activate Rad53 in S phase. The aim of the work reported here is to examine whether Rad53 itself is regulated directly by phosphorylation in a cell-cycle dependent manner and to analyze its effect upon Rad53 checkpoint activity.

Cellular responses to DNA damage differ not only during the cell cycle, but also in respect of the corresponding lesion. Mec1 and Tel1 do not only activate Rad53, but also influence repair and recovery processes at the site of DNA damage. One key function of these kinases is the phosphorylation of the core histone H2A at serine 129 (γH2A), a step that is important for the repair of DNA double strand breaks (DSBs).

A second aim of this thesis is to understand whether Mec1 and Tel1 also induce γH2A at other sites of DNA damage, for example stalled replication forks, which are known to be structurally and functionally distinct from DSBs. In mammalian cells γH2A occurs at senescent telomeres. Yeast telomeres do not senesce spontaneously, yet γH2A might occur at the lesion-like DNA structures at natural chromosome ends. The final aim of this work is to characterize and determine the presence and function of γH2A at these non-DSB sites.

1.7 References

Aboussekhra, A., M. Biggerstaff, M.K. Shivji, J.A. Vilpo, V. Moncollin, V.N. Podust, M. Protic, U. Hubscher, J.M. Egly, and R.D. Wood. 1995. Mammalian DNA nucleotide excision repair reconstituted with purified protein components. *Cell*. 80:859-68.

Adkins, M.W., J.J. Carson, C.M. English, C.J. Ramey, and J.K. Tyler. 2007. The histone chaperone anti-silencing function 1 stimulates the acetylation of newly synthesized histone H3 in S-phase. *J Biol Chem*. 282:1334-40.

Agez, M., J. Chen, R. Guerois, C. van Heijenoort, J.Y. Thuret, C. Mann, and F. Ochsenbein. 2007. Structure of the histone chaperone ASF1 bound to the histone H3 C-terminal helix and functional insights. *Structure*. 15:191-9.

Ahn, J., M. Urist, and C. Prives. 2004. The Chk2 protein kinase. *DNA Repair (Amst)*. 3:1039-47.

Alcasabas, A.A., A.J. Osborn, J. Bachant, F. Hu, P.J. Werler, K. Bousset, K. Furuya, J.F. Diffley, A.M. Carr, and S.J. Elledge. 2001. Mrc1 transduces signals of DNA replication stress to activate Rad53. *Nat Cell Biol*. 3:958-65.

Ampatzidou, E., A. Irmisch, M.J. O'Connell, and J.M. Murray. 2006. Smc5/6 is required for repair at collapsed replication forks. *Mol Cell Biol*. 26:9387-401.

Bao, Y., and X. Shen. 2007. INO80 subfamily of chromatin remodeling complexes. *Mutat Res*. 618:18-29.

Barbour, L., L.G. Ball, K. Zhang, and W. Xiao. 2006. DNA damage checkpoints are involved in postreplication repair. *Genetics*. 174:1789-800.

Barbour, L., and W. Xiao. 2003. Regulation of alternative replication bypass pathways at stalled replication forks and its effects on genome stability: a yeast model. *Mutat Res*. 532:137-55.

Bermejo, R., Y. Doksani, T. Capra, Y.M. Katou, H. Tanaka, K. Shirahige, and M. Foiani. 2007. Top1- and Top2-mediated topological transitions at replication forks ensure fork progression and stability and prevent DNA damage checkpoint activation. *Genes Dev*. 21:1921-36.

Bjergbaek, L., J.A. Cobb, M. Tsai-Pflugfelder, and S.M. Gasser. 2005. Mechanistically distinct roles for Sgs1p in checkpoint activation and replication fork maintenance. *Embo J*. 24:405-17.

Blackburn, E.H. 2001. Switching and signaling at the telomere. *Cell*. 106:661-73.

Bloom, J., and F.R. Cross. 2007. Multiple levels of cyclin specificity in cell-cycle control. *Nat Rev Mol Cell Biol*. 8:149-60.

Bostelman, L.J., A.M. Keller, A.M. Albrecht, A. Arat, and J.S. Thompson. 2007. Methylation of histone H3 lysine-79 by Dot1p plays multiple roles in the response to UV damage in Saccharomyces cerevisiae. *DNA Repair (Amst)*. 6:383-95.

Branzei, D., J. Sollier, G. Liberi, X. Zhao, D. Maeda, M. Seki, T. Enomoto, K. Ohta, and M. Foiani. 2006. Ubc9- and mms21-mediated sumoylation counteracts recombinogenic events at damaged replication forks. *Cell*. 127:509-22.

Brown, J.A., G. Sherlock, C.L. Myers, N.M. Burrows, C. Deng, H.I. Wu, K.E. McCann, O.G. Troyanskaya, and J.M. Brown. 2006. Global analysis of gene function in yeast by quantitative phenotypic profiling. *Mol Syst Biol*. 2:2006 0001.

Bystricky, K., T. Laroche, G. van Houwe, M. Blaszczyk, and S.M. Gasser. 2005. Chromosome looping in yeast: telomere pairing and coordinated movement reflect anchoring efficiency and territorial organization. *J Cell Biol*. 168:375-87.

Byun, T.S., M. Pacek, M.C. Yee, J.C. Walter, and K.A. Cimprich. 2005. Functional uncoupling of MCM helicase and DNA polymerase activities activates the ATR-dependent checkpoint. *Genes Dev*. 19:1040-52.

Calzada, A., B. Hodgson, M. Kanemaki, A. Bueno, and K. Labib. 2005. Molecular anatomy and regulation of a stable replisome at a paused eukaryotic DNA replication fork. *Genes Dev*. 19:1905-19.

Carr, A.M. 1997. Control of cell cycle arrest by the Mec1sc/Rad3sp DNA structure checkpoint pathway. *Curr Opin Genet Dev*. 7:93-8.

Celic, I., H. Masumoto, W.P. Griffith, P. Meluh, R.J. Cotter, J.D. Boeke, and A. Verreault. 2006. The sirtuins hst3 and Hst4p preserve genome integrity by controlling histone h3 lysine 56 deacetylation. *Curr Biol*. 16:1280-9.

Chang, D.J., P.J. Lupardus, and K.A. Cimprich. 2006. Monoubiquitination of proliferating cell nuclear antigen induced by stalled replication requires uncoupling of DNA polymerase and mini-chromosome maintenance helicase activities. *J Biol Chem*. 281:32081-8.

Choy, J.S., and S.J. Kron. 2002. NuA4 subunit Yng2 function in intra-S-phase DNA damage response. *Mol Cell Biol*. 22:8215-25.

Clerici, M., V. Baldo, D. Mantiero, F. Lottersberger, G. Lucchini, and M.P. Longhese. 2004. A Tel1/MRX-dependent checkpoint inhibits the metaphase-to-anaphase transition after UV irradiation in the absence of Mec1. *Mol Cell Biol*. 24:10126-44.

Cobb, J.A., L. Bjergbaek, K. Shimada, C. Frei, and S.M. Gasser. 2003. DNA polymerase stabilization at stalled replication forks requires Mec1 and the RecQ helicase Sgs1. *Embo J*. 22:4325-36.

Cobb, J.A., T. Schleker, V. Rojas, L. Bjergbaek, J.A. Tercero, and S.M. Gasser. 2005. Replisome instability, fork collapse, and gross chromosomal rearrangements arise synergistically from Mec1 kinase and RecQ helicase mutations. *Genes Dev*. 19:3055-69.

Cockell, M., F. Palladino, T. Laroche, G. Kyrion, C. Liu, A.J. Lustig, and S.M. Gasser. 1995. The carboxy termini of Sir4 and Rap1 affect Sir3 localization: evidence for a multicomponent complex required for yeast telomeric silencing. *J Cell Biol*. 129:909-24.

Collins, S.R., K.M. Miller, N.L. Maas, A. Roguev, J. Fillingham, C.S. Chu, M. Schuldiner, M. Gebbia, J. Recht, M. Shales, H. Ding, H. Xu, J. Han, K. Ingvarsdottir, B. Cheng, B. Andrews, C. Boone, S.L. Berger, P. Hieter, Z. Zhang, G.W. Brown, C.J. Ingles, A. Emili, C.D. Allis, D.P. Toczyski, J.S. Weissman, J.F. Greenblatt, and N.J. Krogan. 2007. Functional dissection of protein complexes involved in yeast chromosome biology using a genetic interaction map. *Nature*. 446:806-10.

Dalgaard, J.Z., and A.J. Klar. 2000. swi1 and swi3 perform imprinting, pausing, and termination of DNA replication in S. pombe. *Cell*. 102:745-51.

Deshaies, R.J. 1997. Phosphorylation and proteolysis: partners in the regulation of cell division in budding yeast. *Curr Opin Genet Dev*. 7:7-16.

Dhillon, N., M. Oki, S.J. Szyjka, O.M. Aparicio, and R.T. Kamakaka. 2006. H2A.Z functions to regulate progression through the cell cycle. *Mol Cell Biol*. 26:489-501.

Dionne, I., and R.J. Wellinger. 1996. Cell cycle-regulated generation of single-stranded G-rich DNA in the absence of telomerase. *Proc Natl Acad Sci U S A*. 93:13902-7.

Downs, J.A., M.C. Nussenzweig, and A. Nussenzweig. 2007. Chromatin dynamics and the preservation of genetic information. *Nature*. 447:951-8.

Driscoll, R., A. Hudson, and S.P. Jackson. 2007. Yeast Rtt109 promotes genome stability by acetylating histone H3 on lysine 56. *Science*. 315:649-52.

Dubrana, K., S. Perrod, and S.M. Gasser. 2001. Turning telomeres off and on. *Curr Opin Cell Biol*. 13:281-9.

Dudas, A., and M. Chovanec. 2004. DNA double-strand break repair by homologous recombination. *Mutat Res*. 566:131-67.

Elledge, S.J. 1996. Cell cycle checkpoints: preventing an identity crisis. *Science*. 274:1664-72.

Elledge, S.J., Z. Zhou, J.B. Allen, and T.A. Navas. 1993. DNA damage and cell cycle regulation of ribonucleotide reductase. *Bioessays*. 15:333-9.

Emili, A. 1998. MEC1-dependent phosphorylation of Rad9p in response to DNA damage. *Mol Cell*. 2:183-9.

Emili, A., D.M. Schieltz, J.R. Yates, 3rd, and L.H. Hartwell. 2001. Dynamic interaction of DNA damage checkpoint protein Rad53 with chromatin assembly factor Asf1. *Mol Cell*. 7:13-20.

Enserink, J.M., M.B. Smolka, H. Zhou, and R.D. Kolodner. 2006. Checkpoint proteins control morphogenetic events during DNA replication stress in Saccharomyces cerevisiae. *J Cell Biol*. 175:729-41.

Evans, S.K., and V. Lundblad. 1999. Est1 and Cdc13 as comediators of telomerase access. *Science*. 286:117-20.

Falbo, K.B., and X. Shen. 2006. Chromatin remodeling in DNA replication. *J Cell Biochem*. 97:684-9.

Fillingham, J., M.C. Keogh, and N.J. Krogan. 2006. GammaH2AX and its role in DNA double-strand break repair. *Biochem Cell Biol*. 84:568-77.

Fleck, O., and P. Schar. 2004. Translesion DNA synthesis: little fingers teach tolerance. *Curr Biol*. 14:R389-91.

Foster, E.R., and J.A. Downs. 2005. Histone H2A phosphorylation in DNA double-strand break repair. *Febs J*. 272:3231-40.

Franco, A.A., W.M. Lam, P.M. Burgers, and P.D. Kaufman. 2005. Histone deposition protein Asf1 maintains DNA replisome integrity and interacts with replication factor C. *Genes Dev*. 19:1365-75.

Frei, C., and S.M. Gasser. 2000. The yeast Sgs1p helicase acts upstream of Rad53p in the DNA replication checkpoint and colocalizes with Rad53p in S-phase-specific foci. *Genes Dev*. 14:81-96.

Gambus, A., R.C. Jones, A. Sanchez-Diaz, M. Kanemaki, F. van Deursen, R.D. Edmondson, and K. Labib. 2006. GINS maintains association of Cdc45 with MCM in replisome progression complexes at eukaryotic DNA replication forks. *Nat Cell Biol*. 8:358-66.

Gasser, S.M. 2000. A sense of the end. *Science*. 288:1377-9.

Gasser, S.M., and M.M. Cockell. 2001. The molecular biology of the SIR proteins. *Gene*. 279:1-16.

Giannattasio, M., F. Lazzaro, P. Plevani, and M. Muzi-Falconi. 2005. The DNA damage checkpoint response requires histone H2B ubiquitination by Rad6-Bre1 and H3 methylation by Dot1. *J Biol Chem*.

Gilbert, C.S., C.M. Green, and N.F. Lowndes. 2001. Budding yeast Rad9 is an ATP-dependent Rad53 activating machine. *Mol Cell*. 8:129-36.

Green, E.M., A.J. Antczak, A.O. Bailey, A.A. Franco, K.J. Wu, J.R. Yates, 3rd, and P.D. Kaufman. 2005. Replication-independent histone deposition by the HIR complex and Asf1. *Curr Biol*. 15:2044-9.

Grenon, M., T. Costelloe, S. Jimeno, A. O'Shaughnessy, J. Fitzgerald, O. Zgheib, L. Degerth, and N.F. Lowndes. 2007. Docking onto chromatin via the Saccharomyces cerevisiae Rad9 Tudor domain. *Yeast*. 24:105-19.

Gunjan, A., J. Paik, and A. Verreault. 2005. Regulation of histone synthesis and nucleosome assembly. *Biochimie*. 87:625-35.

Gunjan, A., and A. Verreault. 2003. A Rad53 kinase-dependent surveillance mechanism that regulates histone protein levels in S. cerevisiae. *Cell*. 115:537-49.

Han, J., H. Zhou, B. Horazdovsky, K. Zhang, R.M. Xu, and Z. Zhang. 2007a. Rtt109 acetylates histone H3 lysine 56 and functions in DNA replication. *Science*. 315:653-5.

Han, J., H. Zhou, Z. Li, R.M. Xu, and Z. Zhang. 2007b. Acetylation of lysine 56 of histone H3 catalyzed by Rtt109 and regulated by Asf1 is required for replisome integrity. *J Biol Chem*.

Harrison, J.C., and J.E. Haber. 2006. Surviving the breakup: the DNA damage checkpoint. *Annu Rev Genet*. 40:209-35.

Hartwell, L.H., J. Culotti, J.R. Pringle, and B.J. Reid. 1974. Genetic control of the cell division cycle in yeast. *Science*. 183:46-51.

Hartwell, L.H., J. Culotti, and B. Reid. 1970. Genetic control of the cell-division cycle in yeast. I. Detection of mutants. *Proc Natl Acad Sci U S A*. 66:352-9.

Hartwell, L.H., and T.A. Weinert. 1989. Checkpoints: controls that ensure the order of cell cycle events. *Science*. 246:629-34.

He, Z., L.A. Henricksen, M.S. Wold, and C.J. Ingles. 1995. RPA involvement in the damage-recognition and incision steps of nucleotide excision repair. *Nature*. 374:566-9.

Henikoff, S., and K. Ahmad. 2005. Assembly of variant histones into chromatin. *Annu Rev Cell Dev Biol*. 21:133-53.

Herzberg, K., V.I. Bashkirov, M. Rolfsmeier, E. Haghnazari, W.H. McDonald, S. Anderson, E.V. Bashkirova, J.R. Yates, 3rd, and W.D. Heyer. 2006. Phosphorylation of Rad55 on serines 2, 8, and 14 is required for efficient homologous recombination in the recovery of stalled replication forks. *Mol Cell Biol*. 26:8396-409.

Hodgson, B., A. Calzada, and K. Labib. 2007. Mrc1 and Tof1 Regulate DNA Replication Forks in Different Ways during Normal S Phase. *Mol Biol Cell*.

Hoege, C., B. Pfander, G.L. Moldovan, G. Pyrowolakis, and S. Jentsch. 2002. RAD6-dependent DNA repair is linked to modification of PCNA by ubiquitin and SUMO. *Nature*. 419:135-41.

Hu, F., A.A. Alcasabas, and S.J. Elledge. 2001. Asf1 links Rad53 to control of chromatin assembly. *Genes Dev*. 15:1061-6.

Hug, N., and J. Lingner. 2006. Telomere length homeostasis. *Chromosoma*. 115:413-25.

Hunter, T. 1995. Protein kinases and phosphatases: the yin and yang of protein phosphorylation and signaling. *Cell*. 80:225-36.

Huyen, Y., O. Zgheib, R.A. Ditullio, Jr., V.G. Gorgoulis, P. Zacharatos, T.J. Petty, E.A. Sheston, H.S. Mellert, E.S. Stavridi, and T.D. Halazonetis. 2004.

Methylated lysine 79 of histone H3 targets 53BP1 to DNA double-strand breaks. *Nature*. 432:406-11.

Hyland, E.M., M.S. Cosgrove, H. Molina, D. Wang, A. Pandey, R.J. Cottee, and J.D. Boeke. 2005. Insights into the role of histone H3 and histone H4 core modifiable residues in Saccharomyces cerevisiae. *Mol Cell Biol*. 25:10060-70.

Ira, G., A. Malkova, G. Liberi, M. Foiani, and J.E. Haber. 2003. Srs2 and Sgs1-Top3 suppress crossovers during double-strand break repair in yeast. *Cell*. 115:401-11.

Ito, T., T. Chiba, R. Ozawa, M. Yoshida, M. Hattori, and Y. Sakaki. 2001. A comprehensive two-hybrid analysis to explore the yeast protein interactome. *Proc Natl Acad Sci U S A*. 98:4569-74.

Ivessa, A.S., B.A. Lenzmeier, J.B. Bessler, L.K. Goudsouzian, S.L. Schnakenberg, and V.A. Zakian. 2003. The Saccharomyces cerevisiae helicase Rrm3p facilitates replication past nonhistone protein-DNA complexes. *Mol Cell*. 12:1525-36.

Jenuwein, T., and C.D. Allis. 2001. Translating the histone code. *Science*. 293:1074-80.

Katou, Y., Y. Kanoh, M. Bando, H. Noguchi, H. Tanaka, T. Ashikari, K. Sugimoto, and K. Shirahige. 2003. S-phase checkpoint proteins Tof1 and Mrc1 form a stable replication-pausing complex. *Nature*. 424:1078-83.

Kats, E.S., C.P. Albuquerque, H. Zhou, and R.D. Kolodner. 2006. Checkpoint functions are required for normal S-phase progression in Saccharomyces cerevisiae RCAF- and CAF-I-defective mutants. *Proc Natl Acad Sci U S A*. 103:3710-5.

Kellogg, D.R. 2003. Wee1-dependent mechanisms required for coordination of cell growth and cell division. *J Cell Sci*. 116:4883-90.

Keogh, M.C., J.A. Kim, M. Downey, J. Fillingham, D. Chowdhury, J.C. Harrison, M. Onishi, N. Datta, S. Galicia, A. Emili, J. Lieberman, X. Shen, S. Buratowski, J.E. Haber, D. Durocher, J.F. Greenblatt, and N.J. Krogan. 2006. A phosphatase complex that dephosphorylates gammaH2AX regulates DNA damage checkpoint recovery. *Nature*. 439:497-501.

Klein, F., T. Laroche, M.E. Cardenas, J.F. Hofmann, D. Schweizer, and S.M. Gasser. 1992. Localization of RAP1 and topoisomerase II in nuclei and meiotic chromosomes of yeast. *J Cell Biol*. 117:935-48.

Kondo, T., T. Wakayama, T. Naiki, K. Matsumoto, and K. Sugimoto. 2001. Recruitment of Mec1 and Ddc1 checkpoint proteins to double-strand breaks through distinct mechanisms. *Science*. 294:867-70.

Kops, G.J., B.A. Weaver, and D.W. Cleveland. 2005. On the road to cancer: aneuploidy and the mitotic checkpoint. *Nat Rev Cancer*. 5:773-85.

Kraus, E., W.Y. Leung, and J.E. Haber. 2001. Break-induced replication: a review and an example in budding yeast. *Proc Natl Acad Sci U S A*. 98:8255-62.

Krawitz, D.C., T. Kama, and P.D. Kaufman. 2002. Chromatin assembly factor I mutants defective for PCNA binding require Asf1/Hir proteins for silencing. *Mol Cell Biol*. 22:614-25.

Krings, G., and D. Bastia. 2004. swi1- and swi3-dependent and independent replication fork arrest at the ribosomal DNA of Schizosaccharomyces pombe. *Proc Natl Acad Sci U S A*. 101:14085-90.

Krishnan, V., S. Nirantar, K. Crasta, A.Y. Cheng, and U. Surana. 2004. DNA replication checkpoint prevents precocious chromosome segregation by regulating spindle behavior. *Mol Cell*. 16:687-700.

Kumagai, A., and W.G. Dunphy. 2000. Claspin, a novel protein required for the activation of Chk1 during a DNA replication checkpoint response in Xenopus egg extracts. *Mol Cell*. 6:839-49.

Labib, K., and A. Gambus. 2007. A key role for the GINS complex at DNA replication forks. *Trends Cell Biol*. 17:271-8.

Lambert, S., B. Froget, and A.M. Carr. 2007. Arrested replication fork processing: Interplay between checkpoints and recombination. *DNA Repair (Amst)*.

Lee, S.K., R.E. Johnson, S.L. Yu, L. Prakash, and S. Prakash. 1999. Requirement of yeast SGS1 and SRS2 genes for replication and transcription. *Science*. 286:2339-42.

Lee, W., R.P. St Onge, M. Proctor, P. Flaherty, M.I. Jordan, A.P. Arkin, R.W. Davis, C. Nislow, and G. Giaever. 2005. Genome-wide requirements for resistance to functionally distinct DNA-damaging agents. *PLoS Genet*. 1:e24.

Lehmann, A.R., A. Niimi, T. Ogi, S. Brown, S. Sabbioneda, J.F. Wing, P.L. Kannouche, and C.M. Green. 2007. Translesion synthesis: Y-family polymerases and the polymerase switch. *DNA Repair (Amst)*. 6:891-9.

Lew, D.J. 2003. The morphogenesis checkpoint: how yeast cells watch their figures. *Curr Opin Cell Biol*. 15:648-53.

Liberi, G., G. Maffioletti, C. Lucca, I. Chiolo, A. Baryshnikova, C. Cotta-Ramusino, M. Lopes, A. Pellicioli, J.E. Haber, and M. Foiani. 2005. Rad51-dependent DNA structures accumulate at damaged replication forks in sgs1 mutants defective in the yeast ortholog of BLM RecQ helicase. *Genes Dev*. 19:339-50.

Lindroos, H.B., L. Strom, T. Itoh, Y. Katou, K. Shirahige, and C. Sjogren. 2006. Chromosomal association of the Smc5/6 complex reveals that it functions in differently regulated pathways. *Mol Cell*. 22:755-67.

Lingner, J., J.P. Cooper, and T.R. Cech. 1995. Telomerase and DNA end replication: no longer a lagging strand problem? *Science*. 269:1533-4.

Liu, J.S., S.R. Kuo, and T. Melendy. 2003. Comparison of checkpoint responses triggered by DNA polymerase inhibition versus DNA damaging agents. *Mutat Res*. 532:215-26.

Longhese, M.P., M. Clerici, and G. Lucchini. 2003. The S-phase checkpoint and its regulation in Saccharomyces cerevisiae. *Mutat Res*. 532:41-58.

Lowndes, N.F., and G.W. Toh. 2005. DNA repair: the importance of phosphorylating histone H2AX. *Curr Biol*. 15:R99-R102.

Lundblad, V., and J.W. Szostak. 1989. A mutant with a defect in telomere elongation leads to senescence in yeast. *Cell*. 57:633-43.

Lustig, A.J., and T.D. Petes. 1986. Identification of yeast mutants with altered telomere structure. *Proc Natl Acad Sci U S A*. 83:1398-402.

Lydall, D. 2003. Hiding at the ends of yeast chromosomes: telomeres, nucleases and checkpoint pathways. *J Cell Sci*. 116:4057-65.

Maas, N.L., K.M. Miller, L.G. DeFazio, and D.P. Toczyski. 2006. Cell cycle and checkpoint regulation of histone H3 K56 acetylation by Hst3 and Hst4. *Mol Cell*. 23:109-19.

MacDougall, C.A., T.S. Byun, C. Van, M.C. Yee, and K.A. Cimprich. 2007. The structural determinants of checkpoint activation. *Genes Dev*. 21:898-903.

Majka, J., and P.M. Burgers. 2004. The PCNA-RFC families of DNA clamps and clamp loaders. *Prog Nucleic Acid Res Mol Biol*. 78:227-60.

Majka, J., A. Niedziela-Majka, and P.M. Burgers. 2006. The checkpoint clamp activates Mec1 kinase during initiation of the DNA damage checkpoint. *Mol Cell*. 24:891-901.

Mantiero, D., M. Clerici, G. Lucchini, and M.P. Longhese. 2007. Dual role for Saccharomyces cerevisiae Tel1 in the checkpoint response to double-strand breaks. *EMBO Rep*. 8:380-7.

Marcand, S., E. Gilson, and D. Shore. 1997. A protein-counting mechanism for telomere length regulation in yeast. *Science*. 275:986-90.

Masumoto, H., D. Hawke, R. Kobayashi, and A. Verreault. 2005. A role for cell-cycle-regulated histone H3 lysine 56 acetylation in the DNA damage response. *Nature*. 436:294-8.

Mayer, M.L., I. Pot, M. Chang, H. Xu, V. Aneliunas, T. Kwok, R. Newitt, R. Aebersold, C. Boone, G.W. Brown, and P. Hieter. 2004. Identification of protein complexes required for efficient sister chromatid cohesion. *Mol Biol Cell*. 15:1736-45.

McGowan, C.H., and P. Russell. 2004. The DNA damage response: sensing and signaling. *Curr Opin Cell Biol*. 16:629-33.

Meister, P., A. Taddei, L. Vernis, M. Poidevin, S.M. Gasser, and G. Baldacci. 2005. Temporal separation of replication and recombination requires the intra-S checkpoint. *J Cell Biol*. 168:537-44.

Melo, J., and D. Toczyski. 2002. A unified view of the DNA-damage checkpoint. *Curr Opin Cell Biol*. 14:237-45.

Melo, J.A., J. Cohen, and D.P. Toczyski. 2001. Two checkpoint complexes are independently recruited to sites of DNA damage in vivo. *Genes Dev*. 15:2809-21.

Mendenhall, M.D., and A.E. Hodge. 1998. Regulation of Cdc28 cyclin-dependent protein kinase activity during the cell cycle of the yeast Saccharomyces cerevisiae. *Microbiol Mol Biol Rev*. 62:1191-243.

Mohanty, B.K., N.K. Bairwa, and D. Bastia. 2006. The Tof1p-Csm3p protein complex counteracts the Rrm3p helicase to control replication termination of Saccharomyces cerevisiae. *Proc Natl Acad Sci U S A*. 103:897-902.

Moldovan, G.L., B. Pfander, and S. Jentsch. 2006. PCNA controls establishment of sister chromatid cohesion during S phase. *Mol Cell*. 23:723-32.

Moldovan, G.L., B. Pfander, and S. Jentsch. 2007. PCNA, the maestro of the replication fork. *Cell*. 129:665-79.

Moretti, P., K. Freeman, L. Coodly, and D. Shore. 1994. Evidence that a complex of SIR proteins interacts with the silencer and telomere-binding protein RAP1. *Genes Dev*. 8:2257-69.

Morrison, A.J., J. Highland, N.J. Krogan, A. Arbel-Eden, J.F. Greenblatt, J.E. Haber, and X. Shen. 2004. INO80 and gamma-H2AX interaction links ATP-dependent chromatin remodeling to DNA damage repair. *Cell*. 119:767-75.

Morrison, A.J., J.A. Kim, M.D. Person, J. Highland, J. Xiao, T.S. Wehr, S. Hensley, Y. Bao, J. Shen, S.R. Collins, J.S. Weissman, J. Delrow, N.J. Krogan, J.E. Haber, and X. Shen. 2007. Mec1/Tel1 Phosphorylation of the INO80 Chromatin Remodeling Complex Influences DNA Damage Checkpoint Responses. *Cell*. 130:499-511.

Musacchio, A., and E.D. Salmon. 2007. The spindle-assembly checkpoint in space and time. *Nat Rev Mol Cell Biol*. 8:379-93.

Nevanlinna, H., and J. Bartek. 2006. The CHEK2 gene and inherited breast cancer susceptibility. *Oncogene*. 25:5912-9.

Ng, H.H., R.M. Xu, Y. Zhang, and K. Struhl. 2002. Ubiquitination of histone H2B by Rad6 is required for efficient Dot1-mediated methylation of histone H3 lysine 79. *J Biol Chem*. 277:34655-7.

Nitani, N., K. Nakamura, C. Nakagawa, H. Masukata, and T. Nakagawa. 2006. Regulation of DNA replication machinery by Mrc1 in fission yeast. *Genetics*. 174:155-65.

Nyberg, K.A., R.J. Michelson, C.W. Putnam, and T.A. Weinert. 2002. Toward maintaining the genome: DNA damage and replication checkpoints. *Annu Rev Genet*. 36:617-56.

Ogiwara, H., T. Enomoto, and M. Seki. 2007. The INO80 chromatin remodeling complex functions in sister chromatid cohesion. *Cell Cycle*. 6:1090-5.

Osborn, A.J., and S.J. Elledge. 2003. Mrc1 is a replication fork component whose phosphorylation in response to DNA replication stress activates Rad53. *Genes Dev*. 17:1755-67.

Ozdemir, A., S. Spicuglia, E. Lasonder, M. Vermeulen, C. Campsteijn, H.G. Stunnenberg, and C. Logie. 2005. Characterization of lysine 56 of histone H3 as an acetylation site in Saccharomyces cerevisiae. *J Biol Chem*. 280:25949-52.

Paciotti, V., M. Clerici, G. Lucchini, and M.P. Longhese. 2000. The checkpoint protein Ddc2, functionally related to S. pombe Rad26, interacts with Mec1 and is regulated by Mec1-dependent phosphorylation in budding yeast. *Genes Dev*. 14:2046-59.

Pagano, M. 1997. Cell cycle regulation by the ubiquitin pathway. *Faseb J*. 11:1067-75.

Palladino, F., T. Laroche, E. Gilson, L. Pillus, and S.M. Gasser. 1993. The positioning of yeast telomeres depends on SIR3, SIR4, and the integrity of the nuclear membrane. *Cold Spring Harb Symp Quant Biol*. 58:733-46.

Pan, X., P. Ye, D.S. Yuan, X. Wang, J.S. Bader, and J.D. Boeke. 2006. A DNA integrity network in the yeast Saccharomyces cerevisiae. *Cell*. 124:1069-81.

Papouli, E., S. Chen, A.A. Davies, D. Huttner, L. Krejci, P. Sung, and H.D. Ulrich. 2005. Crosstalk between SUMO and ubiquitin on PCNA is mediated by recruitment of the helicase Srs2p. *Mol Cell*. 19:123-33.

Parrilla-Castellar, E.R., S.J. Arlander, and L. Karnitz. 2004. Dial 9-1-1 for DNA damage: the Rad9-Hus1-Rad1 (9-1-1) clamp complex. *DNA Repair (Amst)*. 3:1009-14.

Pellicioli, A., and M. Foiani. 2005. Signal transduction: how rad53 kinase is activated. *Curr Biol*. 15:R769-71.

Pfander, B., G.L. Moldovan, M. Sacher, C. Hoege, and S. Jentsch. 2005. SUMO-modified PCNA recruits Srs2 to prevent recombination during S phase. *Nature*. 436:428-33.

Pike, B.L., S. Yongkiettrakul, M.D. Tsai, and J. Heierhorst. 2003. Diverse but overlapping functions of the two forkhead-associated (FHA) domains in Rad53 checkpoint kinase activation. *J Biol Chem*. 278:30421-4.

Pommier, Y. 2006. Topoisomerase I inhibitors: camptothecins and beyond. *Nat Rev Cancer*. 6:789-802.

Ramey, C.J., S. Howar, M. Adkins, J. Linger, J. Spicer, and J.K. Tyler. 2004. Activation of the DNA damage checkpoint in yeast lacking the histone chaperone anti-silencing function 1. *Mol Cell Biol*. 24:10313-27.

Recht, J., T. Tsubota, J.C. Tanny, R.L. Diaz, J.M. Berger, X. Zhang, B.A. Garcia, J. Shabanowitz, A.L. Burlingame, D.F. Hunt, P.D. Kaufman, and C.D. Allis. 2006. Histone chaperone Asf1 is required for histone H3 lysine 56 acetylation, a modification associated with S phase in mitosis and meiosis. *Proc Natl Acad Sci U S A*. 103:6988-93.

Redon, C., D.R. Pilch, and W.M. Bonner. 2006. Genetic analysis of Saccharomyces cerevisiae H2A serine 129 mutant suggests a functional relationship between H2A and the sister-chromatid cohesion partners Csm3-Tof1 for the repair of topoisomerase I-induced DNA damage. *Genetics*. 172:67-76.

Redon, C., D.R. Pilch, E.P. Rogakou, A.H. Orr, N.F. Lowndes, and W.M. Bonner. 2003. Yeast histone 2A serine 129 is essential for the efficient repair of checkpoint-blind DNA damage. *EMBO Rep*. 4:678-84.

Ritchie, K.B., J.C. Mallory, and T.D. Petes. 1999. Interactions of TLC1 (which encodes the RNA subunit of telomerase), TEL1, and MEC1 in regulating telomere length in the yeast Saccharomyces cerevisiae. *Mol Cell Biol*. 19:6065-75.

Robert, T., D. Dervins, F. Fabre, and S. Gangloff. 2006. Mrc1 and Srs2 are major actors in the regulation of spontaneous crossover. *Embo J*. 25:2837-46.

Rouse, J., and S.P. Jackson. 2000. LCD1: an essential gene involved in checkpoint control and regulation of the MEC1 signalling pathway in Saccharomyces cerevisiae. *Embo J*. 19:5801-12.

Rouse, J., and S.P. Jackson. 2002. Lcd1p recruits Mec1p to DNA lesions in vitro and in vivo. *Mol Cell*. 9:857-69.

Sancar, A., L.A. Lindsey-Boltz, K. Unsal-Kacmaz, and S. Linn. 2004. Molecular mechanisms of mammalian DNA repair and the DNA damage checkpoints. *Annu Rev Biochem*. 73:39-85.

Sanchez, Y., J. Bachant, H. Wang, F. Hu, D. Liu, M. Tetzlaff, and S.J. Elledge. 1999. Control of the DNA damage checkpoint by chk1 and rad53 protein kinases through distinct mechanisms. *Science*. 286:1166-71.

Sandell, L.L., and V.A. Zakian. 1993. Loss of a yeast telomere: arrest, recovery, and chromosome loss. *Cell*. 75:729-39.

Sanematsu, F., Y. Takami, H.K. Barman, T. Fukagawa, T. Ono, K. Shibahara, and T. Nakayama. 2006. Asf1 is required for viability and chromatin assembly during DNA replication in vertebrate cells. *J Biol Chem*. 281:13817-27.

Santocanale, C., and J.F. Diffley. 1998. A Mec1- and Rad53-dependent checkpoint controls late-firing origins of DNA replication. *Nature*. 395:615-8.

Sar, F., L.A. Lindsey-Boltz, D. Subramanian, D.L. Croteau, S.Q. Hutsell, J.D. Griffith, and A. Sancar. 2004. Human claspin is a ring-shaped DNA-binding protein with high affinity to branched DNA structures. *J Biol Chem*. 279:39289-95.

Schulz, L.L., and J.K. Tyler. 2006. The histone chaperone ASF1 localizes to active DNA replication forks to mediate efficient DNA replication. *Faseb J*. 20:488-90.

Schwartz, M.F., J.K. Duong, Z. Sun, J.S. Morrow, D. Pradhan, and D.F. Stern. 2002. Rad9 phosphorylation sites couple Rad53 to the Saccharomyces cerevisiae DNA damage checkpoint. *Mol Cell*. 9:1055-65.

Schwartz, M.F., S.J. Lee, J.K. Duong, S. Eminaga, and D.F. Stern. 2003. FHA domain-mediated DNA checkpoint regulation of Rad53. *Cell Cycle*. 2:384-96.

Sharp, J.A., E.T. Fouts, D.C. Krawitz, and P.D. Kaufman. 2001. Yeast histone deposition protein Asf1p requires Hir proteins and PCNA for heterochromatic silencing. *Curr Biol*. 11:463-73.

Sharp, J.A., G. Rizki, and P.D. Kaufman. 2005. Regulation of histone deposition proteins Asf1/Hir1 by multiple DNA damage checkpoint kinases in Saccharomyces cerevisiae. *Genetics*. 171:885-99.

Shen, X., G. Mizuguchi, A. Hamiche, and C. Wu. 2000. A chromatin remodelling complex involved in transcription and DNA processing. *Nature*. 406:541-4.

Shimada, K., P. Pasero, and S.M. Gasser. 2002. ORC and the intra-S-phase checkpoint: a threshold regulates Rad53p activation in S phase. *Genes Dev*. 16:3236-52.

Shirahige, K., Y. Hori, K. Shiraishi, M. Yamashita, K. Takahashi, C. Obuse, T. Tsurimoto, and H. Yoshikawa. 1998. Regulation of DNA-replication origins during cell-cycle progression. *Nature*. 395:618-21.

Smith, A.P., J.F. Gimenez-Abian, and D.J. Clarke. 2002. DNA-damage-independent checkpoints: yeast and higher eukaryotes. *Cell Cycle*. 1:16-33.

Smolka, M.B., C.P. Albuquerque, S.H. Chen, K.H. Schmidt, X.X. Wei, R.D. Kolodner, and H. Zhou. 2005. Dynamic changes in protein-protein interaction and protein phosphorylation probed with amine reactive isotope tag. *Mol Cell Proteomics*.

Smolka, M.B., C.P. Albuquerque, S.H. Chen, and H. Zhou. 2007. Proteome-wide identification of in vivo targets of DNA damage checkpoint kinases. *Proc Natl Acad Sci U S A*.

Smolka, M.B., S.H. Chen, P.S. Maddox, J.M. Enserink, C.P. Albuquerque, X.X. Wei, A. Desai, R.D. Kolodner, and H. Zhou. 2006. An FHA domain-mediated protein interaction network of Rad53 reveals its role in polarized cell growth. *J Cell Biol*. 175:743-53.

Sogo, J.M., M. Lopes, and M. Foiani. 2002. Fork reversal and ssDNA accumulation at stalled replication forks owing to checkpoint defects. *Science*. 297:599-602.

Stelter, P., and H.D. Ulrich. 2003. Control of spontaneous and damage-induced mutagenesis by SUMO and ubiquitin conjugation. *Nature*. 425:188-91.

Strom, L., C. Karlsson, H.B. Lindroos, S. Wedahl, Y. Katou, K. Shirahige, and C. Sjogren. 2007. Postreplicative formation of cohesion is required for repair and induced by a single DNA break. *Science*. 317:242-5.

Strom, L., H.B. Lindroos, K. Shirahige, and C. Sjogren. 2004. Postreplicative recruitment of cohesin to double-strand breaks is required for DNA repair. *Mol Cell*. 16:1003-15.

Strom, L., and C. Sjogren. 2005. DNA damage-induced cohesion. *Cell Cycle*. 4:536-9.

Su, T.T. 2006. Cellular responses to DNA damage: one signal, multiple choices. *Annu Rev Genet*. 40:187-208.

Sutton, A., J. Bucaria, M.A. Osley, and R. Sternglanz. 2001. Yeast ASF1 protein is required for cell cycle regulation of histone gene transcription. *Genetics*. 158:587-96.

Suzuki, M., R. Igarashi, M. Sekiya, T. Utsugi, S. Morishita, M. Yukawa, and Y. Ohya. 2004. Dynactin is involved in a checkpoint to monitor cell wall synthesis in Saccharomyces cerevisiae. *Nat Cell Biol*. 6:861-71.

Sweeney, F.D., F. Yang, A. Chi, J. Shabanowitz, D.F. Hunt, and D. Durocher. 2005. Saccharomyces cerevisiae Rad9 acts as a Mec1 adaptor to allow Rad53 activation. *Curr Biol*. 15:1364-75.

Szyjka, S.J., C.J. Viggiani, and O.M. Aparicio. 2005. Mrc1 is required for normal progression of replication forks throughout chromatin in S. cerevisiae. *Mol Cell*. 19:691-7.

Taggart, A.K., S.C. Teng, and V.A. Zakian. 2002. Est1p as a cell cycle-regulated activator of telomere-bound telomerase. *Science*. 297:1023-6.

Takahashi, A., and T. Ohnishi. 2005. Does gammaH2AX foci formation depend on the presence of DNA double strand breaks? *Cancer Lett*. 229:171-9.

Tamburini, B.A., J.J. Carson, M.W. Adkins, and J.K. Tyler. 2005. Functional conservation and specialization among eukaryotic anti-silencing function 1 histone chaperones. *Eukaryot Cell*. 4:1583-90.

Tanaka, K., and P. Russell. 2001. Mrc1 channels the DNA replication arrest signal to checkpoint kinase Cds1. *Nat Cell Biol*. 3:966-72.

Teixeira, M.T., and E. Gilson. 2005. Telomere maintenance, function and evolution: the yeast paradigm. *Chromosome Res*. 13:535-48.

Tercero, J.A., M.P. Longhese, and J.F. Diffley. 2003. A central role for DNA replication forks in checkpoint activation and response. *Mol Cell*. 11:1323-36.

Toczyski, D.P., D.J. Galgoczy, and L.H. Hartwell. 1997. CDC5 and CKII control adaptation to the yeast DNA damage checkpoint. *Cell*. 90:1097-106.

Toh, G.W., and N.F. Lowndes. 2003. Role of the Saccharomyces cerevisiae Rad9 protein in sensing and responding to DNA damage. *Biochem Soc Trans*. 31:242-6.

Torres-Rosell, J., G. De Piccoli, V. Cordon-Preciado, S. Farmer, A. Jarmuz, F. Machin, P. Pasero, M. Lisby, J.E. Haber, and L. Aragon. 2007. Anaphase onset before complete DNA replication with intact checkpoint responses. *Science*. 315:1411-5.

Torres-Rosell, J., F. Machin, S. Farmer, A. Jarmuz, T. Eydmann, J.Z. Dalgaard, and L. Aragon. 2005. SMC5 and SMC6 genes are required for the segregation of repetitive chromosome regions. *Nat Cell Biol*. 7:412-9.

Tourriere, H., and P. Pasero. 2007. Maintenance of fork integrity at damaged DNA and natural pause sites. *DNA Repair (Amst)*.

Tourriere, H., G. Versini, V. Cordon-Preciado, C. Alabert, and P. Pasero. 2005. Mrc1 and Tof1 promote replication fork progression and recovery independently of Rad53. *Mol Cell*. 19:699-706.

Tremethick, D.J. 2007. Higher-order structures of chromatin: the elusive 30 nm fiber. *Cell*. 128:651-4.

Tseng, S.F., J.J. Lin, and S.C. Teng. 2006. The telomerase-recruitment domain of the telomere binding protein Cdc13 is regulated by Mec1p/Tel1p-dependent phosphorylation. *Nucleic Acids Res*. 34:6327-36.

Tsubota, T., C.E. Berndsen, J.A. Erkmann, C.L. Smith, L. Yang, M.A. Freitas, J.M. Denu, and P.D. Kaufman. 2007. Histone H3-K56 acetylation is catalyzed by histone chaperone-dependent complexes. *Mol Cell*. 25:703-12.

Tyler, J.K., C.R. Adams, S.R. Chen, R. Kobayashi, R.T. Kamakaka, and J.T. Kadonaga. 1999. The RCAF complex mediates chromatin assembly during DNA replication and repair. *Nature*. 402:555-60.

Ulrich, H.D. 2005. Mutual interactions between the SUMO and ubiquitin systems: a plea of no contest. *Trends Cell Biol*. 15:525-32.

Unal, E., A. Arbel-Eden, U. Sattler, R. Shroff, M. Lichten, J.E. Haber, and D. Koshland. 2004. DNA damage response pathway uses histone modification to assemble a double-strand break-specific cohesin domain. *Mol Cell*. 16:991-1002.

Van Attikum, H., O. Fritsch, and S.M. Gasser. 2007. Distinct roles for SWR1 and INO80 chromatin remodeling complexes at chromosomal double-strand breaks. *The EMBO Journal advance online publication 30 August 2007*. doi: 10.1038/sj.emboj.760183.

van Attikum, H., O. Fritsch, B. Hohn, and S.M. Gasser. 2004. Recruitment of the INO80 Complex by H2A Phosphorylation Links ATP-Dependent Chromatin Remodeling with DNA Double-Strand Break Repair. *cell*. 119:777-788.

van Attikum, H., and S.M. Gasser. 2005. The histone code at DNA breaks: a guide to repair? *Nat Rev Mol Cell Biol*. 6:757-65.

Verdun, R.E., and J. Karlseder. 2007. Replication and protection of telomeres. *Nature*. 447:924-31.

Viscardi, V., M. Clerici, H. Cartagena-Lirola, and M.P. Longhese. 2005. Telomeres and DNA damage checkpoints. *Biochimie*. 87:613-24.

Wakayama, T., T. Kondo, S. Ando, K. Matsumoto, and K. Sugimoto. 2001. Pie1, a protein interacting with Mec1, controls cell growth and checkpoint responses in Saccharomyces cerevisiae. *Mol Cell Biol*. 21:755-64.

Wang, H., and S.J. Elledge. 2002. Genetic and physical interactions between DPB11 and DDC1 in the yeast DNA damage response pathway. *Genetics*. 160:1295-304.

Ward, I.M., and J. Chen. 2001. Histone H2AX is phosphorylated in an ATR-dependent manner in response to replicational stress. *J Biol Chem*. 276:47759-62.

Weinert, T.A., and L.H. Hartwell. 1988. The RAD9 gene controls the cell cycle response to DNA damage in Saccharomyces cerevisiae. *Science*. 241:317-22.

Wright, J.H., D.E. Gottschling, and V.A. Zakian. 1992. Saccharomyces telomeres assume a non-nucleosomal chromatin structure. *Genes Dev*. 6:197-210.

Wyman, C., and R. Kanaar. 2006. DNA double-strand break repair: all's well that ends well. *Annu Rev Genet*. 40:363-83.

Wysocki, R., A. Javaheri, S. Allard, F. Sha, J. Cote, and S.J. Kron. 2005. Role of Dot1-dependent histone H3 methylation in G1 and S phase DNA damage checkpoint functions of Rad9. *Mol Cell Biol*. 25:8430-43.

Xu, F., K. Zhang, and M. Grunstein. 2005. Acetylation in histone H3 globular domain regulates gene expression in yeast. *Cell*. 121:375-85.

Yarbro, J.W. 1992. Mechanism of action of hydroxyurea. *Semin Oncol*. 19:1-10.

Ye, X., A.A. Franco, H. Santos, D.M. Nelson, P.D. Kaufman, and P.D. Adams. 2003. Defective S phase chromatin assembly causes DNA damage, activation of the S phase checkpoint, and S phase arrest. *Mol Cell*. 11:341-51.

Zegerman, P., and J.F. Diffley. 2003. Lessons in how to hold a fork. *Nat Struct Biol*. 10:778-9.

Zhao, H., and P. Russell. 2004. DNA binding domain in the replication checkpoint protein Mrc1 of Schizosaccharomyces pombe. *J Biol Chem*. 279:53023-7.

Zhao, X., A. Chabes, V. Domkin, L. Thelander, and R. Rothstein. 2001. The ribonucleotide reductase inhibitor Sml1 is a new target of the Mec1/Rad53 kinase cascade during growth and in response to DNA damage. *Embo J*. 20:3544-53.

Zhao, X., E.G. Muller, and R. Rothstein. 1998. A suppressor of two essential checkpoint genes identifies a novel protein that negatively affects dNTP pools. *Mol Cell*. 2:329-40.

Zhao, X., and R. Rothstein. 2002. The Dun1 checkpoint kinase phosphorylates and regulates the ribonucleotide reductase inhibitor Sml1. *Proc Natl Acad Sci U S A*. 99:3746-51.

Zhou, B.B., and J. Bartek. 2004. Targeting the checkpoint kinases: chemosensitization versus chemoprotection. *Nat Rev Cancer*. 4:216-25.

Zou, L., and S.J. Elledge. 2003. Sensing DNA damage through ATRIP recognition of RPA-ssDNA complexes. *Science*. 300:1542-8.

Chapter 2

Cell-cycle dependent phosphorylation of Rad53 modulates its activity in response to DNA damage and affects checkpoint adaptation

Thomas Schleker, Kenji Shimada[1], Ragna Sack[2] and Susan M. Gasser[3]

[1] K. S. performed experiments shown in Sup. Figures 2.2a and 2.4, helped in experiments shown in Figure 2.6, and contributed to the design and choice of experiments.

[2] R. S. performed the mass spectrometric analysis and contributed display of the results in Figure 2.5b and Sup Figure 2.3.

[3] S. G. was supervising choice and analysis of experiments, and manuscript preparation.

2.1 Summary

Genotoxic insults lead to activation of DNA damage checkpoint pathways in all cell cycle stages. This response, however, can differ during the cell cycle. In particular, in S phase a replication checkpoint monitors the stalling of replication forks in addition to the DNA damage sensing checkpoint pathway. Since single-stranded DNA activates the replication checkpoint, it can respond to normal replication events. To accomodate this, there is a cell-cycle specific threshold for Rad53 activation in yeast which means that a higher amount of DNA damage is needed in S phase to activate Rad53.

To better understand this cell-cycle dependent regulation of Rad53 activation we examined whether Rad53 itself is modulated in a cell-cycle dependent manner. We found that a subpopulation of Rad53 is phosphorylated during late G2 and mitosis, leading to a band of slightly lower mobility in SDS-PAGE during G2, M and G1, but not in S phase. This phosphorylation depends on both the mitotic Cdc5 (polo-like kinase) and Cdc28 (cyclin-dependent kinase) activities. Moreover, purified Cdc5 kinase can phosphorylate recombinant Rad53 *in vitro*.

Galactose-induced expression of partial Rad53 fragments mapped the phosphorylation event to the C-terminal part of Rad53. More precisely serines 774 and 789 of Rad53 were found to be phosphorylated in mitotic cells in the absence of DNA damage. By mutagenesis we showed that the phosphorylation of Ser774 is important for mediating the cell-cycle dependent migration pattern, while phosphorylation of Ser789 is important for enhancing Rad53 phosphorylation in response to low levels of DNA damage in the G2/M checkpoint. This activation delays checkpoint adaptation in response to a single irreparable double strand break.

Together these results suggest that in addition to DNA-damage dependent hyperphosphorylation of Rad53, Rad53 is also phosphorylated in a cell-cycle dependent manner on sites that are independent of those that signal the checkpoint response.

Checkpoint adaptation was shown to involve several proteins including Cdc5, the phosphatases Ptc2 and Ptc3 as well as the kinase CK2. CK2 partially acts by phosphorylating Ptc2 to promote Rad53 dephosphorylation after several hours of active checkpoint signaling. We asked whether the cell-cycle specific modification of Rad53 contributes to checkpoint adaptation. We found that Rad53 gets hyperactivated

in a *cka1*Δ *cka*2-8/13 ^{ts} mutant strain at restrictive temperature of 38.5°C in absence of exogenous DNA damage. Similar hyperactivation occurs in response to low amounts of DNA damage at 37°C. In both cases, Rad53 activation is dependent upon DNA damage signaling, but only partially upon *PTC2* and *PTC3* function, since in *ptc2*Δ *ptc3*Δ mutant cells we do not observe Rad53 activation in response to high temperature and only slight Rad53 hyperactivation in response to DNA damage. This suggests that CK2 acts only partially through Ptc2 and Ptc3 for downregulating Rad53 activation. Alternatively, the function of CK2 in checkpoint adaptation may be not only the downregulation of a checkpoint response, but also the continuous checkpoint inactivation during normal checkpoint signaling. If this role were also true in transformed mammalian cells, CK2 inhibition could be used to widen the therapeutic window for cancer therapy.

2.2 Introduction

Very important barriers to tumorigenesis are provided by DNA damage checkpoint pathways (Bartkova et al., 2005; Gorgoulis et al., 2005), which delay cell-cycle progression in the presence of unrepaired DNA damage and inhibit its distribution into daughter cells (Hartwell and Weinert, 1989; Weinert and Hartwell, 1988). Therefore it is not surprising that mutations in DNA checkpoint genes can be found in human cancer-predisposing disorders, such as ATM in ataxia telangiectasia (Savitsky et al., 1995) and Chk2 in Li-Fraumeni syndrome (Bell et al., 1999).

The budding yeast Chk2 homologue Rad53 was identified as an essential serine/threonine kinase whose transcription is upregulated in S phase, suggesting an important role related to DNA replication (Stern et al., 1991; Zheng et al., 1993). Rad53 is an essential component of checkpoint responses in G1, S and G2/M phases of the cell cycle (Weinert et al., 1994; Allen et al., 1994). In addition to its role in checkpoint signaling Rad53 regulates dNTP levels through a second kinase Dun1 (Chen et al., 2007; Elledge et al., 1993). Mec1 (human ATR) is a checkpoint protein acting upstream of Rad53. It is also essential for yeast growth and is required for activation of Rad53 in response to DNA damage. Overexpression of *RAD53* complements the lethality of *Δmec1* mutants (Sanchez et al., 1996). Supression of lethality of both *mec1* and *rad53* mutant strains stems from higher basal activation of Dun1, which in turn inactivates Sml1 (a negative regulator of ribonucleotide reductase). In the absence of either Mec1 or Rad53, Sml1 inhibits ribonucleotide reductase and thereby arrests cell growth (Zhao et al., 2001; Zhao et al., 1998; Zhao and Rothstein, 2002).

Independent of Sml1 inhibition, the activated Mec1/Rad53 signal transduction pathway promotes cell-cycle delay in response to DNA damage or replication blockage. In S phase other functions that depend upon Rad53 are replisome stabilization, facilitated replication restart processes, inhibition of the firing of late origins, prevention of precocious chromosome segregation and regulation of spindle dynamics (Branzei and Foiani, 2006; Krishnan and Surana, 2005). Furthermore Rad53 is required to maintain proper bud site selection and cell morphology in response to replication stress (Enserink et al., 2006; Smolka et al., 2006).

DNA damage is recognized by sensor proteins that associate with the DNA lesion in a more or less direct way. Important for the detection of DNA damage and triggering a

checkpoint response are the Rad24-RFC like complex and the PCNA-like complex of Rad17, Ddc1 and Mec3, as well as Mec1 and its essential cofactor, Ddc2. Double strand breaks are also sensed by a pathway involving the MRX complex (Mre11, Rad50 and Xrs2) and the PI3-like kinase Tel1. Generally in yeast Mec1 has the predominant role of sensing DNA damage and promoting checkpoint arrest (Cobb et al., 2004; Harrison and Haber, 2006). Ddc2 is essential for proper Mec1 checkpoint function (Paciotti et al., 2000; Rouse and Jackson, 2000; Wakayama et al., 2001), as it targets Mec1 to sites of DNA damage by recognizing single-stranded DNA bound by RPA (Rouse and Jackson, 2002; Zou and Elledge, 2003).

During the DNA damage and replication checkpoint activation process, Mec1 and Tel1 then phosphorylate the so-called adaptor proteins, Rad9 or Mrc1 (Alcasabas et al., 2001; Osborn and Elledge, 2003; Schwartz et al., 2002; Sun et al., 1998), which in turn lead to activation of both Rad53 and Chk1 (Harrison and Haber, 2006). In budding yeast this cascade of kinases prevents anaphase by two mechanisms: activated Chk1 stabilizes the anaphase inhibitor Pds1, whereas activated Rad53 inhibits polo-like kinase Cdc5 and therefore cytokinesis (Sanchez et al., 1999). Recently the predicted physical interaction of Mrc1 with the FHA1 domain of Rad53 was confirmed (Smolka et al., 2006) making it likely that Mrc1, like Rad9, is a bona fide adaptor during replication checkpoint activation.

Rad53 activation occurs in a two step mechanism: First a priming phosphorylation by Mec1/Ddc2 occurs and then its activation is amplified by autophosphorylation of Rad53 in trans (Ma et al., 2006). The adaptor proteins Rad9, and presumably also Mrc1, may function as solid state catalysts to mediate interaction between Mec1 and Rad53 and/or scaffold proteins to facilitate Rad53 autophosphorylation in-trans (Gilbert et al., 2001; Pellicioli and Foiani, 2005; Sweeney et al., 2005).

Accordingly Rad53 contains 16 SQ/TQ sites, which are consensus sites for Mec1/Tel1 mediated phosphorylation. Four of these sites form SQ/TQ clusters in front of each Forkhead Homology Associated (FHA) domains, respectively (Kim et al., 1999; Lee et al., 2003b; Traven and Heierhorst, 2005). FHA domains were shown to be phosphospecific protein-protein interaction motifs (Durocher et al., 1999) and show slightly different phosphopeptide binding specificities (Durocher et al., 2000; Liao et al., 1999; Liao et al., 2000). Accordingly also the factors known to interact with the two FHA domains are different. The FHA2 domain (C-terminal of the kinase domain) was found to interact only with phosphorylated Rad9 (Smolka et al., 2006;

Sun et al., 1998; Vialard et al., 1998) and seems to be important only for receiving signal input of the DNA damage checkpoint.

The FHA1 domain of Rad53 was shown to interact with Rad9 as well as with Sgs1, Mrc1, Dbf4, Ptc2, Asf1, Dun1, Mdt1 as well as Rad9 (Bjergbaek et al., 2005; Duncker et al., 2002; Durocher et al., 1999; Emili et al., 2001; Hu et al., 2001; Lee et al., 2003b; Leroy et al., 2003; Pike et al., 2004b; Schwartz et al., 2003). Amazingly a further 25 proteins with a wide variety of biological functions, including transcription factors and septins also bind the Rad53 FHA1 domain (Smolka et al., 2006). Based on these observations the FHA2 domain seems to be mainly implicated for receiving upstream signal input of the DNA damage checkpoint, whereas the FHA1 domain is the major interface for signaling via the replication checkpoint as well as towards downstream target proteins.

Mutation of both FHA domains is required to render yeast strains as sensitive to DNA damaging drugs as *rad53* kinase dead or null mutant strains (Pike et al., 2003; Schwartz et al., 2003). Nonetheless results from Schwartz et al. (2003) suggest that the FHA1 and FHA2 domains have different roles in response to different sources of DNA damage. Yeast strains mutated for the FHA1 domain of Rad53 are very sensitive to HU, which activates the replication checkpoint and the FHA1 domain is required to prevent firing of late origins (Pike et al., 2004a; Schwartz et al., 2003).

Two studies aimed to map all possible Rad53 phosphorylation sites in response to DNA damage. Sweeney et al determined by mass spectrometry phosphorylated amino acid residues in response to the UV-mimetric drug 4-NQO. They found 13 potential Rad53 autophosphorylation sites and 14 occurring independent of Rad53 kinase activity, including Mec1 target sites and one potential CDK site at aa 375 (Sweeney et al., 2005). Smolka et al. instead analysed Rad53 phosphorylation sites in response to MMS and found 32 phosphopeptides in their study, some of them are potential CDK sites (at position 175, 375 and 774) and also occurring in the absence of MMS (Smolka et al., 2005). One clear outcome of both studies is that Rad53 phosphorylation sites in response to DNA damage are not completely overlapping (see also Pellicioli and Foiani, 2005) and that some sites, in particular the potential CDK sites are phosphorylated in the absence of DNA damage signaling. An overview of selected important known phosphorylation sites and Mec1/Tel1 target sites is given in Figure 2.5a.

Shimada et al showed by using an *orc2*-1 mutant with reduced replication rate that the checkpoint response is impaired specifically in S phase due to the lower amount of replication forks (Shimada et al., 2002). The authors propose that the checkpoint in S phase is attenuated and responds in a dose-dependent manner taking into account the amount of replicating DNA. They argue that the cell buffers this endogenous checkpoint signal by a threshold for Rad53 activation which is higher in S phase than in G1 or G2 phase cells. Indeed the G2/M checkpoint is known to have a very high sensitivity to DNA damage, since one DSB is sufficient to trigger Rad53 activation (Pellicioli et al., 2001).

Yeast cells have evolved a system that overrides the DNA-damage induced checkpoint arrest at G2/M after a time-period sufficient for DNA repair, in order to increase strain viability (Galgoczy and Toczyski, 2001; Toczyski et al., 1997). Checkpoint inactivation occurs ideally after repair, and is then called recovery. However, even in the absence of repair yeast cells can override the checkpoint arrest after a certain time. In this case it is called adaptation (Toczyski et al., 1997). In experimental systems this can be demonstrated by inducing an irrepairable DSB with the HO-endonuclease (Sandell and Zakian, 1993; Toczyski et al., 1997). Toczyski et al. screened for adaptation-deficient mutants and identified two genes required for this checkpoint adaptation, casein kinase *CKB2* and polo-like kinase *CDC5*. All adaptation defective mutants show persistent phosphorylation of Rad53, arguing that adaptation involves Rad53 inactivation (Lee et al., 2001; Lee et al., 2003a; Leroy et al., 2003; Pellicioli et al., 2001; Vaze et al., 2002). Not surprisingly, phosphatases have been reported to play an important role for inactivating the checkpoint arrest during recovery or adaptation. For instance in budding yeast the PP2C phosphatases Ptc2 and Ptc3 were shown to bind and inactivate Rad53 in response to an irreparable DSB, and hence are indispensable for checkpoint adaptation and recovery (Leroy et al., 2003).

The activation and identification of phosphorylation sites of Rad53 in response to DNA damage has been studied intensively in the past. Nothing is yet known about whether regulatory modifications outside of DNA damage signaling might contribute to and modulate Rad53 kinase activity in response to DNA damage. In the current study we provide evidence that Rad53 is phosphorylated in a cell-cycle dependent manner independent of a DNA damage checkpoint response. This phosphorylation is required to avoid premature checkpoint adaptation in response to a single irreparable

DSB and contributes to the increased sensitivity of the G2/M checkpoint as compared to the intra-S phase checkpoint. Furthermore our results suggest that CK2 is required to continuously downregulate Rad53 activation in response to DNA damage. CK2 therefore prevents hyperactivation of the checkpoint, which would interfere with normal cell growth and the recovery from DNA damage.

2.3 Materials and methods

2.3.1 Site directed mutagenesis and list of plasmids

Standard molecular biology techniques were used (Sambrook and Russell, 2001). Site directed mutagenesis of plasmid borne *RAD53* was performed with the two-stage QuickChange Site-Directed Mutagenesis using Pfu polymerase, as described (Wang and Malcolm, 1999). Plasmid-bearing *RAD53* (YCplac33-*RAD53)* encodes Rad53 with a C-terminal HA-tag under control of the endogenous promoter (Sugimoto et al., 1997). *rad53*^{CCA1} (Cell Cycle Alanine Mutant 1), a derivative of *RAD53* with S789A and S791A substitutions was kindly provided by Daniel Durocher (originally *rad53*^{A7}, (Sweeney et al., 2005). *rad53*^{CCA2} has the following mutations: S689A S774A S789A S791A E117A (E117A is silent and does not influence the function of the Rad53 FHA1 domain, (Durocher et al., 1999). *rad53*^{S774A} bears a S774A, *rad53*^{S774E} a S774E and *rad53*^{S789E} a S789E mutation. For galactose-inducible expression plasmids pNter (originally pJG47-RAD53-FHA1), pKIN (originally pJG47-RAD53-Kinase) and pCter (originally pJG47-RAD53-FHA2), pCter^{R605A} (originally pJG47-RAD53-FHA2^{R605A}) and pCter^{CCA1} bearing S789A and S791A mutations, express domains of Rad53 with a C-terminal HA-tag (Bjergbaek et al., 2005).

2.3.2 General Yeast culture conditions

Yeast strains used are listed in Supplemental Table 2.1 and were grown at 30°C on YPAD plates or in liquid YPAD medium (YPAD = YPD + 0.002% adenine) if not otherwise stated and where indicated in selective synthetic medium with either glucose, raffinose or galactose (Amberg et al., 2005). SCLGG was synthetic medium with lactic acid (2% final), glycerol (3% final) and glucose (0.05% final).

Deletion strains were made by plasmid-borne or PCR based gene disruption and verified by PCR and phenotypic analysis (Ivanov et al., 1992; Longtine et al., 1998; Wach et al., 1994).

2.3.3 Cell cycle synchronization and blockage

Exponentially growing yeast cultures were synchronized in G1 phase by addition of α-factor at pH 4.5 to 5.0 for one cell cycle stage as described (Braguglia et al., 1998). Nocodazole and benomyl were added at 10-15 μg/ml to cultures adjusted to 1% DMSO. FACS was performed on a Facscalibur Flow Cytometer (BD) as described (Frei and Gasser, 2000).

For specific inhibition of the *cdc28*-AS1 allele, cells were arrested in mitosis by a *cdc16*-1 block (by shifting the temperature to 37°C for 90 min), and one half of the culture was incubated with 17 μM Na-PP1 / 1% DMSO (kindly provided by M. Peter, (Jaquenoud et al., 2002), or with 1% DMSO alone, for 90 min. Blockage of temperature sensitive *CDC* mutants was obtained by shifting cultures from 23°C to the restrictive temperature of 37°C (or 38.5°C for *cka2*-8/13 alleles).

2.3.4 Drop assays and checkpoint activation experiments

Drop assays were a 1:5 or 1:10 dilution series of uniformly grown yeast cultures on plates with and without the corresponding drugs at indicated doses. Pictures were taken after 2-3 days of continuous growth.

2.3.5 Expression of ectopic protein fragments in yeast

For yeast strains bearing plasmids pNter, pKIN and pCter, selective medium (Sraff-trp) was used and protein expression was induced by addition of 2% galactose for 60 min. Proteins were separated on 10% SDS-PAGE, followed by western blot with Mab 12CA5 (anti-HA).

2.3.6 Protein extracts, SDS-Page and Western blot analysis

Whole cell protein extracts were prepared from cell pellets by TCA precipitation according to (Yaffe and Schatz, 1984). Precipitates were washed twice with a solution containing 70% acetone, 20 % ethanol and 10 mM Tris pH7.5 and bromphenol blue to monitor sufficient washing. Proteins were resuspended in SDS sample buffer by sonication and denatured prior to SDS-PAGE on 6% Mini-gels (acrylamide: bisacrylamide ratio of 37.5: 1). Gel running conditions were: constant 10mA per gel

for 3-4 hours at 4°C, hence for 6% gels proteins < 60 kDa have been run out of the gel. Endogenous Rad53 was detected with goat anti-Rad53 (yC-19, Santa Cruz Biotechnology) and tagged proteins with Mab 9E10 (anti-Myc) or Mab 12CA5 (anti-HA) or Mab 3F10 (anti-HA, Roche). Secondary antibodies were commerical HRP linked anti-rabbit, anti-mouse, anti-rat and anti-goat antibodies. Detection was done with the Enhanced Chemi-Luminescence system (Amersham) combined with films or the Chemidoc XRS and Quantity One software (both from Biorad).

2.3.7 Immunoprecipitation and phosphatase treatments

Immunoprecipitation was performed with Mab 9E10 as described (Cobb et al., 2003; Cobb et al., 2005) after addition of protease and phosphatase inhibitors. The phosphatase reaction was performed using alkaline phosphatase (Roche) in a buffer containing 50 mM Tris-Cl pH 8.0, 100 mM NaCl and 2.5 mM $MgCl_2$ (Deak and Templeton, 1997) for 1 hour at 37°C. The reaction was stopped by addition of an equal colume 2x SDS sample buffer and denaturation prior to SDS-PAGE.

2.3.8 Mass spectrometric analysis

Rad53-Myc from cells arrested in mitosis (GA-1745, *cdc15*-2 and GA-1159, *cdc16*-1) was recovered by immunoprecipitation. The coomassie stained bands were processed by reduction and alkylation of the cysteines followed by digestion with trypsin. Tryptic peptides were separated by nano-HPLC (Agilent 1100 nanoLC system, Agilent Technologies) coupled to a 4000 Q TRAP mass spectrometer (Applied Biosystems). In the IDA mode the mass spectrometer cycled through six analyses, one full-scan MS experiment and one enhanced resolution experiment followed by four enhanced product ion experiments. Phosphorylated peptides and phosphorylation sites were determined searching UniProt data base restricted to *Saccharomyces cerevisiae* using Mascot (Matrix Science). Resulting sequences were inspected manually. Multiple reaction monitoring (MRM) analyses were performed for confirmation of the phosphorylation sites as well as for identification of potential CDK sites.

2.3.9 Recombinant protein expression and in vitro phosphorylation

Bacterially expressed substrates for in vitro phosphorylation were GST (pGEX-6P-3), Rad53 GST-Nter (GST-FHA1, Durocher et al., 1999) and Rad53 GST-Cter (GST-FHA2, Durocher et al., 1999) and induced by IPTG and purified with glutathione sepharose 4G (GE Healthcare). As control substrates for CDK Histone H1 (Sigma) was used and for Plk1 Casein (Sigma) was used. The purified recombinant kinases were XeCdc2/Cyclin B (a gift of P. Descombes) and human Plk1 (Proteinkinase.de).
The reaction buffer for in vitro phosphorylation is based upon protocols of Yamaguchi et al. (2005) and Choi et al. (1999) and contains 50 mM Tris pH 7.5, 10 mM $MgCl_2$, 1mM DTT, 3 μCi γATP, 20 μM ATP, 1mM PMSF, 0.1 mM sodiumorthovanadate, 1 mM NaF. The reaction was performed with 10 μg of substrate and 0.1 μg kinase in a total volume of 16 μl for 30 min at 30°C. The reaction was stopped by addition of 2x SDS sample buffer and heating to 95°C for 3 min. The full sample was loaded on 15% SDS-PAGE, the gels were vacuum dried and autoradiography was performed. Quantitive results were obtained by using an Imaging Screen K (Kodak) and Typhoon 9400 Variable Mode Imager (Amersham Bioscience). Images were quantified using Quantity One (Biorad).

2.4 Results

2.4.1 Rad53 is phosphorylated in a cell-cycle dependent manner in the absence of DNA damage

In this study we have addressed the question whether the Rad53 protein itself is modified in a cell-cycle dependent manner, and if this could contribute to the variation in the sensitivity of checkpoint signaling through the cell cycle. Rad53 is phosphorylated in response to DNA damage and this leads to a retarded migration pattern on SDS-PAGE (Sanchez et al., 1996; Sun et al., 1996). We arrested cells in G1 with α-factor, then took samples as cells progressed synchronously through the cell cycle in the absence of DNA damage after release. To see if there are cell-cycle dependent modifications of Rad53, we monitored migration of endogenous Rad53 by SDS-PAGE, maximizing separation by the use of 6% gels (see Material and Methods). We identified a novel cell-cycle dependent mobility shift for a portion of Rad53. This shift was observed in G1 phase, was not seen in S phase, and returned in G2- and M-phase cells as determined by the corresponding FACS profile (see Figure 2.1a). This cell-cycle dependent upshift was also observed in the second cell cycle after α-factor release, demonstrating that the shift was not a response to α-factor synchronization. This upshift was far less dramatic than the altered migration observed for hyperphosphorylated Rad53 in response to DNA damage (Figure 2.1a). We therefore found it important to determine if this novel modification stems from phosphorylation. To answer this question we treated immunoprecipitated Rad53 from G2/M phase cells with alkaline phosphatase (Supplemental Figure 2.1a). Both the DNA-damage dependent Rad53-hypershift and the cell-cycle dependent upshift could be reversed into a sharp band in the presence of alkaline phosphatase, while the addition of a phosphatase inhibitor abolished this effect. We conclude that the cell-cycle dependent shift is due to phosphorylation. DNA damage induced phosphorylation of Rad53 is dependent on the PI3-like kinase Mec1. We therefore asked if the novel cell-cycle dependent phosphorylation of Rad53 requires either Mec1 or the second PI3 kinase in yeast, Tel1. However, we still observe the cell-cycle dependent upshift of Rad53 in both a *mec1*-1 mutant (Figure 2.1b) and in a *mec1*-1 *tel1* double mutant (data not shown). From these results we conclude that the cell-cycle dependent phosphorylation of Rad53 is independent of checkpoint signaling.

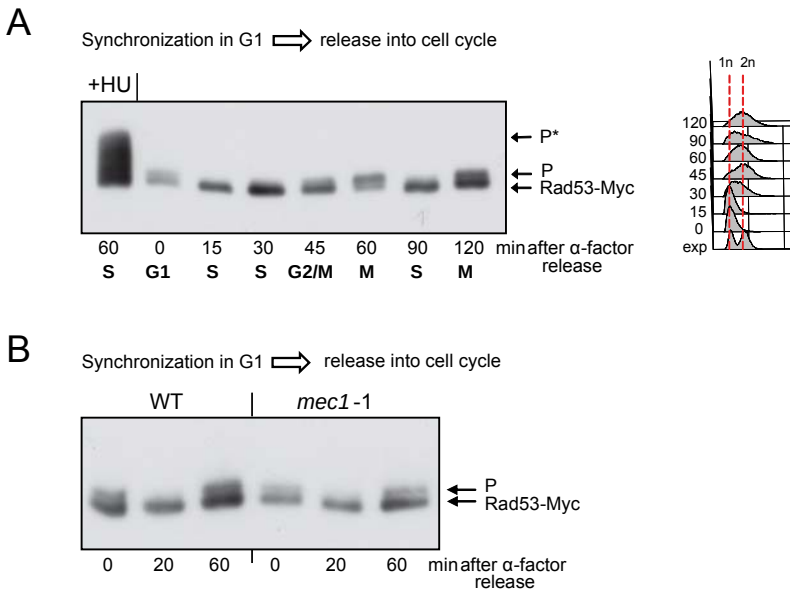

Figure 2.1: Rad53 is phosphorylated in a cell cycle-dependent manner in G1 and G2/M phase in the absence of DNA damage

A: Endogenous Rad53 undergoes a mobility shift on SDS-page in G1 and G2/M but not S phase. Yeast cells with Myc-tagged Rad53 (GA-2019) were blocked in G1 phase by α-factor for 120 min and released synchronously into S phase, samples were taken at the indicated time points and Rad53 migration pattern in the absence of damage was analysed by SDS-PAGE. Rad53 migration upon DNA damage (60 min in HU) represents hyperphosphorylated forms of Rad53 (P*). Western blot analysis was done with anti-Myc. The cell cycle position of the corresponding samples determined by FACS is shown in the right pannel.
B: The cell-cycle dependent phosphorylation of Rad53 is independent of Mec1 checkpoint function. WT (GA-1040) and *mec1*-1 *sml1* (GA-1048) mutant strains with Rad53-Myc were synchronized in G1 phase by α-factor for 75 min and released synchronously into S phase, samples were taken at the indicated time points and Rad53 migration pattern in the absence of damage was analysed by SDS-PAGE and probed with anti-Myc.

2.4.2 Rad53 is phosphorylated in its C-terminal part in a cell-cycle dependent manner

Rad53 contains a central kinase domain flanked by two FHA domains, FHA1 and FHA2, which are required for checkpoint signaling. The FHA1 domain was shown to be required for signaling mediated by the replication checkpoint pathway. The FHA2 domain is involved in the Rad53 response to the DNA damage signaling pathway, by binding the *RAD9* gene product (see section 2.2). To determine whether one of these Rad53 domains is the target of the cell-cycle dependent phosphorylation, we used a galactose-inducible system to express plasmids containing the N-terminal 165 amino acids (aa) including the FHA1 domain (pNter), the central protein part (aa 177-599) including the kinase domain (pKIN), and the C-terminal aa 497-821 including the FHA2 domain (pCter) of Rad53 (Figure 2.2a). To look specifically at Rad53

phosphorylation during M phase these fragments were induced in *cdc15*-2 cells at the non-permissive temperature, which arrests cells in mitosis (Figure 2.2b).

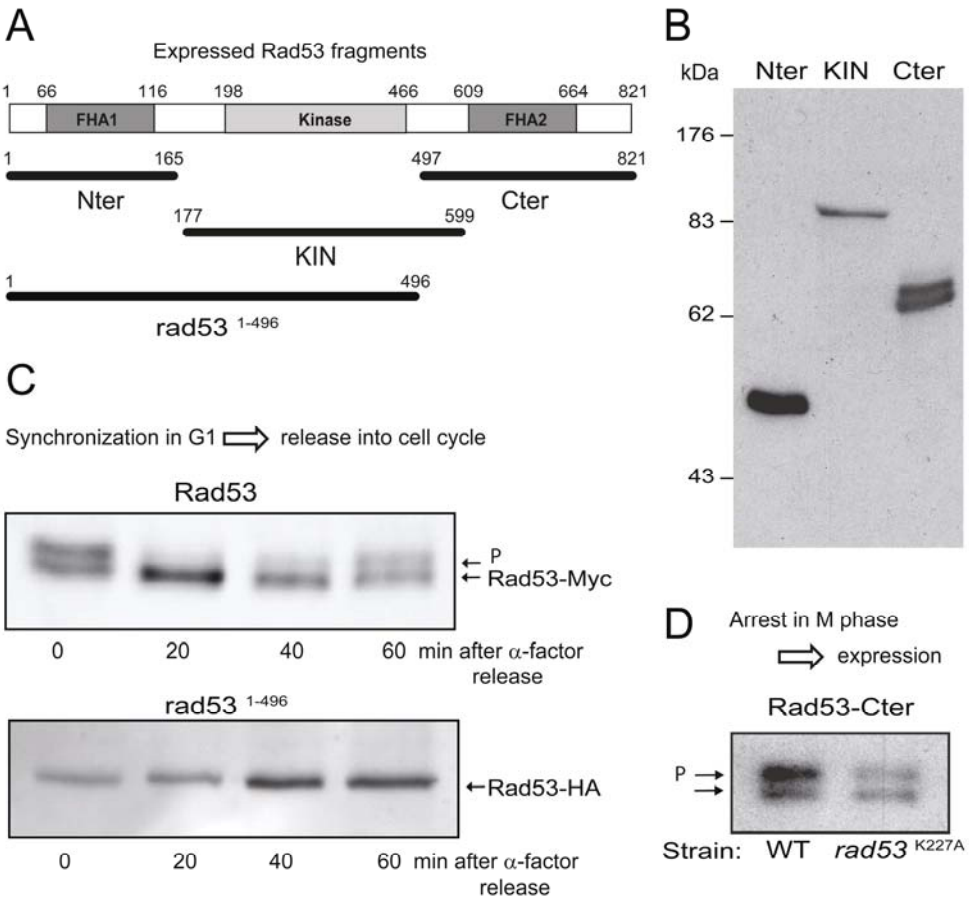

Figure 2.2: The cell-cycle dependent phosphorylation of Rad53 occurs in the C-terminal protein part

A: Schematic representation of Rad53 protein fragments. Protein fragments encoding the N-terminal (Nter), central (KIN) and C-terminal (Cter) regions of Rad53 that were expressed from a Gal-inducible yeast expression vector (Bjergbaek et al., 2005). The truncated form of endogenous Rad53 used in Figure 2.2d is indicated.
B: The protein fragment containing the FHA2 domain (Cter) induces additionally also a slower migrating form in SDS-PAGE during mitosis. A *cdc15*-2 temperature sensitive mutant strain (GA-1745) was grown on selective medium Sraff-trp at 23°C and shifted to restrictive temperature of 37°C for 2 hours. Protein expression was induced by addition of galactose and samples were taken after 60 min. Proteins were separated on 10% SDS-PAGE and probed with anti-HA.
C: Removal of aa 497-821 eliminates the cell-cycle dependent mobility shift in Rad53. WT Rad53-Myc (GA-2019) and Rad53-496HA (GA-3390) were synchronized in G1 phase by α-factor for 90 min and released synchronously into S phase, samples were taken at the indicated time points. Rad53-496HA was analysed on a 10% SDS page and run to the middle of the gel, full length WT control was run as usual on a 6% gel. Proteins were transfered on membrane and probed with anti-HA and anti-Myc, respectively.
D: Rad53 kinase activity is not needed for the C-terminal phosphorylation. WT (GA-2019) and *rad53*^{K227A} (GA-3188) mutant strains were transformed with pCter. Protein expression was induced by addition of galactose to nocodazole and benomyl arrested cells. Protein samples were taken after 60 min and separated on 10% SDS-PAGE and probed with anti-HA.

After *cdc15*-2 arrest, the Cter-fragment but neither Nter- nor KIN-fragments showed an upshift. The same result was obtained for fragments induced in α-factor arrested cells (data not shown). The C-terminal domain of Rad53 thus shows the same cell-cycle modification as full-length Rad53 (see Figure 2.1a). To confirm that the C-terminal sites are the only targets, we monitored cell-cycle dependent phosphorylation

of a truncated form of Rad53, which was created by inserting a HA-tag into the endogenous *RAD53* gene after residue 496, where the Cter domain starts (Figure 2.2a). In the Rad53 496-HA strain, the cell-cycle dependent mobility shift is lost (Figure 2.2c). This confirms that the phosphorylation marks responsible for the cell-cycle dependent upshift are found in the C-terminal aa 497-821 of Rad53.

We then asked whether the Cter upshift is due to an autophosphorylation event. We induced expression from pCter in a Rad53 kinase deficient mutant , *rad53* ^{K227A}, in cells arrested in mitosis with nocodazole. We observed no change in the upshift in comparison to a WT strain (Figure 2.2d). Hence the cell-cycle dependent phosphorylation of Rad53 is not due to Rad53 kinase autophosphorylation. Interestingly, the cell-cycle dependent phosphorylation of Rad53 may depend at least in part on a functional FHA2 domain, since a fragment bearing a mutation which specifically impairs the function of FHA (mutation R605A) showed reduced phosphorylation (Supplemental Figure 2.1b).

2.4.3 The cell-cycle dependent phosphorylation of Rad53 depends upon Cdc5 and Cdc28

To more specifically define the point in the cell cycle at which this novel phosphorylation of Rad53 occurs we looked at Rad53 mobility shifts in various *cdc* mutant strains that arrest at unique points of the cell cycle. We synchronized cells in α-factor and shifted the cultures to restrictive temperature, followed by release from α-factor, to allow cells to accumulate at their arrest points (Figure 2.3a). The *cdc7*-1 mutant arrests at origin firing, yet we note that the upshifted band of Rad53 is maintained even 120 min after α-factor release. This argues that not only passage through the G1/S boundary, but also origin firing must occur before the cell-cycle dependent phosphorylation of Rad53 is reversed. This mutation also rules out that Cdc7 is the Rad53 kinase.

The loss of phospho-Rad53 in S phase is not due to protein turnover (Supplemental Figure 2.2a), nor is it dependent on phosphatases Ptc2 and Ptc3, which dephosphorylate Rad53 during checkpoint adaptation (Leroy et al., 2003). Indeed, the cell-cycle dependent upshift is still reversed in a *ptc2*Δ *ptc3*Δ double deletion strain (Supplemental Figure 2.2b).

Our previous results (Figure 2.1a) suggested that the cell-cycle dependent phosphorylation occurs in G2/M phase cells. We therefore released cells from α-factor into a *cdc15*-2 and a *cdc16*-1 arrest, which reflect metaphase and cytokinesis, respectively. In these strains the Rad53 upshift disappeared for ~ 20 min after α-factor release (S phase) and was observed again upon entry into mitosis (60 min). The modification persisted for the full time of arrest, ruling out a role for the anaphase promoting complex in the phosphorylation event.

To sum up, the cell-cycle dependent phosphorylation of Rad53 occurs during the G2/M phase of the cell cycle and is present until S phase onset (origin firing). We deduce that a mitotic kinase is responsible for the cell-cycle dependent phosphorylation of Rad53; consistently we see that Cter is modified when induced at the mitotic arrest points of either *cdc16*-1 (metaphase) or *cdc15*-2 (telophase). However, it is not efficiently modified at the *cdc28*-4 (G1/S), *cdc4*-3 (G1/S) or *cdc53*-1 (G1/S) arrest points (Figure 2.3b).

Which mitotic kinase phosphorylates Rad53? Rad53 contains several minimal CDK consensus sites (Figure 2.5a) and its human homologue Chk2 was shown to be associated with and phosphorylated by the Polo-like kinase Plk1 (Tsvetkov et al., 2003). Indeed, the polo-like kinase, Cdc5, and the cyclin-dependent kinase, Cdc28, are conserved kinases with important mitotic activity in all species (Nigg, 1998). Based on this knowledge, we asked whether Cdc5 or Cdc28 mediates the cell-cycle dependent phosphorylation of Rad53. We shifted WT and *cdc5*-1 mutant cells to restrictive temperature of 37°C under addition of nocodazole (Figure 2.3c). We observed that in WT cells at 37°C the Rad53 protein is completely upshifted during the nocodazole-induced mitotic arrest. In contrast there is no detectable upshift in the *cdc5*-1 mutant cells at restrictive temperature, while it is detectable at 23°C. This points towards a direct role of Cdc5 in mediating the cell-cycle dependent phosphorylation of Rad53. This result is further substantiated by the observation that Cter is similarly modified in nocodazole, but not in *cdc5*-1 arrested cells (see Figure 2.3b).

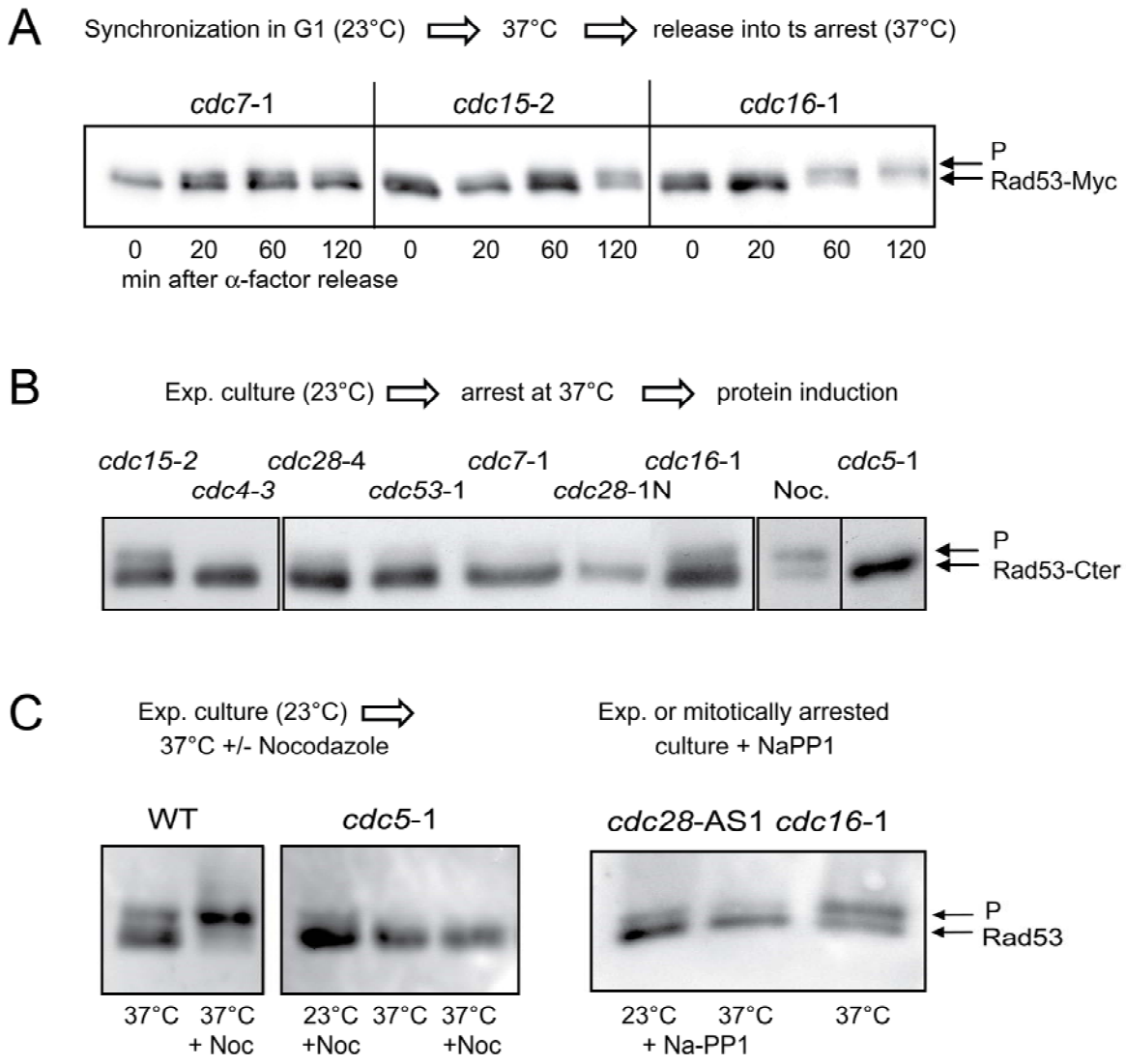

Figure 2.3: The cell cycle-dependent phosphorylation of Rad53 depends upon Cdc5 and partially upon Cdc28 gene function

A: Cells blocked in G1/S (*cdc7*-1), metaphase (*cdc16*-1) or telophase (*cdc15*-2) retain phosphorylated Rad53. Exponentially growing cultures of GA-1945 (*cdc7*-1), GA-1745 (*cdc15*-2) and GA-1159 (*cdc16*-1) were arrested by α-factor at 23°C for 90 min and then shifted in α-factor arrest to 37°C and released after 60 min into the cell cycle at 37°C. Rad53 was separated by SDS-PAGE and probed with anti-Myc.

B: Expression of Cter at different cell cycle arrest points shows the same cell-cycle dependent behavior as endogenous Rad53 and indicates requirement of the mitotic kinase Cdc5. Rad53-Cter was expressed at restrictive temperature in (*cdc15*-2: GA-1745, *cdc16*-1 (GA-2294), *cdc5*-1 (GA-214), *cdc28*-4 (GA-416), *cdc53*-1 (GA-1408), *cdc4*-3 (GA-1188), *cdc7*-1 (GA-1945) and *cdc28*-1N (GA-414) cells. Strains were grown on selective medium Sraff-trp at 23°C and shifted to restrictive temperature of 37°C for 2 hours. Protein expression was induced by addition of galactose and samples were taken after 60 min. Proteins were separated on 10% SDS-PAGE and probed with anti-HA.

C: Mitotic phosphorylation of endogenous Rad53 requires Cdc5 and is reduced if Cdc28 is specifically inhibited. WT (GA-180) and *cdc5*-1 mutant strains (GA-214) were arrested with nocodazole for 120 min either at permissive (23°C) or restrictive temperature (37°C). The *cdc28*-AS1 specific analog Na-PP1 was added to *cdc16*-1 *cdc28*-AS1 mutant cells (GA-2695) at permissive temperature for 180 min or at restrictive temperature for 90 min. Rad53 was separated by SDS-PAGE and probed with anti-Rad53.

The essential role of Cdc28 throughout the cell cycle makes it more difficult to ask if Cdc28 is involved in mediating the cell-cycle dependent phosphorylation of Rad53. For example the *cdc28*-1 mutant strain is known to arrest at START (Pringle and Hartwell, 1981) while the G2 defective allele *cdc28*-1N is defective only in cell cycle transition through G2, yet it maintains its kinase activity (Surana et al., 1991). Consistent with a role for a CDK, we saw a partial reduction of Rad53 upshift in the experiments using the *cdc28*-1 mutant strain and no reduction for the cdc28-1N mutant strain (data not shown). To be able to monitor Cdc28 activity in mitosis, we made use of a *cdc28*-AS1 *cdc16*-1 mutant strain, where Cdc28 can be specifically inhibited by addition of the ATP-analog Na-PP1 in cells arrested in mitosis at the restrictive temperature (Jaquenoud et al., 2002). We arrested cells in mitosis by shifting the culture to the restrictive temperature and added Na-PP1 to part of the culture. We observed a reduction of Rad53 upshift in the *cdc28*AS1 *cdc16*-1 cells treated with the CDK inhibitor Na-PP1 but not in its absence (Figure 2.3c). This result suggests that mitotic CDK is required for, or at least contributes to the cell-cycle dependent upshift of Rad53. Indirect support stems from our observation that there is a bigger upshift in cells arrested by *cdc16*-1, which arrests with elevated CDK activity than by *cdc15*-2 (see Figure 2.3a; Heichman and Roberts, 1996).

It was previously shown that nocodazole arrest activates Rad53 and that this depends completely upon Mad2 (Clemenson and Marsolier-Kergoat, 2006). We therefore looked if our cell-cycle dependent phosphorylation would still occur in a *mad2* mutant. We observed that the cell-cycle dependent phosphorylation of Rad53 is independent of Mad2 (Supplemental Figure 2.2c), and is therefore independent of the previously described mitotic spindle stress.

We next adressed the question whether the C-terminal part of Rad53 is a direct substrate for either Cdc5 or Cdc28 kinases *in vitro.* To address this question we performed an *in vitro* phosphorylation reaction using recombinant, purified GST-Cter as a substrate. The human Cdc5 homolog Plk1 and *Xenopus* CDK (Cdc2/Cyclin B) kinases were added with P^{32} labeled γATP (Figure 2.4a).

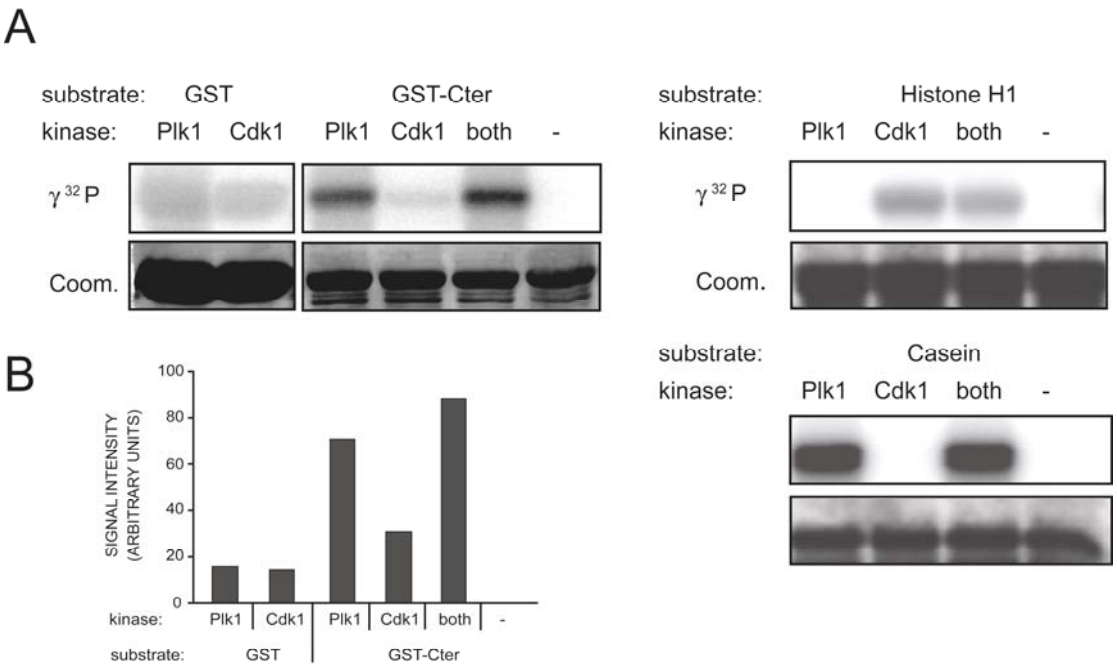

Figure 2.4: The polo-like kinase Plk1 targets the C-terminal part of Rad53

A: Human Plk1 phosphorylates the C-terminal part of Rad53 *in vitro.* Recombinantly expressed GST, Rad53 GST-Nter and Rad53 GST-Cter as well as control substrates Histone H1 and Casein were incubated with recombinant CDK (XeCdc2, CyclinB) and Plk1. Displayed are the autoradiogram showing P^{32} incorporation and the coomassie stained gel for protein loading. **B: Quantification of experiment A shows that Rad53 GST-Cter is phosphorylated efficiently by Plk1 *in vitro*.** Displayed is the signal intensity of the autoradiogram displayed in A.

For the control substrates histone H1 (for CDK) and Casein (for Plk1) were used. This confirmed that the enzymes were active and working properly in the chosen buffer environment. The phosphorylation reaction using GST-Cter as a substrate led to substantial P^{32} incorporation by Plk1, either when Plk1 was added alone or together with CDK (Figure 2.4a). However we observed weak P^{32} incorporation using CDK alone. We saw no significant background phosphorylation of GST alone, instead. Quantification of the signal intensity of P^{32} incorporation normalized to substrate amount, showed a strong increase by Plk1 but a weak one with CDK (Figure 2.4b). While these results confirm that the human Cdc5 homolog Plk1 can phosphorylate the C-terminal part of Rad53 *in vitro*, the lack of effect by human CDK is not conclusive, given the cross species substrate and lack of full-length substrate. We also cannot rule out that CDK-mediated phosphorylation of certain substrates is sensitive to buffer conditions. Our *in vivo* and *in vitro* results strongly suggest that the C-terminal cell-cycle dependent phosphorylation of Rad53 depends on Cdc5 and Cdc28. The presence of consensus motifs for CDK phosphorylation in the Rad53 protein suggests that this latter is also a direct effect.

2.4.4 Serines 774 and 789 in the C-terminal part of Rad53 are phosphorylated in the absence of DNA damage

Our results argue for the involvement of Cdc5 and Cdc28 kinases. Therefore we looked for potential phosphorylation consensus sites for these kinases in Rad53, based on sequence predictions.

It is difficult to predict phosphorylation sites for polo-like kinase because of the absence of a clearly determined consensus motif. However a consensus motive for Plk1 was suggested as D/E-X S/T –Φ-X-D/E (X, any amino acid, Φ, a hydrophobic amino acid, (Nakajima et al., 2003). Interestingly we observe that serine 198 of Rad53 fulfills these consensus criteria of being a polo-like kinase target site. Consistently, we observe that the N-terminal fragment of Rad53 (GST-Nter) gets efficiently phosphorylated by Plk1 (data not shown). We did not detect such a consensus in the C-terminal part of Rad53. On the other hand it has been argued that this consensus is too strict to account for many known Plk1 phosphorylation sites (Moshe et al., 2004).

CDK sites are more readily predictable and the consensus sequence for CDK mediated phosphorylation is S/T-P-X-K/R (Endicott et al., 1999). Some yeast targets contain only the minimal consensus sequence S/T-P (Rudner and Murray, 2000; Ubersax et al., 2003) and Rad53 contains S-P dipeptides at positions 175, 375, 469, 639 and 774. Figure 2.5a depicts these potential CDK sites as well as DNA damage induced phosphorylation sites along the Rad53 protein.

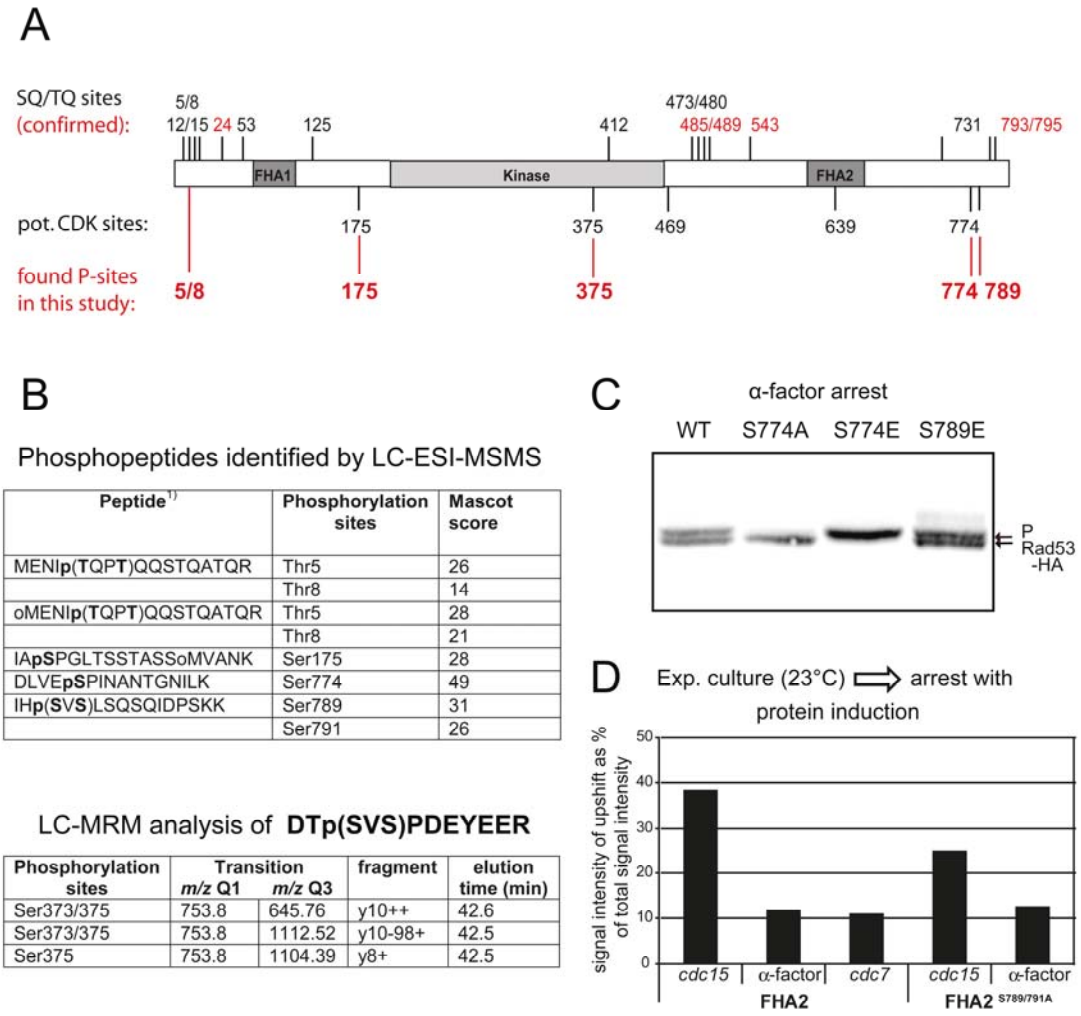

Figure 2.5: Ser774 and Ser789 of Rad53 are found to be phosphorylated in the absence of DNA damage by mass spectrometry

A: Representation of domain structure and known SQ/TQ phosphorylation sites that are important for activation of Rad53 by Mec1/Tel1 in response to DNA damage (Schwartz et al., 2003). Some of these sites were confirmed to be phosphorylated in vivo and are labled red (Smolka et al., 2005; Sweeney et al., 2005). Shown are also potential CDK target sites and sites found in this study as listed in panel B.
B: Mass spectrometric analysis of Rad53 indicates a phosphorylation at Ser774 and Ser789 in the absence of exogenous DNA damage. Represented is the amino acid sequence of the peptide, in which the phosphorylation sites were found. Also further phosphorylation sites found in this study are indicated.
1) The phosphorylated amino acid is in bold preceded by a 'p'. Oxidized methionine is marked with a preceding 'o'.
C: Phosphorylation of Ser774 but not Ser789/791 is required for the cell-cycle dependent upshift in full length Rad53. *rad53 sml1* mutant cell cultures (GA-3455) with the described Rad53 alleles borne on plasmids (*rad53*^{S774A}, *rad53*^{S774E}, *rad53*^{S789E}) were synchronized in α-factor for 90 min. Protein extracts were separated by SDS-PAGE and probed with anti-HA.
D: Ser789/791 is important for the mitotic upshift of Cter. *cdc15*-2 (GA-1745) and *cdc7*-1 (GA-1945) cells containing the indicated plasmids were grown on selective medium Sraff-trp at 23°C and shifted to restrictive temperature of 37°C for 2 hours. Protein expression was induced by addition of galactose and samples were taken after 60 min. WT (GA-2019) cells were correspondingly arrested by α-factor and protein expression was induced. Proteins were separated on 10% SDS-PAGE and probed with anti-HA.

We next determined phosphorylation sites of Rad53 by mass spectrometry. We enriched endogenous C-terminally Myc-tagged Rad53 from mitotically arrested cells by immunoprecipitation and identified phosphorylation sites after tryptic digestion by determining the peptide sequence via LC-MSMS. We used a data dependent analysis approach as well as a candidate based approach for the potential CDK sites. Under

these conditions we found that Ser774 as well as Ser789 and/or Ser791 are phosphorylated in the absence of exogenous DNA damage. The sequences of the peptides and the phosphorylation sites that were found are shown in Figure 2.5b. Representative MSMS spectra of the peptides phosphorylated at Ser774 and at Ser789 are shown in Supplemental Figure 2.3a and 2.3b.

Of the CDK sites predicted from sequence, besides the C-terminal potential CDK site at Ser774, the potential CDK site at Ser175 was also shown to be phosphorylated in mitosis in the absence of DNA damage. Multiple reaction monitoring analyses also indicate a likely modification of Ser373 or 375; but no confirmation was obtained by MSMS sequencing. No evidence was found for a phosphorylation of Ser469 or 639. Besides these phosphorylated CDK sites, and the Ser789 phosphorylation, we also found that the N-terminal Rad53 peptide is acetylated as well as phosphorylated in the absence of DNA damage in mitotic cells. Amino acids 1-17 contain one of the TQ clusters important for Rad53 activation by Mec1/Tel1 in response to DNA damage (Figure 2.5a) and TQ sites at aa 5 and 8 are phosphorylated in the absence of exogenous DNA damage. This is an unexpected finding and could stem either from signaling of low levels of endogenous DNA damage or from a yet unknown function of Mec1 signaling via Rad53 during mitosis, as the benomyl-sensitivity of both, *rad53* and *mec1* mutants may suggest (Supplemental Figure 2.4a).

We focused our further study on analyzing the function of Ser774 and Ser789/791 phosphorylation, as these were the sites confirmed to be phosphorylated within the C-terminal part of Rad53 during mitosis (see Figure 2.5a). To address if phosphorylation of Ser774 or Ser789 is inducing the cell-cycle dependent upshift Rad53 monitored on western blot we mutated first Ser774 to alanine or glutamic acid in HA-tagged full length Rad53 expressed from the endogenous promoter on a CEN/ARS plasmid. We observed that Rad53^{S774A} migrates as the non phosphorylated protein does in α-factor arrested cells, whereas Rad53^{S774E} migrates with the same mobility as the cell-cycle dependent upshifted form of Rad53 (Figure 2.5c). Indeed, mass spectrometry confirmed, that phosphorylated Ser774 mainly occurs in the upshifted fraction of the Rad53 protein (data not shown). However we do not observe any effect on the Rad53 upshift after mutating Ser789 and/or Ser791 in G1 phase cells (Figure 2.5c and Supplemental Figure 2.1c). Rad53 containing Ser639Ala, Ser774Ala, Ser789Ala and Ser791Ala mutations (*rad53*^{CCA2}) migrated the same as *rad53*^{S774A} (Supplemental Figure 2.1c and data not shown). While Ser789/791 phosphorylation

does not contribute to the upshift, this phosphorylation was identified by mass spectrometry of cells arrested in mitosis and the Ser789/791Ala mutation in Cter reduces its upshift by half (Figure 2.5d) This argues that Ser789/791 do function in the DNA damage-independent, cell-cycle dependent phosphorylation of Rad53.

2.4.5 Mutation of the cell cycle dependent phosphorylation sites in Rad53 affects checkpoint adaptation

What is the physiological role of the cell-cycle dependent phosphorylation of Rad53? We made use of plasmid-borne C-terminally HA-tagged Rad53 alleles expressed under control of the endogenous promoter, to address the question if cell growth in the presence of DNA damaging drugs might be impaired in the absence of the cell-cycle dependent phosphorylation sites.

Figure 2.6a shows that *rad53*Δ mutants are not viable on plates containing HU or MMS in concentrations at which WT strains are still able to grow. Similarly sensitive are *rad53*^{A8} and *rad53*^{A9} mutants, as reported previously (Sweeney et al., 2005). In contrast the mutants of interest, in which Ser789 and Ser791 are mutated to alanine (*rad53*^{CCA1}, (Sweeney et al., 2005) or in which Ser639, Ser774, Ser789 and Ser791 are mutated to alanine (*rad53*^{CCA2}), showed no loss of survival in the presence of the genotoxic drugs (HU and MMS, Figure 2.6a) nor after irradiation with X-rays or UV (Supplemental Figure 2.5a).

Rad53 was previously shown to be important for regulation of origin firing (Dohrmann et al., 1999; Duncker et al., 2002; Santocanale and Diffley, 1998). Since we monitor persistence of the cell-cycle dependent phosphorylation event upon replication onset (Figure 2.3a), we asked if cell cycle progression from G1 into and through S phase might be impaired. We monitored cell cycle progression after α-factor release for WT, *rad53*Δ, *rad53*^{CCA1} and *rad53*^{CCA2}. However cell-cycle progression in these mutants was not impaired (Supplemental Figure 2.6a).

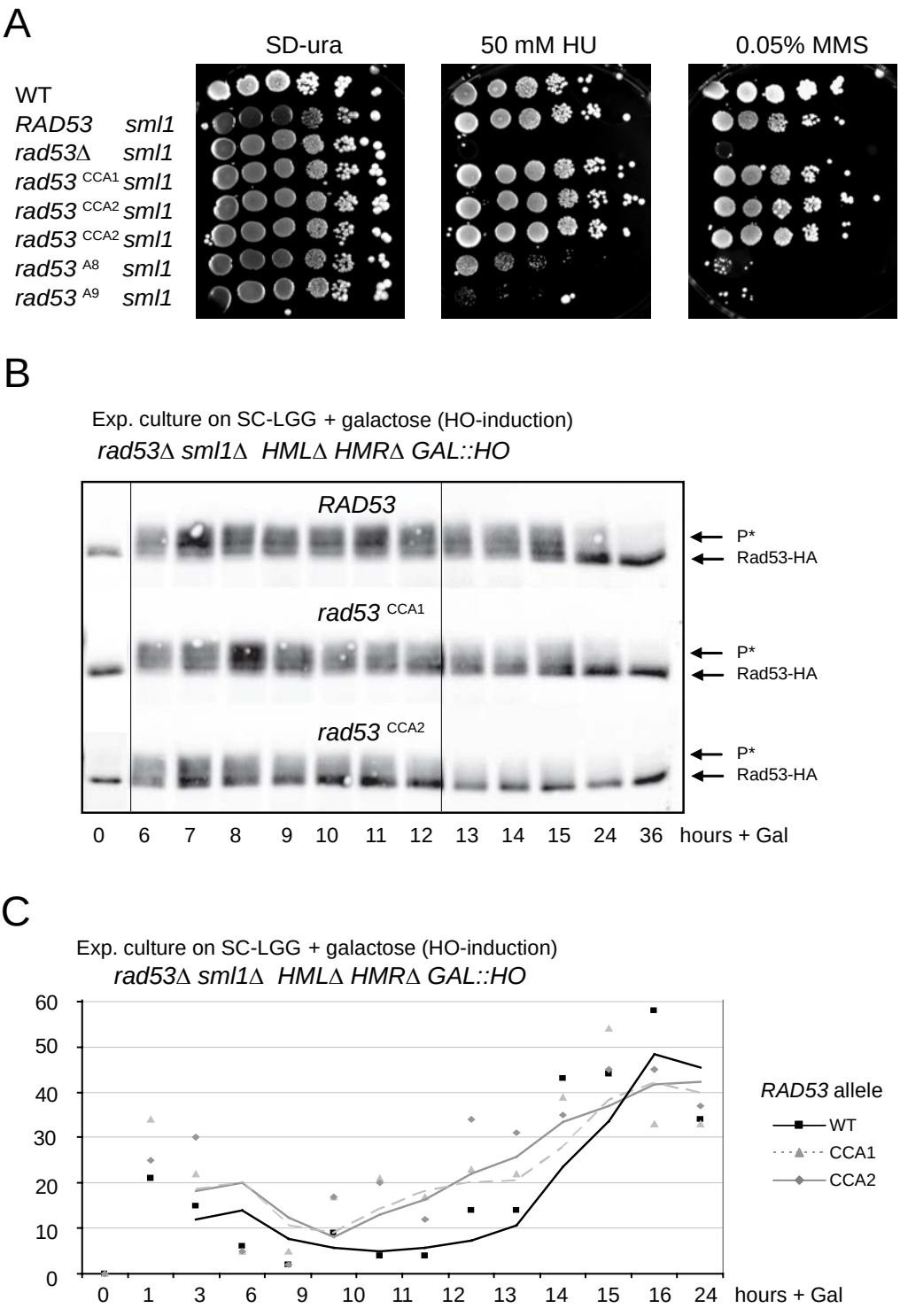

Figure 2.6: Mutation of cell-cycle dependent phosphorylation sites in Rad53 leads to faster adaptation of the G2/M checkpoint.

A: *rad53*^{CCA2} mutant cells have no defect in cell viability or cell growth in response to HU and MMS. Shown is a drop assay of 10 fold serial diluted *rad53 sml1* mutant cell cultures (GA-3455) with the described Rad53 alleles on plasmid for complementation on plates with the indicated drug concentration.

B: Loss of phosphorylation at Ser774 and Ser789/791 leads to faster Rad53 inactivation in response to an irreparable DSB. Exponentially growing yeast strains (GA-1693) bearing the corresponding Rad53 allele on a plasmid were exponentially grown in SLGG-ura medium and the irreparable HO-cut was induced by addition of galactose. Protein samples were taken at the indicated timepoints and separated by SDS-PAGE. Rad53 activation and deactivation kinetics were probed with anti-HA.

C: Rad53 mutation of Ser789 into alanine (and additionally Ser774 into alanine) results in faster adaptation and reentry of cell cycle. The percentage of budded cells was monitored for the corresponding time points of the experiment shown in panel B and is represented as moving average with period =3.

There was also no defect in cell cycle progression for the phosphomimicking mutants *rad53*^{S789E} and *rad53*^{S774E} (Supplemental Figure 2.6). This argues that cell-cycle dependent phosphorylation of Rad53 does not regulate or influence cell-cycle progression itself. Since it is known that the level of damage required for Rad53 activation differs during the cell cycle (Shimada et al., 2002), we next assayed whether the cell-cycle dependent phosphorylation of Rad53 affects its activation in the cell cycle phase where it appears. To address this we monitored Rad53 activation in the *rad53*^{CCA1} and *rad53*^{CCA2} mutants during activation of the G2/M checkpoint. The G2/M checkpoint is highly sensitive to DNA damage, and one DSB is sufficient to trigger Rad53 activation (Pellicioli et al., 2001). Our previous results exclude the possibility, that the G2/M checkpoint would be completely deficient in *rad53*^{CCA1} and *rad53*^{CCA2} mutants. We therefore assayed for a drop in sensitivity. In WT and the corresponding mutant strains we generated a single irreparable DSB using the HO endonuclease, and we monitored Rad53 hyperphosphorylation in response to this DSB over 36 hours (Figure 2.6b). Rad53 WT cells are known to undergo adaptation in response to an irreparable break after 15-18 hours (Pellicioli et al., 2001). It is not yet known to what extent down-regulation (through phosphatases) and/or diminished activation (through impaired DNA damage signaling or constant activating events) affect Rad53 inactivation.

Our results showed that initial Rad53 activation occurred in *rad53*^{CCA1} and *rad53*^{CCA2} mutants as in WT cells (Figure 2.6b 6 hours). However, the fraction of protein undergoing complete hyperphosphorylation is reduced for the *rad53* ^{CCA2} mutant, suggesting that activation is slightly diminished. Interestingly we saw that while the *rad53*^{CCA1} and *rad53*^{CCA2} mutant proteins returned to the unmodified state by 12 hours, the WT Rad53 remained hyperactivated at 12 hours. This effect persisted at later time points. To verify that *rad53*^{CCA1} and *rad53*^{CCA2} mutants indeed have a more rapid checkpoint adaptation we monitored reentry into the cell cycle by counting the number of budded cells at all the time points. This suggests that the cells have adapted and passed into the next cell cycle. Figure 2.6c shows that there are no budded cells when cells respond to the G2/M checkpoint (6 h). However, *rad53*^{CCA1} and *rad53*^{CCA2} mutants start rebudding at 10 hours after break induction, whereas WT cells stay arrested for 12 hours (Figure 2.6c). This shows that *rad53*^{CCA1} and *rad53*^{CCA2} mutants adapt more rapidly after arrest due to an irreparable DSB.

Interestingly, Cdc5 has already been previously implicated in checkpoint adaptation, as demonstrated by the *cdc5-ad* allele (Toczyski et al., 1997). Therefore we checked whether the cell-cycle dependent upshift would still occur in a *cdc5*-ad mutant strain. We observed an identical pattern of Rad53 migration in the *cdc5-ad* mutant in both α-factor and nocodazole (see Supplemental Figure 2.1c). This is reasonable, since we observed for *rad53*^{CCA1} and *rad53*^{CCA2} a faster checkpoint adaptation, while the *cdc5-ad* mutant has a defect in adaptation (Toczyski et al., 1997).

The lower extent of Rad53 hyperphosphorylation at early time points for *rad53*^{CCA2} (Figure 2.6b, 6 hours) suggested that there may be reduced Rad53 activation. To address this possibility, we looked at early Rad53 activation in G2/M (in cells blocked with nocodazole) after treating cells with low amounts of Zeocin (Delacote et al., 2007; Povirk, 1996). Different concentrations of Zeocin were tested to determine the timing and dosage needed for checkpoint activation (data not shown). Supplemental Figure 2.5b shows that the hyperphosphorylation and therefore upshift of Rad53 is diminished in the *rad53*^{CCA2} strain as compared to *RAD53*. This reduced activation is even more obvious in a *rad24* background, which reduces the sensing of DNA damage (Bjergbaek et al., 2005; de la Torre-Ruiz et al., 1998) ; Supplemental Figure 2.5b). This observation is confirmed by quantifying the upshift versus total protein for the *rad53*^{CCA2} allele and the WT *RAD53* (see Supplemental Figure 2.5c). We conclude that the faster adaptation to DNA damage in G2/M phase of the cell cycle in *rad53*^{CCA1} and *rad53*^{CCA2} mutants stems from decreased activation of Rad53 through lack of the cell-cycle dependent phosphorylation.

2.4.6 Rad53 is hyperphosphorylated if CK2 is inactivated and a small amount of DNA damage occurs at the same time

Since the cell-cycle dependent phosphorylation of Rad53 is dependent upon Cdc5, which is also important for checkpoint adaptation, we next tested whether another kinase known to be important for checkpoint adaptation, CK2 (Toczyski et al., 1997), functions in Rad53 phosphorylation. CK2 is encoded by two genes for the catalytic subunits Cka1 and Cka2, and two for the regulatory subunits Ckb1 and Ckb2 (Glover, 1998). A knockout of both catalytic subunits is inviable. We therefore used temperature-sensitive mutant strains, in which the *CKA1* gene is deleted and the *CKA2* gene is replaced by temperature sensitive mutant alleles *cka2*-8 or *cka2*-13.

These deplete CK2 activity at restrictive temperature (Hanna et al., 1995). Strains bearing these mutant alleles do not arrest completely at 37°C, but require 38.5°C (Hanna et al., 1995). To address whether CK2 inactivation affects the cell-cycle dependent phosphorylation of Rad53 or not, we arrested cells in mitosis and inactivated CK2 by shifting these mutants to restrictive temperature. Monitoring the phosphorylation status of Rad53 on Western blot, we observed no disappearance of the cell-cycle dependent phosphorylation of Rad53 in the *cka1*Δ *cka2*-8 or *cka1*Δ *cka2*-13 mutant cells. Instead we detected a hyperphosphorylation of Rad53, similar to the level observed after checkpoint activation (see Figure 2.7a, compare Figure 2.1a). We also noted a slight upshift for *cka1*Δ *CKA2* cells, supporting the idea that high temperatures might create some minor DNA damage or DNA damage-like signaling. Nevertheless, the ratio of hyperphosphorylated/basal Rad53 is strongly altered in the *cka2*-8 or *cka2*-13 mutant cells. In the mutants, the major Rad53 band consists of hyperphosphorylated Rad53. Furthermore, since the result obtained is the same for *cka1*Δ *cka2*-8 and *cka1*Δ *cka2*-13 mutant cells, this hyperphosphorylation does not reflect an allele-specific defect, but rather the inactivation of *CKA2*.

To examine whether this checkpoint activation can be induced by exogenous DNA damage in *cka1*Δ *cka2*-13 mutant cells at sub-restrictive temperature (37°C), which *per se* does not lead to hyperphosphorylation of Rad53 in WT (Figure 2.3a), we generated exogenous DNA damage by adding a small amount of Zeocin (5µg/ml) to the culture. We compared Rad53 migration in nocodazole arrested cells at 23°C, 37°C, 37°C + Zeocin, and 38.5°C. As expected, in WT cells, we do not monitor complete upshift due to hyperphosphorylation at 37°C + Zeocin or at 38.5°C, yet we see strong hyperphosphorylation at both conditions in *cka1*Δ *cka2*-13 mutant cells (Figure 2.7b). Since there is no hyperphosphorylation in *cka1*Δ *cka2*-13 mutant cells at 37°C we conclude that higher temperature, as well as a low amount of DNA damage, induce Rad53 hyperphosphorylation in the absence of CK2.

The lack of CK2 could induce Rad53 hyperphosphorylation by different mechanisms. One possibility is that the lack of CK2 induces a DNA damage signal by itself. This is unlikely, since we observe hyperphosphorylation in *cka1*Δ *cka2*-13 mutant cells at 37°C + Zeocin, however not 37°C (Figure 2.7b).

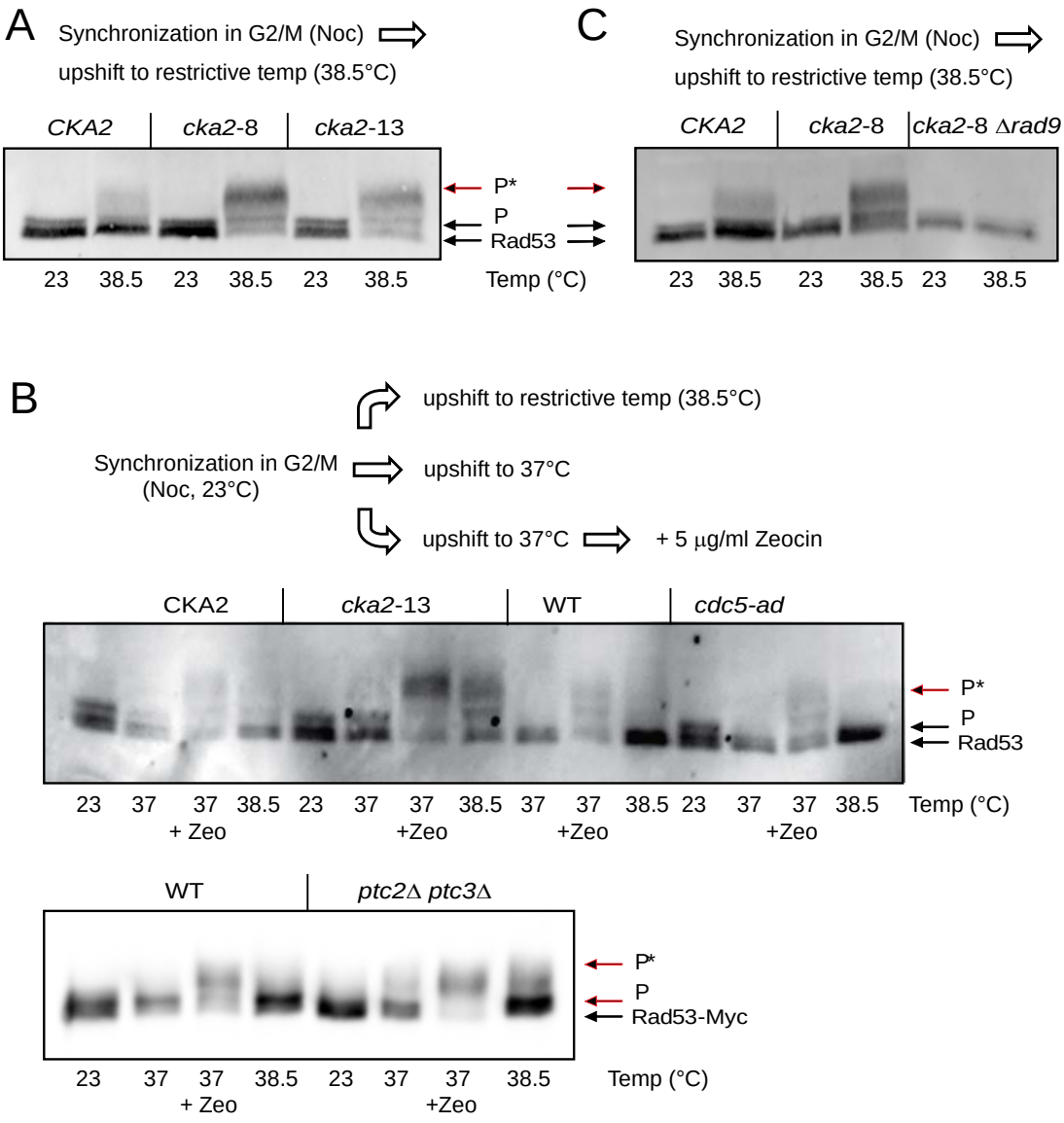

Figure 2.7: Rad53 is hyperphosphorylated if CK2 is inactivated and a small amount of DNA damage occurs

A: Inactivation of CK2 in temperature sensitive mutant strains by high temperature leads to hyperphosphorylation of Rad53 through high temperature. Yeast strains GA-141 (CKA2 *cka1*Δ), GA-142 (*cka2-8 cka1*Δ) and GA-143 (*cka2*-13 *cka1*Δ) were exponentially grown and then arrested with nocodazole and benomyl in mitosis for 120 min, followed by an upshift to 38.5°C to inactivate CK2 ts alleles for 120 min. Shown is Rad53 mobility for samples taken before and after the temperature shift. Protein samples were taken before (Noc) and after temperature shift (38.5°C), separated by SDS-PAGE and probed with anti-Rad53.

B: Hyperphosphorylation of Rad53 can also be induced by a small amount of exogenous DNA damage at subrestrictive temperature and is specific to the involvement of CK2 but not other components of the checkpoint adaptation response. Yeast strains GA-141 (*CKA2 cka1*Δ), GA-142 (*cka2-8 cka1*Δ), GA.143 (*cka2*-13 *cka1*Δ), GA-2019 (wt Rad53-myc), GA-3194 (*ptc2*Δ *ptc3*Δ Rad53-myc), GA-3533 (wt for GA-3530) and GA-3530 (*cdc5-ad*) were exponentially grown and then arrested with nocodazole and benomyl in mitosis, followed by an upshift to 38.5°C for 120 min. or the subrestrictive temperature of 37°C for 90 min to inactivate ts CK2 alleles and then 5µg/ml Zeocin Zeocin was added for 30 min. Shown is Rad53 mobility for samples taken before (Noc) and after the temperature shift +/- Zeocin. Protein samples were taken at the corresponding time points, separated by SDS-PAGE and probed with anti-Rad53.

C: The hyperphosphorylation of Rad53 due to CK2 inactivation at restrictive temperature depends on an intact checkpoint signaling pathway. Yeast strains GA-141 (*CKA2 cka1*Δ), GA-142 (*cka2-8 Δcka1*Δ), GA-4347 (*rad9 CKA2 cka1*Δ) and GA-4348 (*rad9 cka2-8 cka1*Δ) were arrested in mitosis by nocodazole and benomyl for 90 min, followed by shifting the culture to 38.5°C for 90 min. Protein samples were taken before (Noc) and after temperature shift (38.5°C), separated by SDS-PAGE and probed with anti-Rad53.

Since CK2 function is already abolished at 37°C, this makes the creation of *de novo* DNA damage signaling by pure lack of CK2 unlikely. To test if Rad53 hyperphosphorylation in the absence of CK2 requires DNA damage signaling we created a *RAD9* deletion in the *cka1*Δ *cka2*-8 mutant strain. Cells mutated for *RAD9* are impaired for Rad53 activation (de la Torre-Ruiz et al., 1998; Navas et al., 1996) and upon shifting cells to 38.5°C, we accordingly observed no Rad53 hyperphosphorylation in the *cka1*Δ *cka2*-8 *rad9* mutant strain (Figure 2.7c). To test if the temperature sensitivity of CK2 mutants is induced by a checkpoint response, we monitored viability of *cka1*Δ *cka2*-8 *rad9*Δ versus *cka1*Δ *cka2*-8 and *cka1*Δ *CKA2* cells at 30, 37 and 38.5°C. We show that *cka1*Δ *cka2*-8 *rad9*Δ and *cka1*Δ *cka2*-8 were indistinguishable, with equal loss of viability under these conditions (data not shown).

A second possibility for the observed effect of CK2 deficiency on Rad53 hyperphosphorylation would be that CK2 directly phosphorylates Rad53 in response to high temperature, or to low amounts of DNA damage. This then would downregulate the checkpoint response. However, we do not have yet any indication for a direct phosphorylation of Rad53 by CK2.

A third possibility is that CK2 is required for the activation of proteins which downregulate the activation of Rad53 in response to DNA damage. This would lead to lower levels of activation in CK2 WT cells, as opposed to cells mutant for CK2. Obvious candidates would be phosphatases that dephosphorylate activated Rad53. The phosphatases Ptc2 and Ptc3 were shown to dephosphorylate Rad53 during checkpoint adaptation (Leroy et al., 2003) and it was shown recently that CK2 phosphorylates Ptc2 and Ptc3 directly. This phosphorylation increases their enzymatic function, promoting checkpoint adaptation (Guillemain et al., 2007). We therefore tested whether *ptc2*Δ *ptc3*Δ double mutants also show Rad53 hyperphosphorylation at 37°C + Zeocin and at 38.5°C (Figure 2.7b). This is indeed the case.

We also observe no increase in hyperactivation of Rad53 in the adaptation deficient mutant strain, *cdc5-ad*, excluding the possibility that our observation is a general hallmark of all adaptation deficient mutants. Instead this suggests a specific role of CK2 in adaptation.

2.5 Discussion

2.5.1 Phosphorylation of Rad53 in a cell-cycle dependent manner depends on Cdc5 and Cdc28

In the current study we provide evidence that Rad53 is phosphorylated in a cell-cycle dependent manner, independent of the DNA damage checkpoint response. This phosphorylation occurs in mitosis (see Figure 2.1, Figure 2.3). Rad53 was previously shown to be phosphorylated in nocodazole-arrested cells (Clemenson and Marsolier-Kergoat, 2006). In this case activation of the spindle checkpoint was shown to trigger phosphorylation of Rad9 as well as Rad53. This phosphorylation is abolished in spindle defective mutants, such as a *mad2* mutant. We ruled out this pathway for the cell-cycle dependent modification reported here (Supplemental Figure 2.2c). The phosphorylation we observe is therefore novel and un-related to the observations made by Clemenson and Marsolier-Kergoat (2006).

We furthermore observed that the cell-cycle dependent phosphorylation of Rad53 depends on both Cdc5 and Cdc28 (Figure 2.3 and 2.4). Cdc5 is an important regulator of mitosis and its kinase activity is restricted to the G2/M phase of the cell cycle (Cheng et al., 1998). Intriguingly, Cdc5 gets phosphorylated in a Rad53-dependent manner in response to DNA damage (Cheng et al., 1998).

In contrast to human Plk1, which efficiently phosphorylates Rad53 *in vitro*, we did not observe *in vitro* phosphorylation of the C-terminal part of Rad53 by *Xenopus* CDK/Cyclin B. One possible explanation for our observation is that the substrate site can only be phosphorylated by the yeast Cdc28 enzyme in combination with the right cyclin. Cyclin specificity has been shown to be very important for selective phosphorylation of a large number of substrates (Loog and Morgan, 2005). Indeed, we found potential CDK-sites at position 175 and 375 phosphorylated in mitosis in the absence of DNA damage. Phosphorylation of these sites was confirmed by other studies (Smolka et al., 2005; Sweeney et al., 2005).

2.5.2 The cell-cycle dependent phosphorylation of the C-terminus of Rad53 influences the threshold for Rad53 activation

We mapped the mitotic phosphorylation event to the C-terminal part of Rad53 (Figure 2.2). In this part of Rad53 Ser774 and Ser789 were confirmed to be phosphorylated in the absence of DNA damage and mutation of both affect the mitotic Rad53 mobility shift on SDS-PAGE (see Figure 2.5). Also other studies indicate phosphorylation of Rad53 at these positions. Ser774 was indicated, however not clearly confirmed, to be phosphorylated in the absence of DNA damage (Smolka et al., 2005). Smolka et al propose that Ser789 could be the major initial autophosphorylation site of Rad53 (Smolka et al. MCP 2005), whereas Sweeney et al. propose Ser789 as a Mec1/Tel1 target site (Sweeney et al., 2005). We and they, however, find Ser789 phosphorylation in the absence of DNA damage (Sweeney et al., 2005).

Both sites occur in close proximity to two Mec1-phosphorylation sites and phosphorylation of Ser774 as well as Ser789 might influence the interaction dynamics of the close FHA2 domain, or directly the kinase activity of the holoprotein. The FHA2 domain is only known to be targeted via the Rad9-mediated DNA damage checkpoint, therefore we would expect a cell-cycle dependent phosphorylation in the C-terminal part of Rad53 may influence the DNA-damage checkpoint. We looked at activation (Supplemental Figure 2.5) as well as maintenance (Figure 2.6) of Rad53 activation in response to a single DSB or small dose of DSB creating drugs in the corresponding alanine mutants and observe impaired checkpoint function. This result is in accordance with a very sensitive checkpoint in G2/M phase cells and a higher threshold for Rad53 activation in S phase cells (Shimada et al., 2002). The cell-cycle dependent phosphorylation of Rad53 could contribute to such a threshold of Rad53 activation, however not in an exclusive manner, since we do not observe any loss of viability in *rad53*^{CCA1} and *rad53*^{CCA2} mutant cells on plates containing genotoxic drugs (Figure 2.6).

Rad53 is effector kinase of the checkpoint signaling pathway, which might be influenced also at other stages. Evidence for this comes from human cells, where once again CDK regulates the checkpoint response. ATRIP, the human Ddc2 homologue, was shown to be phosphorylated by CDK, and mutation of the phosphoacceptor site caused a defect in the maintenance of the G2/M checkpoint (Myers et al., 2007). Also DNA damage detection by sensor proteins might be limited in S phase. Following up

the study of Shimada et al. (2002), we found that higher levels of the sensor protein Rad24 can stimulate Rad53 activation via the intra-S-phase checkpoint response in an *orc2*-1 mutant strain. This result suggests that DNA damage sensing an upstream checkpoint signaling might be limiting in S phase (Schleker, 2003). In another study it was suggested that also partial loss of the Rad53 kinase by reduction of its protein levels provides cells with a growth advantage through premature checkpoint inactivation in the presence of MMS-induced alkylating damage but not in response to HU-stalled replication forks (Cordon-Preciado et al., 2006). This observation was strictly limited to alkylating damage, where checkpoint activation occurs in S phase cells (Tercero et al., 2003).

2.5.3 How does the cell-cycle dependent phosphorylation influence adaptation?

As a unicellular organism where the alternative to growth is death, yeast cells seem have to evolved to override the DNA-damage induced checkpoint arrest and reenter cell cycle in response to limited damage after a time-period sufficient for DNA repair, increasing strain viability (Galgoczy and Toczyski, 2001; Toczyski et al., 1997).

The observation that activation as well as maintenance of the checkpoint (faster adaptation) are affected when the cell-cycle dependent phosphorylation sites Ser774 and Ser789 are mutated, suggests a model where constant signal input is needed to maintain an active checkpoint response and to avoid early adaptation. We propose that the cell-cycle dependent phosphorylation lowers the signal threshold needed to reach Rad53 activation by reducing the number of Mec1-mediated phosphorylation events needed to activate Rad53. In this model, where the DNA damage signal would reduce after some time, even though the damage is not repaired, cells lacking the cell-cycle dependent phosphorylation of Rad53 would adapt earlier. This idea, that preventing checkpoint adaptation requires constant signal input is also supported by the results obtained for checkpoint activation in a *cka1*Δ *cka2*^{ts} mutant strain (see Figure 2.7).

Whether yeast cells undergo checkpoint adaptation or not depends also on the amount of DNA damage, since WT yeast cells can only adapt to one DSB, and not to two irreparable breaks (Lee et al., 1998). In addition, the mutation of proteins involved in DSB processing and repair, such as yKu70 and yKu80, Rad51, Tid1, Srs2 and Rfa1 also influence the timing and occurrence of checkpoint adaptation (Lee et al., 1998;

Lee et al., 2001; Lee et al., 2003a; Vaze et al., 2002). The adaptation defective phenotype for yeast mutants naturally depends on an induced checkpoint response, beings relieved by mutation of *RAD9* (Toczyski et al., 1997). Since Rad9 functions exclusively through Rad53, it is not surprising that Rad53 inactivation and loss of its checkpoint kinase activity is the key event in both checkpoint recovery and adaptation (Pellicioli et al., 2001; Vaze et al., 2002). Phosphatases have been reported to play an important role in the inactivation of the checkpoint arrest induced by DNA damage. Notably, in budding yeast the PP2C phosphatases Ptc2 and Ptc3 were shown to bind and inactivate Rad53 during adaptation and both are indispensable for the adaptation event (Leroy et al., 2003). Similarily the human PP2C phosphatase Wip1, which dephosphorylates human Chk2 at Thr68, is critical for the reversal of Chk2 activation in response to DNA damage (Fujimoto et al., 2006).

The mechanism of Rad53 inactivation by Ptc2 and Ptc3 most likely is regulated by CK2. CK2 is necessary for *in vivo* interaction between Ptc2 and the FHA1 domain of Rad53 through phosphorylating the FHA-domain binding motif at Thr376 of Ptc2, as shown *in vitro* (Guillemain et al., 2007). Likewise *ckb1*Δ and *ckb2*Δ mutant cells are also defective for adaptation (Toczyski et al., 1997). However Guillemain and coworkers concluded that the effect of CK2 depletion upon adaptation is much stronger and can therefore not only be mediated through Ptc2/Ptc3. Consistent with this conclusion we do not observe checkpoint hyperactivation in *ptc2/ptc3* mutant cells, yet we do see this in cells mutated for CK2 function (see Figure 2.7). Recently a third phosphatase, Pph3, was shown to be required for stalled replication fork restart and recovery from DNA damage by dephosphorylating Rad53 (O'Neill et al., 2007). Pph3 in a complex with Psy2 was furthermore shown to interact with the kinase domain of Rad53 (O'Neill et al., 2007). Since Pph3 seems to act mainly in S phase, it would be interesting to address whether Pph3 removes the cell-cycle dependent phosphorylation of Rad53 during normal cell cycle progression.

Ccd5 has also been proposed to act in a feedback mechanism to turn off Rad53 kinase activity (Pellicioli et al., 2001). However, how exactly Cdc5 would downregulate the DNA damage checkpoint pathway is still an open question (Lee et al., 2005a). It has been shown previously that Cdc5 overproduction can override a Rad53 induced checkpoint arrest (Sanchez et al., 1999). But this is most likely through promoting mitotic exit, because Rad53-dependent inhibition of Cdc5 inhibits mitotic exit and causes G2/M arrest. Overexpression of PTC2 rescues adaptation deficient *cdc5-ad*

mutants, probably by directly reversing Rad53 activation (Leroy et al., 2003). Checkpoint adaptation may be influenced by multiple pathways or at multiple points of the same signaling pathway. If *cdc5-ad* would be a gain-of-function mutant, this would explain both our model for Cdc5 phosphorylation contributing to Rad53 activation, as well as the adaptation-deficiency of *cdc5-ad* mutants. In this respect, it is important to note that an interaction between Cdc5 and Rad53 has been conserved through evolution. Human Plk1 and Chk2 were shown to interact and colocalise to centrosomes and the midbody. Recombinant Plk1 can phosphorylate Chk2 *in vitro*, Plk1 overexpression further enhanced phosphorylation of Chk2 at Thr-68, promoting activity of Chk2 (Ahn et al., 2004). Finally the stress response protein Plk3 is activated in response to DNA damage in an ATM dependent manner and was shown to interact with Chk2, enhancing its activity (Bahassi el et al., 2002). Our data in yeast corresponds with the stimulatory effect of Plk3 phosphorylation on Chk2 activity. Since both Plk1 and Plk3 can complement the essential Cdc5 function in *Saccharomyces cerevisiae*, we propose that these functions are conserved (Ouyang et al., 1997; Lee and Erikson, 1997).

2.5.4 Inhibition of CK2 leads to hyperactivation of Rad53 in response to DNA damage

One possibility for how Rad53 hyperphosphorylation could be influenced by CK2, would be via the chaperone protein Cdc37. CK2 and Cdc37 are organized in a positive feedback loop that promotes the activation of many protein kinases (Bandhakavi et al., 2003). We therefore analysed Rad53 hyperactivation in *cdc37* ^{ts} mutant cells (kindly provided by D. Picard), however did not observe any difference to WT cells (data not shown). We therefore do not know for the moment if CK2 acts directly or indirectly on Rad53. Further candidates for indirect action are direct interaction partners of Rad53, Asf1 and Sgs1. Both are likely CK2 targets (personal prediction for Sgs1 and homepage of the Glover lab for Asf1: http://www.bmb.uga.edu/glover/ck2substrates.html). Asf1 mutant cells show no changed hyperphosphorylation pattern as observed for *cka2*-8 or *cka2*-13 mutant cells in Figure 2.7a and 2.7b (data not shown). A potential CK2 site lays in an evolutionary conserved region in the N-terminal part of Sgs1 at aa positions 423/424 (data not shown). Sgs1 is known to interact with the FHA1 domain of Rad53 (Bjergbaek et al.,

2005) and interestingly phosphorylated amino acids 423 and 424 would fit the ideal consensus for recognition by the Rad53 FHA1 domain (Durocher et al., 1999; Durocher et al., 2000; Yongkiettrakul et al., 2004). Mutation of these sites does not lead to hypersensitivity on cells containing HU and MMS (data not shown); however a careful analysis of Rad53 hyperphosphorylation is still required.

Yeast cells pretreated with heat shock at 38°C were shown to repair Bleomycin-induced DSBs more efficiently than control strains (Keszenman et al., 2000). The authors associate this higher efficiency of DNA repair with heat shock induced activation of genes from a regulatory network involving DNA repair, heat shock response and DNA metabolism genes. Our results of monitoring Rad53 activation by heat shock instead suggest that this protective function of heat shock in the respect of subsequent DNA damage might stem from DNA damage caused by the heat shock itself. Supporting this idea, even higher temperatures such as used for the hyperthermic treatment of tumors, induce DNA damage (Hilger et al., 2005).
Targeting of checkpoint kinases is generally thought to be therapeutically interesting for chemosensitization of tumor cells and chemoprotection of normal cells to widen the narrow window of DNA-damaging chemotherapeutics (Zhou and Bartek, 2004).
However also the specific induction of checkpoint-mediated apoptosis in tumor cells through selectable induction of E2F1, named "Activated Checkpoint Therapy", may be a promising therapeutic approach (Li et al., 2003). The human Rad53 homologue Chk2 might be a particularly suitable target for such an approach, since Chk2 overexpression can drive cancer cells into apoptosis and senescence (Chen et al., 2005). We observed in yeast that CK2 inhibition enhances the checkpoint response in the presence of low amounts of DNA damage that do not activate the checkpoint in WT cells. If our observation is conserved through evolution, this could potentially be used to elict a checkpoint mediated apoptotic response in tumor cells, particularly in combination with local radiation or hyperthermic treatment.

There are indications that this could be true. Firstly downregualtion of CK2 is associated with replicative and H_2O_2-induced senescence (Ryu et al., 2006). Secondly CK2 has an anti-apoptotic function; since most tumors are overexpressing CK2, and on several CK2 inhibitors could induce apoptosis in tumor cells (Ahmed et al., 2002; Pagano et al., 2006). Thirdly CK2 could relocalize to distinct nuclear structures in

response to UV-irradiation, Ionizing Radiation and heat shock (Gerber et al., 2000; Yamane and Kinsella, 2005). If future experiments would validate that DNA damage checkpoints may be hyperactivated in response to small amounts of DNA damage in mammalian cells a combined therapy of local irradiation with CK2 inhibitors might drive tumor cells into apoptosis and senescence.

2.6 Acknowledgements

The authors acknowledge support from the Novartis Research Foundation, the Swiss Cancer League, the Swiss National Science Foundation, European RTN Checkpoints and Cancer. We thank colleagues of the FMI facilities for technical help.

We thank D. Durocher for providing us the rad53$^{A7,\ A8\ and\ A9}$ mutant strains and M. Peter for providing us the *cdc28*-AS1 mutant strain as well as the analog Na-PP1.

We thank S. Jackson for vectors for expression of recombinant Rad53 protein fragments and M-Tsai-Pflugfelder for creating pNter, pKin and pCter. We thank D. Toczyski and L. Hartwell, B. Pike and J. Heierhorst, D. Picard and K. Nasmyth and members of the Gasser lab for yeast strains.

We thank members of the Gasser lab for helpful discussions and Dr. Brietta Pike for critically reading of the manuscript. T. Schleker would like to thank the members of his thesis committee Primo Schär, Dirk Schübeler and Maria Pia Longhese for helpful suggestions.

2.7 References

Ahmed, K., D.A. Gerber, and C. Cochet. 2002. Joining the cell survival squad: an emerging role for protein kinase CK2. *Trends Cell Biol*. 12:226-30.

Ahn, J., M. Urist, and C. Prives. 2004. The Chk2 protein kinase. *DNA Repair (Amst)*. 3:1039-47.

Alcasabas, A.A., A.J. Osborn, J. Bachant, F. Hu, P.J. Werler, K. Bousset, K. Furuya, J.F. Diffley, A.M. Carr, and S.J. Elledge. 2001. Mrc1 transduces signals of DNA replication stress to activate Rad53. *Nat Cell Biol*. 3:958-65.

Allen, J.B., Z. Zhou, W. Siede, E.C. Friedberg, and S.J. Elledge. 1994. The SAD1/RAD53 protein kinase controls multiple checkpoints and DNA damage-induced transcription in yeast. *Genes Dev*. 8:2401-15.

Amberg, D.C., D.J. Burke, and J.N. Strathern. 2005. Methods in Yeast Genetics: A Cold Spring Harbor Laboratory Course Manual 2005 Edition. Cold Spring Harbor Laboratory Press, Cold Spring Harbor, New York, United States of America.

Bahassi el, M., C.W. Conn, D.L. Myer, R.F. Hennigan, C.H. McGowan, Y. Sanchez, and P.J. Stambrook. 2002. Mammalian Polo-like kinase 3 (Plk3) is a multifunctional protein involved in stress response pathways. *Oncogene*. 21:6633-40.

Bandhakavi, S., R.O. McCann, D.E. Hanna, and C.V. Glover. 2003. Genetic interactions among ZDS1,2, CDC37, and protein kinase CK2 in Saccharomyces cerevisiae. *FEBS Lett*. 554:295-300.

Bartkova, J., Z. Horejsi, K. Koed, A. Kramer, F. Tort, K. Zieger, P. Guldberg, M. Sehested, J.M. Nesland, C. Lukas, T. Orntoft, J. Lukas, and J. Bartek. 2005. DNA damage response as a candidate anti-cancer barrier in early human tumorigenesis. *Nature*. 434:864-70.

Bell, D.W., J.M. Varley, T.E. Szydlo, D.H. Kang, D.C. Wahrer, K.E. Shannon, M. Lubratovich, S.J. Verselis, K.J. Isselbacher, J.F. Fraumeni, J.M. Birch, F.P. Li, J.E. Garber, and D.A. Haber. 1999. Heterozygous germ line hCHK2 mutations in Li-Fraumeni syndrome. *Science*. 286:2528-31.

Bjergbaek, L., J.A. Cobb, M. Tsai-Pflugfelder, and S.M. Gasser. 2005. Mechanistically distinct roles for Sgs1p in checkpoint activation and replication fork maintenance. *Embo J*. 24:405-17.

Braguglia, D., P. Heun, P. Pasero, B.P. Duncker, and S.M. Gasser. 1998. Semi-conservative replication in yeast nuclear extracts requires Dna2 helicase and supercoiled template. *J Mol Biol*. 281:631-49.

Branzei, D., and M. Foiani. 2006. The Rad53 signal transduction pathway: Replication fork stabilization, DNA repair, and adaptation. *Exp Cell Res*. 312:2654-9.

Chen, C.R., W. Wang, H.A. Rogoff, X. Li, W. Mang, and C.J. Li. 2005. Dual induction of apoptosis and senescence in cancer cells by Chk2 activation: checkpoint activation as a strategy against cancer. *Cancer Res*. 65:6017-21.

Chen, S.H., M.B. Smolka, and H. Zhou. 2007. Mechanism of Dun1 activation by Rad53 phosphorylation in Saccharomyces cerevisiae. *J Biol Chem*. 282:986-95.

Cheng, L., L. Hunke, and C.F. Hardy. 1998. Cell cycle regulation of the Saccharomyces cerevisiae polo-like kinase cdc5p. *Mol Cell Biol*. 18:7360-70.

Choi, K.S., Y.W. Eom, Y. Kang, M.J. Ha, H. Rhee, J.W. Yoon, and S.J. Kim. 1999. Cdc2 and Cdk2 kinase activated by transforming growth factor-beta1 trigger

apoptosis through the phosphorylation of retinoblastoma protein in FaO hepatoma cells. *J Biol Chem*. 274:31775-83.

Clemenson, C., and M.C. Marsolier-Kergoat. 2006. The spindle assembly checkpoint regulates the phosphorylation state of a subset of DNA checkpoint proteins in Saccharomyces cerevisiae. *Mol Cell Biol*. 26:9149-61.

Cobb, J.A., L. Bjergbaek, K. Shimada, C. Frei, and S.M. Gasser. 2003. DNA polymerase stabilization at stalled replication forks requires Mec1 and the RecQ helicase Sgs1. *Embo J*. 22:4325-36.

Cobb, J.A., T. Schleker, V. Rojas, L. Bjergbaek, J.A. Tercero, and S.M. Gasser. 2005. Replisome instability, fork collapse, and gross chromosomal rearrangements arise synergistically from Mec1 kinase and RecQ helicase mutations. *Genes Dev*. 19:3055-69.

Cobb, J.A., K. Shimada, and S.M. Gasser. 2004. Redundancy, insult-specific sensors and thresholds: unlocking the S-phase checkpoint response. *Curr Opin Genet Dev*. 14:292-300.

Cordon-Preciado, V., S. Ufano, and A. Bueno. 2006. Limiting amounts of budding yeast Rad53 S-phase checkpoint activity results in increased resistance to DNA alkylation damage. *Nucleic Acids Res*. 34:5852-62.

de la Torre-Ruiz, M.A., C.M. Green, and N.F. Lowndes. 1998. RAD9 and RAD24 define two additive, interacting branches of the DNA damage checkpoint pathway in budding yeast normally required for Rad53 modification and activation. *Embo J*. 17:2687-98.

Deak, J.C., and D.J. Templeton. 1997. Regulation of the activity of MEK kinase 1 (MEKK1) by autophosphorylation within the kinase activation domain. *Biochem J*. 322 (Pt 1):185-92.

Delacote, F., L. Deriano, S. Lambert, P. Bertrand, Y. Saintigny, and B.S. Lopez. 2007. Chronic exposure to sublethal doses of radiation mimetic Zeocin selects for clones deficient in homologous recombination. *Mutat Res*. 615:125-33.

Dohrmann, P.R., G. Oshiro, M. Tecklenburg, and R.A. Sclafani. 1999. RAD53 regulates DBF4 independently of checkpoint function in Saccharomyces cerevisiae. *Genetics*. 151:965-77.

Duncker, B.P., K. Shimada, M. Tsai-Pflugfelder, P. Pasero, and S.M. Gasser. 2002. An N-terminal domain of Dbf4p mediates interaction with both origin recognition complex (ORC) and Rad53p and can deregulate late origin firing. *Proc Natl Acad Sci U S A*. 99:16087-92.

Durocher, D., J. Henckel, A.R. Fersht, and S.P. Jackson. 1999. The FHA domain is a modular phosphopeptide recognition motif. *Mol Cell*. 4:387-94.

Durocher, D., I.A. Taylor, D. Sarbassova, L.F. Haire, S.L. Westcott, S.P. Jackson, S.J. Smerdon, and M.B. Yaffe. 2000. The molecular basis of FHA domain:phosphopeptide binding specificity and implications for phospho-dependent signaling mechanisms. *Mol Cell*. 6:1169-82.

Elledge, S.J., Z. Zhou, J.B. Allen, and T.A. Navas. 1993. DNA damage and cell cycle regulation of ribonucleotide reductase. *Bioessays*. 15:333-9.

Emili, A., D.M. Schieltz, J.R. Yates, 3rd, and L.H. Hartwell. 2001. Dynamic interaction of DNA damage checkpoint protein Rad53 with chromatin assembly factor Asf1. *Mol Cell*. 7:13-20.

Endicott, J.A., M.E. Noble, and J.A. Tucker. 1999. Cyclin-dependent kinases: inhibition and substrate recognition. *Curr Opin Struct Biol*. 9:738-44.

Enserink, J.M., M.B. Smolka, H. Zhou, and R.D. Kolodner. 2006. Checkpoint proteins control morphogenetic events during DNA replication stress in Saccharomyces cerevisiae. *J Cell Biol*. 175:729-41.

Frei, C., and S.M. Gasser. 2000. The yeast Sgs1p helicase acts upstream of Rad53p in the DNA replication checkpoint and colocalizes with Rad53p in S-phase-specific foci. *Genes Dev*. 14:81-96.

Fujimoto, H., N. Onishi, N. Kato, M. Takekawa, X.Z. Xu, A. Kosugi, T. Kondo, M. Imamura, I. Oishi, A. Yoda, and Y. Minami. 2006. Regulation of the antioncogenic Chk2 kinase by the oncogenic Wip1 phosphatase. *Cell Death Differ*. 13:1170-80.

Galgoczy, D.J., and D.P. Toczyski. 2001. Checkpoint adaptation precedes spontaneous and damage-induced genomic instability in yeast. *Mol Cell Biol*. 21:1710-8.

Gerber, D.A., S. Souquere-Besse, F. Puvion, M.F. Dubois, O. Bensaude, and C. Cochet. 2000. Heat-induced relocalization of protein kinase CK2. Implication of CK2 in the context of cellular stress. *J Biol Chem*. 275:23919-26.

Gilbert, C.S., C.M. Green, and N.F. Lowndes. 2001. Budding yeast Rad9 is an ATP-dependent Rad53 activating machine. *Mol Cell*. 8:129-36.

Glover, C.V., 3rd. 1998. On the physiological role of casein kinase II in Saccharomyces cerevisiae. *Prog Nucleic Acid Res Mol Biol*. 59:95-133.

Gorgoulis, V.G., L.V. Vassiliou, P. Karakaidos, P. Zacharatos, A. Kotsinas, T. Liloglou, M. Venere, R.A. Ditullio, Jr., N.G. Kastrinakis, B. Levy, D. Kletsas, A. Yoneta, M. Herlyn, C. Kittas, and T.D. Halazonetis. 2005. Activation of the DNA damage checkpoint and genomic instability in human precancerous lesions. *Nature*. 434:907-13.

Guillemain, G., E. Ma, S. Mauger, S. Miron, R. Thai, R. Guerois, F. Ochsenbein, and M.C. Marsolier-Kergoat. 2007. Mechanisms of checkpoint kinase Rad53 inactivation after a double-strand break in Saccharomyces cerevisiae. *Mol Cell Biol*. 27:3378-89.

Hanna, D.E., A. Rethinaswamy, and C.V. Glover. 1995. Casein kinase II is required for cell cycle progression during G1 and G2/M in Saccharomyces cerevisiae. *J Biol Chem*. 270:25905-14.

Harrison, J.C., and J.E. Haber. 2006. Surviving the breakup: the DNA damage checkpoint. *Annu Rev Genet*. 40:209-35.

Hartwell, L.H., and T.A. Weinert. 1989. Checkpoints: controls that ensure the order of cell cycle events. *Science*. 246:629-34.

Heichman, K.A., and J.M. Roberts. 1996. The yeast CDC16 and CDC27 genes restrict DNA replication to once per cell cycle. *Cell*. 85:39-48.

Hilger, I., A. Rapp, K.O. Greulich, and W.A. Kaiser. 2005. Assessment of DNA damage in target tumor cells after thermoablation in mice. *Radiology*. 237:500-6.

Hu, F., A.A. Alcasabas, and S.J. Elledge. 2001. Asf1 links Rad53 to control of chromatin assembly. *Genes Dev*. 15:1061-6.

Ivanov, E.L., V.G. Korolev, and F. Fabre. 1992. XRS2, a DNA repair gene of Saccharomyces cerevisiae, is needed for meiotic recombination. *Genetics*. 132:651-64.

Jaquenoud, M., F. van Drogen, and M. Peter. 2002. Cell cycle-dependent nuclear export of Cdh1p may contribute to the inactivation of APC/C(Cdh1). *Embo J*. 21:6515-26.

Keszenman, D.J., E. Carmen Candreva, and E. Nunes. 2000. Cellular and molecular effects of bleomycin are modulated by heat shock in Saccharomyces cerevisiae. *Mutat Res*. 459:29-41.

Kim, S.T., D.S. Lim, C.E. Canman, and M.B. Kastan. 1999. Substrate specificities and identification of putative substrates of ATM kinase family members. *J Biol Chem*. 274:37538-43.

Krishnan, V., and U. Surana. 2005. Taming the spindle for containing the chromosomes. *Cell Cycle*. 4:376-9.

Lee, K.S., and R.L. Erikson. 1997. Plk is a functional homolog of Saccharomyces cerevisiae Cdc5, and elevated Plk activity induces multiple septation structures. *Mol Cell Biol*. 17:3408-17.

Lee, K.S., J.E. Park, S. Asano, and C.J. Park. 2005. Yeast polo-like kinases: functionally conserved multitask mitotic regulators. *Oncogene*. 24:217-29.

Lee, S.E., J.K. Moore, A. Holmes, K. Umezu, R.D. Kolodner, and J.E. Haber. 1998. Saccharomyces Ku70, mre11/rad50 and RPA proteins regulate adaptation to G2/M arrest after DNA damage. *Cell*. 94:399-409.

Lee, S.E., A. Pellicioli, A. Malkova, M. Foiani, and J.E. Haber. 2001. The Saccharomyces recombination protein Tid1p is required for adaptation from G2/M arrest induced by a double-strand break. *Curr Biol*. 11:1053-7.

Lee, S.E., A. Pellicioli, M.B. Vaze, N. Sugawara, A. Malkova, M. Foiani, and J.E. Haber. 2003a. Yeast Rad52 and Rad51 recombination proteins define a second pathway of DNA damage assessment in response to a single double-strand break. *Mol Cell Biol*. 23:8913-23.

Lee, S.J., M.F. Schwartz, J.K. Duong, and D.F. Stern. 2003b. Rad53 phosphorylation site clusters are important for Rad53 regulation and signaling. *Mol Cell Biol*. 23:6300-14.

Leroy, C., S.E. Lee, M.B. Vaze, F. Ochsenbien, R. Guerois, J.E. Haber, and M.C. Marsolier-Kergoat. 2003. PP2C phosphatases Ptc2 and Ptc3 are required for DNA checkpoint inactivation after a double-strand break. *Mol Cell*. 11:827-35.

Li, Y., X. Sun, J.T. LaMont, A.B. Pardee, and C.J. Li. 2003. Selective killing of cancer cells by beta -lapachone: direct checkpoint activation as a strategy against cancer. *Proc Natl Acad Sci U S A*. 100:2674-8.

Liao, H., I.J. Byeon, and M.D. Tsai. 1999. Structure and function of a new phosphopeptide-binding domain containing the FHA2 of Rad53. *J Mol Biol*. 294:1041-9.

Liao, H., C. Yuan, M.I. Su, S. Yongkiettrakul, D. Qin, H. Li, I.J. Byeon, D. Pei, and M.D. Tsai. 2000. Structure of the FHA1 domain of yeast Rad53 and identification of binding sites for both FHA1 and its target protein Rad9. *J Mol Biol*. 304:941-51.

Longtine, M.S., A. McKenzie, 3rd, D.J. Demarini, N.G. Shah, A. Wach, A. Brachat, P. Philippsen, and J.R. Pringle. 1998. Additional modules for versatile and economical PCR-based gene deletion and modification in Saccharomyces cerevisiae. *Yeast*. 14:953-61.

Loog, M., and D.O. Morgan. 2005. Cyclin specificity in the phosphorylation of cyclin-dependent kinase substrates. *Nature*. 434:104-8.

Ma, J.L., S.J. Lee, J.K. Duong, and D.F. Stern. 2006. Activation of the checkpoint kinase Rad53 by the phosphatidyl inositol kinase-like kinase Mec1. *J Biol Chem*. 281:3954-63.

Moshe, Y., J. Boulaire, M. Pagano, and A. Hershko. 2004. Role of Polo-like kinase in the degradation of early mitotic inhibitor 1, a regulator of the anaphase promoting complex/cyclosome. *Proc Natl Acad Sci U S A*. 101:7937-42.

Myers, J.S., R. Zhao, X. Xu, A.J. Ham, and D. Cortez. 2007. Cyclin-dependent kinase 2 dependent phosphorylation of ATRIP regulates the G2-M checkpoint response to DNA damage. *Cancer Res*. 67:6685-90.

Nakajima, H., F. Toyoshima-Morimoto, E. Taniguchi, and E. Nishida. 2003. Identification of a consensus motif for Plk (Polo-like kinase) phosphorylation reveals Myt1 as a Plk1 substrate. *J Biol Chem*. 278:25277-80.

Navas, T.A., Y. Sanchez, and S.J. Elledge. 1996. RAD9 and DNA polymerase epsilon form parallel sensory branches for transducing the DNA damage checkpoint signal in Saccharomyces cerevisiae. *Genes Dev*. 10:2632-43.

Nigg, E.A. 1998. Polo-like kinases: positive regulators of cell division from start to finish. *Curr Opin Cell Biol*. 10:776-83.

O'Neill, B.M., S.J. Szyjka, E.T. Lis, A.O. Bailey, J.R. Yates, 3rd, O.M. Aparicio, and F.E. Romesberg. 2007. Pph3-Psy2 is a phosphatase complex required for Rad53 dephosphorylation and replication fork restart during recovery from DNA damage. *Proc Natl Acad Sci U S A*. 104:9290-5.

Osborn, A.J., and S.J. Elledge. 2003. Mrc1 is a replication fork component whose phosphorylation in response to DNA replication stress activates Rad53. *Genes Dev*. 17:1755-67.

Ouyang, B., H. Pan, L. Lu, J. Li, P. Stambrook, B. Li, and W. Dai. 1997. Human Prk is a conserved protein serine/threonine kinase involved in regulating M phase functions. *J Biol Chem*. 272:28646-51.

Paciotti, V., M. Clerici, G. Lucchini, and M.P. Longhese. 2000. The checkpoint protein Ddc2, functionally related to S. pombe Rad26, interacts with Mec1 and is regulated by Mec1-dependent phosphorylation in budding yeast. *Genes Dev*. 14:2046-59.

Pagano, M.A., L. Cesaro, F. Meggio, and L.A. Pinna. 2006. Protein kinase CK2: a newcomer in the 'druggable kinome'. *Biochem Soc Trans*. 34:1303-6.

Paulovich, A.G., R.U. Margulies, B.M. Garvik, and L.H. Hartwell. 1997. RAD9, RAD17, and RAD24 are required for S phase regulation in Saccharomyces cerevisiae in response to DNA damage. *Genetics*. 145:45-62.

Pellicioli, A., and M. Foiani. 2005. Signal transduction: how rad53 kinase is activated. *Curr Biol*. 15:R769-71.

Pellicioli, A., S.E. Lee, C. Lucca, M. Foiani, and J.E. Haber. 2001. Regulation of Saccharomyces Rad53 checkpoint kinase during adaptation from DNA damage-induced G2/M arrest. *Mol Cell*. 7:293-300.

Pike, B.L., A. Hammet, and J. Heierhorst. 2001. Role of the N-terminal forkhead-associated domain in the cell cycle checkpoint function of the Rad53 kinase. *J Biol Chem*. 276:14019-26.

Pike, B.L., N. Tenis, and J. Heierhorst. 2004a. Rad53 kinase activation-independent replication checkpoint function of the N-terminal forkhead-associated (FHA1) domain. *J Biol Chem*. 279:39636-44.

Pike, B.L., S. Yongkiettrakul, M.D. Tsai, and J. Heierhorst. 2003. Diverse but overlapping functions of the two forkhead-associated (FHA) domains in Rad53 checkpoint kinase activation. *J Biol Chem*. 278:30421-4.

Pike, B.L., S. Yongkiettrakul, M.D. Tsai, and J. Heierhorst. 2004b. Mdt1, a novel Rad53 FHA1 domain-interacting protein, modulates DNA damage tolerance

and G(2)/M cell cycle progression in Saccharomyces cerevisiae. *Mol Cell Biol*. 24:2779-88.

Povirk, L.F. 1996. DNA damage and mutagenesis by radiomimetic DNA-cleaving agents: bleomycin, neocarzinostatin and other enediynes. *Mutat Res*. 355:71-89.

Pringle, J.R., and L.H. Hartwell. 1981. The Saccharomyces cerevisiae cell cycle, in The Molecular Biology of the Yeast Saccharomyces: Life Cycle and Inheritance. Cold Spring Harbor Laboratory, Cold Spring Harbor, NY.

Rouse, J., and S.P. Jackson. 2000. LCD1: an essential gene involved in checkpoint control and regulation of the MEC1 signalling pathway in Saccharomyces cerevisiae. *Embo J*. 19:5801-12.

Rouse, J., and S.P. Jackson. 2002. Lcd1p recruits Mec1p to DNA lesions in vitro and in vivo. *Mol Cell*. 9:857-69.

Rudner, A.D., and A.W. Murray. 2000. Phosphorylation by Cdc28 activates the Cdc20-dependent activity of the anaphase-promoting complex. *J Cell Biol*. 149:1377-90.

Ryu, S.W., J.H. Woo, Y.H. Kim, Y.S. Lee, J.W. Park, and Y.S. Bae. 2006. Downregulation of protein kinase CKII is associated with cellular senescence. *FEBS Lett*. 580:988-94.

Sambrook, J., and D. Russell. 2001. Molecular cloning: A laboratory manual. Cold Spring Harbor Laboratory Press, Cold Spring Harbor, New York.

Sanchez, Y., J. Bachant, H. Wang, F. Hu, D. Liu, M. Tetzlaff, and S.J. Elledge. 1999. Control of the DNA damage checkpoint by chk1 and rad53 protein kinases through distinct mechanisms. *Science*. 286:1166-71.

Sanchez, Y., B.A. Desany, W.J. Jones, Q. Liu, B. Wang, and S.J. Elledge. 1996. Regulation of RAD53 by the ATM-like kinases MEC1 and TEL1 in yeast cell cycle checkpoint pathways. *Science*. 271:357-60.

Sandell, L.L., and V.A. Zakian. 1993. Loss of a yeast telomere: arrest, recovery, and chromosome loss. *Cell*. 75:729-39.

Santocanale, C., and J.F. Diffley. 1998. A Mec1- and Rad53-dependent checkpoint controls late-firing origins of DNA replication. *Nature*. 395:615-8.

Savitsky, K., A. Bar-Shira, S. Gilad, G. Rotman, Y. Ziv, L. Vanagaite, D.A. Tagle, S. Smith, T. Uziel, S. Sfez, M. Ashkenazi, I. Pecker, M. Frydman, R. Harnik, S.R. Patanjali, A. Simmons, G.A. Clines, A. Sartiel, R.A. Gatti, L. Chessa, O. Sanal, M.F. Lavin, N.G. Jaspers, A.M. Taylor, C.F. Arlett, T. Miki, S.M. Weissman, M. Lovett, F.S. Collins, and Y. Shiloh. 1995. A single ataxia telangiectasia gene with a product similar to PI-3 kinase. *Science*. 268:1749-53.

Schleker, T. 2003. Search for limiting factors in S phase checkpoint activation of Saccharomyces cerevisiae: RAD24 and MRC1 overexpression partially restore Rad53p activation under conditions of lowered replication rates. *In* Département de Biologie Moléculaire. Vol. Certificat de Biologie Moléculaire (DEA/Masters). Université de Genève, Genève.

Schwartz, M.F., J.K. Duong, Z. Sun, J.S. Morrow, D. Pradhan, and D.F. Stern. 2002. Rad9 phosphorylation sites couple Rad53 to the Saccharomyces cerevisiae DNA damage checkpoint. *Mol Cell*. 9:1055-65.

Schwartz, M.F., S.J. Lee, J.K. Duong, S. Eminaga, and D.F. Stern. 2003. FHA domain-mediated DNA checkpoint regulation of Rad53. *Cell Cycle*. 2:384-96.

Shimada, K., and S.M. Gasser. 2007. The origin recognition complex functions in sister-chromatid cohesion in Saccharomyces cerevisiae. *Cell*. 128:85-99.

Shimada, K., P. Pasero, and S.M. Gasser. 2002. ORC and the intra-S-phase checkpoint: a threshold regulates Rad53p activation in S phase. *Genes Dev*. 16:3236-52.

Smolka, M.B., C.P. Albuquerque, S.H. Chen, K.H. Schmidt, X.X. Wei, R.D. Kolodner, and H. Zhou. 2005. Dynamic changes in protein-protein interaction and protein phosphorylation probed with amine reactive isotope tag. *Mol Cell Proteomics*.

Smolka, M.B., S.H. Chen, P.S. Maddox, J.M. Enserink, C.P. Albuquerque, X.X. Wei, A. Desai, R.D. Kolodner, and H. Zhou. 2006. An FHA domain-mediated protein interaction network of Rad53 reveals its role in polarized cell growth. *J Cell Biol*. 175:743-53.

Stern, D.F., P. Zheng, D.R. Beidler, and C. Zerillo. 1991. Spk1, a new kinase from Saccharomyces cerevisiae, phosphorylates proteins on serine, threonine, and tyrosine. *Mol Cell Biol*. 11:987-1001.

Sugimoto, K., S. Ando, T. Shimomura, and K. Matsumoto. 1997. Rfc5, a replication factor C component, is required for regulation of Rad53 protein kinase in the yeast checkpoint pathway. *Mol Cell Biol*. 17:5905-14.

Sun, Z., D.S. Fay, F. Marini, M. Foiani, and D.F. Stern. 1996. Spk1/Rad53 is regulated by Mec1-dependent protein phosphorylation in DNA replication and damage checkpoint pathways. *Genes Dev*. 10:395-406.

Sun, Z., J. Hsiao, D.S. Fay, and D.F. Stern. 1998. Rad53 FHA domain associated with phosphorylated Rad9 in the DNA damage checkpoint. *Science*. 281:272-4.

Surana, U., H. Robitsch, C. Price, T. Schuster, I. Fitch, A.B. Futcher, and K. Nasmyth. 1991. The role of CDC28 and cyclins during mitosis in the budding yeast S. cerevisiae. *Cell*. 65:145-61.

Sweeney, F.D., F. Yang, A. Chi, J. Shabanowitz, D.F. Hunt, and D. Durocher. 2005. Saccharomyces cerevisiae Rad9 acts as a Mec1 adaptor to allow Rad53 activation. *Curr Biol*. 15:1364-75.

Tercero, J.A., M.P. Longhese, and J.F. Diffley. 2003. A central role for DNA replication forks in checkpoint activation and response. *Mol Cell*. 11:1323-36.

Thomas, B.J., and R. Rothstein. 1989. Elevated recombination rates in transcriptionally active DNA. *Cell*. 56:619-30.

Toczyski, D.P., D.J. Galgoczy, and L.H. Hartwell. 1997. CDC5 and CKII control adaptation to the yeast DNA damage checkpoint. *Cell*. 90:1097-106.

Traven, A., and J. Heierhorst. 2005. SQ/TQ cluster domains: concentrated ATM/ATR kinase phosphorylation site regions in DNA-damage-response proteins. *Bioessays*. 27:397-407.

Tsvetkov, L., X. Xu, J. Li, and D.F. Stern. 2003. Polo-like kinase 1 and Chk2 interact and co-localize to centrosomes and the midbody. *J Biol Chem*. 278:8468-75.

Ubersax, J.A., E.L. Woodbury, P.N. Quang, M. Paraz, J.D. Blethrow, K. Shah, K.M. Shokat, and D.O. Morgan. 2003. Targets of the cyclin-dependent kinase Cdk1. *Nature*. 425:859-64.

Vaze, M.B., A. Pellicioli, S.E. Lee, G. Ira, G. Liberi, A. Arbel-Eden, M. Foiani, and J.E. Haber. 2002. Recovery from checkpoint-mediated arrest after repair of a double-strand break requires Srs2 helicase. *Mol Cell*. 10:373-85.

Vialard, J.E., C.S. Gilbert, C.M. Green, and N.F. Lowndes. 1998. The budding yeast Rad9 checkpoint protein is subjected to Mec1/Tel1-dependent hyperphosphorylation and interacts with Rad53 after DNA damage. *Embo J*. 17:5679-88.

Wach, A., A. Brachat, R. Pohlmann, and P. Philippsen. 1994. New heterologous modules for classical or PCR-based gene disruptions in Saccharomyces cerevisiae. *Yeast*. 10:1793-808.

Wakayama, T., T. Kondo, S. Ando, K. Matsumoto, and K. Sugimoto. 2001. Pie1, a protein interacting with Mec1, controls cell growth and checkpoint responses in Saccharomyces cerevisiae. *Mol Cell Biol*. 21:755-64.

Wang, W., and B.A. Malcolm. 1999. Two-stage PCR protocol allowing introduction of multiple mutations, deletions and insertions using QuikChange Site-Directed Mutagenesis. *Biotechniques*. 26:680-2.

Weinert, T.A., and L.H. Hartwell. 1988. The RAD9 gene controls the cell cycle response to DNA damage in Saccharomyces cerevisiae. *Science*. 241:317-22.

Weinert, T.A., G.L. Kiser, and L.H. Hartwell. 1994. Mitotic checkpoint genes in budding yeast and the dependence of mitosis on DNA replication and repair. *Genes Dev*. 8:652-65.

Wood, J.S., and L.H. Hartwell. 1982. A dependent pathway of gene functions leading to chromosome segregation in Saccharomyces cerevisiae. *J Cell Biol*. 94:718-26.

Yaffe, M.P., and G. Schatz. 1984. Two nuclear mutations that block mitochondrial protein import in yeast. *Proc Natl Acad Sci U S A*. 81:4819-23.

Yamaguchi, T., H. Goto, T. Yokoyama, H. Sillje, A. Hanisch, A. Uldschmid, Y. Takai, T. Oguri, E.A. Nigg, and M. Inagaki. 2005. Phosphorylation by Cdk1 induces Plk1-mediated vimentin phosphorylation during mitosis. *J Cell Biol*. 171:431-6.

Yamane, K., and T.J. Kinsella. 2005. CK2 inhibits apoptosis and changes its cellular localization following ionizing radiation. *Cancer Res*. 65:4362-7.

Yongkiettrakul, S., I.J. Byeon, and M.D. Tsai. 2004. The ligand specificity of yeast Rad53 FHA domains at the +3 position is determined by nonconserved residues. *Biochemistry*. 43:3862-9.

Zhao, X., A. Chabes, V. Domkin, L. Thelander, and R. Rothstein. 2001. The ribonucleotide reductase inhibitor Sml1 is a new target of the Mec1/Rad53 kinase cascade during growth and in response to DNA damage. *Embo J*. 20:3544-53.

Zhao, X., E.G. Muller, and R. Rothstein. 1998. A suppressor of two essential checkpoint genes identifies a novel protein that negatively affects dNTP pools. *Mol Cell*. 2:329-40.

Zhao, X., and R. Rothstein. 2002. The Dun1 checkpoint kinase phosphorylates and regulates the ribonucleotide reductase inhibitor Sml1. *Proc Natl Acad Sci U S A*. 99:3746-51.

Zheng, P., D.S. Fay, J. Burton, H. Xiao, J.L. Pinkham, and D.F. Stern. 1993. SPK1 is an essential S-phase-specific gene of Saccharomyces cerevisiae that encodes a nuclear serine/threonine/tyrosine kinase. *Mol Cell Biol*. 13:5829-42.

Zhou, B.B., and J. Bartek. 2004. Targeting the checkpoint kinases: chemosensitization versus chemoprotection. *Nat Rev Cancer*. 4:216-25.

Zou, L., and S.J. Elledge. 2003. Sensing DNA damage through ATRIP recognition of RPA-ssDNA complexes. *Science*. 300:1542-8.

2.7 Supplementary Material

2.7.1 Supplementary Table

Strain	Genotype	Origin and Background
GA-141	**MATa,** cka1::HIS3, cka2::TRP1, pCKA2::LEU2 (CEN/ARS)	orig. YDH6 (Hanna et al., 1995), **YPH250**
GA-142	**MATa,** cka1::HIS3, cka2::TRP1, pcka2-8ts::LEU2 (CEN/ARS)	orig. YDH8 (Hanna et al., 1995), **YPH250**
GA-143	**MATa,** cka1::HIS3, cka2::TRP1, pcka2-13ts::LEU2 (CEN/ARS)	orig. YDH13 (Hanna et al., 1995), **YPH250**
GA-161	**MATa,** *ura1, his7, cdc16*-1	H16C1A1 (Wood and Hartwell, 1982), **A364a**
GA-180	**MATa,** *ade2*-1, *trp1*-1, *his3*-11, -15, *ura3*-1, *leu2*-3,-112, *can1*-100	(Thomas and Rothstein, 1989), **W303-1A**
GA-181	**MATalpha,** *ade2*-1, *trp1*-1, *his3*-11, -15, *ura3*-1, *leu2*-3,-112, *can1*-100	(Thomas and Rothstein, 1989), **W303-1B**
GA-414	**MAT alpha,** cdc28-1N in GA-181	orig. KNY 1992 (Surana et al., 1991), **W303**
GA-416	**MAT alpha,** cdc28-4 in GA-181	orig. KNY 1990 (Surana et al., 1991), **W303**
GA-871	**MATa,** *his3, leu2, ura3, trp1*	(Paulovich et al., 1997), **A364a**
GA-903	**MATa,** sml1 in GA-871	(Paulovich et al., 1997), **A364a**
GA-904	**MATa,** mec1-1 sml1in GA-871	(Paulovich et al., 1997), **A364a**
GA-1040	**MATa,** rad53::RAD53-13Myc-KanMX in GA-871	(Frei and Gasser, 2000), **A364a**
GA-1048	**MATa,** rad53::RAD53-13Myc-KanMX in GA-904	(Frei and Gasser, 2000), **A364a**
GA-1081	**MATalpha,** hml::ADE1 hmr::ADE1 ade3::GALHO *ade1, leu2-3,112, lys5, trp1::hisG, ura3-52*	(Lee et al., 1998), **JMK179**
GA-1148	**MATa,** rad9::LEU2	S114 (D. Shore), **W303**
GA-1159	**MATa,** rad53::RAD53-13Myc-KanMX in GA-161	Ch. Frei, **A364a**
GA-1351	**MATa,** rad53-11, DBF4-Myc::LEU2	P.Pasero, **W303**
GA-1408	**MATa,** cdc53-1 in GA-180	K. Shimada, **W303**
GA-1693	**MATalpha,** rad53::KanMX, sml1::TRP1 in GA-1081	K. Dubrana, **JMK179**
GA-1745	**MATa,** cdc15-2 in GA-1906	K. Shimada, **W303**
GA-1868	**MATa,** mad2::URA3	yMP77 (M. Peter), **W303**
GA-1906	**MATa,** cdc15-2, rad53::RAD53-13Myc-KanMX in GA-180	(Shimada and Gasser, 2007), **W303**
GA-1907	**MATa,** mad2::URA3 in GA-1906	K. Shimada, **W303**
GA-1945	**MATa,** cdc7-1 in GA-1906	K. Shimada, **W303**
GA-2019	**MATa,** rad53::RAD53-13Myc-KanMX in GA-180, rad5-535::RAD5	K. Shimada, **W303**
GA-2084	**MATalpha,** mec1-1	P. Pasero (orig.T. Weinert), **W303**
GA-2135	**MATa**, mrc1-2::KanMX, HIS3	(Alcasabas et al., 2001), **W303**
GA-2294	**MATalpha,** cdc16-1 in GA-181	K. Shimada, **W303**
GA-2474	**MATa,** mec1-100::LEU2	(Cobb et al., 2005), **W303**
GA-2695	**MATa,** cdc16-1, cdc28::cdc28AS1 in GA-180	(Jaquenod et al. Embo J 2002), **W303**
GA-3188	**MATa,** rad53-K227A, sml1::HIS	(Pike et al., 2001), **W303**
GA-3194	**MATa,** ptc2::URA3, ptc3::HIS3 in GA-2019	T. Schleker, **W303**
GA-3388	**MATa,** rad53::RAD53-3HA-HIS in GA-903	T. Schleker, **A364a**
GA-3390	**MATa,** rad53::RAD53posN496-3HA-HIS in GA-903	T. Schleker, **A364a**
GA-3455	**MATa,** sml1::KanMX6 rad53::HIS3MX6 in GA-180	K. Shimada, **W303**
GA-3530	**MATΔ,** cdc5-ad in GA-3533	(Toczyski et al., 1997), **LS20**
GA-3533	**MATΔ,** cyh2 can1 lys5 ade2 ade3::GalHO trp1 his3 ura3 leu2	(Toczyski et al., 1997), **LS20**
GA-3636	**MATa,** rad24::TRP1 in GA-3455	T. Schleker, **W303**
GA-3666	**MATa,** chk1::HIS3 in GA-3455	K. Shimada, **W303**
GA-4347	**MATa,** rad9::URA3 in GA-141	T. Schleker
GA-4348	**MATa,** rad9::URA3 in GA-142	T. Schleker

Supplemental Table 2.1: Yeast strains used in this study.

References for Supplemental Table 2.1:

Alcasabas, A.A., A.J. Osborn, J. Bachant, F. Hu, P.J. Werler, K. Bousset, K. Furuya, J.F. Diffley, A.M. Carr, and S.J. Elledge. 2001. Mrc1 transduces signals of DNA replication stress to activate Rad53. *Nat Cell Biol*. 3:958-65.

Cobb, J.A., T. Schleker, V. Rojas, L. Bjergbaek, J.A. Tercero, and S.M. Gasser. 2005. Replisome instability, fork collapse, and gross chromosomal rearrangements arise synergistically from Mec1 kinase and RecQ helicase mutations. *Genes Dev*. 19:3055-69.

Frei, C., and S.M. Gasser. 2000. The yeast Sgs1p helicase acts upstream of Rad53p in the DNA replication checkpoint and colocalizes with Rad53p in S-phase-specific foci. *Genes Dev*. 14:81-96.

Hanna, D.E., A. Rethinaswamy, and C.V. Glover. 1995. Casein kinase II is required for cell cycle progression during G1 and G2/M in Saccharomyces cerevisiae. *J Biol Chem*. 270:25905-14.

Lee, S.E., J.K. Moore, A. Holmes, K. Umezu, R.D. Kolodner, and J.E. Haber. 1998. Saccharomyces Ku70, mre11/rad50 and RPA proteins regulate adaptation to G2/M arrest after DNA damage. *Cell*. 94:399-409.

Paulovich, A.G., R.U. Margulies, B.M. Garvik, and L.H. Hartwell. 1997. RAD9, RAD17, and RAD24 are required for S phase regulation in Saccharomyces cerevisiae in response to DNA damage. *Genetics*. 145:45-62.

Pike, B.L., A. Hammet, and J. Heierhorst. 2001. Role of the N-terminal forkhead-associated domain in the cell cycle checkpoint function of the Rad53 kinase. *J Biol Chem*. 276:14019-26.

Shimada, K., and S.M. Gasser. 2007. The origin recognition complex functions in sister-chromatid cohesion in Saccharomyces cerevisiae. *Cell*. 128:85-99.

Surana, U., H. Robitsch, C. Price, T. Schuster, I. Fitch, A.B. Futcher, and K. Nasmyth. 1991. The role of CDC28 and cyclins during mitosis in the budding yeast S. cerevisiae. *Cell*. 65:145-61.

Thomas, B.J., and R. Rothstein. 1989. Elevated recombination rates in transcriptionally active DNA. *Cell*. 56:619-30.

Toczyski, D.P., D.J. Galgoczy, and L.H. Hartwell. 1997. CDC5 and CKII control adaptation to the yeast DNA damage checkpoint. *Cell*. 90:1097-106.

Wood, J.S., and L.H. Hartwell. 1982. A dependent pathway of gene functions leading to chromosome segregation in Saccharomyces cerevisiae. *J Cell Biol*. 94:718-26.

2.7.2 Supplementary Figures

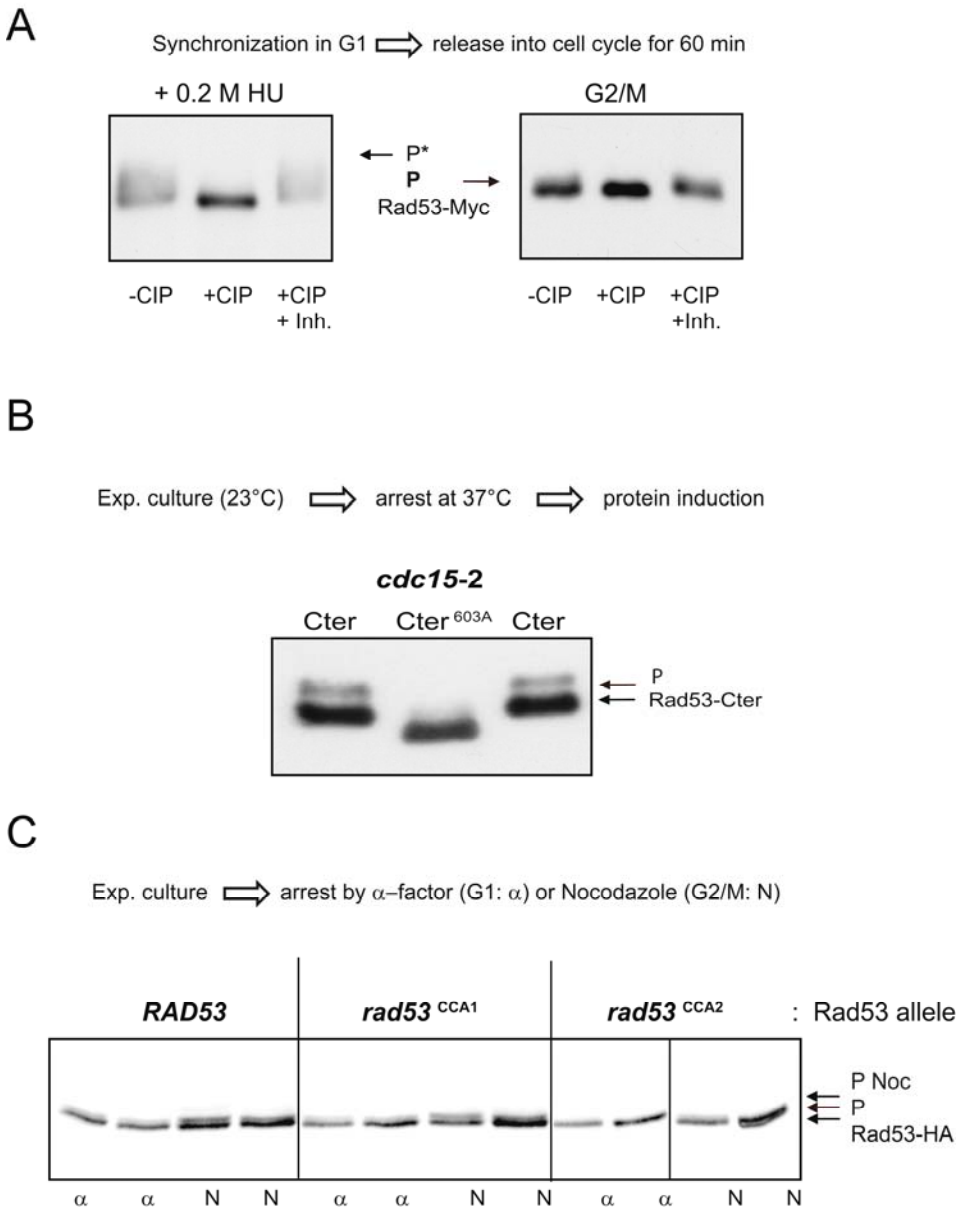

Sup. Fig. 2.1: The cell cycle-dependent upshift of Rad53 is due to phosphorylation, depends partially upon a functional FHA2 domain and still occurs in a *cdc5-ad* mutant strain.

A: The cell-cycle dependent mobility shift of Rad53 is due to phosphorylation.
Cells with Myc-tagged Rad53 (GA-2019) were blocked by α-factor for 75 min and released into fresh YPAD medium +/- 0.2 M HU for 60 min. (G2/M). Rad53-Myc was immunoprecipitated and either mock treated, or incubated with CIP +/- phosphatase inhibitor and separated by SDS-PAGE and probed with anti-Myc.
B: The upshift of Rad53-Cter is reduced in presence of a non-functional FHA2 domain (R603A).
An exponentially growing culture of a *cdc15*-2 mutant strain (GA-1745) was arrested at restrictive temperature of 37°C for 120 min. and protein expression was induced by addition of galactose and samples were taken after 60 min. Protein samples were separated on 10% SDS-PAGE and probed with anti-HA.
C: The cell-cycle dependent upshift still occurs in a *cdc5-ad* mutant strains.
The yeast strains GA-3533 (WT) and GA-3530 (*cdc5-ad*) were transformed with plasmid-borne HA-tagged Rad53 alleles RAD53, *rad53*^{CCA1} and *rad53*$^{CCA2.}$ Exponentially grown cultures were arrested either by nocodazole or α-factor for 90 minutes. Protein samples were separated on 6% SDS-PAGE and probed with anti-HA.

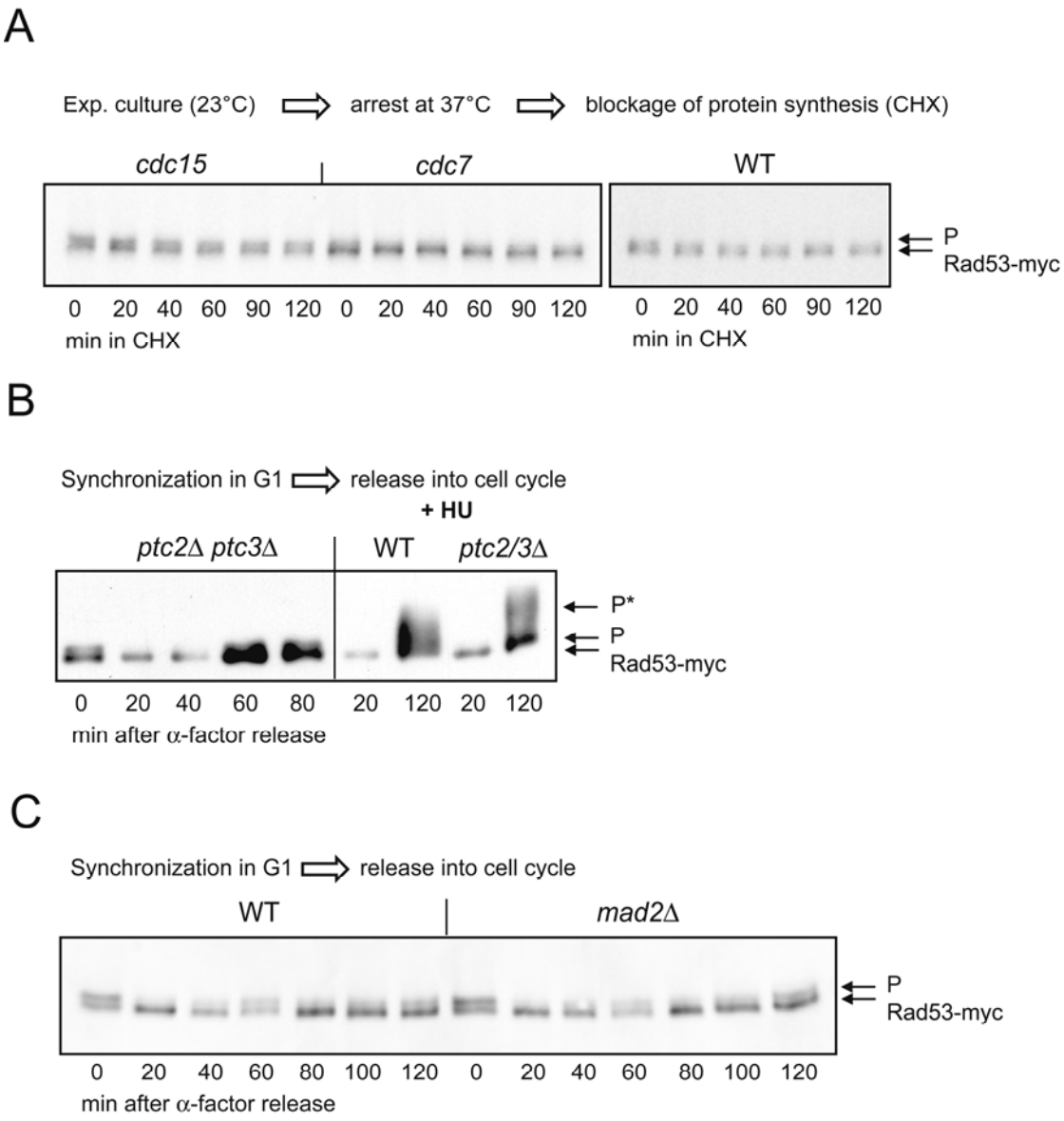

Supplemental Figure 2.2: Upshifted Rad53 protein is not unstable and upshift does not depend on Ptc2, Ptc3 and Mad2.

A: Rad53 is stable in *cdc15*-2 or *cdc7*-1 arrested cells.
Exponentially growing cultures of a *cdc15*-2 (GA-1745) and *cdc7*-1 (GA-1945) were arrested at restrictive temperature of 37°C for 90 min and *de novo* protein synthesis was blocked by addition of 25 µg/ml Cyclohexamide and samples were taken over a period of 120 minutes. Protein stability was also monitored for exponentially growing WT (GA-2019). Protein samples were separated by SDS-PAGE and probed with anti-Myc.
B: The cell-cycle dependent up/downshift still occurs in a *ptc2 ptc3* double mutant.
WT (GA-2019) and *ptc2 ptc3* double mutant strains (GA-3194) were synchronized by α-factor in G1 phase for 90 min and released into the cell cycle for up to 120 minutes +/- HU. Protein samples were taken at the indicated time points, separated by SDS-PAGE and probed with anti-Myc.
C: The cell-cycle dependent up/downshift still occurs in a *mad2* mutant.
Exponentially grown WT (GA-1906) and *mad2* mutant strains (GA-1907) were synchronized by α-factor in G1 phase for 90 min. and released into the cell cycle for up to 120 minutes. Protein samples were taken at the indicated time points, separated by SDS-PAGE and probed with anti-Myc.

A

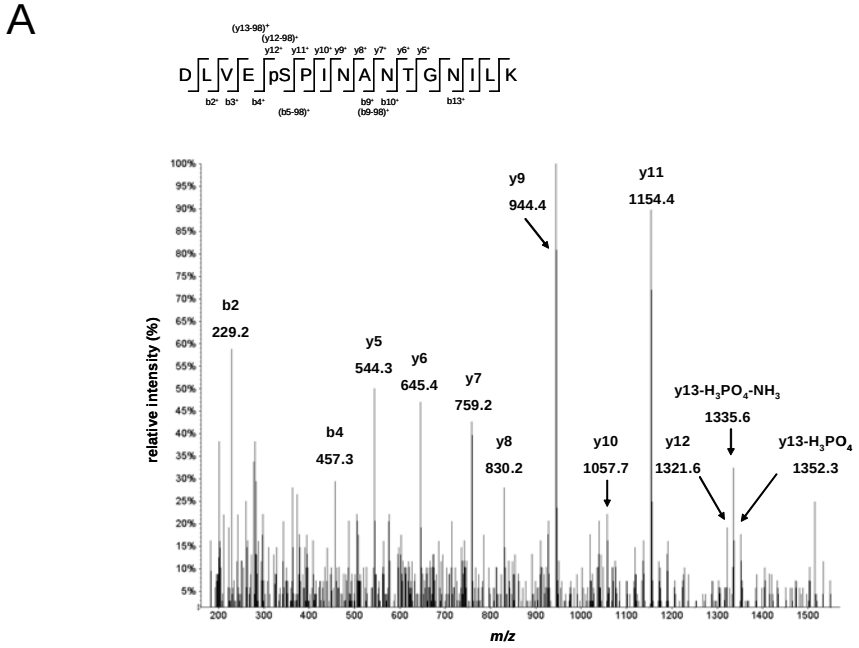

B

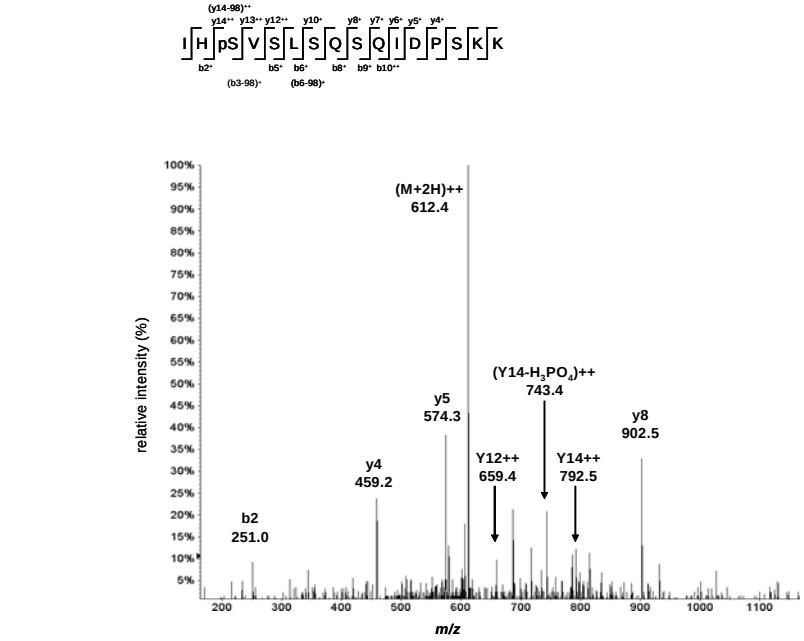

Supplemental Figure 2.3: Mass spectrometric spectra showing Rad53 Ser774 and Ser789 phosphorylation

A: Mass spectrometic spectrum showing that Ser774 is phosphorylated in mitotic Rad53 in the absence of exogenous DNA damage. Shown is the MSMS spectrum of *m/z* 889.38
B: Mass spectrometic spectrum showing that Ser789 is phosphorylated in mitotic Rad53 in the absence of exogenous DNA damage. Shown is the MSMS spectrum of *m/z* 612.1

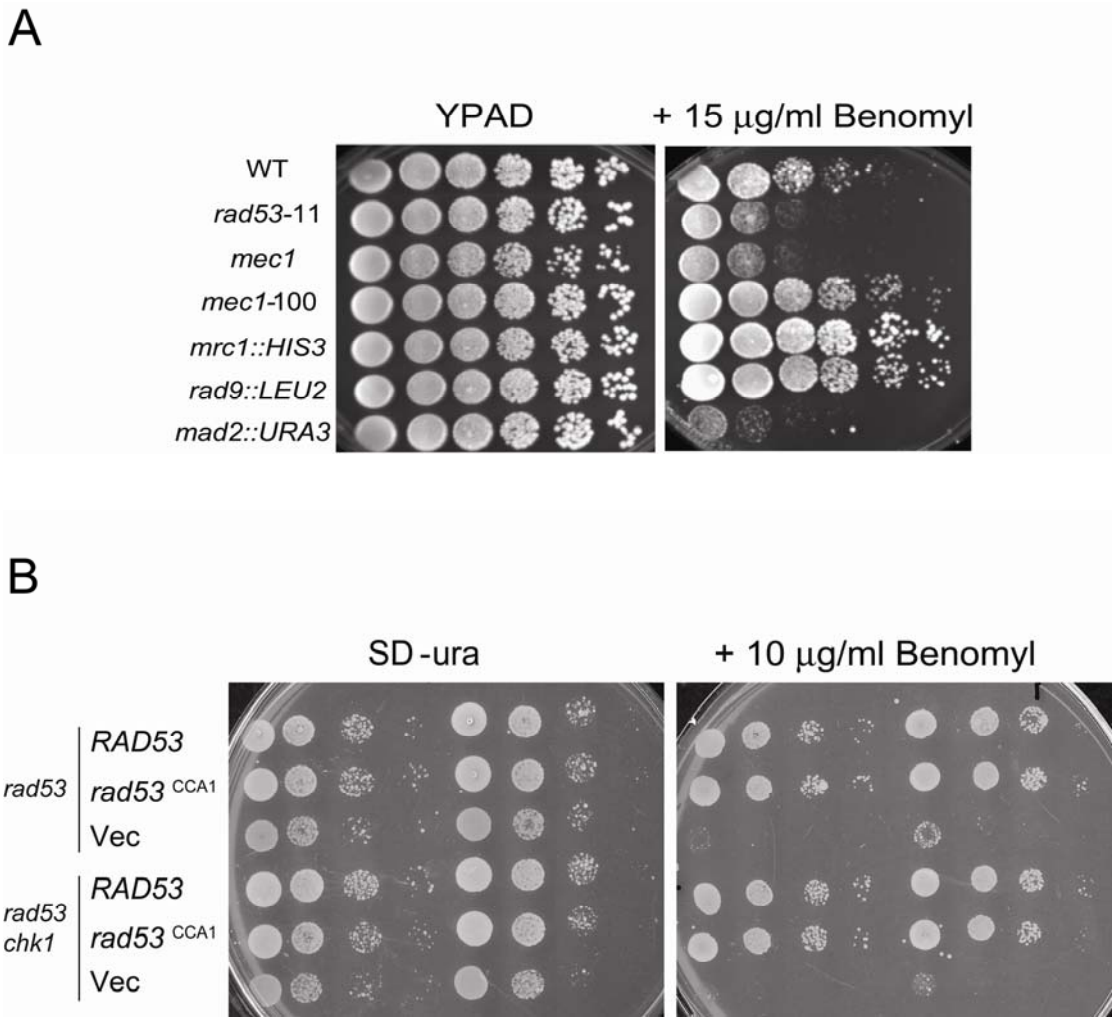

Supplemental Figure 2.4: *rad53* and *mec1* mutant strains are sensitive to benomyl

A: *rad53* and *mec1* mutant strains show a defect in cell viability in response to benomyl independent of Rad9 and Mrc1. WT (GA-180), *rad53*-11 (GA-1351), *mec1* (GA-2084), *mec1*-100 (GA-2474), *mrc1* (GA-2135), *rad9* (GA-1148) and *mad2* (GA-1868) mutant strains were dropped in a 5 fold serial dilution series on plates containing benomyl.
B: Mutation of the cell-cycle dependent phosphorylation in Rad53 does not lead to a sensitivity to benomyl. *rad53 sml1* (GA-3455) and *rad53 chk1 sml1* (GA-3666) mutant were transformed with plassmide-borne Rad53 WT and rad53^{CCA1} mutant allele. Shown is a drop assay of a 5 fold serial diluted yeast cells on plates containing benomyl.

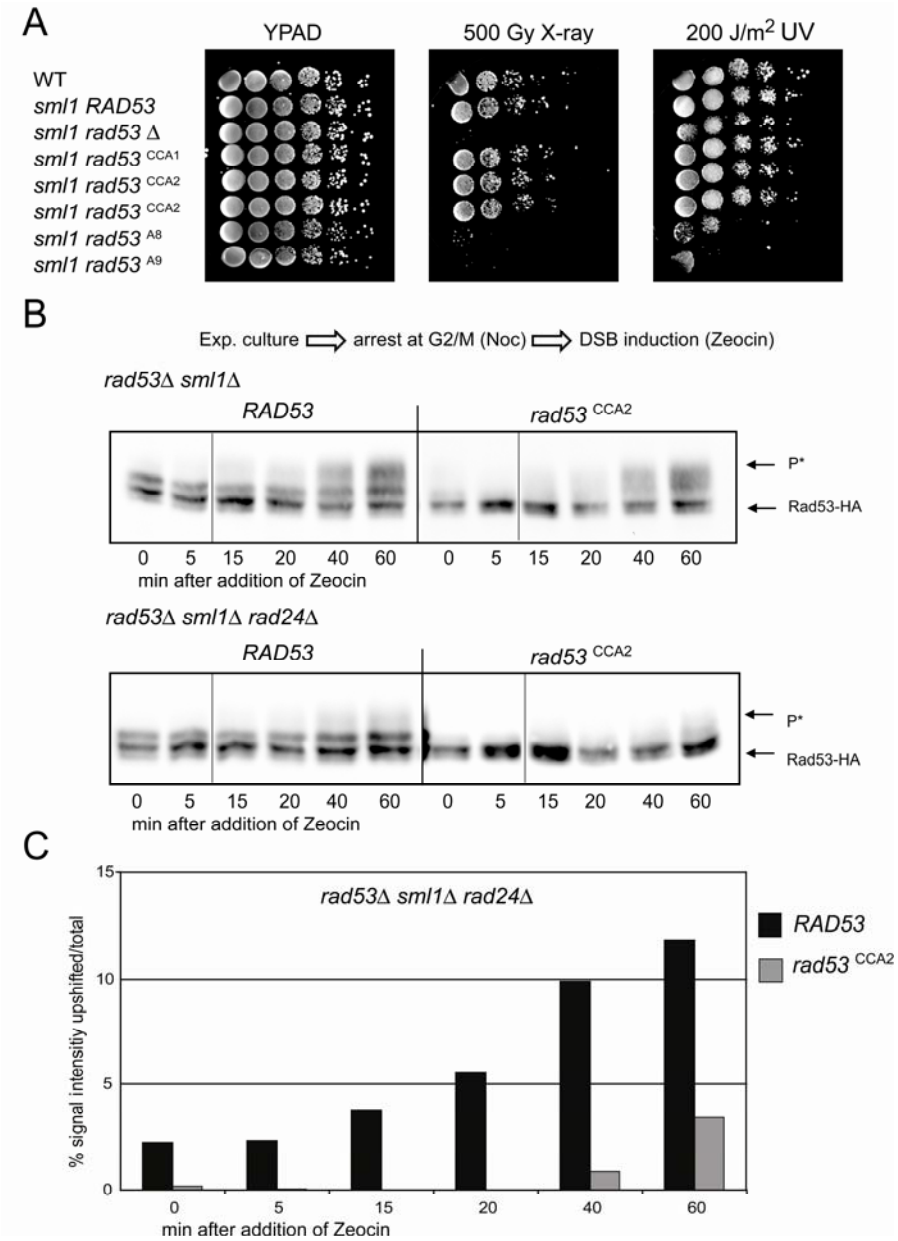

Supplemental Figure 2.5: Checkpoint activation is partially impaired in the *rad53*^{CCA2} mutant

A: *rad53*^{CCA1} and *rad53*^{CCA2} mutants have no increased sensitivity to X-ray and UV irradiation.
rad53^{CCA1} and *rad53*^{CCA2} alleles have no defect in cell viability in response to irradiation by X-rays and UV. Shown is a drop assay of 10 fold serial diluted *rad53 sml* mutant cell cultures (GA-3455) with the described Rad53 alleles on plasmid for complementation on plates after irradiation with the indicated irradiation dose.
B: Lack of mitotic phosphorylation at Ser774 and Ser789/791 leads to a lower extend of Rad53 hyperphosphorylation in response to Zeocin-induced DSBs.
rad53 sml (GA-3455) and *rad53 rad24 sml1* (GA-3636) mutant strains were transformed with pRAD53 and p*rad53* ^{CCA2}. Exponentially growing cells were shifted to YPAD medium, blocked with nocodazole in G2/M for 90 min and then DSBs were induced by addition of 5 µg/ml Zeocin. Protein samples were taken for the indicated time points, separated by SDS-PAGE and probed with anti-HA.
C: Quantification of Rad53 hyperphosphorylation.
The ushifted versus total Rad53 protein in the *rad24* mutant strain of the experiment shown in B was quantified using Quantity One.

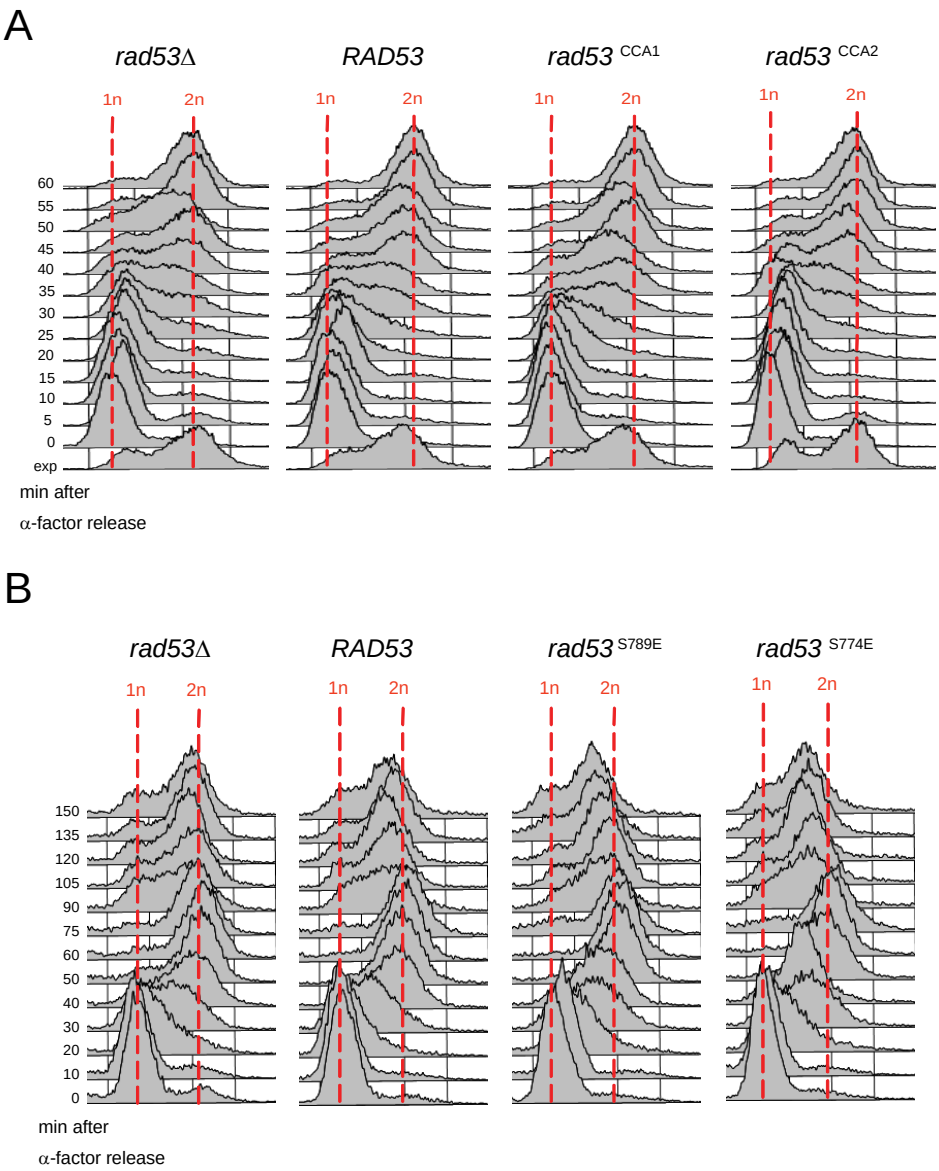

Supplemental Figure 2.6: The analysed *rad53* alleles show a normal cell cycle progression

A: *rad53*^{CCA1} and *rad53*^{CCA2} mutant strains have a normal S phase progression.
The yeast strain GA-3455 (*rad53 sml1*) was transformed with *RAD53*, *rad53*^{CCA1} and *rad53*$^{CCA2.}$ Control is a strain transformed with empty vector pYCP50. Exponentially grown cultures were arrested by α-factor in G1 phase for 90 min. and released into S phase. Cell cycle position of the synchronized cultures after release in 5 minute intervals was determined by FACS.
B: Rad53 phosphomimicking mutants have normal cell cycle progression.
The yeast strain GA-3455 (*rad53 sml1*) was transformed with *RAD53*, *rad53*^{S774E} and *rad53*^{S789E}.
Control is a strain transformed with empty vector pYCP50. Exponentially grown cultures were arrested by α-factor in G1 phase for 90 min. and released into the cell cycle. Cell cycle position of the synchronized cultures after release was determined by FACS.

Chapter 3

Histone H2A is phosphorylated by Mec1 at hydroxyurea-stalled replication forks

published as

Replisome instability, fork collapse, and gross chromosomal rearrangements arise synergistically from Mec1 kinase and RecQ helicase mutations

Jennifer A. Cobb, Thomas Schleker[4], Vanesa Rojas, Lotte Bjergbaek, José Antonio Tercero and Susan M. Gasser

published in:
Genes and Development. 2005 Dec 15;19(24):3055-69.

[4] T. S. contributed data shown in Figure 7 of the paper.

3.1 Summary

Cells are especially sensitive to genotoxic events during DNA replication and have therefore evolved a surveillance system, the intra-S-phase checkpoint that ensures the fidelity and completion of DNA replication before the onset of mitosis. Besides DNA damage, which activates the checkpoint in all cell cycle phases, an S-phase specific replication checkpoint responds to stalled replication forks and has an important role in maintaining replication fork structural integrity.

Stalling of replication forks in *Saccharomyces cerevisiae* by hydroxyurea treatment leads to stabilization of DNA polymerases and recruitment of checkpoint proteins (e.g. the ATR homologue Mec1), which can be observed by Chromatin Immunoprecipitation.

It was shown that the recruitment of checkpoint proteins and especially Mec1 leads to recruitment or modification of downstream components which initiate DNA repair. One of the major targets of ATR/ATM kinases in the damage response is modification of a C-terminal serine residue in the H2A variant, H2AX (in mammals) or H2A itself in yeast. The modified form of H2A (γH2A) spreads for roughly 25 kb to either side of an induced DSB and its modification reflects the activities of both Mec1 and Tel1 (the ATM homologue). At DSBs H2A phosphorylation is necessary for the recruitment and loading of cohesin, which favors repair from the sister chromatid, as well as the INO80 and SWR1 nucleosome remodeller complexes.

Checkpoint signaling and DNA repair mechanisms at stalled forks are still less well understood. We therefore analysed if γH2A would be present at stalled replication forks. By using Chromatin immunoprecipitation with a phospho-epitope specific antibody we monitor abundant phosphorylation of histone H2A at serine 129 at HU-arrested replication forks. The distribution is similar to that of the stabilized replication polymerase, DNA Polε. This phosphorylation is highly reduced in a *mec1* mutant strain and persists at a higher level in a *tel1* mutant strain. This is in contrast to the situation at DSBs, where both, Mec1 and Tel1 are required for efficient H2A-phosphorylation.

3.2 Copy of the publication (Cobb et al., 2005)

Replisome instability, fork collapse, and gross chromosomal rearrangements arise synergistically from Mec1 kinase and RecQ helicase mutations

Jennifer A. Cobb,[1] Thomas Schleker,[3] Vanesa Rojas,[2] Lotte Bjergbaek,[1,4] José Antonio Tercero,[2] and Susan M. Gasser[1,3,5]

[1]Frontiers in Genetics NCCR Program, University of Geneva, CH-1211 Geneva 4, Switzerland; [2]Centro de Biología Molecular "Severo Ochoa," Universidad Autónoma de Madrid/CSIC, Cantoblanco, 28049-Madrid, Spain; [3]Friedrich Miescher Institute for Biomedical Research, CH-4058 Basel, Switzerland

The yeast checkpoint kinases Mec1 and Rad53 are required for genomic stability in the presence of replicative stress. When replication forks stall, the stable maintenance of replisome components requires the ATR kinase Mec1/Ddc2 and the RecQ helicase Sgs1. It was unclear whether either Mec1 or Sgs1 action requires the checkpoint effector kinase, Rad53. By combining *sgs1Δ* with checkpoint-deficient alleles, we can now distinguish the role of Mec1 at stalled forks from that of Rad53. We show that the S-phase-specific *mec1-100* allele, like the *sgs1Δ* mutation, partially destabilizes DNA polymerases at stalled forks, yet combining the *mec1-100* and *sgs1Δ* mutations leads to complete disassociation of the replisome, loss of RPA, irreversible termination of nucleotide incorporation, and compromised recovery from hydroxyurea (HU) arrest. These events coincide with a dramatic increase in both spontaneous and HU-induced chromosomal rearrangements. Importantly, in *sgs1Δ* cells, RPA levels at stalled forks do not change, although Ddc2 recruitment is compromised, explaining the partial Sgs1 and Mec1 interdependence. Loss of Rad53 kinase, on the other hand, does not affect the levels of DNA polymerases at arrested forks, but leads to MCM protein dissociation. Finally, confirming its unique role during replicative stress, Mec1, and not Tel1, is shown to modify fork-associated histone H2A.

[*Keywords*: Replicative stress; checkpoint; DNA polymerases; Mec1; Sgs1; chromosome instability]

Supplemental material is available at http://www.genesdev.org.

Received August 3, 2005; revised version accepted October 24, 2005.

Intact S-phase checkpoint mechanisms are essential for cell survival and proliferation in the presence of DNA replicative stress, which can be caused by the stalling of replication forks at DNA lesions, at DNA-bound protein complexes (Ivessa et al. 2003), or as a result of reduced nucleotide levels induced by the addition of hydroxyurea (HU). Importantly, DNA replication defects and genomic instability are both hallmarks of oncogenic transformation. Indeed, cancer cells appear to persist in a state of perpetual replicative stress, which correlates with low but continuous signs of an activated DNA damage response, such as histone H2AX and CHK2 phosphorylation (Halazonetis 2004). In budding yeast, the ATR kinase homolog Mec1 and its downstream effector kinase Rad53, the hCHK2 homolog, are both central to the DNA damage checkpoint signaling cascade.

A role for ATM-related kinases in the cellular response to replication fork stalling is conserved in all eukaryotes. The affinity of the mammalian ATRIP for replication protein A (RPA) suggests a model in which ATR-ATRIP is recruited to sites of damage or to abnormal structures generated at stalled replication forks that contain extended regions of RPA-bound single-stranded DNA (ssDNA) (Zou and Elledge 2003). Mec1 requires a cofactor Ddc2, the counterpart to mammalian ATRIP, and loss of either subunit abrogates the checkpoint-dependent phosphorylation of Rad53 and Pds1 proteins, precluding a checkpoint response (Paciotti et al. 2000). Once recruited, Mec1 may act by phosphorylating fork-associated targets such as RPA (Brush et al. 1996; Kim and Brill 2003; Bartrand et al. 2004) or the replication/checkpoint adaptor protein Mrc1 (Alcasabas et al. 2001; Osborn and Elledge 2003).

[4]Present address: Department of Molecular Biology, Aarhus University, DK-8000 Aarhus C, Denmark.
[5]Corresponding author.
E-MAIL susan.gasser@fmi.ch; FAX 41-61-697-39-76.
Article and publication are at http://www.genesdev.org/cgi/doi/10.1101/gad.361805.

In mammals, the ATR kinase was also shown to bind and phosphorylate the RecQ helicase BLM (Davies et al. 2004; Li et al. 2004). RecQ helicases are a family of 3′–5′ DNA-unwinding enzymes conserved from bacteria to man, which includes a single budding yeast homolog called Sgs1. Mutations in three of five human RecQ helicases are responsible for genetic disorders that correlate with chromosomal loss, increase rates of translocation, and cause premature aging or cancer (for review, see Mohaghegh and Hickson 2001). BLM helicase, like the yeast Sgs1 protein, associates with DNA repair foci in S-phase cells, and was recently shown to be an intermediary in the response to stalled replication forks, physically interacting with 53BP1 and γ-H2AX in human cells (Sengupta et al. 2004).

In budding yeast, elimination of Sgs1 helicase leads to elevated rates of meiotic and mitotic recombination (Watt et al. 1996), increased frequencies of spontaneous gross chromosomal rearrangements (GCR) (Myung and Kolodner 2002), as well as aberrant DNA replication phenotypes (Versini et al. 2003; Liberi et al. 2005). When replication forks are stalled by the addition of HU, *sgs1*-deficient cells suffer a partial loss of fork-associated DNA polymerases (Cobb et al. 2003). It was proposed but not proven that the chromosome instability arises from loss of polymerases at stalled forks.

One way to categorize the various phenotypes associated with a loss of Sgs1 is to determine whether or not they require its helicase activity, and/or the associated type I topoisomerase, Top3. For instance, Sgs1 contributes to the activation of Rad53 in response to HU, on a pathway that is redundant with break-induced signaling pathways (Frei and Gasser 2000). This activity requires intact Sgs1, but neither its helicase function nor the activity of Top3 (Bjergbaek et al. 2005). In contrast, the contribution of Sgs1 to replication fork stability on HU requires both the helicase activity and Top3 interaction (Cobb et al. 2003; Bjergbaek et al. 2005). Moreover, loss of Sgs1's polymerase stabilizing function appears to be epistatic with loss of the strand-exchange factor Rad51, consistent with the observation that Rad51-dependent cruciform structures accumulate at stalled forks in *sgs1* cells (Liberi et al. 2005).

By monitoring cells as they synchronously enter S phase, we have shown that both Mec1/Ddc2 and Mrc1 are required to stabilize DNA polymerase ε (pol ε) and α (pol α) at stalled replication forks during the first hour of HU-induced arrest (Cobb et al. 2003; Katou et al. 2003; Bjergbaek et al. 2005). This occurs prior to Rad53 kinase activation. Consistently, fork-bound polymerases remain bound at stalled forks in cells that carry a complete *rad53* deletion (Cobb et al. 2003). Inexplicably, however, an active-site mutation, *rad53*-K227A, appears to provoke a partial loss of both DNA pol ε and pol α on HU (Lucca et al. 2004). Other differences in the response to replicative stress have been reported for different checkpoint mutants. For instance, a complete deletion of *mec1* increased the rate of spontaneous GCR far more significantly than the loss of the G2 damage checkpoint in *rad9* or *rad53* cells (Kolodner et al. 2002). Nonetheless, the survival rate of a *rad53* mutant after exposure to HU was just as compromised as a *mec1*Δ strain (Weinert et al. 1994), and strains lacking Rad53 are unable to resume replication after fork stalling (Lopes et al. 2001; Tercero et al. 2003). While these studies suggest that the functions of Mec1/Ddc2 and Rad53 kinase at stalled forks are distinct, they do not reveal how their modes of action differ.

Past results supported the argument that Sgs1, Mrc1, Mec1/Ddc2, and Rad53 all contribute to cellular recovery after replication fork arrest, yet the relationship between the maintenance of engaged replicative polymerases and prevention of irreversible fork collapse remained unclear, because these proteins act on overlapping pathways. Here we dissect the roles of the Mec1/Ddc2 complex and Rad53 kinase in preserving replication fork integrity, by combining an S-phase-specific allele of *mec1* with a complete deletion of *sgs1*. We detect a dramatic synergism between *sgs1*Δ and *mec1-100* mutations in promoting fork collapse and in destabilizing replication polymerases at stalled forks, a defect that cannot be attributed to impaired activation of the downstream kinase Rad53. The *sgs1* and *mec1-100* mutations affect the binding of RPA and Mec1/Ddc2 at stalled forks differentially, and collectively lead to complete polymerase loss. This is not the case in cells lacking Rad53, although other replisome components, like the MCM helicase, are found displaced from stalled forks in this mutant. Finally, we recover phosphorylated H2A at stalled replication forks and show that its modification depends exclusively on Mec1. These data directly link the loss of polymerases and RPA from forks and an inability to recover from replicative stress, with dramatic increases in both spontaneous and HU-induced chromosomal rearrangements. This suggests mechanisms through which ATR and BLM maintain genomic stability.

Results

Sgs1p and Mec1p contribute independently to genomic stability and cell viability

Previous studies have implicated the *Saccharomyces cerevisiae* replication checkpoint in the suppression of spontaneous genomic instability (for review, see Kolodner et al. 2002). Cells with deletions for Mec1 were shown to be highly synergistic with the loss of Sgs1 for GCR (Myung and Kolodner 2002). Surprisingly, the synergism with *sgs1* was much less pronounced for mutants that lose the DNA damage-induced checkpoint response, such as *rad24*, *rad53*, or *tel1* (Myung and Kolodner 2002). While this suggested a special relationship between the S-phase functions of Sgs1 and Mec1, there were no data to link this instability to their roles at stalled replication forks.

Given that the complete deletion of *MEC1* compromises both the intra-S and the G2/M checkpoint responses, we made use of the *mec1-100* allele, which is deficient for the replication checkpoint but which maintains a functional G2/M arrest in response to strand

breaks (Paciotti et al. 2001). The mutation reflects two amino acid substitutions ($F^{1179}S$ and $N^{1700}S$), upstream of the C-terminal PI3-kinase domain in a region shared with the fission yeast and mammalian ATM/ATR enzymes. We introduced the appropriate markers to monitor GCR and backcrossed to generate isogenic strains bearing either the *mec1-100* allele, an *sgs1* deletion, or both. Spontaneous and HU-induced GCR, and viability during chronic exposure to HU, were then monitored. Finally, we scored the strains for their ability to recover from nucleotide depletion and resume DNA replication.

The rate of spontaneous GCR monitored in the *mec1-100* allele is 187-fold above that in wild-type cells, while that of *sgs1*Δ increases by 67-fold (Table 1). By deleting *sgs1* in the *mec1-100* background, we see the rate of GCRs rise synergistically to a value 573-fold above the wild-type rate. This phenotype is unique to the *mec1-sgs1* combination; in *rad53-11 sgs1*Δ cells, GCR rates are 177-fold above wild type, which is not even additive (177 < 67 + 123-fold). Therefore, with respect to chromosome instability, the *mec1-100* allele shows synergistic effects with *sgs1*Δ much like *mec1*Δ (Myung and Kolodner 2002). This genetic interaction becomes even more severe when cells are treated with 0.2 M HU. Under these conditions, *mec1-100* cells showed a 6×10^3-fold increase in GCR rate over wild type, and the double mutant reaches 1.62×10^5 times the wild-type GCR rate (Table 1). This elevated GCR rate in *mec1-100 sgs1*Δ cells is dramatically exacerbated by HU, increasing by another 667-fold (+HU/–HU), while the same ratio is 2.4-fold in wild-type cells (Table 1).

Coincident with this extreme chromosome instability, we monitor a severe loss of cell viability both when the double mutant is plated on low levels of HU (Fig. 1A), or after cells have been arrested for increasing periods of time on HU, and released for growth in the absence of drug (Fig. 1B). Although neither *sgs1*Δ nor *mec1-100* mutations alone are highly sensitive, the *mec1-100 sgs1*Δ cells are nearly as compromised as the *mec1*Δ strain. This is not suppressed by up-regulating dNTP levels (i.e., by *sml1* deletion) (Fig. 1B), which is necessary for viability in the *mec1*Δ background. Observing the S-phase-specific defects of the *mec1-100* strain and its high rates of GCR, we speculated that this mutation might be sufficient to irreversibly destabilize replication polymerases and cause fork collapse, as reported for the more pleiotropic *mec1*Δ mutation (Tercero and Diffley 2001; Cobb et al. 2003).

Combining mec1-100 *and* sgs1Δ *mutations synergistically promotes fork collapse*

When yeast cells enter S phase in media containing HU, early origins fire normally, yet the rate of replication is severely reduced due to low dNTP levels. In wild-type cells, DNA polymerases remain fork-associated or progress very slowly along the chromosome, allowing efficient recovery when nucleotide levels are restored. In *mec1*Δ cells, on the other hand, forks that encounter damage collapse (Tercero and Diffley 2001). To see if fork collapse correlates with the synergistic effects on GCR rates scored for the *mec1-100 sgs1*Δ double mutant, we monitored replication fork progression in HU with a density isotope substitution method (Fig. 2; Tercero et al. 2000), using probes that recognize DNA fragments at the origin (fragment 1) or at a site ~15 kb away (fragment 2). This monitors nucleotide incorporation genome-wide, as well as locally.

In wild-type, *sgs1*Δ and *mec1-100* single mutant cells, we clearly detect the replication of fragment 1 by 120 min in HU, although between 30% and 35% of the forks stall within this zone. Little of fragment 2 becomes fully replicated (Fig. 2A,C), consistent with data from Santocanale and Diffley (1998), who found that most forks stall within 10 kb of an origin in cells exposed to high concentrations of HU. In *mec1-100 sgs1*Δ cells, on the other hand, no replication of fragment 1 can be detected under identical conditions (Fig. 2D). Given that there are no differences for the timing of S-phase onset, budding index (Supplementary Fig. 1), and bubble arc appearance (Fig. 3), nor in the level of Orc2 recovered at origins by chromatin immunoprecipitation (ChIP), we conclude that the *mec1-100 sgs1*Δ strain, unlike either single mutant, suffers severe attenuation of fork progression on HU.

To monitor the reversibility of fork stalling in these cultures, cells were released from HU arrest by placing them in fresh, drug-free media. Under these conditions, wild-type, *mec1-100*, and *sgs1*Δ cells all resume DNA replication satisfactorily (Fig. 2A–C). By 80 min, both fragments 1 and 2 are fully replicated, indicating that a large fraction of replication forks recover and continue DNA synthesis after HU removal. In contrast, the *mec1-100 sgs1*Δ double mutant shows significant amounts of unreplicated DNA even after release into fresh media (Fig. 2D). We estimate that significantly fewer than 50% of the replication forks resume DNA synthesis in the

Table 1. *Effect of* sgs1Δ *and* mec1-100 *mutations on spontaneous and HU-induced GCR rates*

Genotype	GCR	GCR after 0.2M HU	Fold increase (+HU/–HU)
Wild-type (S288c)	$2.4\ [0.7–4.1] \times 10^{-10}$ (1)	$5.6\ [0.7–10.0] \times 10^{-10}$ (1)	2.4
*sgs1*Δ	$1.6\ [0.3–28.4] \times 10^{-8}$ (67)	$6.9\ [3.2–10.6] \times 10^{-8}$ (123)	4.4
mec1-100	$4.5\ [2.4–6.6] \times 10^{-8}$ (187)	$3.4\ [3.0–3.8] \times 10^{-6}$ (6000)	75.3
rad53-11	$3.0\ [2.0–3.9] \times 10^{-8}$ (123)	[a]	N/D
*sgs1*Δ *mec1-100*	$1.4\ [1.2–1.6] \times 10^{-7}$ (573)	$9.1\ [4.8–13.4] \times 10^{-5}$ (162,000)	667
*sgs1*Δ *rad53-11*	$4.2\ [3.7–4.7] \times 10^{-8}$ (177)	[a]	N/D

[a]Too few survivors were recovered under these conditions to determine rates of GCR. [ ] indicates the highest and lowest rates observed in the fluctuation tests. The numbers in parentheses are the fold increases in the rate relative to that of the wild-type strain.

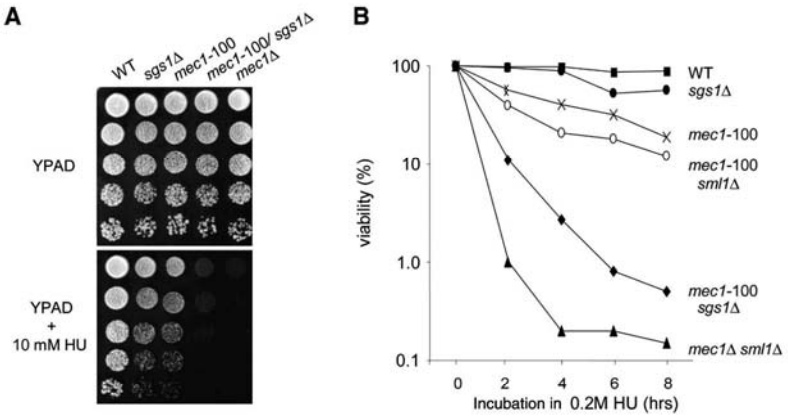

Figure 1. Highly synergistic effects of *mec1-100* and *sgs1*Δ mutations on chromosome stability and recovery from HU. (*A*) Drop assays on YPD ± 10 mM HU were performed with exponentially growing cultures of the indicated W303-1a (GA-180) derivates, using a 1:5 serial dilution series: *sgs1*Δ (GA-1761), *mec1-100* (GA-2474), *mec1-100 sml1*Δ (GA-2478), *mec1-100 sgsl*Δ (GA-2514), or *mec1*Δ *sml1*Δ (GA-2895). (*B*) Cell viability was monitored as colony outgrowth from cultures synchronized by α-factor and held in YPD + 0.2 M HU for indicated times.

double mutant, since the replication of fragments 1 and 2 could initiate from any origin on the chromosomal arm to complete replication by 80 min. We conclude that a high fraction of DNA replication forks collapse irreversibly in the *mec1-100 sgs1*Δ strain on HU. This is reminiscent of the fork collapse reported for the *mec1*Δ strain on MMS (Tercero and Diffley 2001), and is likely to account for the loss of viability observed for these cells (Figs. 1B, 2D).

Sgs1 and Mec1 cooperate to stabilize DNA polymerases at stalled replication forks

To see if fork collapse and high GCR rates are due to a loss of replicative polymerases at forks, we performed ChIP for both DNA pol α and pol ε, comparing wild-type and mutant strains as they synchronously enter S phase in the presence of 0.2 M HU (Cobb et al. 2003; Bjergbaek et al. 2005). During the first hour in HU, the abundance of Myc-tagged DNA pol ε and HA-tagged DNA pol α was analyzed at the early-firing origin ARS607 (filled symbols) by real-time PCR (rtPCR). As a negative control, we probed for a site +14 kb away from the origin (Fig. 3B, open symbols). The values plotted are direct ratios of the mean rates of fragment accumulation monitored by rt-PCR in immunoprecipitates over control precipitates.

In Figure 3D, we show that both DNA pol ε and pol α are efficiently associated with ARS607 by 20 min after release from a pheromone arrest. In the absence of HU, the polymerases progress rapidly through both the origin and distal sites, and genomic replication is completed by ~30 min (Cobb et al. 2003). However, in HU-containing medium, both polymerases remain associated with the stalled fork for ~60 min (Fig. 3D, filled symbols), and migrate slowly into the fragment at +14 kb by 60 min (Fig. 3D, open symbols and stippled lines). When the same assay is performed in either *sgs1*Δ or *mec1-100* cells, we see a partial loss of DNA pol ε and pol α at ARS607 (2- to 2.5-fold reduction) as compared with the isogenic wild-type strain (Fig. 3D–F).

A much more striking loss of polymerases occurs in the *mec1-100 sgs1*Δ cells. We see that both DNA pol ε and pol α levels drop to near background levels at ARS607 (Fig. 3G), as occurs in *mec1*Δ and *mec1*Δ *sgs1*Δ cells (Supplementary Fig. 2). We also observe a transient enrichment of DNA pol α and pol ε at the late-firing origin ARS501 in *mec1-100* cells (Supplementary Fig. 3), confirming that late origins fire precociously in these mutants (Santocanale and Diffley 1998). ARS501 serves as a positive control both for the assay and the *mec1-100* defect for Rad53 activation (Fig. 4A,B; Paciotti et al. 2001; Tercero et al. 2003).

The drop in polymerase levels in *mec1-100 sgs1*Δ cells is not due to aberrant initiation timing as demonstrated by 2D gel analysis of replication intermediates (Fig. 3A). Furthermore, it is presumed that prereplication complexes are not disrupted, since Orc2 recovery at ARS607 is similar in wild-type and mutant cells (Fig. 3C). Finally, the budding index is not significantly altered in any of these mutants, either in the presence or absence of HU (Supplementary Fig. 1), and progression through S phase in the absence of HU occurs normally (see ChIP for DNA pol ε and FACS analysis) (Supplementary Fig. 4). Thus, there must be a true reduction in the level of replicative enzymes bound to stalled forks in *mec1-100 sgs1*Δ cells. This correlates with an accumulation of aberrant X-shaped structures in neutral-neutral 2D gels of *mec1-100 sgs1*Δ mutants treated ~20 min with HU (Fig. 3A, see arrow). These may reflect nonproductive fork-associated recombination events.

Polymerase stability at stalled forks is independent of Rad53 checkpoint activation

We next asked whether the defects on HU reflect the double mutant's inability to activate Rad53 kinase and thereby delay progression into mitosis. Indeed, *rad53*Δ cells, like both the *mec1*Δ and *mec-100 sgs1*Δ double mutant, are known to lose viability after exposure to high HU concentrations (Desany et al. 1998; Lopes et al. 2001), and irreversible fork collapse was reported to occur in both *rad53*Δ and *mec1*Δ strains on MMS (Tercero and Diffley 2001). Our previous work indicated that DNA polymerases remained efficiently bound at stalled

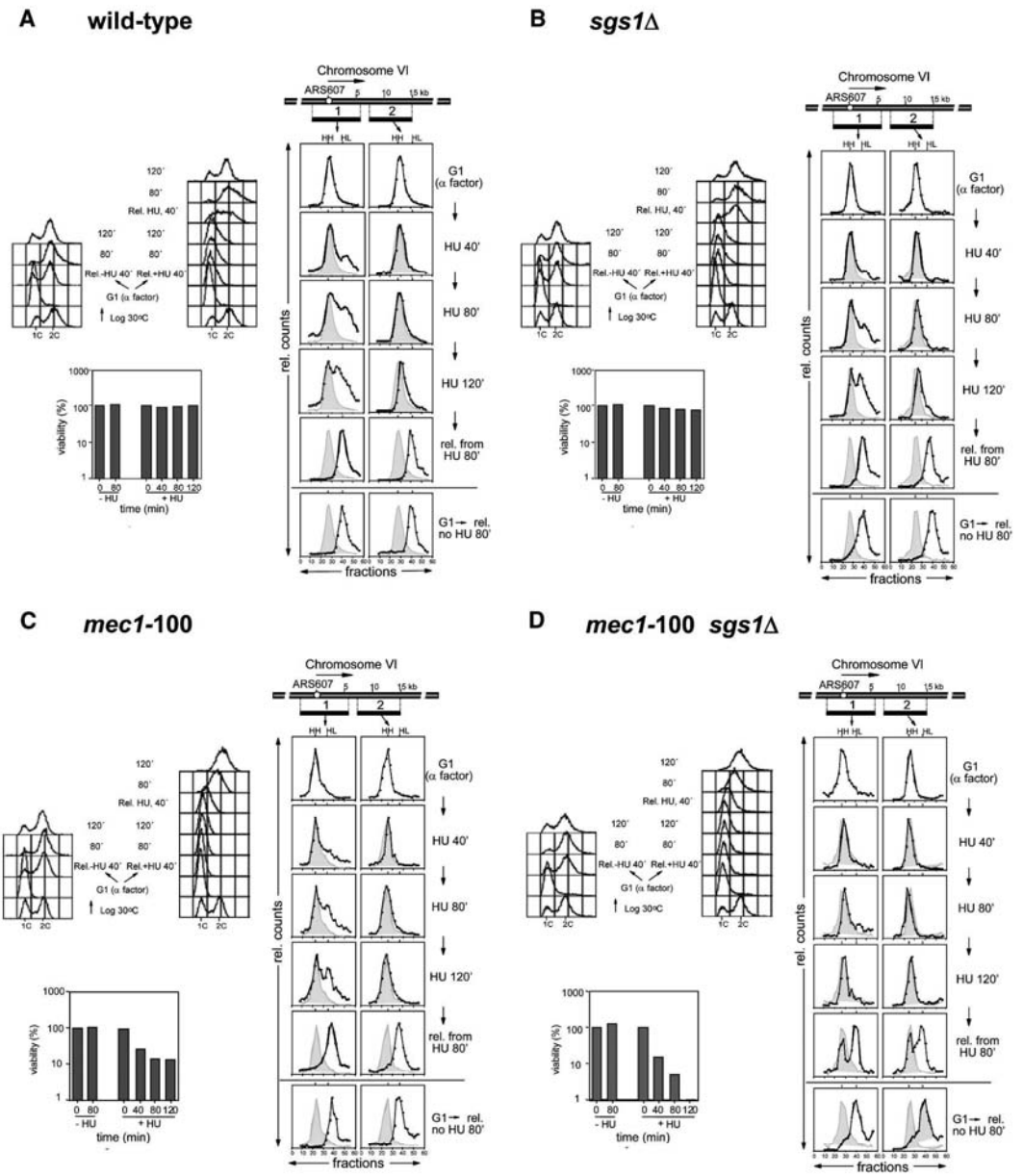

Figure 2. Replication fork collapse in *mec1-100 sgs1*Δ mutants. For all panels, cells were grown in minimal medium with heavy (H) isotopes and blocked in G1 with α-factor. The cultures were held in α-factor for an additional 30 min in light (L) isotope before dividing and releasing into fresh medium ± 0.2 M HU. Samples were taken at 40, 80, and 120 min, when cells were released from HU and their recovery was monitored. DNA content as determined by flow cytometry and cell viability for all strains was scored at the indicated time points. A time course of DNA replication at ARS607 was analyzed by density transfer after release from α-factor arrest into medium with 0.2 M HU, using specific probes recognizing the ClaI/SalI fragments 1 and 2. The relative amounts of radioactivity in the hybridized DNA are plotted against the gradient fraction number. The positions of unreplicated (heavy–heavy, HH) and fully replicated heavy–light (HL) are indicated. At later time points, the position of the initial HH peak is shown for comparison (gray area). Corresponding FACS analysis and survival assays are shown for each isogenic strain bearing the following mutations: wild-type (YJT110) (*A*); *sgs1*Δ (YVR1) (*B*); *mec1-100* (GA-2931) (*C*); and *mec1-100 sgs1*Δ (GA-2930) (*D*).

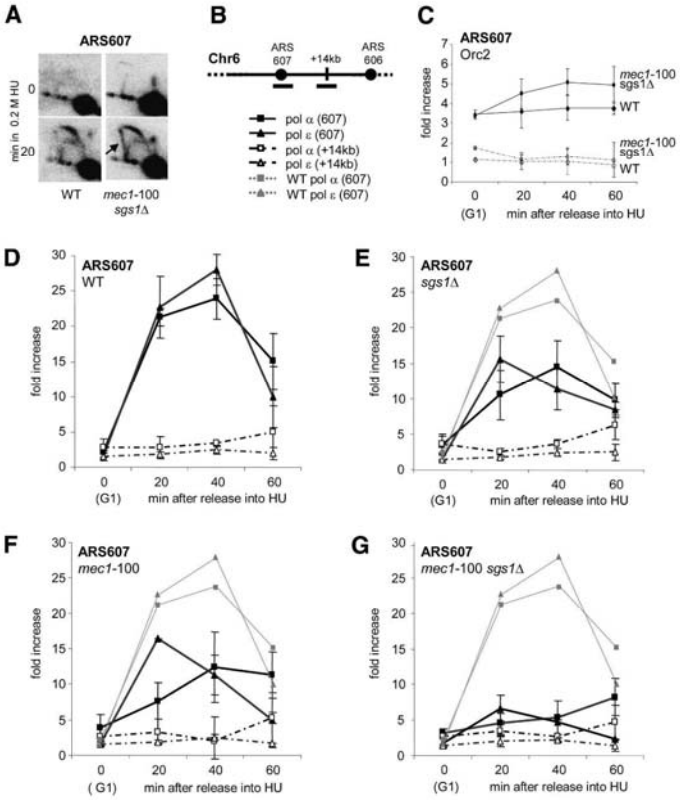

Figure 3. Loss of DNA polymerases at stalled replication forks in *mec1-100 sgs1*Δ cells. (*A*) Neutral/neutral 2D gel analysis was performed at ARS607 in wild-type (GA-1020) and *mec1-100 sgs1*Δ (GA-2514) cells released from α-factor arrest into YPD + 0.2 M HU. Genomic DNA was prepared from cells collected at 0 (G1) or 20 min after release, and the Southern transfer was probed with a 2.6-kb fragment spanning ARS607. (*B*) Primers were designed to amplify genomic regions on Chr 6 corresponding to early-firing origin ARS607 (filled symbols) and a nonorigin site, +14 kb (open symbols). ChIP was performed on cultures synchronized in G1 by α-factor arrest, and released into prewarmed YPD + 0.2 M HU, prior to fixation with 1% formaldehyde at the indicated time points. (*C*) ChIP with anti-Myc (9E10) is used to quantify Myc-Orc2 presence at ARS607 in isogenic wild-type (GA-2897, diamonds) and *mec1-100 sgs1*Δ (GA-2896, ovals) cells. (*D–G*) ChIP with anti- Myc (9E10) or anti-HA (12CA5) precipitated HA-tagged DNA pol α (squares) or Myc-tagged DNA pol ε (diamonds). The strains used were wild-type strains GA-2238 and GA-2448 in *D*; *sgs1*Δ strains GA-2256 and GA-2450 in *E*; *mec1-100* strains GA-2567 and GA-2515 in *F*; and *mec1-100 sgs1*Δ strains GA-2578 and GA-2516 in *G*. In *E–G*, wild-type signals are shown as light-gray dashed lines for comparison. Controls and quantitation are described in Materials and Methods. Standard deviation is calculated from duplicate runs and multiple independent experiments.

forks in a *rad53*Δ strain (Cobb et al. 2003), yet in these experiments the *rad53*Δ mutation was coupled with *sml1*Δ, to prevent cell death (Zhao et al. 1998). The *sml1* mutation up-regulates ribonucleotide reductase genes (*RNR1-4*), which might conceivably influence replisome stability indirectly. Thus, to test whether the loss of Rad53 activity contributes to the synergism between the *mec1-100* and *sgs1*Δ mutations, we tested a recessive, activity-dead allele called *rad53-11*, which fails to become phosphorylated and to activate the checkpoint, yet which does not require *sml1* deletion for survival (Weinert et al. 1994; Pellicioli et al. 1999).

An in-gel Rad53 autophosphorylation assay confirms that on HU, Rad53 is activated by 60 min in wild-type cells, but is inactive in a *rad53-11* mutant, and is strongly reduced in the *mec1-100* allele (Paciotti et al. 2001). In the *mec1-100 sgs1*Δ strain, we see slightly more Rad53 activity, perhaps reflecting the higher rates of DNA breakage and activation of the G2 checkpoint through Rad9 (Fig. 4A,B). Since impaired Rad53 activation might accelerate progression into mitosis, we tested whether we could enhance the viability of the double mutant by providing time for recovery from HU. Delaying the G2/M transition by placing the HU-arrested cells transiently in nocodazole-containing media, did not, however, increase survival (Supplementary Fig. 5), arguing that the loss of viability in *mec1-100* or *mec1-100 sgs1*Δ strains is not due simply to premature entry into mitosis or uncontrolled spindle elongation.

We next analyzed the effect of the *rad53-11* allele on DNA polymerase stability at HU-arrested forks by monitoring whether a loss of Rad53 activity is synergistic with the deletion of *sgs1*. ChIP experiments performed with an isogenic *rad53-11* mutant show nearly identical levels of DNA pol ε and pol α at ARS607 as the wild-type and the *rad53*Δ *sml1*Δ control strains (Fig. 4C; Cobb et al. 2003). In these mutant samples, we also detect the recruitment of DNA polymerases to the late-firing origin ARS501, confirming that Rad53 failed to activate the checkpoint response that suppresses late origin firing (Supplementary Fig. 3; Santocanale and Diffley 1998). Importantly, when *rad53-11* is combined with a deletion of *sgs1*, we detect no synergism whatsoever, and the levels of fork-associated DNA pol ε and pol α are identical to the levels scored in *sgs1*Δ cells (Fig. 4D). Thus, the loss of DNA polymerases at stalled forks in *mec1* cells, and in the *mec1-100 sgs1*Δ double mutant, does not reflect Mec1's role as an activator of Rad53 kinase and its downstream checkpoint response. This result supports the hypothesis that both Mec1 and Sgs1 have a Rad53-independent function at replication forks (Desany et al. 1998; Tercero and Diffley 2001; Bjergbaek et al. 2005).

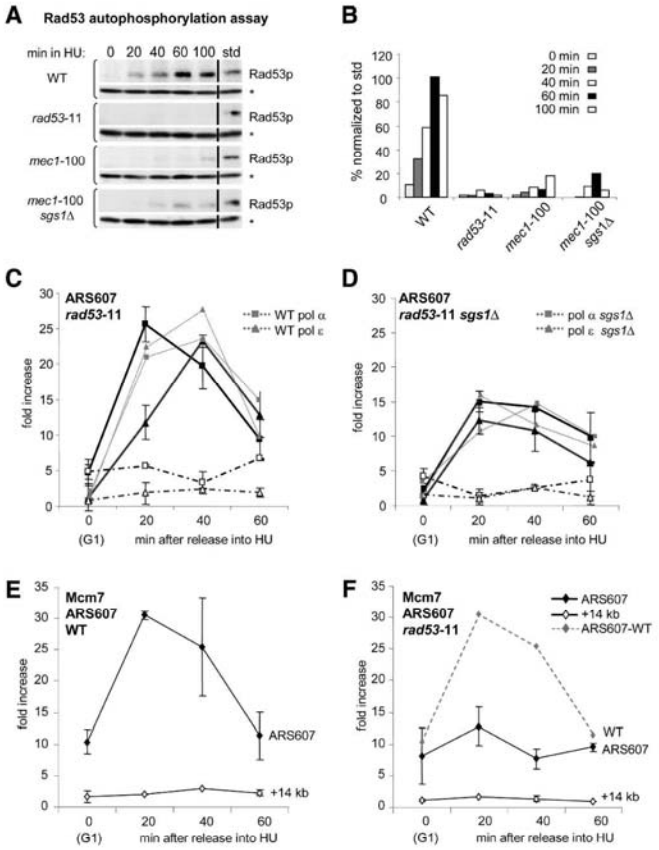

Figure 4. Rad53 is needed to stabilize MCM proteins but not DNA polymerases at stalled forks. (*A*) ISA analysis of Rad53 autophosphorylation was performed on wild-type (GA-1020), *rad53-11* (GA-2240), *mec1-100* (GA-2474), and *mec1-100 sgs1*Δ (GA-2514) cells. For each strain, the *upper* box shows the incorporation of γ^{32}-ATP into Rad53, and the *bottom* panel shows the same blot probed with anti-RNaseH42 to normalize loading (*). Time (in minutes) after α-factor release is indicated *above* each panel, and "std" is 5 µL of a standard containing a known amount of a HU-activated Rad53. For every sample, protein concentration was determined by Coomassie blue staining prior to equally loading gels. Dried filters were exposed for equal times on a Bio-Rad PhosphorImager, before reprobing for RNaseH42 to normalize signals. (*B*) Quantification of Rad53 autophosphorylation displayed as a normalized percentage of std. Shown is an average of two experiments with standard deviations between 5% and 15%. (*C*,*D*) ChIP was performed as described in Figure 3 for HA-tagged DNA pol α (squares) and Myc-tagged DNA pol ε (diamonds) in *rad53-11* strain GA-2574 and *rad53-11 sgs1*Δ strain GA-2576. (*E*,*F*) ChIP was performed for Myc-tagged Mcm7 (diamonds) in cultures released from α-factor into 0.2 M HU as in Figure 3 using wild type (GA-1003) and *rad53-11* (GA-3054). rtPCR was performed as described for ARS607 (filled symbols) and +14 kb (open symbols). Wild-type and *sgs1*Δ signals are shown in light-gray dashed lines for comparison.

Why then are stalled replication forks unable to recover in the absence of Rad53 activity? One of the phenotypes of *rad53*-deficient cells arrested on HU is the accumulation of long stretches of ssDNA at stalled forks (Sogo et al. 2002), which could result from an uncoupling of polymerases from the MCM helicase (Byun et al. 2005). Similarly, cells lacking the histone chaperone Asf1, which interacts with Rad53, show aberrant replisome stability with the MCM helicase being displaced along the template (Franco et al. 2005). To see if the *rad53-11* strain would have a similar phenotype, we monitored MCM proteins at replication forks stalled on HU, as described above. Indeed, fork-associated Mcm7 levels drop significantly in the *rad53-11* mutant, and it does not move into the +14-kb fragment (Fig. 4E,F). Similar results were obtained for a tagged Mcm4 subunit, where we see that Rad53 checkpoint activation, but not Sgs1, is necessary for Mcm4 maintenance (Supplementary Fig. 6). Thus, the primary defect at stalled forks in *rad53*-deficient cells appears to be the displacement of MCM proteins, which does not necessarily lead to polymerase loss. We do not know whether MCM proteins become displaced along the DNA fiber, or are completely lost from stalled forks.

RPA recovery at replication forks is diminished in the mec1-100 sgs1Δ *double mutant*

To identify the mechanisms through which *mec1-100* and *sgs1*Δ cells lose functional replication forks, we looked at factors that might be differently regulated by Mec1 and Rad53, yet which also interact with Sgs1. One likely candidate was the single-strand binding complex, RPA, which interacts strongly with Sgs1 both in the presence and absence of HU (Cobb et al. 2003). This interaction is conserved, as BLM and WRN helicases both bind human RPA tightly (Brosh et al. 2000; Doherty et al. 2005). Importantly, functional RPA is known to be necessary for the recruitment of pol α-primase (Tanaka and Nasmyth 1998) and pol ε to active forks (Lucca et al. 2004), and the phosphorylation of Rpa2 in response to DNA damage requires Mec1, but not Rad53 (Brush et al. 1996; Kim and Brill 2003). Indeed, in response to HU, Rpa2 is fully phosphorylated in the *rad53-11* mutant, yet lacks damage-specific modifications in the *mec1*-deficient strain. To see if the presence of RPA was affected by either the *mec1-100* or *sgs1*Δ mutation, we assayed for Rpa1 at stalled forks, as described in Figure 3.

Rpa1 was immunoprecipitated from wild-type and mutant cells synchronously released into S phase in the

presence of 0.2 M HU (Fig. 5A). In wild-type, *sgs1*Δ, and *mec1-100* cells, there is no significant change in the level of Rpa1 present at the early firing origin ARS607 in HU-arrested cells (Fig. 5A–C). On the other hand, there is a striking and complete loss of Rpa1 at stalled forks in the *mec1-100 sgs1*Δ double mutant (Fig. 5D). This effect is even more severe than that observed for *mec1*Δ cells (Fig. 5E). These results indicate that Mec1 activity is necessary to maintain RPA at stalled forks, which was not the case for the Rad53 kinase (Tanaka and Nasmyth 1998). Given that Rpa1 remains bound in the *mec1-100* mutant, but is lost when this mutation is coupled with *sgs1*Δ (Fig. 5D), we conclude that Sgs1 activity must contribute to Rpa1 binding when Mec1 activity is compromised. Loss of Rpa1 correlates with irreversible fork collapse and high GCR rates in the *mec1-100 sgs1*Δ double mutant.

We monitored Rpa1 binding at the late-firing origin ARS501 in the same set of strains under identical conditions. Consistent with a lack of activated Rad53 and the precocious firing of late origins, Rpa1 is present at ARS501 in *mec1-100* and *mec1*Δ cells, yet it is absent in the *mec1-100 sgs1*Δ double mutant (Fig. 5F; see also Tanaka and Nasmyth 1998). This suggests that RPA binding is destabilized at both early- and late-firing origins in the double mutant.

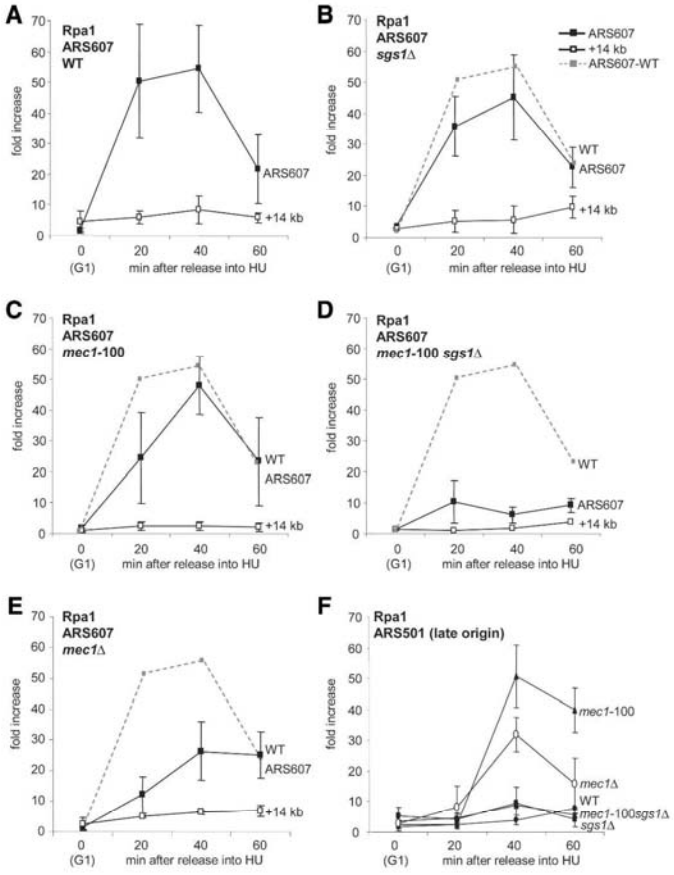

Figure 5. Rpa1 is displaced from stalled replication forks in *mec1-100 sgs1*Δ cells. ChIP was performed on Myc-tagged Rpa1 (squares) in cultures release from α-factor into 0.2 M HU as described in Figure 3 using the following strains: wild-type (GA-1113) (*A*), *sgs1*Δ (GA-2439) (*B*), *mec1-100* (GA-2571) (*C*), *mec1-100 sgs1*Δ (GA-2581) (*D*), and *mec1*Δ *sml1*Δ (GA-2582) (*E*). rtPCR-amplified regions correspond to ARS607 (filled symbols) and +14 kb (open symbols), with the wild-type signal for Rpa1 shown as a dashed line. From the same experiment, the level of Myc-Rpa1 at the late origin ARS501 is shown for indicated wild-type and mutant strains.

Mec1–Ddc2 recruitment to forks is compromised in sgs1Δ, *but not in* mec1-100, *cells*

The Mec1/Ddc2 complex has been shown to be recruited to stalled forks (Katou et al. 2003; Osborn and Elledge 2003), apparently through the affinity of Ddc2 for RPA (Zou and Elledge 2003). Given that Sgs1 binds Rpa1, it was possible that the RecQ helicase might influence the association of Mec1/Ddc2 near stalled forks. To test whether Mec1/Ddc2 recruitment is altered in *mec1-100* or *sgs1*Δ mutants, we monitored the recruitment of the Ddc2 protein to ARS607 by ChIP (Fig. 6). The presence of Ddc2 is assumed to reflect the binding of the Mec1/Ddc2 heterodimer, since in both yeast and human cells, the vast majority of the Mec1/ATR kinase is recovered in a complex with Ddc2/ATRIP (Rouse and Jackson 2002; Zou and Elledge 2003) and *DDC2* disruption completely abrogates the checkpoint response (Paciotti et al. 2000).

For Ddc2 localization we use an HA epitope-tagged version of the protein that is fully functional, based on the cellular response and viability under DNA-damaging conditions (data not shown). Consistent with previous reports (Katou et al. 2003; Osborn and Elledge 2003), we see that HA-Ddc2 is recruited to ARS607 in wild-type cells during an HU arrest, peaking at ~40 min after release from pheromone arrest (Fig. 6A). This is 20 min

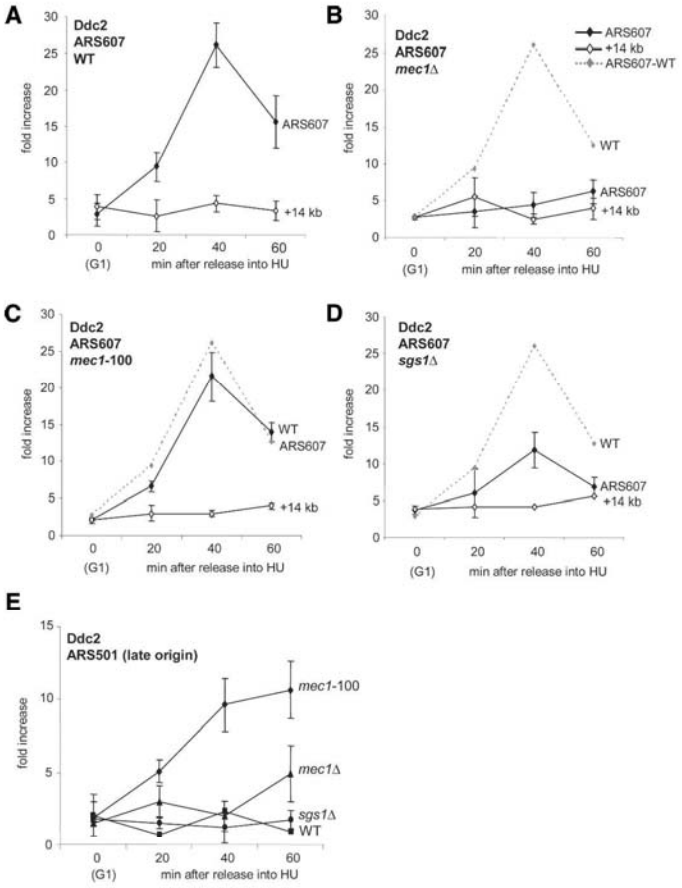

Figure 6. Ddc2 recruitment drops in *sgs1*Δ but not *mec1-100* strains. ChIP was performed on HA-tagged Ddc2 (diamonds) in cultures released from α-factor into 0.2 M HU exactly as described in Figure 3 using the following strains: wild-type (GA-2462) (*A*), *mec1*Δ (GA-2463) (*B*), *mec1-100* (GA-2475) (*C*), and *sgs1*Δ (GA-2519) (*D*). rtPCR-amplified regions correspond to ARS607 (filled symbols) and +14 kb (open symbols), with the wild-type signal for Ddc2 shown as a dashed line. From the same experiment, the level of Ddc2 at the late origin ARS501 is shown for indicated wild-type and mutant strains (*E*).

later than the first appearance of DNA polymerases or Sgs1 helicase at early-firing origins (Cobb et al. 2003), but coincides with Mec1 appearance by ChIP (data not shown). We find that in *mec1*Δ cells, Ddc2 recruitment to stalled forks is completely abolished (Fig. 6B). In the *mec1-100* background, on the other hand, we see no significant drop in the efficiency of Ddc2 binding to stalled forks (Fig. 6C). These data support previous immunofluorescence studies that showed the proper association of Ddc2 with S-phase-specific repair foci in the *mec1-100* allele in response to MMS (Tercero et al. 2003). We argue that the instability of polymerases does not stem from an absence of mec1-100/Ddc2 complex recruitment, but rather from altered activity of the complex, supporting the hypothesis that Mec1/Ddc2 targets fork-associated proteins to stabilize the replisome (Cha and Kleckner 2002; Osborn and Elledge 2003).

We next examined Ddc2 recruitment in *sgs1*Δ cells. We see a partial, but reproducible twofold decrease in the amount of Ddc2 recovered at stalled forks (Fig. 6D). This is all the more noteworthy because we do not detect a significant drop in Rpa1 levels in this strain (Fig. 5B). This may mean that *sgs1*-deficient cells accumulate inappropriate strand exchanges (Liberi et al. 2005) that preclude efficient Mec1 binding. Alternatively, Sgs1 may be needed for a conformational change in RPA that favors either Mec1/Ddc2 and/or DNA polymerase interaction (see Discussion).

Finally, we monitored whether the Mec1/Ddc2 complex is recruited to late-firing origins, or whether it only binds those that fire early and then stall. Indeed, Ddc2 is recovered at the late origin ARS501 when it is inappropriately activated in the *mec1-100* mutant, but not in wild-type or *sgs1*Δ cells (Fig. 6E). This shows that Mec1/Ddc2 can be recruited to any active fork arrested by HU, and argues that the unscheduled firing of late origins is a further source of damage that requires Mec1 action.

Mec1-dependent H2A phosphorylation at stalled replication forks

Histone H2A or its variant H2AX is a critical target of ATR and ATM kinases at sites of double-strand breaks (DSB), and it also becomes modified in response to HU in mammalian cells (for review, see Liu et al. 2003; Thiriet and Hayes 2005). This modification helps recruit downstream kinases as well as chromatin-modifying enzymes, to maintain the checkpoint arrest. In budding

yeast, the two major H2A isoforms both carry the serine at position 129, typical of H2AX, which becomes phosphorylated in response to damage by either Tel1 or Mec1 kinase, but not by Dun1 or Rad53 (Downs et al. 2000; Shroff et al. 2004). Similarly, both ATR and ATM kinases modify H2AX in fission yeast and vertebrates (Nakamura et al. 2004). Given that loss of the C-terminal phospho-acceptor serine increases sensitivity to S-phase damage (MMS), we examined whether or not H2A-P is directly associated with stalled forks.

Phospho-specific antibodies to H2A-P (a gift from W. Bonner, NIH, Bethesda, MD) were used to monitor the presence of the modified histone near HU-arrested replication forks. In parallel, we precipitated the Myc-tagged DNA pol ε to confirm fork position (data not shown). Using the indicated primers, we detect a strong enrichment of H2A-P at stalled forks in wild-type cells treated with HU, while in its absence we detect no significant phosphorylation of H2A-P (Fig. 7B,C). Thus H2A-P modification is specific to stalled forks and not to replication per se.

To see if this phosphorylation event is mediated by both Tel1 and Mec1, as shown for DSBs, we performed the HU arrest and quantitative H2A ChIP experiment in appropriate mutants. The amount of H2A-P at stalled forks in the *mec1*Δ strain drops to background levels, but there is no significant change in the *tel1*Δ strain (Fig. 7D). Given that there is no DNA PK homolog in yeast, this suggests that Mec1 alone modifies yeast H2A at stalled replication forks. This unique function underscores the singular importance of Mec1 during replication fork stalling and recovery (Cha and Kleckner 2002), quite apart from its ability to activate the downstream checkpoint kinase Rad53. The cross-talk between Mec1 and Sgs1 may be further reflected in the ability of RecQ helicases to be bound and potentially regulated by H2A-P (Nakamura et al. 2004; Sengupta et al. 2004).

Discussion

Chromosomal breaks and rearrangements are not only correlated with neoplastic transformation but also can cause malignancy. Previous work showed that in yeast an increase in both spontaneous and induced rearrangements is strikingly elevated in cells mutated for ATM, and even more so for cells lacking ATR, or its ortholog Mec1 (Kolodner et al. 2002). It was recently proposed that gross chromosomal rearrangements of this type are likely to arise from stalled forks (Lambert et al. 2005). We now use the synthetic behavior of a double mutant to show that this increase in chromosomal breaks and rearrangements correlates strictly with replication fork collapse, which entails a rapid displacement of DNA polymerases and RPA. This is due, in turn, to the loss of Mec1(ATR) kinase activity on substrates at sites of replication stalling. A partial loss-of-function mutant, *mec1-100*, which has very minor phenotypes on its own, has highly synergistic rates of GCR and replication fork collapse when coupled with deletion of the gene encoding the RecQ helicase Sgs1.

The simplest interpretation of our findings is as follows: In a strain that bears a mutated but catalytically active Mec1 kinase, *mec1-100*, we find a partial displacement of polymerases, although RPA remains bound and the Mec1–Ddc2 complex is recruited to stalled forks at near wild-type levels. The *mec1-100* mutation allows a fairly efficient resumption of replication after removal of HU, although the strain shows a slight sensitivity to HU. We conclude that in this background there is a second pathway that stabilizes the replisome, or allows its re-establishment, enabling recovery from HU arrest. This second pathway depends almost entirely on the activity of the RecQ helicase, Sgs1, because in the *mec1-100 sgs1*Δ double mutant we observe a complete collapse of replication forks. This coincides with the displacement not only of replicative polymerases, but also of RPA.

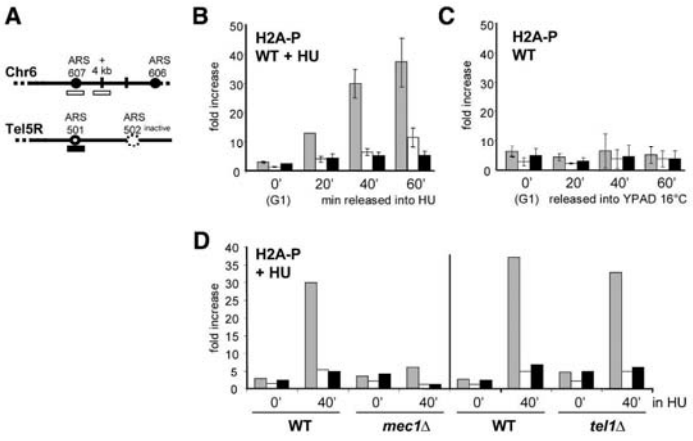

Figure 7. Modification of H2A at replication forks is Mec1-specific. (*A*) Primers as previously described in Figure 3 were used to amplify the early-firing origin ARS607 (stippled) and an origin-proximal site (+4 kb; white), or late-firing origin ARS501 (black). (*B*) ChIP was performed on a wild-type (GA-2448) culture as described in Figure 3, released from α-factor into 0.2 M HU, using a phospho-specific rabbit polyclonal antibody recognizing the Ser 129-P H2A epitope (a gift from W. Bonner). Myc-tagged DNA pol ε was precipitated in parallel (data not shown). (*C*) ChIP for H2A-P as in *B* was performed on a wild-type culture following synchronous release from pheromone arrest into YPD at 16°C, in the absence of HU. (*D*) ChIP as described in *B* except that the strains used were *mec1*Δ (GA-2588) and *tel1*Δ (GA-2002). Here the ratio of absolute fold enrichments is reported after the rtPCR signals are normalized to a wild-type control in duplicate independent experiments: The scaling factor is 1.00 for *mec1*Δ and 0.268 for *tel1*Δ. Error bars were similar for both wild-type and mutant strains.

Coincident with these events, there is a synergistic increase in gross chromosomal rearrangements, presumably reflecting strand breakage, and the abolition of fork recovery potential. Enhanced strand breakage was also reported to occur on replicating DNA in *Xenopus* extracts depleted for XBLM helicase, although the mechanisms leading to such instability were not addressed (Li et al. 2004).

There are three important conclusions from our observations: First, based on the strong synergism observed coordinately for gross chromosomal rearrangements, polymerase displacement, and loss of fork recovery potential, we argue that these events are mechanistically linked. Second, we have identified fork-associated targets that are dependent on Rad53 checkpoint activation (MCM proteins) or that are unique to Mec1, being Rad53-independent (DNA polymerases and H2A-P at forks). Third, we elucidate the role played by Sgs1 helicase in this process and find that Sgs1 becomes essential to promote polymerase stability in the *mec1-100* background. This suggests that Mec1/Ddc2 and Sgs1 contribute independently to polymerase stabilization, and that either Sgs1 or the partial *mec1-100* activity is sufficient to ensure fork recovery (Fig. 8). Given that both Sgs1 and Mec1/Ddc2 bind RPA, and that RPA in turn promotes DNA pol α/primase initiation, it was not unexpected that both pathways for replisome stability converge on RPA, which itself is a target of checkpoint kinase modification (for review, see Binz et al. 2004).

How can Sgs1 directly modulate RPA function, if the level of RPA bound at stalled forks does not change in an *sgs1*Δ strain? It is well-established that RPA can bind ssDNA in two modes, a high-affinity footprint that covers 29–30 nucleotides (nt), and a less tightly bound "primosome" complex that associates with DNA pol α/primase, leaving an RPA–DNA contact of ~10 nt (for review, see Binz et al. 2004; Arunkumar et al. 2005). RPA is also known to bind the virally encoded helicase, large T antigen (Tag) through its 70-kDa and 32-kDa subunits. It was recently shown that interaction with Tag provokes a conformational change in RPA that strongly favors formation of a primosome complex with DNA pol α/primase, switching RPA's DNA-binding mode. Given that RecQ helicases, notably, BLM, WRN, and Sgs1, all bind the large RPA subunits with high affinity (Brosh et al. 2000; Cobb et al. 2003; Doherty et al. 2005), we propose that Sgs1, like Tag, may induce a conformational change in RPA that promotes its interaction with DNA pol α. This may, in turn, promote primosome formation at stalled forks (see Fig. 8). While the Sgs1 function is not absolutely essential in the presence of fully functional Mec1 kinase, it becomes critical for maintenance of replicative polymerases in the *mec1-100* background. We propose that the maintenance of RPA at stalled forks in the *sgs1*Δ strain reflects the binding of RPA in its non-primosome, high-affinity form (Arunkumar et al. 2005). This may be influenced by checkpoint kinase-induced phosphorylation. Because Sgs1 is also necessary for maximal Mec1/Ddc2 levels at stalled forks, a tertiary complex of RPA, Sgs1, and Mec1/Ddc2 may also exist. Intriguingly, BLM and Sgs1 are targets of ATR-family kinases that are activated in response to fork-associated damage (Brush and Kelly 2000; Davies et al. 2004; Li et al. 2004).

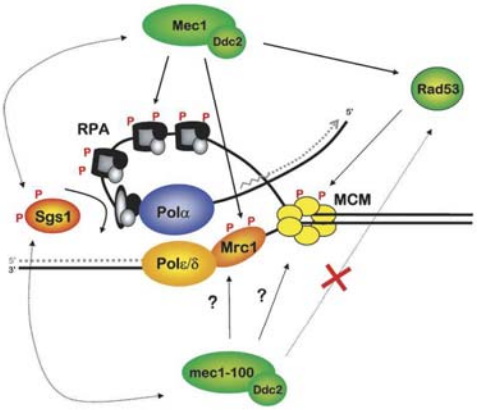

Figure 8. Mec1/Ddc2 and Sgs1 stabilize RPA and DNA polymerases at stalled forks. This model summarizes the pathways that stabilize the replisome in cells exposed to HU. Sgs1, like large T antigen, is proposed to provoke a conformational change in RPA that promotes stable binding of DNA pol α as a primosome. Mec1/Ddc2 kinase also acts on Mrc1 to stabilize polymerases, while Rad53 either uncouples or displaces the MCM complex.

What other targets of Mec1/Ddc2 are essential to stabilize the replisome? This pathway involves proteins other than the Sgs1 helicase, and is undoubtedly tightly regulated. With respect to DNA pol α and pol ε, it has been proposed that hyperphosphorylation of RPA by PI3-related kinases alters the interaction of RPA with several ligands, reducing its affinity for Tag, DNA pol α, and ATR, while increasing affinity for p53 (for review, see Binz et al. 2004). A partially modified form of RPA may change its mode of DNA binding such that it is able to maintain or re-establish contact with DNA pol α/primase, to allow resumption of DNA replication recovery once conditions improve. Mrc1 is also an important target of Mec1 kinase at stalled forks, and in *mrc1*Δ mutants, DNA pol ε is also partially destabilized on HU (Katou et al. 2003; Bjergbaek et al. 2005). Given that this effect is synergistic with loss of Sgs1, while loss of Rad53 is not (Fig. 4), we propose that Mrc1 also contributes to replisome stability at stalled forks on a pathway separate from Sgs1 (Fig. 8). Finally, we find that H2A phosphorylation at stalled forks depends on Mec1, but not Tel1. This observation clearly distinguishes the "stalled fork" response from the "DNA damage" response, where Mec11/Tel1 kinase redundancy has been established (Nakamura et al. 2004; Shroff et al. 2004). The modification of H2A at stalled forks may regulate the accessibility of DNA to enzymes involved in repair and fork restart.

A critical target of Mec1 kinase is, of course, Rad53, and we show here that a loss of Rad53 kinase activity leads to a drop in MCM levels at stalled forks, although

Table 2. S. cerevisiae *strains used in this study*

Strain	Genotype	Source
GA-180	MATa, *ade2*-1, *trp1*-1, *his3*-11, -15, *ura3*-1, *leu2*-3,-112, *can1*-100	R. Rothstein (W303-1A)
GA-1003	MATa, *ade2*-1, *trp1*-1, *his3*-11, -15, *ura3*-1, *leu2*-3,-112, *can1*-100; CDC47-6Myc::URA	Tanaka and Nasmyth 1998
GA-1020	MATa, *ade2*-1, *trp1*-1, *his3*-11, -15, *ura3*-1, *leu2*-3,-112, *can1*-100, *pep4*::*LEU2*	R. Rothstein (W303-1A)
GA-1113	MATa, *ade2*-1, *trp1*-1, *his3*-11, -15, *ura3*-1, *leu2*-3,-112, *can1*-100; *RFA1-18Myc*::*TRP1* from K7141	This study Tanaka and Nasmyth 1998
GA-1761	GA-1020 with *sgs1*::*TRP1*	Bjergbaek et al. 2005
GA-2002	GA-1020 with *tel1*::*URA3*; *Rad53-13Myc*::*KanMX6*	This study
GA-2238	MATa, *ade2*-1, *trp1*-1, *his3*-11, -15, *ura3*-1, *leu2*-3,-112, *can1*-100, *CDC17-3HA*::*TRP1*	Aparicio et al. 1999
GA-2239	MATa, *ade2*-1, *trp1*-1, *his3*-11, -15, *ura3*-1, *leu2*-3,-112, *can1*-100, *CDC17-3HA*::*TRP1*; *rad53*-11	Aparicio et al. 1999
GA-2240	MATa, *ade2*-1, *trp1*-1, *his3*-11, -15, *ura3*-1, *leu2*-3,-112, *can1*-100 *rad53*-11	Aparicio et al. 1999
GA-2256	GA-2238 with *sgs1*::*LEU2*	This study
GA-2439	GA-1113 with *sgs1*::*LEU2*	This study
GA-2448	GA-1020 with *POL2*-13Myc::*KanMX6*	Bjergbaek et al. 2005
GA-2450	GA-1020 with *sgs11-3*::*TRP1*, *POL2*-13Myc::*KanMX6*	Bjergback et al. 2005
GA-2462	MATa, *ade2*-1, *trp1*-1, *his3*-11, -15, *ura3*-1, *leu2*-3,-112, *can1*-100, *DDC2-3HA*::*URA3*, same as YLL683.8/4A	Paciotti et al. 2001
GA-2463	MATa, *ade2*-1, *trp1*-1, *his3*-11, -15, *ura3*-1, *leu2*-3,-112, *can1*-100, *DDC2-3HA*::*URA3*, *mec1*::*HIS3*, *sml1*::*KanMX6*, same as DMP3048	Paciotti et al. 2001
GA-2474	MATa, *ade2*-1, *trp1*-1, *his3*-11, -15, *ura3*-1, *leu2*-3,-112, *can1*-100, *mec1*-100::*LEU2(HIS3)*, derived from DMP3343/6C	This study Paciotti et al. 2001
GA-2475	GA-2474 with *DDC2-3HA*::*URA3*	This study
GA-2478	MATa, *ade2*-1, *trp1*-1, *his3*-11, -15, *ura3*-1, *leu2*-3,-112, *can1*-100, *mec1*-100::*LEU2(HIS3)*, *sml1*::*KanMX6* derived from DMP3343/6C	This study Paciotti et al. 2001
GA-2514	GA-2474 with *sgs11-3*::*TRP1*	This study
GA-2515	GA-2474 with *POL2-13Myc*::*KanMX6*	This study
GA-2516	GA-2474 with *sgs11-3*::*TRP1*, *POL2-13Myc*::*KanMX6*	This study
GA-2519	GA-2462 with *sgs11-3*::*TRP1*	This study
GA-2567	GA-2474 with *CDC17-3HA*::*TRP1*	This study
GA-2571	GA-2474 with *RFA1-18Myc*::*TRP1*	This study
GA-2574	GA-2239 with *POL2-13Myc*::*KanMX6*	This study
GA-2576	GA-2239 with sgs1::LEU2, *POL2*-13Myc::*KanMX6*	This study
GA-2578	GA-2474 with *sgs11-3*::*LEU2*; *CDC17-3HA*::*TRP1*	This study
GA-2581	GA-2474 with *sgs11-3*::*LEU2*; *RFA1-18Myc*::*TRP1*	This study
GA-2582	GA-1113 with *mec1*::*HIS3*, *sml1*::*KanMX6*	This study
GA-2588	GA-180 with *POL2-13Myc*::*KanMX6*, *mec1*::*HIS3*, *sml1*::*KanMX6*	This study
GA-2895	GA-180 with *mec1*::*HIS3*, *sml1*::*KanMX6*	This study
GA-2896	MATa, *ade2*-1, *trp1*-1, *his3*-11, -15, *ura3*-1, *leu2*-3,-112, *can1*-100, ORC2-9Myc::LEU2, *sgs11-3*::*TRP1*; *mec1*-100:: *LEU2 (HIS3)*	This study
GA-2897	MATa, *ade2*-1, *trp1*-1, *his3*-11, -15, *ura3*-1, *leu2*-3,-112, *can1*-100, ORC2-9Myc::LEU2	This study
GA-2930	YJT110 with *sgs1*::*KanMX6*, *mec1*-100::*LEU2(HIS3)*	This study
GA-2931	YJT110 with *mec1*-100::*LEU2(HIS3)*	This study
GA-3050	MATa, *CAN1*, *hxt13*::*URA3* same as E1557	Lengronne and Schwob 2002
GA-3053	GA-3050 with *mecl*-100::*LEU2(HIS3)*, *sgs1*::*TRP*	This study
GA-3054	GA-1003 with *rad53*-11	This study
GA-3056	GA-3050 with *sgs11-3*::*TRP*	This study
GA-3057	GA-3050 with *mec1*-100::*LEU2(HIS3)*	This study
GA-3062	GA-3050 with rad53-11	This study
GA-3063	GA-3050 with rad53-11, *sgs11-3*::*TRP*	This study
YJT110	W303 MATa with *ARS608*::*HIS3*;*ARS609*::*TRP1*, *ADE+*	Tercero et al. 2003
YVR1	YJT110 with *sgs1*::*KanMX6*	Tercero et al. 2003

fork-associated levels of DNA pol α and pol ε, and RPA, remain stable (Fig. 4; Tanaka and Nasmyth 1998; Cobb et al. 2003 for *rad53*Δ *sml1*Δ). We propose that some of the MCM modifications attributed to ATR-like kinases are actually due to the effector kinase Rad53 (Cortez et al. 2004; Yoo et al. 2004; Byun et al. 2005). The inefficient maintenance of MCM helicase could lead indirectly to fork collapse through an uncoupling of DNA unwinding from DNA synthesis. This is consistent with the high levels of ssDNA that accumulate at stalled forks in HU-arrested *rad53*-deficient cells (Sogo et al. 2002). Also consistent with our results, we note that

DNA pol α levels actually increase at stalled forks in strains lacking Asf1, a histone chaperone and Rad53-binding protein, while MCM helicase becomes mislocalized from the replisome (Franco et al. 2005).

It is thus also possible that some of the defects in *rad53* cells that lead to fork collapse are linked to the role of Rad53 in regulating histone levels during a checkpoint response. Rad53 down-regulates histones to release the histone chaperone Asf1 (Emili et al. 2001). Consistently, overexpression of Asf1 can partially suppress the lethality of a *rad53* mutation on HU. Importantly, the ability of a cell to survive histone overexpression and degrade histones is independent of Mec1, and requires an intact Rad53 kinase (Gunjan and Verreault 2003). This further distinguishes the functions of Mec1 and Sgs1 during replicative stress from those of Rad53.

What are the implications of the dramatic synergy detected between a partial defect in the ATR kinase and RecQ helicase mutation? Since many cancer therapies still rely on DNA-damaging agents that create irreparable damage in S phase, our results support the argument that cell death might be significantly increased if ATR kinase and BLM helicase activities were coordinately compromised during treatment with HU or DNA intercalating drugs. To test this, it will be important to see if the ATR/RecQ synergy observed in yeast similarly enhances HU sensitivity in higher eukaryotic cells.

Materials and methods

All strains used are listed in Table 2 and are derived from either S288C for the GCR assays or W303-1a (*MAT***a** *ade2-1 ura3-1 his3-11,15 trp1-1 leu2-3,112 can1-100*) for all other experiments. Viability was calculated by plating ~500 cells in triplicate onto YPD plates and scoring after 3 d at 30°C. Drop assays were a 1:5 dilution series of uniformly diluted cultures on YPD plates ± 10 mM HU.

GCR rates were calculated as in Myung and Kolodner (2002) for the following strains derived from the wild-type strain GA-3050 (same as E1557 in S288c background) (Lengronne and Schwob 2002): *sgs1*Δ (GA-3056), *mec1-100* (GA-3057), and *mec1-100 sgs1*Δ (GA-3053), *rad53-11* (GA-3062), *rad53-11 sgs1*Δ (GA- 3063) cells were grown in YPD overnight to a density of 0.5×10^6 cells/mL, and incubated ± 0.2 M HU for 2 h, washed, and grown in YPD overnight. GCR rates were determined by scoring Can^r-FOA^r colonies due to loss of *URA3* and *CAN1* genes on Chr 5L. Values reported are from two to three different experiments using five colonies per strain, and mutation rates were calculated by fluctuation analysis (Lea and Coulson 1948).

ChIP was performed using either monoclonal antibodies against HA (12CA5) to precipitate HA-tagged Ddc2 and HA-tagged pol α, Myc (9E10) to precipitate Myc-tagged DNA pol ε, Myc-tagged Mcm7, and Myc-tagged Orc2, or phospho-specific rabbit polyclonal antibody against an epitope containing H2AS129P (a gift from W. Bonner) as described (Cobb et al. 2003), with IP washes at 0.5 M NaCl. In all cases cells were synchronized in G1 with α-factor at 30°C and then released into S phase in either the presence of 0.2 M HU at 30°C or YPD alone at 16°C. BSA-saturated Dynabeads incubated with the same cell extracts served as the background control for each time point. rtPCR quantifies DNA that was amplified with a Perkin-Elmer ABI Prism 7700 or 7000 Sequence Detector System. Sequences of the primers/probes used are available upon request. The data for each strain are averaged over two or three independent ChIP experiments with rtPCR performed in triplicate or duplicate where indicated (standard deviation is shown by error bars). The fold increase represents the ratio of the signal accumulation rates obtained from the antibody-coupled Dynabeads (IP) divided by the signal obtained from BSA-coated Dynabeads (background) after both signals were first normalized to the signal from the input fraction (Cobb et al. 2003). rtPCR monitors T½ within the exponential curve of product accumulation, and the replicate samples ensure a highly quantitative evaluation of product accumulation.

Neutral 2D gel analysis was performed as described (Huberman et al. 1987) with yeast genomic DNA isolated from 7×10^8 cells using a G-20 column (QIAGEN) followed by digestion with PstI and ClaI. Density transfer assays were performed and analyzed as described (Tercero et al. 2000). Rad53 in situ autophosphorylation assay (ISA) is described in Bjergbaek et al. (2005) and Pellicioli et al. (1999). Rat anti-RnaseH42 was kindly provided by U. Wintersberger (University of Vienna, Vienna, Austria) was used to normalize ISA signals.

Acknowledgments

We thank M.P. Longhese, W. Bonner and U. Wintersberger for reagents and P. Pasero, K. Shimada, H. Van Attikum, E. Fanning, and J. Diffley for helpful discussions. The Gasser laboratory thanks the Swiss Cancer League, Swiss National Science Foundation, European RTN Checkpoints and Cancer, and fellowships from the American Cancer Society to J.A.C. (PF-01-142-01-CCG) and the Danish Cancer Society to L.B. (DP00060). J.A.T.'s work is supported by grants BMC2003-00699 from Ministerio de Educación y Ciencia and GR/SAL/0144/2004 from Comunidad de Madrid and by an institutional grant from Fundación Ramón Areces to the CBMSO.

References

Alcasabas, A.A., Osborn, A.J., Bachant, J., Hu, F., Werler, P.J., Bousset, K., Furuya, K., Diffley, J.F., Carr, A.M., and Elledge, S.J. 2001. Mrc1 transduces signals of DNA replication stress to activate Rad53. *Nat. Cell Biol.* **3:** 958–965.

Aparicio, O.M., Stout, A.M., and Bell, S.P. 1999. Differential assembly of Cdc45p and DNA polymerases at early and late origins of DNA replication. *Proc. Natl. Acad. Sci.* **96:** 9130–9135.

Arunkumar, A.I., Klimovich, V., Jiang, X., Ott, R.D., Mizoue, L., Fanning, E., and Chazin, W.J. 2005. Insights into hRPA32 C-terminal domain-mediated assembly of the simian virus 40 replisome. *Nat. Struct. Mol. Biol.* **12:** 332–339.

Bartrand, A.J., Iyasu, D., and Brush, G.S. 2004. DNA stimulates Mec1-mediated phosphorylation of replication protein A. *J. Biol. Chem.* **279:** 26762–26767.

Binz, S.K., Sheehan, A.M., and Wold, M.S. 2004. RPA phosphorylation and the cellular response to DNA damage. *DNA repair* **3:** 1015–1024.

Bjergbaek, L., Cobb, J.A., Tsai-Pflugfelder, M., and Gasser, S.M. 2005. Mechanistically distinct roles for the RecQ helicase Sgs1p at stalled replication forks. *EMBO J.* **24:** 405–417.

Brosh Jr., R.M., Li, J.L., Kenny, M.K., Karow, J.K., Cooper, M.P., Kureekattil, R.P., Hickson, I.D., and Bohr, V.A. 2000. Replication protein A physically interacts with the Bloom's syndrome protein and stimulates its helicase activity. *J. Biol. Chem.* **275:** 23500–23508.

Brush, G.S. and Kelly, T.J. 2000. Phosphorylation of the RPA large subunit in the *S. cerevisiae* checkpoint response. *Nucleic Acids Res.* **28:** 3725–3732.

Brush, G.S., Morrow, D.M., Hieter, P., and Kelly, T.J. 1996. The ATM homologue MEC1 is required for phosphorylation of RPA in yeast. *Proc. Natl. Acad. Sci.* **93:** 15075–15080.

Byun, T.S., Pacek, M., Yee, M.C., Walter, J.C., and Cimprich, K.A. 2005. Functional uncoupling of MCM helicase and DNA polymerase activities activates the ATR-dependent checkpoint. *Genes & Dev.* **19:** 1040–1052.

Cha, R.S. and Kleckner, N. 2002. ATR homolog Mec1 promotes fork progression, thus averting breaks in replication slow zones. *Science* **297:** 602–606.

Cobb, J.A., Bjergbaek, L., Shimada, K., Frei, C., and Gasser, S.M. 2003. DNA polymerase stabilization at stalled replication forks requires Mec1 and the RecQ helicase Sgs1. *EMBO J.* **22:** 4325–4336.

Cortez, D., Glick, G., and Elledge, S.J. 2004. Minichromosome maintenance proteins are direct targets of the ATM and ATR checkpoint kinases. *Proc. Natl. Acad. Sci.* **101:** 10078–10083.

Davies, S.L., North, P.S., Dart, A., Lakin, N.D., and Hickson, I.D. 2004. Phosphorylation of the Bloom's syndrome helicase and its role in recovery from S-phase arrest. *Mol. Cell. Biol.* **24:** 1279–1291.

Desany, B.A., Alcasabas, A.A., Bachant, J.B., and Elledge, S.J. 1998. Recovery from DNA replicational stress is the essential function of the S-phase checkpoint pathway. *Genes & Dev.* **12:** 2956–2970.

Doherty, K.M., Sommers, J.A., Gray, M.D., Lee, J.W., von Kobbe, C., Thoma, N.H., Kureekattil, R.P., Kenny, M.K., and Brosh Jr., R.M. 2005. Physical and functional mapping of the RPA interaction domain of the Werner and Bloom syndrome helicases. *J. Biol. Chem.* **280:** 29494–29505.

Downs, J.A., Lowndes, N.F., and Jackson, S.P. 2000. A role for *S. cerevisiae* histone H2A in DNA repair. *Nature* **408:** 1001–1004.

Emili, A., Schieltz, D.M., Yates III, J.R., and Hartwell, L.H. 2001. Dynamic interaction of DNA damage checkpoint protein Rad53 with chromatin assembly factor Asf1. *Mol. Cell* **7:** 13–20.

Franco, A.A., Lam, W.M., Burgers, P.M., and Kaufman, P.D. 2005. Histone deposition protein Asf1 maintains DNA replisome integrity and interacts with replication factor C. *Genes & Dev.* **19:** 1365–1375.

Frei, C. and Gasser, S.M. 2000. The yeast Sgs1 helicase acts upstream of Rad53 in the DNA replication checkpoint and colocalizes with Rad53 in S-phase-specific foci. *Genes & Dev.* **14:** 81–96.

Gunjan, A. and Verreault, A. 2003. Rad53 kinase-dependent surveillance mechanism that regulates histone protein levels in *S. cerevisiae*. *Cell* **115:** 537–549.

Halazonetis, T.D. 2004. Constitutively active DNA damage checkpoint pathways as the driving force for the high frequency of *p53* mutations in human cancer. *DNA Repair* **3:** 1057–1062.

Huberman, J.A., Spotila, L.D., Nawotka, K.A., el-Assouli, S.M., and Davis, L.R. 1987. The in vivo origin of the yeast 2 micron plasmid. *Cell* **51:** 473–481.

Ivessa, A.S., Lenzmeier, B.A., Bessler, J.B., Goudsouzian, L.K., Schnakenberg, S.L., and Zakian, V.A. 2003. The *S. cerevisiae* helicase Rrm3p facilitates replication past nonhistone protein–DNA complexes. *Mol. Cell* **12:** 1525–1536.

Katou, Y., Kanoh, Y., Bando, M., Noguchi, H., Tanaka, H., Ashikari, T., Sugimoto, K., and Shirahige, K. 2003. S-phase checkpoint proteins Tof1 and Mrc1 form a stable replication-pausing complex. *Nature* **424:** 1078–1083.

Kim, H.S. and Brill, S.J. 2003. MEC1-dependent phosphorylation of yeast RPA1 in vitro. *DNA Repair* **2:** 1321–1335.

Kolodner, R.D., Putnam, C.D., and Myung, K. 2002. Maintenance of genome stability in *Saccharomyces cerevisiae*. *Science* **297:** 552–557.

Lambert, S., Watson, A., Sheedy, D.M., Martin, B., and Carr, A.M. 2005. Gross chromosomal rearrangements and elevated recombination at an inducible site-specific replication fork barrier. *Cell* **121:** 689–702.

Lea, D.E. and Coulson, C.A. 1948. The distribution of the numbers of mutants in bacterial populations. *J. Genet.* **49:** 264–285.

Lengronne, A. and Schwob, E. 2002. The yeast CDK inhibitor Sic1 prevents genomic instability by promoting replication origin licensing in late G1. *Mol. Cell* **9:** 1067–1078.

Li, W., Kim, S.M., Lee, J., and Dunphy, W.G. 2004. Absence of BLM leads to accumulation of chromosomal DNA breaks during both unperturbed and disrupted S phases. *J. Cell Biol.* **165:** 801–812.

Liberi, G., Maffioletti, G., Lucca, C., Chiolo, I., Baryshnikova, A., Cotta-Ramusino, C., Lopes, M., Pellicioli, A., Haber, J.E., and Foiani, M. 2005. Rad51-dependent DNA structures accumulate at damaged replication forks in *sgs1* mutants defective in the yeast ortholog of BLM RecQ helicase. *Genes & Dev.* **19:** 339–350.

Liu, J.S., Kuo, S.R., and Melendy, T. 2003. Comparison of checkpoint responses triggered by DNA polymerase inhibition versus DNA damaging agents. *Mutat. Res.* **532:** 215–226.

Lopes, M., Cotta-Ramusino, C., Pellicioli, A., Liberi, G., Plevani, P., Muzi-Falconi, M., Newlon, C.S., and Foiani, M. 2001. The DNA replication checkpoint response stabilizes stalled replication forks. *Nature* **412:** 557–561.

Lucca, C., Vanoli, F., Cotta-Ramusino, C., Pellicioli, A., Liberi, G., Haber, J., and Foiani, M. 2004. Checkpoint-mediated control of replisome-fork association and signalling in response to replication pausing. *Oncogene* **23:** 1205–1213.

Mohaghegh, P. and Hickson, I.D. 2001. DNA helicase deficiencies associated with cancer predisposition and premature ageing disorders. *Hum. Mol. Genet.* **10:** 741–746.

Myung, K. and Kolodner, R.D. 2002. Suppression of genome instability by redundant S-phase checkpoint pathways in *Saccharomyces cerevisiae*. *Proc. Natl. Acad. Sci.* **99:** 4500–4507.

Nakamura, T.M., Du, L.L., Redon, C., and Russell, P. 2004. Histone H2A phosphorylation controls Crb2 recruitment at DNA breaks, maintains checkpoint arrest, and influences DNA repair in fission yeast. *Mol. Cell. Biol.* **24:** 6215–6230.

Osborn, A.J. and Elledge, S.J. 2003. Mrc1 is a replication fork component whose phosphorylation in response to DNA replication stress activates Rad53. *Genes & Dev.* **17:** 1755–1767.

Paciotti, V., Clerici, M., Lucchini, G., and Longhese, M.P. 2000. The checkpoint protein Ddc2, functionally related to *S. pombe* Rad26, interacts with Mec1 and is regulated by Mec1-dependent phosphorylation in budding yeast. *Genes & Dev.* **14:** 2046–2059.

Paciotti, V., Clerici, M., Scotti, M., Lucchini, G., and Longhese, M.P. 2001. Characterization of mec1 kinase-deficient mutants and of new hypomorphic mec1 alleles impairing subsets of the DNA damage response pathway. *Mol. Cell. Biol.* **21:** 3913–3925.

Pellicioli, A., Lucca, C., Liberi, G., Marini, F., Lopes, M., Plevani, P., Romano, A., Di Fiore, P.P., and Foiani, M. 1999.

Activation of Rad53 kinase in response to DNA damage and its effect in modulating phosphorylation of the lagging strand DNA polymerase. *EMBO J.* **18:** 6561–6572.

Rouse, J. and Jackson, S.P. 2002. Lcd1p recruits Mec1p to DNA lesions in vitro and in vivo. *Mol. Cell* **9:** 857–869.

Santocanale, C. and Diffley, J.F. 1998. A Mec1- and Rad53-dependent checkpoint controls late-firing origins of DNA replication. *Nature* **395:** 615–618.

Sengupta, S., Robles, A.I., Linke, S.P., Sinogeeva, N.I., Zhang, R., Pedeux, R., Ward, I.M., Celeste, A., Nussenzweig, A., Chen, J., et al. 2004. Functional interaction between BLM helicase and 53BP1 in a Chk1-mediated pathway during S-phase arrest. *J. Cell Biol.* **166:** 801–813.

Shroff, R., Arbel-Eden, A., Pilch, D., Ira, G., Bonner, W.M., Petrini, J.H., Haber, J.E., and Lichten, M. 2004. Distribution and dynamics of chromatin modification induced by a defined DNA -double-strand break. *Curr. Biol.* **14:** 1703–1711.

Sogo, J.M., Lopes, M., and Foiani, M. 2002. Fork reversal and ssDNA accumulation at stalled replication forks owing to checkpoint defects. *Science* **297:** 599–602.

Tanaka, T. and Nasmyth, K. 1998. Association of RPA with chromosomal replication origins requires an Mcm protein, and is regulated by Rad53, and cyclin- and Dbf4-dependent kinases. *EMBO J.* **17:** 5182–5191.

Tercero, J.A. and Diffley, J.F. 2001. Regulation of DNA replication fork progression through damaged DNA by the Mec1/Rad53 checkpoint. *Nature* **412:** 553–557.

Tercero, J.A., Labib, K., and Diffley, J.F.X. 2000. DNA synthesis at individual replication forks requires the essential initiation factor Cdc45p. *EMBO J.* **19:** 2082–2093.

Tercero, J.A., Longhese, M.P., and Diffley, J.F. 2003. A central role for DNA replication forks in checkpoint activation and response. *Mol. Cell* **11:** 1323–1336.

Thiriet, C. and Hayes, J.J. 2005. Chromatin in need of a fix: Phosphorylation of H2AX connects chromatin to DNA repair. *Mol. Cell* **18:** 617–622.

Versini, G., Comet, I., Wu, M., Hoopes, L., Schwob, E., and Pasero, P. 2003. The yeast Sgs1 helicase is differentially required for genomic and ribosomal DNA replication. *EMBO J.* **22:** 1939–1949.

Watt, P.M., Hickson, I.D., Borts, R.H., and Louis, E.J. 1996. SGS1, a homologue of the Bloom's and Werner's syndrome genes, is required for maintenance of genome stability in *S. cerevisiae*. *Genetics* **144:** 935–945.

Weinert, T.A., Kiser, G.L., and Hartwell, L.H. 1994. Mitotic checkpoint genes in budding yeast and the dependence of mitosis on DNA replication and repair. *Genes & Dev.* **8:** 652–665.

Yoo, H.Y., Shevchenko, A., Shevchenko, A., and Dunphy, W.G. 2004. Mcm2 is a direct substrate of ATM and ATR during DNA damage and DNA replication checkpoint responses. *J. Biol. Chem.* **279:** 53353–53364.

Zhao, X., Muller, E.G., and Rothstein, R. 1998. A suppressor of two essential checkpoint genes identifies a novel protein that negatively affects dNTP pools. *Mol. Cell* **2:** 329–340.

Zou, L. and Elledge, S.J. 2003. Sensing DNA damage through ATRIP recognition of RPA–ssDNA complexes. *Science* **300:** 1542–1548.

Chapter 4

Histone H2A ^{S129} phosphorylation occurs at replicating rDNA and naturally elongating telomeres in *Saccharomyces cerevisiae.*

Thomas Schleker, Haico van Attikum[5], Véronique Kalck[6] and Susan M. Gasser[7]

[5] H.vA. performed microscopy and data analysis of the results shown in figure 4.5a, and Q-PCR for Figure 4.2f, and contributed to the design and choice of experiments.

[6] V.K. did immunofluorescence stainings and, together with T.S., microscopic acquisition and image processing.

[7] S.G. was supervising choice and analysis of experiments, and manuscript preparation.

4.1 Summary

The rapid phosphorylation of histone H2A at serine 129 (γH2A) by Mec1 and Tel1 is thought to help signal DNA double-strand breaks to the DNA repair machinery. We have previously reported that Mec1-mediated H2A phosphorylation occurs at stalled replication forks (see Chapter 3). In the current study, we found high levels of γH2A at the rDNA locus and telomeres during the S phase of yeast cells growing normally. We found that γH2A is a marker of sub-telomeric nucleosomes that depends mainly on Tel1 kinase. These constitutive levels further increased during the elongation of critically short telomeres. We showed that γH2A contributes to telomeric anchoring in S-phase yeast cells, possibly in parallel to the yKu and Sir4 anchoring pathways. This demonstrates that γH2A is not only important for signaling DNA damage, but also serves to influence interphase nuclear organization by affecting telomere positioning.

4.2 Introduction

Exogenous DNA damage (e.g. irradiation-induced DNA double-stranded breaks, or DSBs) as well as endogenous genotoxic events (e.g. DNA breaks generated by replication fork collapse) occur in cells throughout their lifecycle. Eukaryotic cells have evolved efficient checkpoint and repair pathways to maintain genomic stability in response to DNA damage. Both pathways are influenced by chromatin. Not only do histone marks and chromatin modifiers influence gene regulation and higher order chromatin structure, but they are also determining factors in DNA repair (Ataian and Krebs, 2006; van Attikum and Gasser, 2005).

One of the best characterized repair and checkpoint pathways is the cellular response to a DSB which involves relocalization of checkpoint and repair factors to nuclear foci, which can be visualized by fluorescence microscopy. The first chromatin mark found in such nuclear foci that appeared to be specific to the DNA damage response was the phosphorylation of the histone H2A variant H2AX (γH2AX). γH2AX occurs in megabase regions surrounding DNA DBSs in mammalian cells (Rogakou et al., 1999). This H2AX phosphorylation motif is conserved in *Saccharomyces cerevisiae* in the major H2A isoform. Modification of H2A serine 129 depends on both Mec1 (ATR homologue) and Tel1 (ATM homologue) kinases. Analogous to the situation in mammalian cells, this modification spreads over 25kb either side of an induced DSB (Shroff et al., 2004). γH2A is important for DSB repair because it modifies the recruitment of the chromatin remodeling complex INO80, which promotes efficient end resection (van Attikum et al., 2004; Morrison et al., 2004), and of cohesin, which is required for post-replicative repair of the DSB (Strom et al., 2004; Unal et al., 2004). Two recent reports have proposed that γH2A also aids in the recruitment of the checkpoint adaptor protein Rad9 (Javaheri et al., 2006; Toh et al., 2006).

Besides at DSBs, γH2A was also detected by chromatin immunoprecipitation (ChIP) at replication forks stalled by incubation in the chemotherapeutic agent hydroxyurea (HU), which provokes dNTP depletion (Cobb et al., 2005). In this case, H2A phosphorylation depended nearly exclusively on Mec1. This specific requirement for Mec1 for fork-associated γH2A appears to be conserved in human cells, since hydroxyurea-induced γH2AX depends on ATR (Ward and Chen, 2001).

Yeast strains bearing mutations for serine 129 in both genomic copies of histone H2A are more sensitive to DNA-damaging agents than WT cells (Downs et al., 2000; Redon et al., 2003). Redon et al. (Redon et al., 2003) showed that *h2a*^{S129A} mutant strains lacking the phosphorylation site at serine 129 are particularly sensitive to camptothecin (CPT). CPT inhibits topoisomerase I, an enzyme that relaxes DNA supercoiling by nicking the DNA double-strand, rotating the broken strand and religating DNA. CPT blocks these topoisomerase I cleavage complexes and once the complex is hit by the replisome, this leads to the formation of DSBs (Pommier, 2006). γH2A is not required under these conditions for the checkpoint signaling via *RAD24* and *RAD9* genes, which rather indicates a role of γH2A in the repair of CPT-induced DSBs (Redon et al. 2003). Since transient topoisomerase I cleavage complexes also occur in the absence of the drug, sporadic CPT-like DNA damage during replication and transcription will occur even in normal cells. In S phase, this kind of damage will be high in regions in which topoisomerase I is particularly active. This could lead to the manifestation of replication slow zones, as described by Cha and Kleckner (Cha and Kleckner, 2002).

Not all segments of the yeast genome are replicated with the same ease. There are some regions that are difficult to replicate. Those include tRNA genes, origins, and transcriptional silencers, as well as the rDNA locus and sub-telomeric and telomeric DNA. At these sites, replication forks pause or slow down at non-histone protein-DNA complexes, and error-free replication fork progression requires additional proteins, e.g. the helicase Rrm3 (Azvolinsky et al., 2006; Ivessa et al., 2003; Ivessa et al., 2002; Ivessa et al., 2000; Torres et al., 2004). This impairment coincides with the occurrence of silent chromatin, which in budding yeast is found at mating-type loci, at telomeres, and in the rDNA. Interestingly, the rDNA locus (Voelkel-Meiman et al., 1987) and also telomeres (Linardopoulou et al., 2005; Rudd et al., 2007) are recombination hotspots during normal cell growth.

The observation (Harvey et al., 2005; Redon et al., 2003) that histone H2A gets phosphorylated at serine 129 even in the absence of exogenous DNA damage, as monitored by western blots indicates that it might be required to maintain genomic stability during normal cell growth. If this is the case, γH2A should occur at known recombination hotspots during normal yeast cell growth as these are the rDNA locus and telomeres. A further indication that this might be the case is the observation that topoisomerase I is enriched in the nucleolus (Muller et al., 1985) and replication of

the rDNA coincides temporarily with transcription as observed by electron microscopy (Saffer and Miller, 1986).

With respect to telomeres, it is interesting to note that many DNA damage proteins are found at normal yeast telomeres, and are required for telomere length maintenance (reviewed in Viscardi et al., 2005). In particular, the H2A phosphorylating kinases Tel1 and, in its absence, Mec1 are required for telomere maintenance. *mec1 tel1* double mutants undergo a senescence phenotype like a *tlc1* mutant strain with depleted telomerase function (Greenwell et al., 1995; Ritchie et al., 1999; Tseng et al., 2006).

Whereas telomerase is in principle still catalytically active, telomerase recruitment is impaired in the *mec1 tel1* double-mutant strain (Chan et al., 2001; Goudsouzian et al., 2006; Tseng et al., 2006).

The presence of γH2A in the absence of exogenous DNA damage inspired us to analyze where these substantial levels of γH2A are located during normal cell growth.

In the current study we analyzed the cellular localization of γH2A in normally growing yeast cells by immunofluorescence and chromatin immunoprecipitation experiments. We observed an increase in γH2A during S phase, and particularly high levels of γH2A at the rDNA and at telomeres, supporting the theory that γH2A is a marker of endogenous checkpoint-blind DNA damage that is created by the replication of recombination hotspots. This modification depends on Mec1, while at telomeres the levels of γH2A depend mainly on Tel1. Interestingly, γH2A levels increase during the elongation of short telomeres, possibly mimicking a DSB response.

4.3 Materials and Methods

4.3.1 Yeast strains, culture methods, and general techniques

Yeast strains used in this study (Supplemental Table 4.1) were of W303 background unless otherwise indicated. Deletion strains were made by plasmid-borne or PCR-based gene disruption and were verified by PCR and phenotypic analysis (Ivanov et al., 1992; Longtine et al., 1998; Wach et al., 1994).

Strains were grown in YPAD at 30°C unless otherwise indicated. The experiments monitoring γH2A levels at elongation of short telomeres were performed as described in Marcand et al. (1999) in rich medium containing raffinose, galactose, and/or glucose. Culture conditions for live microscopy were according to Hediger et al. (2002).

Telomeric silencing was assayed on SC medium. For assaying silencing of the *URA3* gene, SC-ura and SC+0.1% 5-fluoro-orotic acid were used; the *ADE2* silencing assay was performed on SC medium containing half of the normal amount of adenine (0.125%). Southern blot analysis of telomere length was performed according to Hediger et al. (2002).

4.3.2 Antibody production

Polyclonal rabbit antibodies against γH2A were generated by Sigma Genosys. The phosphopeptide CKATKA[pSer]QEL was synthesized, conjugated to KLH, and injected into two rabbits. The corresponding crude antisera (SG-2397 and SG-2398) were passed through a column with the non-phosphorylated peptide attached, followed by affinity purification on a column with the coupled phosphopeptide. The populations of antibodies of both eluates were therefore highly specific to the phosphorylated domain of the peptide used as the antigen. This specificity was confirmed using ELISA.

Mouse monoclonal antibody SG1-25J14 was generated by immunizing mice against the phosphopeptide CKATKA[pSer]QEL coupled to KLH, preparation of splenocytes and preparation of fusion cell lines. Phosphoepitope-specific monoclonal antibodies were produced by subcloning and verified by ELISA and western blot.

4.3.3 Immunofluorescence and live fluorescence microscopy

Immunofluorescence on yeast spheroplasts was done according to Klein et al. (1992), except that cells were incubated in 0.1 μg/ml DAPI for 10 min and then mounted with ProLong Gold Antifade Reagent (Invitrogen).

Primary antibodies used in this study are: Rabbit anti-γH2A (SG-2397); monoclonal mouse anti-γH2A SG1-25J14; mouse anti-TAT1 (Woods et al., 1989); monoclonal mouse anti-Nop1 (monoclonal antibody A66; Teixeira et al., 1997); and monoclonal mouse anti-pore Mab414 (Covance).

Secondary antibodies used were: Donkey anti-mouse DTAF (Jackson ImmunoResearch); donkey anti-rabbit Cy5 (Jackson ImmunoResearch); donkey anti-rabbit Alexa 555 (Invitrogen); donkey anti-rabbit Alexa 647 (Invitrogen); goat anti-mouse Alexa 488 (Invitrogen); goat anti-mouse Alexa 647 (Invitrogen).

Pictures were obtained on Zeiss LSM 510 or 510 Meta microscopes with the 100× objective and 1.4 numeric aperture. Pictures were then deconvoluted using Huygens professional scientific volume software (Scientific Volume Imaging: www.svi.nl). Co-localization and 3D surface-rendering and spot-tracking was done using Imaris (Bitplane AG). Live fluorescence microscopy and quantitative analysis of telomere spot position were performed on a Tillvision-driven Olympus IX70 microscope as described in Hediger et al. (2002).

4.3.4 Immunoblot analysis

Whole-cell protein extracts were prepared from exponentially growing yeast cells by TCA-precipitation. MMS treatment was in a final concentration of 0.1% MMS for 2 hours. Recombinant histones were expressed in bacteria and purified according to Luger et al. (1997) and Shen et al. (2003).

Proteins were separated on 15% SDS-PAGE and transferred, or spotted on a nitrocellulose membrane. γH2A was detected by sequential incubations with polyclonal rabbit anti-γH2A (SG-2397/SG-2398), horseradish peroxidase conjugated goat anti-rabbit antibody (Jackson ImmunoResearch), and the Enhanced Chemi-Luminescence system (Amersham); or by using monoclonal mouse anti-γH2A SG1-25J14, horseradish peroxidase conjugated goat anti-mouse antibody (Jackson ImmunoResearch), and the Enhanced Chemi-Luminescence system (Amersham).

4.3.5 Chromatin immunoprecipitation

ChIP was done using rabbit anti-γH2A (SG-2397) and performed and analyzed as described (Cobb et al., 2003; Cobb et al., 2005), except that IP wash buffers contained 0.25M LiCl. 1% Trasylol and other protease inhibitors were added in principle as previously described (Strahl-Bolsinger et al., 1997). 10 mM NaF, 1.25 mM NaPPi and 2.5 mM $NaVO_5$ were added as phosphatase inhibitors. BSA-saturated dynabeads incubated with the same extract served as the background control, and DNA for IP and input was quantified by qPCR on a Perkin-Elmer ABI Prism 7000 sequence-detection system. The sequences of primers and probes used are available upon request. Error bars shown are SD of the mean of at least two independent ChIPs: qPCRs were done in duplicate.

4.4 Results

4.4.1 High γH2A levels occur in normally growing yeast cells

Histone H2A is phosphorylated at serine 129 (γH2A) in response to DNA DSBs, and plays an important role in the repair of nuclear DSBs (van Attikum and Gasser, 2005). In a previous report (Cobb et al., 2005) we showed, using ChIP, that γH2A occurs at high levels at stalled replication forks. The nearly exclusive dependence of this phosphorylation upon Mec1 indicates that this signaling cascade is different from that at DSBs, where H2A is a target of both Mec1 and Tel1 kinases. In the current study, we characterized the occurrence of γH2A in unperturbed cells and in response to different kinds of genotoxic insults.

To perform this study, we generated polyclonal rabbit anti-yeast γH2A antibodies SG-2397 and SG-2398) and a monoclonal mouse anti-yeast γH2A antibody (SG1-25J14). All antibodies showed high specificity for the C-terminal phosphoepitope around serine 129 of histone H2A, which we used for immunization, based on Elisa and western blot analysis (data not shown). The majority of experiments were performed with affinity-purified rabbit anti-γH2A SG-2397. Our first step was to characterize this antibody thoroughly (see Figure 4.1). To assess the specificity of the rabbit anti-γH2A antibody (SG-2397) for its target epitope, we performed a dot blot analysis using the serine 129-phosphorylated oligopeptide and its non-phosphorylated form as control (data not shown). The antibody also showed high specificity for histone H2A phosphorylation at serine 129 on western blots of whole-cell extracts. It even recognizes recombinant histone H2A with phosphomimicking glutamic acid substitution of the serine at position 129, although it does not recognize recombinant phosphorylation-free WT H2A (Figure 4.1a). When DNA damage was induced by MMS in WT and mutant cells in which the phosphor-acceptor serine 129 was substituted by a stop codon, histone H2A was modified only in WT cells. Indeed, γH2A generates a clear signal in extracts from exponentially growing WT cells, and this signal increases in the presence of MMS. No signal is detected in the *h2a*^{S129*} mutant cells, where serine 129 is substituted with a stop codon. In a previous study (see Cobb et al., 2005 in Chapter 3 and Figure 4.1b) we showed by ChIP that high levels of γH2A occur at *ARS607* in response to stalled replication forks.

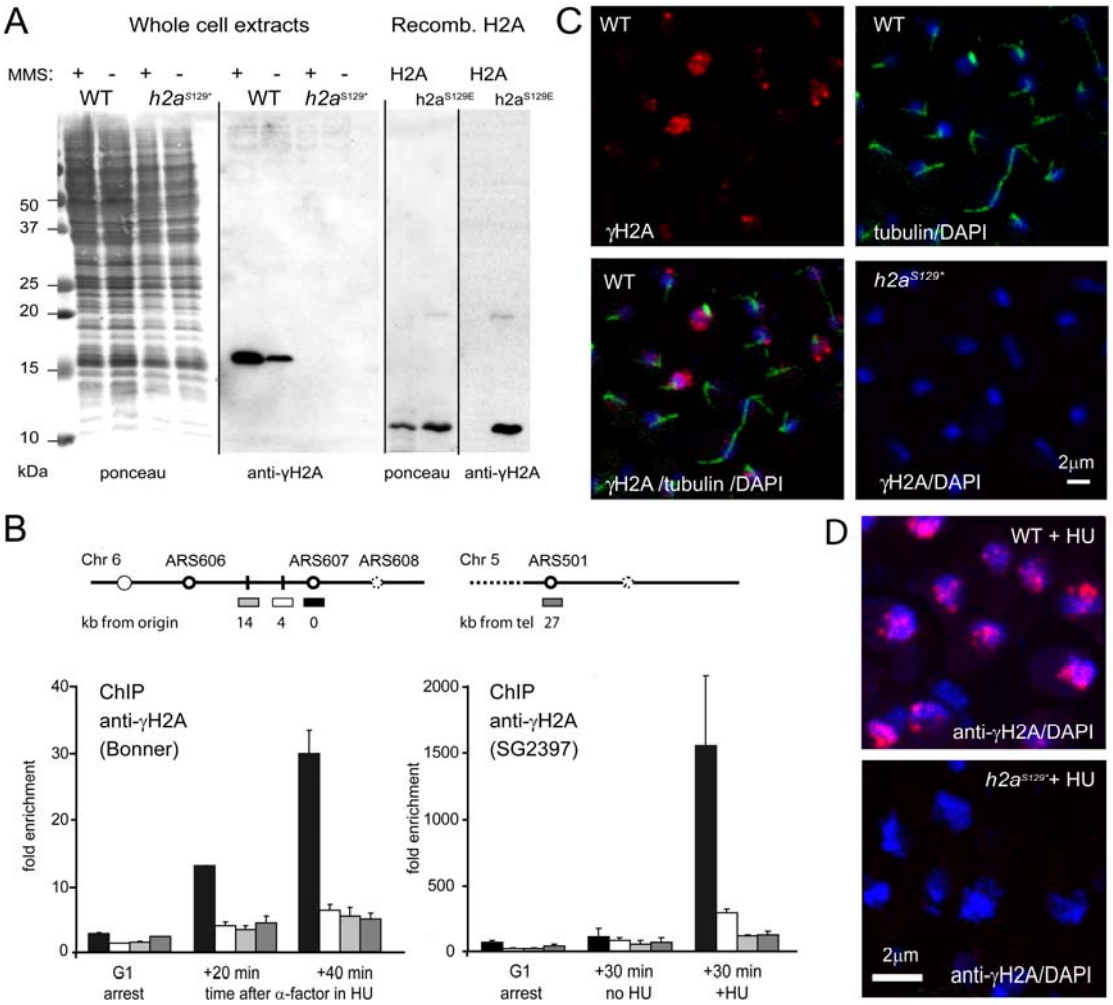

Figure 4.1: Characterization of a new anti-γH2A antibody

A: Rabbit anti-γH2A (SG-2397) is specific for phosphorylated histone H2A.
Whole-cell extracts from exponentially growing WT (GA-180) and *h2a*^{S129*} (GA-3285) strains with or without 0.1% MMS (2h) were separated using 15% SDS-PAGE and probed with anti-γH2A (SG-2397). The righthand panel shows a parallel blot of bacterially expressed histone H2A and *h2a*^{S129E}.
B: High γH2A levels at stalled replication forks are HU-dependent.
ChIP was performed on WT cultures (GA-180) after α-factor arrest and release into YPD +/- 0.2M HU as indicated. qPCR monitored *ARS607* and sites at +4 and +14, as well as the late-firing origin *ARS501*. Results with antibody SG-2397 are compared with those obtained with rabbit anti-γH2A (kind gift of W. Bonner; Cobb et al. 2005). Enrichment is compared to BSA-coated beads.
C: γH2A forms nuclear foci in S phase in the absence of exogenous DNA damage.
WT yeast cells (GA-180) were exponentially grown and IF was performed for γH2A using antibody SG-2397 (1:50) and donkey anti-rabbit Cy5 (1:50) as well as anti-TAT1 (1:50) and donkey anti-mouse DTAF (1:50). DNA was stained with DAPI. In the lower right panel, *h2a*^{S129*}-mutant cells (GA-3285) released into YPD for 40 min after α-factor arrest, were stained with anti-γH2A (SG-2397) and DAPI.
D: γH2A is specifically recognized in IF.
WT (GA-180) and *h2a*^{S129*}-mutant strains (GA-3285) were incubated for 60 min with 0.2M HU and IF was done as described for panel B.

Those experiments were performed with a rabbit anti-γH2A antibody kindly provided by W. Bonner. To confirm that result, we performed ChIP with anti-γH2A SG-2397 on cells released from α-factor arrest either into a normal S phase, or into medium containing 0.2 M HU. We determined the enrichment of γH2A at *ARS607* and a fragment 4 kb away from *ARS607*, and with probes at 14 kb from *ARS607 (FAB1)* as

well as a probe at the late-firing origin *ARS501* as controls. Using SG-2397, we see a very strong enrichment of γH2A at *ARS607*, with signals ~50-fold higher than the results obtained with the Bonner antibody (Cobb et al., 2005 and Figure 4.1b).
However, levels of γH2A at the control regions *FAB1* and *ARS501* remained low, confirming a high specificity of SG-2397 at stalled replication forks surrounding *ARS607*. We next asked if this antibody reflected a specific response to stalling of replication forks by HU, rather than a general response to S phase. γH2A stayed at background levels around *ARS607* after releasing cells into normal S phase without induced arrest or damage (Figure 4.1b, 30 min). These data are in perfect agreement with those in Cobb et al. (2005).
Given that we detected γH2A by western blot even in the absence of exogenous DNA damage (Figure 4.1a), we wanted to ask if this was due to sporadic DNA damage in single cells or a general non-damage related background for all the cells in the cell culture. In this context, it is important to note that mammalian γH2AX forms distinct foci in cells after its phosphorylation (Rogakou et al., 1999). We therefore performed immunofluorescence (IF) staining in exponentially growing WT as well as $h2a^{S129*}$ mutant cells (Figure 4.1c). We observed γH2A foci formation in WT but not in mutant cells in the absence of exogenous DNA damage. IF confirmed the ChIP and western blot data: in a yeast culture synchronously released from G1-arrest into HU we detected bright γH2A foci in almost all cells (Figure 4.1d), while IF signals were absent in similarly treated $h2a^{S129*}$ cells (Figure 4.1d). These experiments confirmed earlier results on HU-treated cells, validated our new antibody, and indicated that unperturbed S-phase cells may contain phosphorylated H2A.

4.4.2 Normally growing yeast cells have high levels of γH2A in S phase

Using ChIP we found γH2A at stalled replication forks, and a previous study in mammalian cells had linked the formation of γH2AX foci to the occurrence of replication-dependent DNA DSBs (Furuta et al., 2003). We were therefore interested in whether the level of spontaneous γH2A signal observed varied during cell cycle progression. In particular, we wanted to see if it might be linked to replication. We determined the total amount of nuclear γH2A by quantifying the signal intensity of a single yeast cell in an exponentially growing WT cell culture. The yeast cells were assigned to the corresponding cell cycle phase by cell shape and by monitoring

spindle morphology using microtubule-IF (see representative examples for the different cell cycle stages in Figure 4.2a). We calculated the mean signal intensity of γH2A over a large number of cells. We found a significant (5-fold) increase in IF signal during S phase, with a peak in G2 and anaphase, as compared to G1 phase (see Figure 4.2a).

These results indicate that H2A phosphorylation at serine 129 in exponentially growing yeast cells occurs mainly in S phase and persists until the end of anaphase.

To confirm this result by other means, we monitored global γH2A levels during an unperturbed cell cycle using western blot (Figure 4.2b). Proper release from α-factor arrest and cell cycle progression was confirmed by determining budding index. We used mouse anti-γH2A (SG1-25J14) to determine γH2A levels for samples every 15 minutes after release from synchronization in G1 into the cell cycle using α-factor. By quantifying the luminescence on the western blot, we determined that the γH2A signal in an unperturbed cell cycle is <10% of the level detected in MMS-treated cells. Again, we saw an increase in the signal during the progression of cells into S and G2 phase (15, 30, and 45 min after α-factor release) as compared with equally loaded G1 (0 min) and random culture samples (data not shown). We also observed a decrease in signal for late M/G1-phase cells (60 and 75 min) and an increase for the second cell cycle (90 and 105 min), despite a significant loss of cell synchronization. This result reinforces the result obtained by IF (Figure 4.2a) and we conclude that γH2A levels increase during an unperturbed S phase.

It is known that there are different functional zones in the cell nucleus. Yeast does not have any chromosomal territories, and therefore the main differentiating factor is proximity to the nuclear periphery versus internal positioning of chromosomal DNA. For example, it is known that late firing origins and rDNA, as well as telomeres, are constrained at the nuclear periphery (Bystricky et al., 2005; Heun et al., 2001) and a common characteristic of these chromosome domains is replication in late S/G2 phase of the cell cycle, where we observe that the γH2A signal becomes maximal. To see if cellular γH2A signals in naturally growing yeast cells are associated or enriched in the internal versus peripheral zone of the yeast nucleus, we performed IF co-staining for γH2A and nuclear pores on exponentially growing WT cells (Figure 4.2c). We observed that γH2A often localized to the nuclear periphery and sometimes even co-localized with nuclear pores (see, for example, the projection for the upper nucleus in Figure 4.2c). To determine the position of γH2A for the three-dimensional nucleus,

we used 3D surface reconstruction of the nuclear pore with spot rendering to visualize loci with an intensive γH2A signal. We found that in most cells many of the brightest γH2A foci were localized at the nuclear periphery.

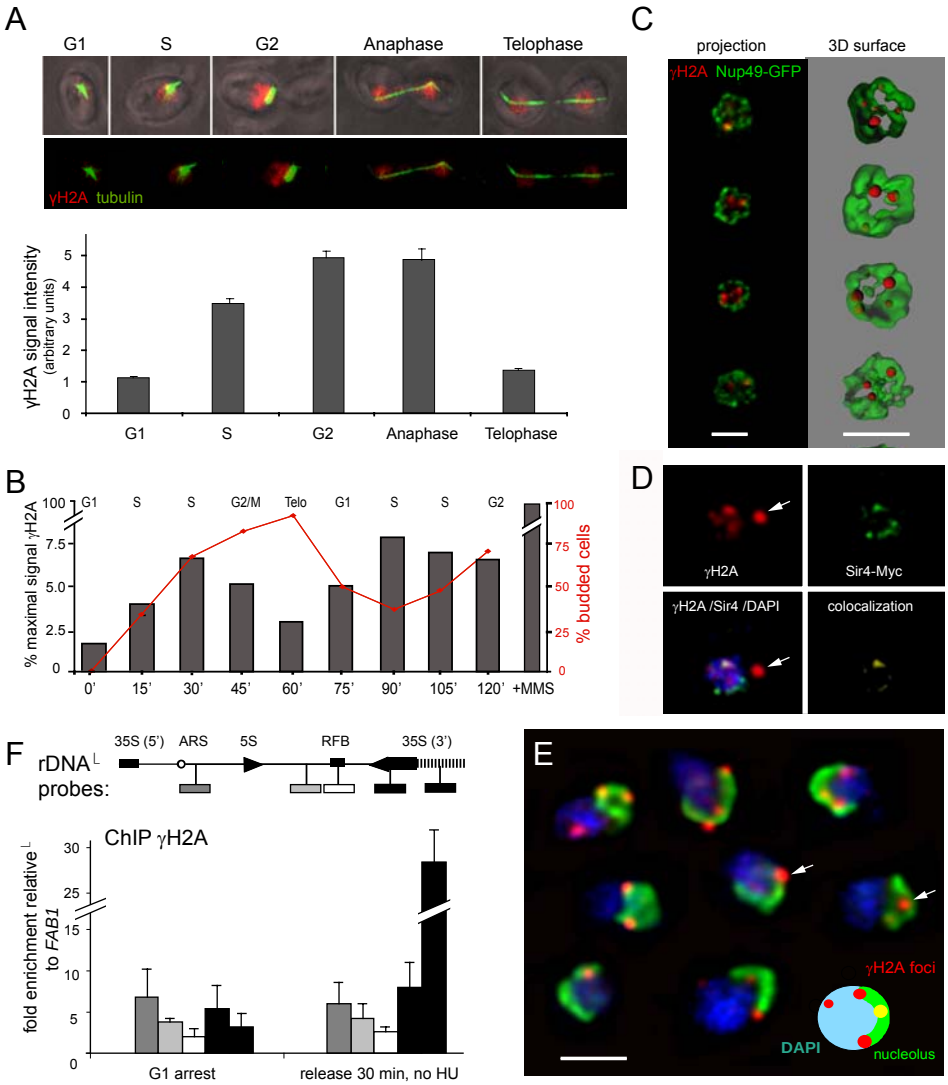

Figure 4.2: γH2A is present in foci in an unperturbed S phase and maps to the rDNA

A: Total γH2A levels increase during S phase and peak in M phase.
Exponentially growing diploid WT cells (GA-659) were stained by IF for γH2A (SG-2397) and TAT1. Cell cycle stages were scored by cell shape (phase microscopy) and spindle morphology. The graph shows the mean + SD of nuclear γH2A signal intensity for the following numbers of cells: G1, n=185; S, n=135; G2, n=83; anaphase, n=35; telophase, n=102.
B: γH2A levels during a synchronized but unperturbed cell cycle.
WT (GA-180) cells were released from α-factor into YPAD and protein samples were taken every 15 min. The γH2A signal on a western blot was normalized to histone levels and is presented with budding index vs. time. 100% = γH2A in MMS-treated cells run on the same western blot.
C: γH2A foci occur near nuclear pores.
IF was performed on exponentially growing WT cells (GA-180) using SG-2397 (anti-γH2A) and Mab414 (anti-pore). On the left is a projection of a stack of confocal images and on the right a 3D surface reconstruction. Bar = 2µm.
D: γH2A foci co-localize partially with telomere-bound Sir4.
Exponentially growing cells bearing Myc-tagged Sir4 (GA-1275) were released from α-factor arrest into YPD for 60 min. IF detected Sir4-Myc (Mab 9E10) and γH2A (SG-2397). Arrows indicate bright γH2A foci that are not telomeric.
E. Bright S-phase γH2A foci are nucleolar.
Exponentially growing cells (GA-1275) were fixed and stained for γH2A (SG-2397), NOP1 (Mab anti-NOP1), and DAPI (blue). Cell-cycle stage was determined by cell shape (phase microscopy). Bar = 2µm.
F. ChIP mapped high levels of γH2A within the 35S rRNA gene.
ChIP for γH2A was performed on WT cells (GA-180) after α-factor arrest and release into YPAD without HU for 30 min. The qPCR probes are indicated in the rDNA repeat. Values obtained were normalized to *FAB1*.

However, we also see clear examples of internal γH2A foci. To determine whether γH2A is found at clustered telomeres at the periphery, we co-stained with Sir4. Sir4 staining is a marker of such telomeres, leading to a staining of the nucleus in a punctate pattern (Palladino et al., 1993a). As Figure 4.2d shows, we often saw partial co-localization between γH2A and Sir4 in late S/G2-phase WT cells. Hence, some of the γH2A signal seems to be at telomeres, though in many cases the brightest γH2A foci are distinct from Sir4 foci.

4.4.3 Very bright γH2A foci occur in the nucleolus in S phase and emanate from γH2A at the 35S ORF in the rDNA

While analyzing the results shown in Figure 4.2d, our attention was attracted by another observation. Figure 4.2d shows an example of a very bright spot of γH2A formed outside the nuclear DNA stained by DAPI. Interestingly, the only place in the nucleus where DAPI staining is absent is the nucleolus. To confirm that γH2A co-localized with the nucleolus, we performed IF staining for Nop1, which is a global marker of the nucleolus and γH2A. We observed that, in a majority of S-phase cells (69%, n=95), there were at least one or more bright spots in or next to the nucleolus (see representative examples in Figure 4.2e). This is specific for S phase, since in 93% (n=81) of G1-phase cells and 70% of telophase cells (n=54) there were no bright γH2A spots associated with the nucleolus. We suspected that this bright spot formation at the nucleolus in S-phase cells could be a main contributing factor for the globally enhanced γH2A signal intensity per nucleus that we observed (see Figure 4.2a), since it is known that viable mutations of components of the cellular DNA replication machinery, e.g. the helicase Sgs1, often show phenotypes concerning the replication of the rDNA (Kaliraman et al., 2001; Versini et al., 2003).

One reason for the rDNA-associated damage is that replication occurs at the same time as transcription. To avoid any collisions between forks and the transcription machinery, rDNA repeats contain replication fork barriers (Lambert et al., 2007). We therefore addressed the question of whether we could monitor the position of γH2A along the rDNA in S-phase cells using ChIP and qPCR throughout the rDNA repeat (see Figure 4.2f). As expected, we saw no high levels at the RFB or other loci in G1 phase, but some enrichment of γH2A could be seen close to the ARS and in the 35S

ORF. Surprisingly, in S phase there was no enrichment at the RFB, but a high enrichment for a region in the 35S ORF. We conclude that the bright γH2A foci we observed at the nucleolus of S-phase cells are not due to γH2A phosphorylation generated by replication problems at the RFB, but are due to γH2A phosphorylation in the 35S ORF.

4.4.4 γH2A is an integral component of sub-telomeric chromatin throughout the cell cycle

Other domains that induce replicational stress at high levels are telomeres. Telomeric sequences pose two specific problems for replication: The terminal repeats of the lagging strand must be extended by telomerase; and the heterochromatic and non-nucleosomal telosome poses a barrier to the replication fork. We therefore did ChIP with the rabbit anti-γH2A (SG-2397) after synchronization with α-factor, and probed with qPCR for γH2A enrichment at regions 0.5 and 1.8 kb from Tel6R, as well as control regions 7.5 and 90 kb (*FAB1*) away from the telomeric repeat (Figure 4.3a). Throughout the cell cycle, we observed very high levels of γH2A at the telomeric regions, as compared with *FAB1*, for timepoints ranging from 0 to 120 min after α-factor release. Levels of γH2A at the telomeres seemed to reach a maximum in late S phase. Interestingly, levels of γH2A were already low 7.5 kb from the TG repeat, showing that the signal does not spread as far as it was shown to for DSBs. In contrast, it localizes to the region with specific telomeric chromatin structure covered with the SIR complex (Hecht et al., 1996). Interestingly, we also observed a significant drop in the levels of sub-telomeric γH2A in a *sir3* mutant strain (Supplemental Figure 4.5).

To rule out non-specific binding of the antibody, we performed ChIP for exponentially growing $h2a^{S129*}$ mutant cell samples. Figure 4.3b shows that only in WT cells did we see γH2A enrichment at telomeres, while in the $h2a^{S129*}$ mutant strain there was no such enrichment. Our absolute enrichment values range up to 3,000-fold, and we therefore noticed a relatively high variation in these absolute values due to fluctuating background signal. This variation became relatively small by normalizing the fold enrichment obtained for telomeric probes to the enrichment obtained for the internal locus *FAB1*, where we only detected background levels for γH2A during normal cell cycle progression (see Figure 4.3a and Cobb et al., 2005).

We compared the level of this late S-phase telomeric γH2A, which is HU-independent, to that recovered at an HU-arrested replication fork. These two signals, monitored in the same experiment, were of nearly the same magnitude (Supplemental Figure 4.1).

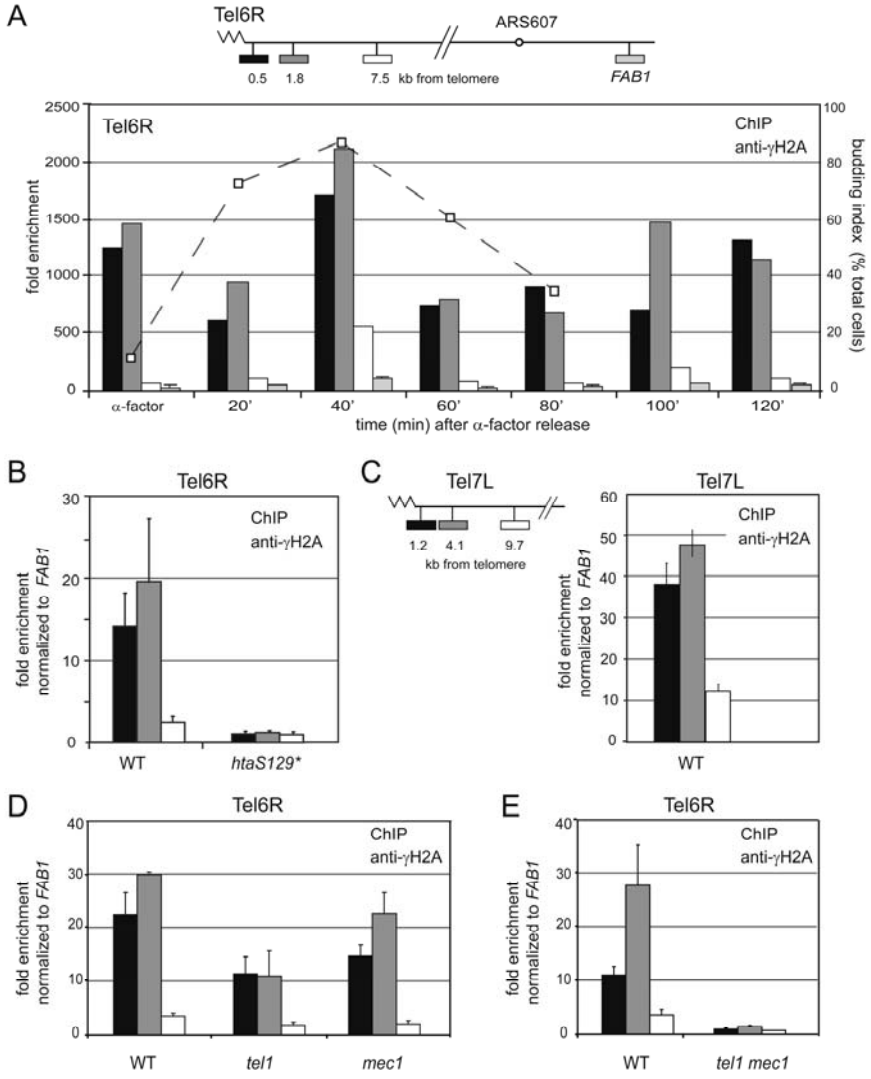

Figure 4.3: γH2A occurs at telomeres and is primarily Tel1-dependent

A: H2A is phosphorylated at Tel6R.
γH2A-ChIP was performed on WT cells (GA-2448) after α-factor arrest and release into YPAD. Samples were taken every 20 min, and progression through the cell cycle was monitored by the budding index. qPCR used probes at 0.5, 1.8 and 7.5 kb from the Tel6R TG-repeat and an internal control locus *FAB1*.
B: γH2A is specifically recognized in ChIP experiments.
γH2A-ChIP was performed on exponentially growing WT (GA-180) and $h2a^{S129*}$ (GA-3285) cells as in A for Tel6R.
C: H2A is phosphorylated at Tel7L.
γH2A-ChIP was performed on exponentially growing WT (GA-2263; S288C background) cells, and qPCR probes are indicated for Tel7L. This experiment rules out the possibility that the telomere-associated signals are background- or strain-specific. The mean of two experiments was normalized to *FAB1*.
D: Telomeric γH2A depends mainly on Tel1 kinase.
γH2A-ChIP was performed on exponentially growing WT (GA-2448), *tel1*Δ (GA-2507), and *mec1*Δ *sml1*Δ (GA-1702) strains as in A. Strains lacking *mec1* carry an *sml1* deletion, which suppresses lethality but does not affect γH2A levels on its own (cf. WT in D vs E).
E: γH2A is completely abolished in *mec1 tel1* double mutant strains.
ChIP was performed on early passage WT (*sml1*Δ, GA-2312) and *mec1*Δ *tel1*Δ *sml1*Δ (GA-2978) strains. Tel6R probes were as in A, and data was normalized to *FAB1*.

Since the presence of γH2A at Tel6R and the co-staining with Sir4 (Figure 4.2d) indicated that γH2A is a general mark of budding yeast telomeres during exponential growth, we also monitored γH2A levels at another telomere, Tel7L. We performed this in yeast from the S288C background to ensure primer sequence functionality. Figure 4.3c shows that we obtained a high relative enrichment for γH2A near Tel7L, confirming the generality of γH2A proximity to telomeres.

4.4.5 Phosphorylation of histone H2A at telomeres is mainly mediated by Tel1

Serine 129 in histone H2A is followed by glutamine (Q) and is thus a target of PI3-like kinases. At DSBs, this phosphorylation is mediated by Mec1 and Tel1, whereas at stalled replication forks it depends strongly on Mec1. To determine which kinase mediates γH2A at telomeres, we performed ChIP for γH2A in exponentially growing *mec1* and *tel1* mutant strains. We observed that γH2A levels relative to *FAB1* at Tel6R were considerably lower in the *tel1* mutant strain, whereas they were only slightly lower than WT in the *mec1* mutant strain (Figure 4.3d). Therefore, H2A phosphorylation at telomeres seems to be mainly mediated by Tel1, but γH2A levels at telomeres are still high in a *tel1* mutant. Even if a *mec1* mutant has only slightly diminished levels of γH2A at the telomeres, it was a substitute for the function of Tel1 in a *tel1* mutant. We therefore assayed γH2A levels in WT and *mec1 tel1* double-mutant strains (Figure 4.3e). We observed that H2A phosphorylation at telomeres was abolished completely in the $h2a^{S129*}$ mutant strain (see Figure 4.3b and data not shown). From these results we conclude that H2A phosphorylation at telomeres is mainly mediated by Tel1, with a smaller contribution from the Mec1 kinase. The Mec1 contribution may increase in the absence of Tel1, consistent with genetic data, implicating Mec1 in telomere maintenance in a *tel1* mutant (Ritchie et al., 1999).

4.4.6 Elongation of telomeres induces higher γH2A levels

Both Tel1 and Mec1 are required to maintain telomere homeostasis. We note that *mec1 tel1* double mutants undergo senescence through continuous telomere shortening (Ritchie et al., 1999). However, the corresponding single mutants of either kinase have shorter but stable telomeres, indicating that both can regulate telomere elongation (Viscardi et al., 2005). Because we saw a negative effect on telomeric γH2A levels in both single mutants, we decided to ask whether the elongation of a

specific telomere would correlate with higher levels of γH2A. Longer telomeres have a lower probability of elongation than short telomeres (Teixeira et al., 2004). To compare γH2A levels specifically at elongating short telomeres with γH2A levels at telomeres of normal length, we made use of a system developed and kindly provided by the Gilson laboratory (Marcand et al., 1999). This system makes use of the counting mechanism at telomeres which is mediated by sub-telomeric TG_{1-3} repeats as Rap1 binding sites (Figure 4.4a).

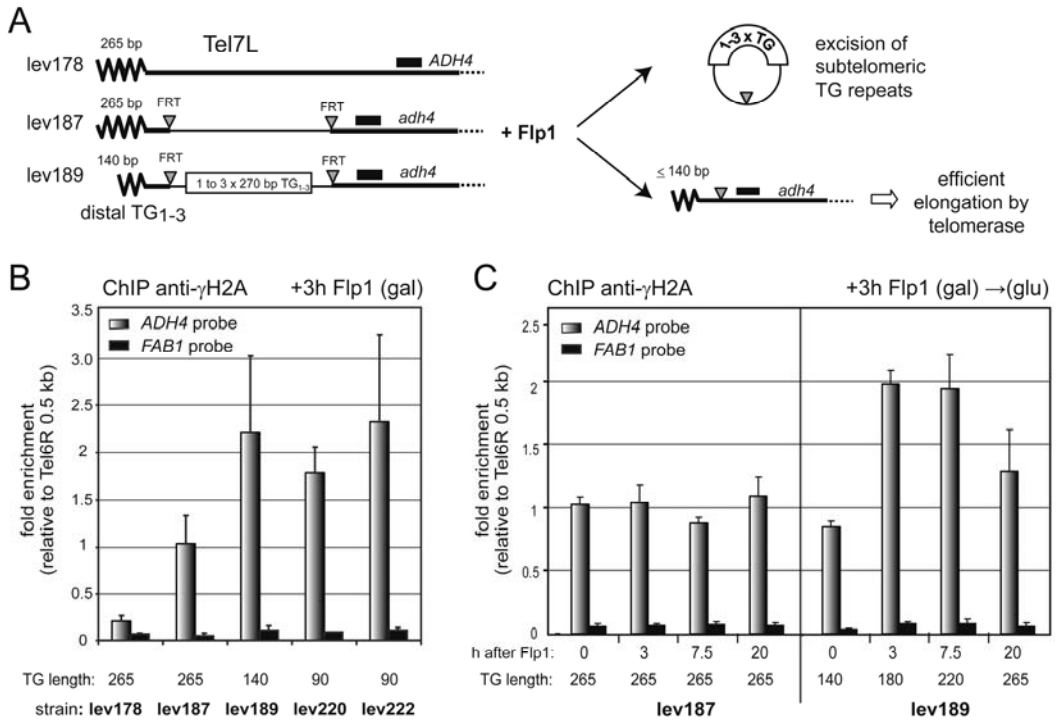

Figure 4.4: γH2A is preferentially found at elongating short telomeres

A: A system for rapid generation of a single short telomere was described by Marcand et al. (1999).
FRT sites are integrated at Tel7L to allow controlled excision by Flp1 recombinase of a sub-telomeric fragment containing 0 to 3 copies of a 270bp TG repeat. The presence of a sub-telomeric TG repeat leads to shorter terminal tracts. qPCR probes are within *ADH4* and *FAB1* (see Figure 4.3) After Flp1-induced excision the *ADH4* probe is 0.5kb from the terminal repeat.
B: γH2A-ChIP was performed in the indicated strains bearing *GAL10::FLP* and either no FRT sites (lev178) or FRT motifs flanking 0 (lev187), 1 (lev189), 2 (lev220), or 3 (lev222) copies of a 270bp TG tract.
Terminal TG lengths are indicated below the graph. Samples were taken for γH2A-ChIP after *GAL10::FLP1* after 3h in 2% galactose. qPCR data for *ADH4* or at the internal *FAB1* site are normalized to γH2A levels at Tel6R-0.5kb (see Figure 4.2).
C: γH2A levels increase at elongating telomeres.
γH2A-ChIP, as described for panel B, is shown for strains having WT terminal TG length (lev187, 265bp) or short terminal tracts (lev189, 140bp). *GAL10::FLP1* cells were grown for 3h on galactose and then placed in YPAD and samples were taken after 0, 3, 7.5, and 20 hours of exponential growth. qPCR is as in B.

A variable number of TG_{1-3} repeats, all 270 bp long, is integrated as a construct flanked by FRT sites between the ADH4 locus and the natural TG_{1-3} repeat of telomere 7L. Internal TG_{1-3} repeats in yeast strains with integration (lev189, lev220, and lev222) lead to the shortening of distal TG_{1-3} in comparison to yeast strains that

have no insertion (lev178 and lev187). After induction of Flp1-mediated recombination, Tel7L is sensed as critically short due to loss of internal TG_{1-3} repeats and it is then elongated proficiently during the next cell cycles to achieve WT length and telomere length equilibrium. We used these strains to monitor γH2A levels at telomeres of different TG_{1-3}-repeat length (Figure 4.4b). We performed ChIP with the γH2A antibody SG-2397 and qPCR for a probe located at the *adh4* locus, which after recombination is located 0.5 kb from the TG_{1-3} repeat and equidistant to the 0.5 kb probe at telomere 6R. As expected for lev189 with WT TG_{1-3}-repeat length, the relative enrichment of γH2A is around one-fold, whereas it stays significantly lower for lev178, due to a lack of recombination and hence a longer distance to the *adh4* probe. All three strains with shorter TG_{1-3} repeats (lev189 with 140 bp, lev220 and lev222 with 90 bp) are therefore prone to elongation back to WT length of around 265 bp (as in lev187), and they show higher levels of γH2A relative to Tel6R and therefore a relative enrichment of more than 1. Both Tel1 and Mec1 are required for the recruitment of telomerase, and we thus next tested whether enhanced γH2A levels are linked to telomere elongation during out-growth after sudden shortening of the TG repeat (Figure 4.4c). We compared the enrichment for γH2A at the *adh4* locus relative to Tel6R in lev187 (with telomeres of WT length) and in lev189, with a strain whose telomere shortens and then gets elongated during the next generations (Marcand et al., 1999). After exponential growth for 1.85 generations (3 h), 5.25 generations (7.5 h), and 13 generations (20 h), we observed that the relative enrichment for lev187 at *adh4* stays at around one-fold for all the timepoints taken. This is expected for a telomere in equilibrium if elongation would positively influence γH2A levels. In contrast, we observed a fold enrichment higher than 1 for lev189 after 3 and 7.5 h. γH2A levels are therefore doubled at a short Tel7L relative to Tel6R during its elongation, which is very proficient in early generations and decreases over time (Marcand et al., 1999), as we could see for the 20 h timepoint. Although our results did not exclude a residual γH2A pool at all telomeres independently of their TG_{1-3}-repeat length, our results demonstrated a positive correlation between γH2A levels and telomere elongation of critically shortened telomeres. This may implicate γH2A in the cellular response to telomeric uncapping.

Telomeric uncapping can also be induced by shifting up a *cdc13*-1 mutant strain to restrictive temperature. We therefore monitored cellular γH2A levels in WT, $h2a^{S129*}$, and *cdc13*-1 mutant strains after shifting to restrictive temperature by IF using mouse

monoclonal anti-γH2A (Supplemental Figure 4.2). However, under these conditions phosphorylation of histone H2A filled the nuclear space and we detected no selective telomere labeling. Nonetheless, in the *cdc13*-1 *h2a*^{S129*} double mutant the checkpoint response, as monitored by Rad53 activation, was normal even at restrictive temperature. This shows that γH2A is not essential for establishing a checkpoint response at uncapped telomeres, but its hyperphosphorylation did coincide with telomere uncapping.

4.4.7 γH2A is not essential for establishing telomeric silencing, but affects nuclear anchoring of telomeres in S phase

Is γH2A essential for telomerase activity? If γH2A were essential for telomerase action, its elimination would induce a senescence phenotype, as is observed in *est1*, *tlc1*, or *est2* deletion strains. We checked whether this was the case by repeatedly re-streaking the *h2a*^{S129*} mutant, yet no senescence phenotype was scored (cf. *tlc1* in Supplemental Figure 4.3a). Moreover, the *h2a*^{S129*} mutation did not suppress senescence when coupled with an *est1* deletion (data not shown).

We reasoned that the telomerase recruiting function of γH2A may be masked by other telomerase regulation pathways, as is the case in the *tel1*Δ strain, where telomere length is maintained at a shorter, but stable length (Greenwell et al., 1995; Ritchie et al., 1999). However, this was not the case in cells lacking γH2A: We performed a Southern blot comparing *XhoI*-digested genomic DNA from isogenic WT, *h2a*^{S129*}, *yku70*, and *rif1* mutants probed with the telomeric repeat. In the *yku70* mutant, TG_{1-3} repeats shortened, and in the *rif1* strain they lengthened, yet telomere length in the *h2a*^{S129*} mutant remained comparable to the WT control (Supplemental Figure 4.3b). There were indications that two of the four *h2a*^{S129*} colonies tested had slightly longer telomeres and/or of variations in Y'-containing telomere ends (see arrows). This may indicate increased or promiscuous recombination events (Supplemental Figure 4.3b). However, in an assay for recombination-dependent survivors of telomerase inactivation, survivors arose in the *h2a*^{S129*} *est1* double mutant with almost the same efficiency as in an *est1* single mutant (Supplemental Figure 4.3c).

Telomeres are anchored to the periphery, and Tel6R, for which we observed high levels of γH2A throughout the cell cycle, is anchored by parallel pathways involving Ku and Sir proteins in interphase (Hediger et al., 2002). The Sir proteins might be

affecting telomeric chromatin structure, and this might also be true for histone modifications. To understand whether γH2A is important for anchoring Tel6R, we introduced lac operator sites at telomere 6R in the *h2a*^{S129*} mutant strain as has been previously reported (Hediger et al., 2002), and compared Tel6R by live fluorescence imaging of GFP-lac repressor fusion proteins, forming a spot (Figure 4.5a).

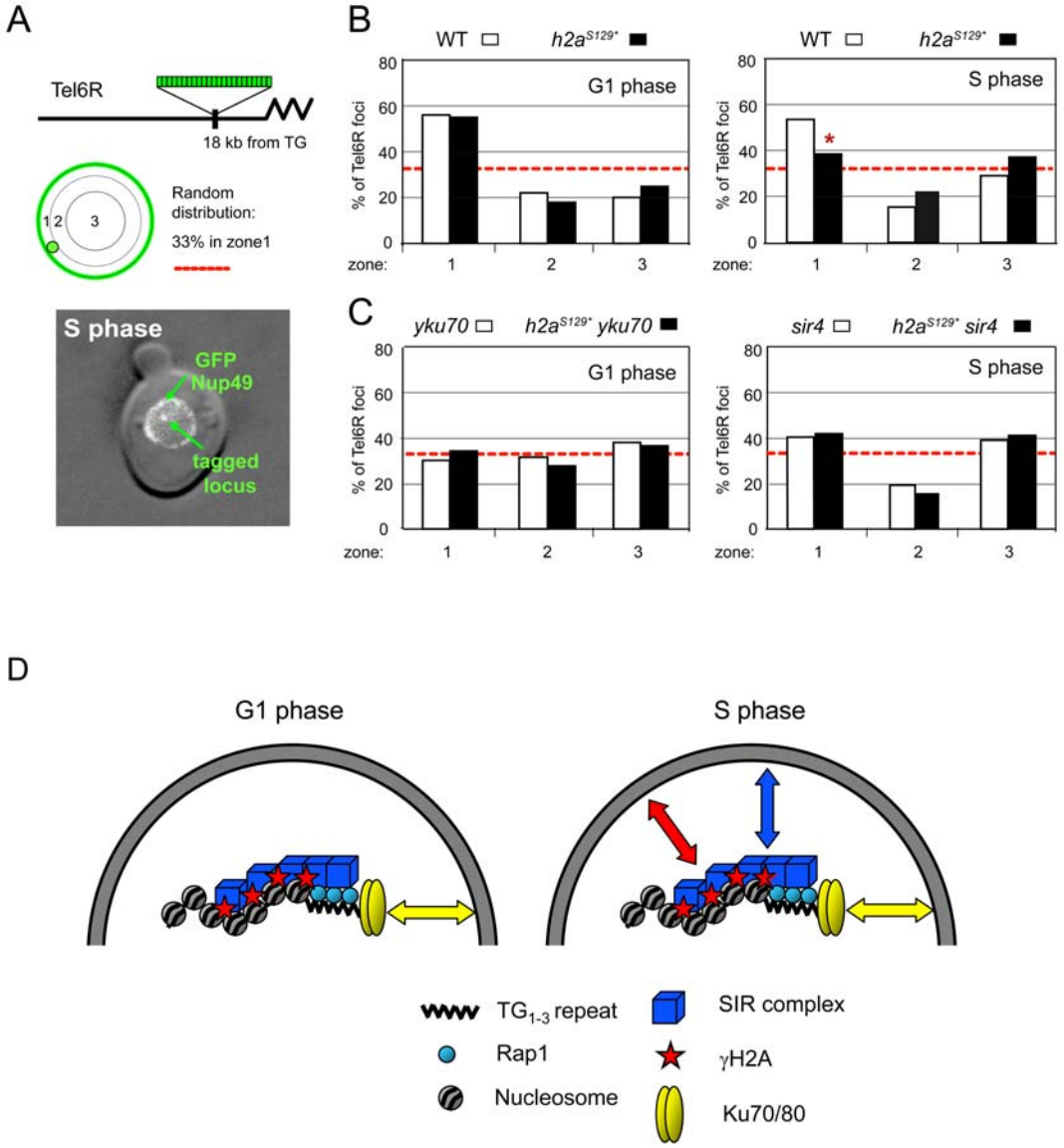

Figure 4.5: Loss of γH2A influences telomeric anchoring at the nuclear periphery

A: Tel6R was tagged with a *lacO* array in WT (GA-1561), *h2a*^{S129*} (GA-4112), *h2a*^{S129*} *ku70* (GA-4159), and *h2a*^{S129*} *sir4* (GA-4169) strains.
Expression of *lac*I-GFP and the pore protein Nup49-GFP, coupled with live 3D microscopy, allowed scoring of the Tel6R position relative to three zones of equal surface (Hediger et al., 2002). Zone1 spans the nuclear envelope.
B and C: Anchoring of Tel6R at the nuclear periphery is compromised by the *h2a*^{S129*} mutation in S-phase.
The P values for zone 1 enrichment in G1 cells are: GA-1561, P=9.14×10^{-10} (n=147); GA-4112, P=2.4×10^{-7} (n=114); GA-4159, P=0.76 (n=89); and GA-4169, P=9.25×10^{-4} (n=105). For S-phase cells: GA-1561, P=2.67×10^{-6} (n=108); GA-4112, P=0.28 (n=71); GA-4159, P=0.40 (n=85); and GA-4169, P=0.028 (n=127). Data for *ku70* and *sir4* mutant strains are derived from Hediger et al. (Hediger et al., 2002).
D: Anchoring of Tel6R in S phase cells depends on γH2A.
Anchoring of Tel6R at the nuclear periphery is mediated in G1-phase cells via the Ku70/Ku80 heterodimer. In S-phase cells, anchoring depends on Ku70/80 and also Sir4, and as novel finding of this study also on γH2A.

Telomere to pore distance was determined in the focal plane, and the spot was classified as being in one of three zones of equal surface area, with zone 1 being the most peripheral zone. In WT strains, Tel6R was significantly anchored in G1- and S-phase cells (Figure 4.5b and Hediger et al., 2002). Although the anchoring of Tel6R was unaltered in the *h2a*^{S129*} mutant strain in G1 phase, it assumed a near-random distribution in S-phase cells (Figure 4.5b).

It has been previously shown that *yku70* mutation compromises anchoring in both G1 and S phases, while *sir4* mutants only reduce Tel6R anchoring in S phase (Hediger et al., 2002; Taddei et al., 2004a). Since this is similar to the *h2a*^{S129*} phenotype, we scored the epistasis of *h2a*^{S129*} with either *yku70* or *sir4* deletions in G1- and S-phase cells. As expected, loss of γH2A did not bypass or aggravate the loss of attachment detected in the *yku70*-deficient strain in either G1- or S-phase cells (Figure 4.5c and data not shown). More importantly, however, we saw no additive effects with the *sir4* mutation, which indicates that γH2A either acts downstream of, or alongside, the Sir4-Esc1 pathway (Figure 4.5c). We conclude that the anchoring of Tel6R in S phase via telomeric chromatin requires both γH2A and Sir4 (Figure 4.5d).

We tested whether γH2A was necessary for the association of Sir4 with telomeres, and the ensuing telomere position effect (TPE), which confers repression on sub-telomeric genes. We investigated a potential function of γH2A in telomeric silencing by monitoring the survival of WT, *yku70*, and *h2a*^{S129*} mutant strains, where each of the strains had a *URA3* gene integrated in the sub-telomeric, and hence normally silenced, region of Tel7L by drop assay on medium containing 5-FOA (Supplemental Figure 4.4a). As expected, we saw that the WT strain survived on medium containing 5-FOA due to telomeric silencing of the *URA3* gene, whereas the *yku70*-mutant strain showed, as expected, a low survival rate due to loss of telomeric silencing. The *h2a*^{S129*}-mutant strain grew like WT, indicating functional telomeric silencing. The *URA*-FOA assay selected for silent states and thus was not sensitive to minor reductions in repression. To further confirm that telomeric chromatin was silenced in an *h2a*^{S129*} mutant, we monitored silencing of an *ADE2* gene integrated at truncated Tel6R by monitoring colony sectoring. *ADE2* repression at Tel6R led to red-colored colonies (Supplemental Figure 4.4b). Again, in WT and the *h2a*^{S129*} mutant we saw red-colored yeast cells, indicating proficient telomeric silencing, although we noted a higher fraction of white sectors in the mutant, indicating that Tel6R repression was slightly reduced when compared with the WT. Similar results were obtained for an

ADE2 construct at Tel5R (data not shown). This argues that loss of γH2A slightly weakens TPE, although SIR complexes are still able to bind. This slight defect in silencing is reminiscent of the situation observed in other mutants that compromise anchorage through the SIR pathway, notably in *esc1*-deletion strains (Taddei et al., 2004a).

4.5 Discussion

In this study we have shown that substantial levels of γH2A occur in normally growing yeast cells. Levels increase significantly during S phase and stay high until the end of mitosis. We further observed foci formation during these phases of the cell cycle. We provide evidence that a major genomic locus which contains S-phase specific γH2A is the rDNA. We propose that nucleolar γH2A foci stem from endogenous replication problems that occur spontaneously during cell growth.
We further showed that γH2A is an integral component of sub-telomeric chromatin throughout the cell cycle. We monitored the dependence of the levels of γH2A on Mec1 and Tel1. Tel1 had a dominant contribution, which indicates a link to telomere length control. Indeed, monitoring γH2A levels during the elongation of critically shortened telomeres, we saw that elongation of telomeres and γH2A levels correlate. It is therefore possible that γH2A is a marker of critically short and elongating telomeres, and may play a role in telomerase recruitment.
Finally, we observed that γH2A influences telomeric anchoring. This is a novel function for H2A phosphorylation. We will now address how this novel function might be connected to the known role of γH2A in DNA damage repair.

4.5.1 Is γH2A during normal cell cycle progression a marker of endogenous replication stress?

In a previous report, we observed high levels of γH2A at HU-stalled replication forks (Cobb et al., 2005) and Figure 4.1c). This phosphorylation of H2A depends on Mec1 which, like its human counterpart ATR, has a predominant role in the replication checkpoint pathway (Zou, 2007) and plays a further direct role in stabilizing stalled replication forks (Cobb et al., 2003; Cobb et al., 2005). In the current study, we observed high levels of γH2A in exponentially growing yeast cells, where levels increased dramatically during S phase and stayed high until the end of telophase (see Figure 4.2a/b). Interestingly, this phenomenon seems to be conserved in evolution, since DNA damage-independent mitotic phosphorylation of H2AX also occurs in normally growing mammalian cells (McManus and Hendzel, 2005). This pool of γH2AX shows the same increase during the cell cycle over S phase with a maximum in mitosis.

We observed very bright γH2A foci in S-phase cells which were associated with the nucleolus (see Figure 4.2e/f). Ribosomal DNA has a characteristic replication fork barrier (RFB) in order to avoid head-on collisions between replication and transcription polymerases. The RFB is known to be a recombination hotspot (Lambert et al., 2007). Thus, one possibility is that γH2A foci in the nucleolus stem from endogenous replication problems. Using ChIP we found that γH2A levels were low at the nucleosome-free RFB (Fritze et al., 1997), yet a significant S-phase specific enrichment was found within the 35S rRNA gene. This is consistent with bright nucleolar γH2A foci arising from S-phase specific collisions between replication and transcription events (Takeuchi et al., 2003). γH2A may also reflect a PI3-like kinase response to damage in the rDNA which was recently shown to down-regulate RNA Pol I in mammalian cells (Kruhlak et al. 2007). Given that the phosphorylation occurs in the 35S gene, the signal is unlikely to stem from a head-on collision between a replication fork and the transcription machinery. It may instead stem from replication forks that encounter the transcription machinery in a unidirectional manner. Transcripts of the 35S ORF have consistently been detected, using electron microscopy, ahead of the replication fork (Saffer and Miller, 1986).

Replication problems can also arise from the replication fork hitting transient topoisomerase I cleavage complexes (see Introduction) and thereby inducing a CPT-like response. Because the *h2a*^{S129*} mutant strains are very sensitive to CPT, γH2A may also be required to maintain genomic stability of the rDNA locus in the context of endogenous replicative damage like CPT-induced damage. The endogenous damage created in the rDNA locus is checkpoint-blind (Torres-Rosell et al., 2005). In this context it is important to recall that γH2A is important for cohesin loading at DSBs (see Introduction), and that cohesion inhibits asymmetrical recombination in the rDNA repeats while favoring homologous recombination (HR) (Huang et al., 2006). This efficient HR may be the reason why the rDNA damage is checkpoint-blind.

Various lines of evidence have indicated a role for γH2A in checkpoint-blind DNA damage. A genetic analysis has indicated that histone H2A serine 129 phosphorylation acts in the same pathway as Tof1 and Csm3 for the repair of CPT-induced DNA damage (Redon et al., 2006). Tof1 interacts with the replisome and is

important for maintaining replication fork stability after hydroxyurea treatment (Katou et al., 2003) as well as for pausing replication forks at the replication fork barrier in the rDNA (Calzada et al., 2005; Tourriere et al., 2005). Both Tof1 and Csm3 have been shown to be important for sister chromatid cohesion and for repair from sister chromatids (Mayer et al., 2004; Xu et al., 2004). We have previously shown that γH2A is also associated with stalled replication forks (Cobb et al. 2005), and since it is required at DSBs for the recruitment of cohesin (see above) it is tempting to speculate that γH2A, together with Tof1 and Csm3, may be important for maintaining replication fork integrity after replication fork stalling, by enabling appropriate recombination from the replicated sister chromatid. Cohesin loading at DSBs was also shown to depend upon a related pair of coiled-coil proteins, Smc5 and Smc6 (Potts et al., 2006). Smc5/6 complexes can be found close to rDNA repeats and at telomeres of normally growing yeast cells, as well as at DSBs and collapsed replication forks (Lindroos et al., 2006; Torres-Rosell et al., 2005). Furthermore, replication is delayed in *smc5* and *smc6* mutants, particularly at the rDNA locus (Torres-Rosell et al., 2007). In *S. pombe*, Smc5/6 is similarly required for the repair of collapsed replication forks and has functions that are both dependent on and independent of replication. Smc6 is not required for the recruitment of recombination proteins, but for effective resolution of intermediates in the homologous recombination process. When Smc6 function is compromised, the resulting recombination-dependent DNA-intermediates accumulate after a release from replication arrest and are not recognized by the G2/M checkpoint (Ampatzidou et al., 2006). This repair pathway might be particularly important in the rDNA because of its repeat structure, since excision of rDNA circles causes aging in yeast (Sinclair and Guarente, 1997). Interestingly, for fission yeast it has been shown that the intra-S-phase checkpoint separates replication and recombination temporally. Perturbing this system can cause a dramatic collapse of the replication fork (Meister et al., 2005). Therefore, the interplay between checkpoint function and recombination must be tightly regulated. It is an intriguing possibility that γH2A is important for regulating replication fork stability in the rDNA by recruiting Smc5 and Smc6 as well as cohesin to checkpoint-blind replication fork structures.

4.5.2 Is γH2A a marker of telomere elongation?

In the current study we detected substantial levels of γH2A at yeast telomeres during an unperturbed cell cycle (see Figure 4.3), a finding that has not previously been reported. Mammalian γH2AX had been previously associated with senescent telomeres, which activate a checkpoint response, but not with telomeres of normal length. Telomeric shortening in mammals provokes a DNA damage response, which entails the recruitment and activation of checkpoint proteins as well as formation of γH2AX foci as markers of senescent telomeres (d'Adda di Fagagna et al., 2003; Hao et al., 2004). There are numerous reasons why γH2AX has not been observed at mammalian telomeres unless they are senescent. First, unlike yeast telomeres, human telomeres form a particular higher order chromatin structure, the T-loop, which protects the 3' overhang (de Lange, 2002). Moreover, the DNA damage response appears to be repressed by POT1, which targets the ATR pathway, and by TRF2, which inhibits ATM (Denchi and de Lange, 2007). Nonetheless, components of the DNA damage response, as well as recombination, are required to form a functional post-replicative T-looped telomere in mammalian cells (Verdun and Karlseder, 2006). To our knowledge, this T-loop structure does not occur in yeast. Normal yeast telomeres may resemble DSBs more closely than mammalian telomeres. It is thought that short yeast telomeres are recognized as DSBs during their replication (Viscardi et al., 2007), even though induction of a single short telomere does not elicit a checkpoint response (Sabourin et al., 2007).

Recently, weak γH2AX signals were reported in proliferating human cells, but not in hTERT-immortalized cells, indicating that the authors were detecting a senescent cell fraction of a proliferating cell culture (Meier et al., 2007). Consistent with this, these authors observed the highest γH2AX levels at the shortest telomeres of senescent cells. Short telomeres also induce a DNA damage response in budding yeast (IJpma and Greider, 2003), and thus "being short" does influence γH2A levels at telomeres, even in yeast.

DNA replication at yeast telomeres occurs in mid/late S phase of the cell cycle (Raghuraman et al., 2001) and, although replication is initiated at chromosomal origins, it is completed by the elongation of the distal $TG_{1\text{-}3}$ repeat by telomerase. This elongation occurs in late S and G2 phases of the cell cycle (Diede and Gottschling, 1999; Marcand et al., 2000). Tel1 and Mec1 are recruited to the telomeres at specific

times in the cell cycle and, furthermore, Tel1 and Mec1 function in a mutually exclusive manner. Tel1 is particularly important for the recruitment of telomerase (Goudsouzian et al., 2006; Takata et al., 2004; Tseng et al., 2006). Furthermore, it has been shown that telomerase, as well as Tel1, preferentially associate with short telomeres (Sabourin et al., 2007).

We examined γH2A levels in *tel1*- and *mec1*-mutant strains, and found a significant reduction in the *tel1*-mutant strain. Since Tel1, and not Mec1, is the major kinase involved in telomere elongation in a normal situation, these results indicate that γH2A might be linked to, or at least coincide with, telomere elongation by telomerase. Along this line, we note that in budding yeast the recruitment of the MRX complex occurs in late S phase (Takata et al., 2005), particularly where there are short telomeres (Viscardi et al., 2007). Since both γH2A and MRX are also part of the DNA damage response at DSBs, this could also be a common phenomenon for telomeres.

It remains unclear whether all telomeres in a given yeast cell bear H2A phosphorylation, or if only a fraction of telomeres gets highly phosphorylated.

If telomerase action is linked to γH2A phosphorylation in S phase, then only a fraction of telomeres would be modified, since telomerase is regulated by a switch between extendible and non-extendible telomerase states, and telomerase has an increased preference for shorter telomeres (Teixeira et al., 2004). One indication that this would indeed be the case is that we did not observe complete co-localization between Sir proteins which bind all telomeres and γH2A (see Figure 4.2d). Moreover, telomere uncapping in a *cdc13*-1 temperature-sensitive allele dramatically increased nuclear γH2A levels (see Supplemental Figure 4.2), indicating that H2A phosphorylation caused by normal cell cycle progression and uncapping/senescence are additive events.

We decided to address this question by looking at γH2A levels during elongation of a critically short telomere using a system developed by the Gilson laboratory (see Figure 4.4c). We observed that γH2A levels at a rapidly shortened telomere, which has a higher chance of getting elongated, are nearly double those found on a telomere of normal TG_{1-3} repeat length. This result clearly demonstrates that telomere elongation is a positive regulator of γH2A levels at yeast telomeres. It would be interesting to examine whether or not this feature is conserved throughout evolution.

As Figure 4.3e shows, only in *mec1 tel1* double mutants is telomeric γH2A lost, while in the *tel1* mutant they are reduced by half. Having determined that telomere elongation positively affects γH2A levels, and having attributed this to the function of Tel1 kinase, why then should Mec1 contribute to γH2A phosphorylation?

We concluded previously that, for the γH2A foci in the rDNA locus, γH2A becomes phosphorylated in response to endogenous DNA damage. We observed that γH2A can be associated with chromosomal loci, which are known to be covered by silent chromatin, containing the SIR complex (Pryde and Louis, 1999). And indeed we monitored the dependence of γH2A on SIR-loading (see Supplemental Figure 4.5). Telomeric heterochromatin boundaries require NuA4-dependent acetylation of the histone H2A isoform Htz1 to restrict silent chromatin at those boundaries (Babiarz et al., 2006). From these data we deduce a possible anti-correlation between γH2A and Htz1 at telomeric/sub-telomeric chromatin. γH2A and Htz1 have already been previously linked in a model, indicating exchange of both isoforms during repair of DSBs by the chromatin remodeling factor SWR1 (van Attikum and Gasser, 2005).

Besides the occurrence of γH2A at telomeres throughout the cell cycle, we observed a general increase in γH2A levels during S phase (Figure 4.2a). Consistent with our previous finding that the amount of γH2A in the whole nucleus, as well as in the rDNA, increases during S phase, we suspect that telomeric γH2A may also arise from endogenous DNA damage created during replication. Telomeres are known to be hyper-recombinogenic. It is possible that telomeres, like the rDNA, provide obstacles to the replication fork due to the presence of SIR proteins and the non-nucleosomal telosome structure (Ivessa et al., 2003; Ivessa et al., 2002). Indeed, we also observed high γH2A levels in *HML* and *HMR* (data not shown). Co-incidence with Smc5 and Smc6 (see previous part of Discussion) indicates that, at least in part, similar repair processes might occur at those heterochromatic loci and correlate with histone H2A phosphorylation.

4.5.3 What is the function of γH2A at telomeres?

Smith and coworkers proposed a model for telomerase regulation that entails a shift in structure through the cell cycle (Smith et al., 2003). According to this model, telomeric chromatin consists of distinct protein complexes at different stages of the cell cycle, including a cycle of association of Rap1 versus Rif1 or Rif2, which in turn

determine accessibility of the chromosome end for telomerase (Smith et al., 2003). Since our observations link γH2A to telomeric elongation, γH2A might also influence this aspect of telomeric chromatin.

It was previously proposed by Downs and coworkers that γH2A affects nucleosomal structure (Downs et al., 2000), but recent work in budding yeast and mammalian cells argues against a direct impact of γH2A/γH2AX on chromatin structure (Fink et al., 2007; Kruhlak et al., 2006). γH2A might instead serve as a histone mark for the recruitment repair factors, rather than directly influencing chromatin structure. An intriguing possibility is that γH2A at stalled or collapsed replication forks in the rDNA, as well as at telomeres, is also important for recruiting the INO80 complex in the same way as it is at DSBs (Downs et al., 2004; Morrison et al., 2004);(van Attikum et al., 2004). INO80 complex mutants are very sensitive to HU (van Attikum et al., 2004), and the Arp8 component of the INO80 complex shows synthetic genetic defects with DNA replication checkpoint genes (Pan et al., 2006).

A correlation exists between the delocalization of telomeres from the nuclear periphery and a reduction in their length in *tel1*-mutant strains (Hediger et al., 2006). Furthermore, Berthiau and coworkers (Berthiau et al., 2006) showed that the absence of Tel1 induces a change in the structure of sub-telomeric chromatin. We have not observed any difference in telomere length between $h2a^{S129*}$-mutant and WT strains (see Supplemental Figure 4.3b). However, the fact that we observed an S-phase specific anchoring defect in the $h2a^{S129*}$ mutant (Figure 4.5) indicates that anchoring is more easily affected by this histone modification than telomere length regulation. The molecular details on how telomeric γH2A affects anchoring in S phase are unknown, but it does act epistatically to SIR proteins. The partial dependence of γH2A levels upon the SIR complex, and equidistant spreading, might argue for this possibility, although we cannot exclude the fact that γH2A mediates telomeric anchoring in a third independent pathway (Figure 4.5d). Even in mammals, γH2AX influences the nuclear positioning of telomeres, yet in a different manner. Murine H2AX regulates meiotic telomere clustering during prophase I (Fernandez-Capetillo et al., 2003).

We and others have shown (T. Kitada and M. Grunstein, personal communication) that γH2A correlates with SIR spreading at telomeres. Therefore it was an obvious question to address: is telomeric silencing affected in an $h2a^{S129*}$-mutant strain (see Supplemental Figure 4.4)? We found only a slight reduction in silencing in the strain

with a nonphosphorylatable H2A. This result is in agreement with data from Wyatt and coworkers (Wyatt et al., 2003), indicating that phosphorylation of histone H2A serine 129 plays a small role in telomeric silencing. This small effect, however, is amplified when it is combined with phosphorylation of histone H2A threonine 126.
In this context we note that not only is serine 129 of H2A phosphorylated in response to DNA damage, but also serine 122 and threonine 126. These sites, in the C-terminal part of H2A, show a complex pattern of phosphorylation in response to different kinds of DNA damage (Harvey et al., 2005; Moore et al., 2006; Wyatt et al., 2003). Therefore, the function of γH2A may be masked because it is embedded in a complex pattern of histone modifications. These authors also postulate a dual role of H2A in DNA damage and telomere position effect. In the next part, we will discuss what other possible roles γH2A has, besides DSB repair.

4.5.4 A function of γH2A beyond telomeres and DSBs?

It was generally believed that the occurrence of mammalian γH2AX foci is strictly linked to the occurrence of DSBs (Takahashi and Ohnishi, 2005), even in the case of replication arrest. In a previous report, we provided evidence that γH2A also occurs at replication forks stalled by HU in a Mec1-dependent manner (Cobb et al., 2005). Here we were able to show that high levels of γH2A occur in the rDNA repeats and at telomeres. We argued that this may also be due to endogenous replicative DNA damage.
The question that future work will have to address is whether the presence of γH2A reflects a role for this modification in DNA repair. γH2A may have independent functions in addition to telomere anchoring, such as influencing gene expression. There are several links between telomeric chromatin and repair.
First, upon DNA damage, KU and SIR proteins become re-localized to DSBs, and induce a slight drop in telomeric silencing (Martin et al., 1999; McAinsh et al., 1999; Mills et al., 1999). Second, the efficiency of DSB repair is particularly high close to telomeres (Ricchetti et al., 2003), and thus depends upon anchoring of the telomere and interaction with the nuclear pore complex (Taddei and Gasser, 2006; Therizols et al., 2006). This cross-talk between telomeres and zones of DNA damage may be mediated by γH2A.

Short yeast telomeres are recognized by the checkpoint as DNA damage, but do not reach the threshold for cell-cycle arrest (Sabourin et al., 2007; Viscardi et al., 2007). Telomeres were thought to be a storage place for DNA damage response factors in an unchallenged situation (Martin et al., 1999). It will be interesting to address how γH2A might influence such a balance, and it opens up the possibility that high levels of γH2A may be responsible for the higher repair efficiency in sub-telomeric regions by facilitating the recruitment of repair factors to the site of damage.

It has been shown that dephosphorylation of γH2A by a complex containing the phosphatase Pph3 regulates recovery from DNA damage (Keogh et al., 2006). This report further demonstrated that γH2A needs to be evicted by chromatin remodelers before dephosphorylation. γH2A eviction at a DSB depends on the chromatin remodeling complex INO80 (Van Attikum et al., 2007). These observations make it clear that γH2A signaling in response to DSBs is a dynamic process involving phosphorylation by Mec1 and Tel1, and eviction by chromatin remodelers, followed by dephosphorylation. We observed a strong increase in nuclear γH2A levels through S phase. These higher levels stay until anaphase, and then suddenly decrease. It will be important to determine which factors regulate the dynamics of H2A phosphorylation at telomeres, as well as determining how this influences telomeric anchoring, telomere metabolism, and sub-telomeric gene expression.

Note added in proof:

The presence of γH2A at natural yeast telomeres was confirmed during the preparation of this manuscript by Kim et al. (2007).

4.6 Acknowledgements

The authors acknowledge support from the Novartis Research Foundation, the Swiss Cancer League, the Swiss National Science Foundation, European RTN Checkpoints and Cancer, and fellowships from EMBO and the Human Frontiers Science Program to HvA. We thank colleagues from the FMI Microscope and Imaging Department, as well as the Protein Synthesis and Monoclonal Antibodies Facilities for technical help. We thank William Bonner for yeast γH2AX antibody, and E. Gilson, S. Marcand, S. Jackson, J. Lingner, D. Shore, and many members of the Gasser laboratory for yeast strains, and M. Tsai-Pflugfelder and K. Bystricky for recombinant histones. We thank Oliver Fritsch and Primo Schär for communicating rDNA primer sequences.

T. Schleker would like to thank the members of his thesis committee Primo Schär, Dirk Schübeler and Maria Pia Longhese for helpful suggestions.

4.7 References

Ampatzidou, E., A. Irmisch, M.J. O'Connell, and J.M. Murray. 2006. Smc5/6 is required for repair at collapsed replication forks. *Mol Cell Biol*. 26:9387-401.

Ataian, Y., and J.E. Krebs. 2006. Five repair pathways in one context: chromatin modification during DNA repair. *Biochem Cell Biol*. 84:490-504.

Azvolinsky, A., S. Dunaway, J.Z. Torres, J.B. Bessler, and V.A. Zakian. 2006. The S. cerevisiae Rrm3p DNA helicase moves with the replication fork and affects replication of all yeast chromosomes. *Genes Dev*. 20:3104-16.

Babiarz, J.E., J.E. Halley, and J. Rine. 2006. Telomeric heterochromatin boundaries require NuA4-dependent acetylation of histone variant H2A.Z in Saccharomyces cerevisiae. *Genes Dev*. 20:700-10.

Berthiau, A.S., K. Yankulov, A. Bah, E. Revardel, P. Luciano, R.J. Wellinger, V. Geli, and E. Gilson. 2006. Subtelomeric proteins negatively regulate telomere elongation in budding yeast. *Embo J*. 25:846-56.

Bystricky, K., T. Laroche, G. van Houwe, M. Blaszczyk, and S.M. Gasser. 2005. Chromosome looping in yeast: telomere pairing and coordinated movement reflect anchoring efficiency and territorial organization. *J Cell Biol*. 168:375-87.

Calzada, A., B. Hodgson, M. Kanemaki, A. Bueno, and K. Labib. 2005. Molecular anatomy and regulation of a stable replisome at a paused eukaryotic DNA replication fork. *Genes Dev*. 19:1905-19.

Cha, R.S., and N. Kleckner. 2002. ATR homolog Mec1 promotes fork progression, thus averting breaks in replication slow zones. *Science*. 297:602-6.

Chan, S.W., J. Chang, J. Prescott, and E.H. Blackburn. 2001. Altering telomere structure allows telomerase to act in yeast lacking ATM kinases. *Curr Biol*. 11:1240-50.

Cobb, J.A., L. Bjergbaek, K. Shimada, C. Frei, and S.M. Gasser. 2003. DNA polymerase stabilization at stalled replication forks requires Mec1 and the RecQ helicase Sgs1. *Embo J*. 22:4325-36.

Cobb, J.A., T. Schleker, V. Rojas, L. Bjergbaek, J.A. Tercero, and S.M. Gasser. 2005. Replisome instability, fork collapse, and gross chromosomal rearrangements arise synergistically from Mec1 kinase and RecQ helicase mutations. *Genes Dev*. 19:3055-69.

d'Adda di Fagagna, F., P.M. Reaper, L. Clay-Farrace, H. Fiegler, P. Carr, T. Von Zglinicki, G. Saretzki, N.P. Carter, and S.P. Jackson. 2003. A DNA damage checkpoint response in telomere-initiated senescence. *Nature*. 426:194-8.

de Lange, T. 2002. Protection of mammalian telomeres. *Oncogene*. 21:532-40.

Denchi, E.L., and T. de Lange. 2007. Protection of telomeres through independent control of ATM and ATR by TRF2 and POT1. *Nature*.

Diede, S.J., and D.E. Gottschling. 1999. Telomerase-mediated telomere addition in vivo requires DNA primase and DNA polymerases alpha and delta. *Cell*. 99:723-33.

Downs, J.A., S. Allard, O. Jobin-Robitaille, A. Javaheri, A. Auger, N. Bouchard, S.J. Kron, S.P. Jackson, and J. Cote. 2004. Binding of Chromatin-Modifying Activities to Phosphorylated Histone H2A at DNA Damage Sites. *Mol Cell*. 16:979-90.

Downs, J.A., N.F. Lowndes, and S.P. Jackson. 2000. A role for Saccharomyces cerevisiae histone H2A in DNA repair. *Nature*. 408:1001-4.

Fernandez-Capetillo, O., B. Liebe, H. Scherthan, and A. Nussenzweig. 2003. H2AX regulates meiotic telomere clustering. *J Cell Biol*. 163:15-20.

Fink, M., D. Imholz, and F. Thoma. 2007. Contribution of the Serine 129 of Histone H2A to Chromatin Structure. *Mol Cell Biol*.

Fritze, C.E., K. Verschueren, R. Strich, and R.E. Esposito. 1997. Direct evidence for SIR2 modulation of chromatin structure in yeast rDNA. *EMBO JOURNAL*. 16:6495-6509.

Furuta, T., H. Takemura, Z.Y. Liao, G.J. Aune, C. Redon, O.A. Sedelnikova, D.R. Pilch, E.P. Rogakou, A. Celeste, H.T. Chen, A. Nussenzweig, M.I. Aladjem, W.M. Bonner, and Y. Pommier. 2003. Phosphorylation of histone H2AX and activation of Mre11, Rad50, and Nbs1 in response to replication-dependent DNA double-strand breaks induced by mammalian DNA topoisomerase I cleavage complexes. *J Biol Chem*. 278:20303-12.

Goudsouzian, L.K., C.T. Tuzon, and V.A. Zakian. 2006. S. cerevisiae Tel1p and Mre11p are required for normal levels of Est1p and Est2p telomere association. *Mol Cell*. 24:603-10.

Greenwell, P.W., S.L. Kronmal, S.E. Porter, J. Gassenhuber, B. Obermaier, and T.D. Petes. 1995. TEL1, a gene involved in controlling telomere length in S. cerevisiae, is homologous to the human ataxia telangiectasia gene. *Cell*. 82:823-9.

Hao, L.Y., M.A. Strong, and C.W. Greider. 2004. Phosphorylation of H2AX at short telomeres in T cells and fibroblasts. *J Biol Chem*. 279:45148-54.

Harvey, A.C., S.P. Jackson, and J.A. Downs. 2005. Saccharomyces cerevisiae histone H2A Ser122 facilitates DNA repair. *Genetics*. 170:543-53.

Hecht, A., S. Strahl-Bolsinger, and M. Grunstein. 1996. Spreading of transcriptional repressor SIR3 from telomeric heterochromatin. *Nature*. 383:92-6.

Hediger, F., A.S. Berthiau, G. van Houwe, E. Gilson, and S.M. Gasser. 2006. Subtelomeric factors antagonize telomere anchoring and Tel1-independent telomere length regulation. *Embo J*. 25:857-67.

Hediger, F., F.R. Neumann, G. Van Houwe, K. Dubrana, and S.M. Gasser. 2002. Live imaging of telomeres: yKu and Sir proteins define redundant telomere-anchoring pathways in yeast. *Curr Biol*. 12:2076-89.

Heun, P., T. Laroche, M.K. Raghuraman, and S.M. Gasser. 2001. The positioning and dynamics of origins of replication in the budding yeast nucleus. *J Cell Biol*. 152:385-400.

Huang, J., I.L. Brito, J. Villen, S.P. Gygi, A. Amon, and D. Moazed. 2006. Inhibition of homologous recombination by a cohesin-associated clamp complex recruited to the rDNA recombination enhancer. *Genes Dev*. 20:2887-901.

IJpma, A.S., and C.W. Greider. 2003. Short telomeres induce a DNA damage response in Saccharomyces cerevisiae. *Mol Biol Cell*. 14:987-1001.

Ivanov, E.L., V.G. Korolev, and F. Fabre. 1992. XRS2, a DNA repair gene of Saccharomyces cerevisiae, is needed for meiotic recombination. *Genetics*. 132:651-64.

Ivessa, A.S., B.A. Lenzmeier, J.B. Bessler, L.K. Goudsouzian, S.L. Schnakenberg, and V.A. Zakian. 2003. The Saccharomyces cerevisiae helicase Rrm3p facilitates replication past nonhistone protein-DNA complexes. *Mol Cell*. 12:1525-36.

Ivessa, A.S., J.Q. Zhou, V.P. Schulz, E.K. Monson, and V.A. Zakian. 2002. Saccharomyces Rrm3p, a 5' to 3' DNA helicase that promotes replication fork

progression through telomeric and subtelomeric DNA. *Genes Dev*. 16:1383-96.

Ivessa, A.S., J.Q. Zhou, and V.A. Zakian. 2000. The Saccharomyces Pif1p DNA helicase and the highly related Rrm3p have opposite effects on replication fork progression in ribosomal DNA. *Cell*. 100:479-89.

Javaheri, A., R. Wysocki, O. Jobin-Robitaille, M. Altaf, J. Cote, and S.J. Kron. 2006. Yeast G1 DNA damage checkpoint regulation by H2A phosphorylation is independent of chromatin remodeling. *Proc Natl Acad Sci U S A*. 103:13771-6.

Kaliraman, V., J.R. Mullen, W.M. Fricke, S.A. Bastin-Shanower, and S.J. Brill. 2001. Functional overlap between Sgs1-Top3 and the Mms4-Mus81 endonuclease. *Genes Dev*. 15:2730-40.

Katou, Y., Y. Kanoh, M. Bando, H. Noguchi, H. Tanaka, T. Ashikari, K. Sugimoto, and K. Shirahige. 2003. S-phase checkpoint proteins Tof1 and Mrc1 form a stable replication-pausing complex. *Nature*. 424:1078-83.

Keogh, M.C., J.A. Kim, M. Downey, J. Fillingham, D. Chowdhury, J.C. Harrison, M. Onishi, N. Datta, S. Galicia, A. Emili, J. Lieberman, X. Shen, S. Buratowski, J.E. Haber, D. Durocher, J.F. Greenblatt, and N.J. Krogan. 2006. A phosphatase complex that dephosphorylates gammaH2AX regulates DNA damage checkpoint recovery. *Nature*. 439:497-501.

Kim, J.A., M. Kruhlak, F. Dotiwala, A. Nussenzweig, and J.E. Haber. 2007. Heterochromatin is refractory to gamma-H2AX modification in yeast and mammals. *J Cell Biol*. 178:209-18.

Klein, F., T. Laroche, M.E. Cardenas, J.F. Hofmann, D. Schweizer, and S.M. Gasser. 1992. Localization of RAP1 and topoisomerase II in nuclei and meiotic chromosomes of yeast. *J Cell Biol*. 117:935-48.

Kruhlak, M.J., A. Celeste, G. Dellaire, O. Fernandez-Capetillo, W.G. Muller, J.G. McNally, D.P. Bazett-Jones, and A. Nussenzweig. 2006. Changes in chromatin structure and mobility in living cells at sites of DNA double-strand breaks. *J Cell Biol*. 172:823-34.

Lambert, S., B. Froget, and A.M. Carr. 2007. Arrested replication fork processing: Interplay between checkpoints and recombination. *DNA Repair (Amst)*.

Linardopoulou, E.V., E.M. Williams, Y. Fan, C. Friedman, J.M. Young, and B.J. Trask. 2005. Human subtelomeres are hot spots of interchromosomal recombination and segmental duplication. *Nature*. 437:94-100.

Lindroos, H.B., L. Strom, T. Itoh, Y. Katou, K. Shirahige, and C. Sjogren. 2006. Chromosomal association of the Smc5/6 complex reveals that it functions in differently regulated pathways. *Mol Cell*. 22:755-67.

Longtine, M.S., A. McKenzie, 3rd, D.J. Demarini, N.G. Shah, A. Wach, A. Brachat, P. Philippsen, and J.R. Pringle. 1998. Additional modules for versatile and economical PCR-based gene deletion and modification in Saccharomyces cerevisiae. *Yeast*. 14:953-61.

Luger, K., T.J. Rechsteiner, A.J. Flaus, M.M. Waye, and T.J. Richmond. 1997. Characterization of nucleosome core particles containing histone proteins made in bacteria. *J Mol Biol*. 272:301-11.

Marcand, S., V. Brevet, and E. Gilson. 1999. Progressive cis-inhibition of telomerase upon telomere elongation. *Embo J*. 18:3509-19.

Marcand, S., V. Brevet, C. Mann, and E. Gilson. 2000. Cell cycle restriction of telomere elongation. *Curr Biol*. 10:487-90.

Martin, S.G., T. Laroche, N. Suka, M. Grunstein, and S.M. Gasser. 1999. Relocalization of telomeric Ku and SIR proteins in response to DNA strand breaks in yeast. *Cell*. 97:621-33.

Mayer, M.L., I. Pot, M. Chang, H. Xu, V. Aneliunas, T. Kwok, R. Newitt, R. Aebersold, C. Boone, G.W. Brown, and P. Hieter. 2004. Identification of protein complexes required for efficient sister chromatid cohesion. *Mol Biol Cell*. 15:1736-45.

McAinsh, A.D., S. Scott-Drew, J.A. Murray, and S.P. Jackson. 1999. DNA damage triggers disruption of telomeric silencing and Mec1p-dependent relocation of Sir3p. *Curr Biol*. 9:963-6.

McManus, K.J., and M.J. Hendzel. 2005. ATM-dependent DNA damage-independent mitotic phosphorylation of H2AX in normally growing mammalian cells. *Mol Biol Cell*. 16:5013-25.

Meier, A., H. Fiegler, P. Munoz, P. Ellis, D. Rigler, C. Langford, M.A. Blasco, N. Carter, and S.P. Jackson. 2007. Spreading of mammalian DNA-damage response factors studied by ChIP-chip at damaged telomeres. *Embo J*.

Meister, P., A. Taddei, L. Vernis, M. Poidevin, S.M. Gasser, and G. Baldacci. 2005. Temporal separation of replication and recombination requires the intra-S checkpoint. *J Cell Biol*. 168:537-44.

Mills, K.D., D.A. Sinclair, and L. Guarente. 1999. MEC1-dependent redistribution of the Sir3 silencing protein from telomeres to DNA double-strand breaks. *Cell*. 97:609-20.

Moore, J.D., O. Yazgan, Y. Ataian, and J.E. Krebs. 2006. Diverse roles for histone H2A modifications in DNA damage response pathways in yeast. *Genetics*.

Morrison, A.J., J. Highland, N.J. Krogan, A. Arbel-Eden, J.F. Greenblatt, J.E. Haber, and X. Shen. 2004. INO80 and gamma-H2AX interaction links ATP-dependent chromatin remodeling to DNA damage repair. *Cell*. 119:767-75.

Muller, M.T., W.P. Pfund, V.B. Mehta, and D.K. Trask. 1985. Eukaryotic type I topoisomerase is enriched in the nucleolus and catalytically active on ribosomal DNA. *Embo J*. 4:1237-43.

Palladino, F., T. Laroche, E. Gilson, A. Axelrod, L. Pillus, and S.M. Gasser. 1993. SIR3 and SIR4 proteins are required for the positioning and integrity of yeast telomeres. *Cell*. 75:543-55.

Pan, X., P. Ye, D.S. Yuan, X. Wang, J.S. Bader, and J.D. Boeke. 2006. A DNA integrity network in the yeast Saccharomyces cerevisiae. *Cell*. 124:1069-81.

Pommier, Y. 2006. Topoisomerase I inhibitors: camptothecins and beyond. *Nat Rev Cancer*. 6:789-802.

Potts, P.R., M.H. Porteus, and H. Yu. 2006. Human SMC5/6 complex promotes sister chromatid homologous recombination by recruiting the SMC1/3 cohesin complex to double-strand breaks. *Embo J*. 25:3377-88.

Pryde, F.E., and E.J. Louis. 1999. Limitations of silencing at native yeast telomeres. *Embo J*. 18:2538-50.

Raghuraman, M.K., E.A. Winzeler, D. Collingwood, S. Hunt, L. Wodicka, A. Conway, D.J. Lockhart, R.W. Davis, B.J. Brewer, and W.L. Fangman. 2001. Replication Dynamics of the Yeast Genome. *Science*. 294:115-121.

Redon, C., D.R. Pilch, and W.M. Bonner. 2006. Genetic analysis of Saccharomyces cerevisiae H2A serine 129 mutant suggests a functional relationship between H2A and the sister-chromatid cohesion partners Csm3-Tof1 for the repair of topoisomerase I-induced DNA damage. *Genetics*. 172:67-76.

Redon, C., D.R. Pilch, E.P. Rogakou, A.H. Orr, N.F. Lowndes, and W.M. Bonner. 2003. Yeast histone 2A serine 129 is essential for the efficient repair of checkpoint-blind DNA damage. *EMBO Rep*. 4:678-84.

Ricchetti, M., B. Dujon, and C. Fairhead. 2003. Distance from the chromosome end determines the efficiency of double strand break repair in subtelomeres of haploid yeast. *J Mol Biol*. 328:847-62.

Ritchie, K.B., J.C. Mallory, and T.D. Petes. 1999. Interactions of TLC1 (which encodes the RNA subunit of telomerase), TEL1, and MEC1 in regulating telomere length in the yeast Saccharomyces cerevisiae. *Mol Cell Biol*. 19:6065-75.

Rogakou, E.P., C. Boon, C. Redon, and W.M. Bonner. 1999. Megabase chromatin domains involved in DNA double-strand breaks in vivo. *J Cell Biol*. 146:905-16.

Rudd, M.K., C. Friedman, S.S. Parghi, E.V. Linardopoulou, L. Hsu, and B.J. Trask. 2007. Elevated rates of sister chromatid exchange at chromosome ends. *PLoS Genet*. 3:e32.

Sabourin, M., C.T. Tuzon, and V.A. Zakian. 2007. Telomerase and Tel1p Preferentially Associate with Short Telomeres in S. cerevisiae. *Mol Cell*.

Saffer, L.D., and O.L. Miller, Jr. 1986. Electron microscopic study of Saccharomyces cerevisiae rDNA chromatin replication. *Mol Cell Biol*. 6:1148-57.

Shen, X., R. Ranallo, E. Choi, and C. Wu. 2003. Involvement of actin-related proteins in ATP-dependent chromatin remodeling. *Mol Cell*. 12:147-55.

Shroff, R., A. Arbel-Eden, D. Pilch, G. Ira, W.M. Bonner, J.H. Petrini, J.E. Haber, and M. Lichten. 2004. Distribution and dynamics of chromatin modification induced by a defined DNA double-strand break. *Curr Biol*. 14:1703-11.

Sinclair, D.A., and L. Guarente. 1997. Extrachromosomal rDNA circles--a cause of aging in yeast. *Cell*. 91:1033-42.

Smith, C.D., D.L. Smith, J.L. DeRisi, and E.H. Blackburn. 2003. Telomeric protein distributions and remodeling through the cell cycle in Saccharomyces cerevisiae. *Mol Biol Cell*. 14:556-70.

Strahl-Bolsinger, S., A. Hecht, K. Luo, and M. Grunstein. 1997. SIR2 and SIR4 interactions differ in core and extended telomeric heterochromatin in yeast. *Genes Dev*. 11:83-93.

Strom, L., H.B. Lindroos, K. Shirahige, and C. Sjogren. 2004. Postreplicative recruitment of cohesin to double-strand breaks is required for DNA repair. *Mol Cell*. 16:1003-15.

Taddei, A., and S.M. Gasser. 2006. Repairing subtelomeric DSBs at the nuclear periphery. *Trends Cell Biol*. 16:225-8.

Taddei, A., F. Hediger, F.R. Neumann, C. Bauer, and S.M. Gasser. 2004. Separation of silencing from perinuclear anchoring functions in yeast Ku80, Sir4 and Esc1 proteins. *EMBO J*. 23:1301-1312.

Takahashi, A., and T. Ohnishi. 2005. Does gammaH2AX foci formation depend on the presence of DNA double strand breaks? *Cancer Lett*. 229:171-9.

Takata, H., Y. Kanoh, N. Gunge, K. Shirahige, and A. Matsuura. 2004. Reciprocal association of the budding yeast ATM-related proteins Tel1 and Mec1 with telomeres in vivo. *Mol Cell*. 14:515-22.

Takata, H., Y. Tanaka, and A. Matsuura. 2005. Late S phase-specific recruitment of Mre11 complex triggers hierarchical assembly of telomere replication proteins in Saccharomyces cerevisiae. *Mol Cell*. 17:573-83.

Takeuchi, Y., T. Horiuchi, and T. Kobayashi. 2003. Transcription-dependent recombination and the role of fork collision in yeast rDNA. *Genes Dev*. 17:1497-506.

Teixeira, M.T., M. Arneric, P. Sperisen, and J. Lingner. 2004. Telomere length homeostasis is achieved via a switch between telomerase- extendible and -nonextendible states. *Cell*. 117:323-35.

Teixeira, M.T., S. Siniossoglou, S. Podtelejnikov, J.C. Benichou, M. Mann, B. Dujon, E. Hurt, and E. Fabre. 1997. Two functionally distinct domains generated by in vivo cleavage of Nup145p: a novel biogenesis pathway for nucleoporins. *Embo J*. 16:5086-97.

Therizols, P., C. Fairhead, G.G. Cabal, A. Genovesio, J.C. Olivo-Marin, B. Dujon, and E. Fabre. 2006. Telomere tethering at the nuclear periphery is essential for efficient DNA double strand break repair in subtelomeric region. *J Cell Biol*. 172:189-99.

Toh, G.W., M. O'Shaughnessy A, S. Jimeno, I.M. Dobbie, M. Grenon, S. Maffini, A. O'Rorke, and N.F. Lowndes. 2006. Histone H2A phosphorylation and H3 methylation are required for a novel Rad9 DSB repair function following checkpoint activation. *DNA Repair (Amst)*. 5:693-703.

Torres-Rosell, J., G. De Piccoli, V. Cordon-Preciado, S. Farmer, A. Jarmuz, F. Machin, P. Pasero, M. Lisby, J.E. Haber, and L. Aragon. 2007. Anaphase onset before complete DNA replication with intact checkpoint responses. *Science*. 315:1411-5.

Torres-Rosell, J., F. Machin, S. Farmer, A. Jarmuz, T. Eydmann, J.Z. Dalgaard, and L. Aragon. 2005. SMC5 and SMC6 genes are required for the segregation of repetitive chromosome regions. *Nat Cell Biol*. 7:412-9.

Torres, J.Z., J.B. Bessler, and V.A. Zakian. 2004. Local chromatin structure at the ribosomal DNA causes replication fork pausing and genome instability in the absence of the S. cerevisiae DNA helicase Rrm3p. *Genes Dev*. 18:498-503.

Tourriere, H., G. Versini, V. Cordon-Preciado, C. Alabert, and P. Pasero. 2005. Mrc1 and Tof1 promote replication fork progression and recovery independently of Rad53. *Mol Cell*. 19:699-706.

Tseng, S.F., J.J. Lin, and S.C. Teng. 2006. The telomerase-recruitment domain of the telomere binding protein Cdc13 is regulated by Mec1p/Tel1p-dependent phosphorylation. *Nucleic Acids Res*. 34:6327-36.

Unal, E., A. Arbel-Eden, U. Sattler, R. Shroff, M. Lichten, J.E. Haber, and D. Koshland. 2004. DNA damage response pathway uses histone modification to assemble a double-strand break-specific cohesin domain. *Mol Cell*. 16:991-1002.

Van Attikum, H., O. Fritsch, and S.M. Gasser. 2007. Distinct roles for SWR1 and INO80 chromatin remodeling complexes at chromosomal double-strand breaks. *The EMBO Journal advance online publication 30 August 2007*. doi: 10.1038/sj.emboj.760183.

van Attikum, H., O. Fritsch, B. Hohn, and S.M. Gasser. 2004. Recruitment of the INO80 Complex by H2A Phosphorylation Links ATP-Dependent Chromatin Remodeling with DNA Double-Strand Break Repair. *cell*. 119:777-788.

van Attikum, H., and S.M. Gasser. 2005. The histone code at DNA breaks: a guide to repair? *Nat Rev Mol Cell Biol*. 6:757-65.

Verdun, R.E., and J. Karlseder. 2006. The DNA damage machinery and homologous recombination pathway act consecutively to protect human telomeres. *Cell*. 127:709-20.

Versini, G., I. Comet, M. Wu, L. Hoopes, E. Schwob, and P. Pasero. 2003. The yeast Sgs1 helicase is differentially required for genomic and ribosomal DNA replication. *Embo J*. 22:1939-49.

Viscardi, V., D. Bonetti, H. Cartagena-Lirola, G. Lucchini, and M.P. Longhese. 2007. MRX-dependent DNA Damage Response to Short Telomeres. *Mol Biol Cell*. 18:3047-58.

Viscardi, V., M. Clerici, H. Cartagena-Lirola, and M.P. Longhese. 2005. Telomeres and DNA damage checkpoints. *Biochimie*. 87:613-24.

Voelkel-Meiman, K., R.L. Keil, and G.S. Roeder. 1987. Recombination-stimulating sequences in yeast ribosomal DNA correspond to sequences regulating transcription by RNA polymerase I. *Cell*. 48:1071-9.

Wach, A., A. Brachat, R. Pohlmann, and P. Philippsen. 1994. New heterologous modules for classical or PCR-based gene disruptions in Saccharomyces cerevisiae. *Yeast*. 10:1793-808.

Ward, I.M., and J. Chen. 2001. Histone H2AX is phosphorylated in an ATR-dependent manner in response to replicational stress. *J Biol Chem*. 276:47759-62.

Woods, A., T. Sherwin, R. Sasse, T.H. MacRae, A.J. Baines, and K. Gull. 1989. Definition of individual components within the cytoskeleton of Trypanosoma brucei by a library of monoclonal antibodies. *J Cell Sci*. 93 (Pt 3):491-500.

Wyatt, H.R., H. Liaw, G.R. Green, and A.J. Lustig. 2003. Multiple roles for Saccharomyces cerevisiae histone H2A in telomere position effect, Spt phenotypes and double-strand-break repair. *Genetics*. 164:47-64.

Xu, H., C. Boone, and H.L. Klein. 2004. Mrc1 is required for sister chromatid cohesion to aid in recombination repair of spontaneous damage. *Mol Cell Biol*. 24:7082-90.

Zou, L. 2007. Single- and double-stranded DNA: building a trigger of ATR-mediated DNA damage response. *Genes Dev*. 21:879-85.

4.8 Supplemental Material

4.8.1 Supplemental Table

Strain	Genotype	Origin and Background
GA-157	**MATa,** *his7, ura1*	orig. H13C1A2, 13a (Wood and Hartwell, 1982), **A364a**
GA-158	**MATalpha,** *his7, ura1*	orig. H13C1B2, 13b (Wood and Hartwell, 1982), **A364a**
GA-172	**MATa/alpha,** mating of GA-157 and GA-158	(Thomas and Rothstein, 1989), **W303-1B**
GA-180	**MATa,** *ade2*-1, *trp1*-1, *his3*-11, -15, *ura3*-1, *leu2*-3,-112, *can1*-100	(Wood and Hartwell, 1982), **A364a**
GA-181	**MATalpha,** *ade2*-1, *trp1*-1, *his3*-11, -15, *ura3*-1, *leu2*-3,-112, *can1*-100	(Thomas and Rothstein, 1989), **W303-1A**
GA-196	**MATa/alpha,** mating of GA-180 and GA-181	orig. RS862**,** (Stone et al., 1991), **W303**
GA-278	**MATa** sir3::TRP1 can1-100 in GA-180	(Thomas and Rothstein, 1989), **W303**
GA-659	**MATa/alpha** ho::LYS2 RAP1-GFP-LEU2::rap1ura3, leu2::hisG arg4	orig. AHY111, (Hayashi et al., 1998), **SK1**
GA-1020	**MATa,** *ade2*-1, *trp1*-1, *his3*-11, -15, *ura3*-1, *leu2*-3,-112, *can1*-100, *pep4*	(Cobb et al., 2003), **W303**
GA-1053	**MATalpha,** TelVII::URA3, lys2::HMLEI::ADE2 in GA-181	orig. LM11 (Maillet et al., 2001), **W303**
GA-1054	**MATalpha,** hdf1::kanMX in GA-1053	orig. LM79 (Maillet et al., 2001), **W303**
GA-1081	**MATalpha,** hml::ADE1 hmr::ADE1 ade3::GALHO ade1, leu2-3,112, lys5, trp1::hisG ura3-5	(Lee et al., 1998), **JMK179**
GA-1275	**MATa,** SIR4-13Myc-kanMX6, can1 deletion, Δade2 Δtrp1 Δcan1ade2 deletion TelVR::ADE2-TEL(+)	(Perrod et al., 2001), **W303**
GA-1461	**MATa, -**lac op and LexA binding sites (TRP1) at ARS 607 -lac I-GFP (HIS3) at his3-15, NUP49GFP as the only copy (ura-) in GA-180	(Taddei et al., 2004b), **W303**
GA-1561	**MATalpha,** lac O and LexA binding sites (TRP1) at ARS 609 -lac I-GFP (HIS3) at his3-15 in GA-181**,** NUP49GFP as the only copy (ura-)	this laboratory - P. Heun, **W303**
GA-1702	**MATa,** can1-100 pep4::LEU2 ; Sgs1-myc::HIS; sml1::KanMX6 mec1::TRP in GA-1020 J.	this laboratory - J. Cobb, **W303**
GA-1852	**MATa,** rif1::TRP1 telVIIL::URA3 in GA-180	orig. YG526 from D. Shore, **W303**
GA-1917	**MATa** ade2-1 can1-100 his3-11,15::GFP-LacI-HIS3 trp1-1 ura3-1 leu2-3,112, nup49::NUP49-GFP-URA3, TELVI-R::lacO-lexAop-TRP1-ADE2-TG	Hediger et al. 2002, **W303**
GA-1949	**MATa,** NUP49-GFP, yku70::*Ca*URA3 -lacO and LexA binding sites (TRP1) at ARS 607-lac I-GFP (HIS3) at his3-15 -NUP49GFP (ura-)	(Taddei et al., 2004b), **W303**
GA-2220	**MATalpha,** Esc1-13Myc::KanMX, ku70::HIS5,TelVII::URA3, lys2::HMLEI::ADE2	this laboratory - A. Taddei, **W303**
GA-2263	**MATa,** his3 del200, leu2 del0 met15 del0 trp1 del0 ura3 del0	this laboratory - H. Van Attikum, **JMK179**
GA-2312	**MAT alpha,** Ino80-13myc-KanMX4 sml1::TRP1 in GA-1081	orig. BY4733, Euroscarf, **S288C**
GA-2448	**MATa,** GA-1020 with *POL2*-13Myc_*KanMX6*	Bjergbaek et al. 2005, **W303**
GA-2507	**MATa,** can1-100 SGS1-13MYC-HIS3 tel1::URA3 pep4::LEU2 in GA-1020	this laboratory - L. Bjergbaek, **W303**
GA-2961	**MATalpha,** hta1-S129*/hta2-S129* in GA-181 (W303)	orig. JDY22 (Downs et al., 2000), **W303**
GA-2978	**MATalpha,** hml::ADE1 hmr::ADE1 ade3::GALHO Ino80-13myc-KanMX4 sml1::TRP1 mec1::NatMX4 tel1::URA3	this laboratory - H. Van Attikum , **JMK179**
GA-3030	**MATa/alpha,** tlc1::hphMx / TLC1 in GA-180 mated with GA-181	this laboratory - H. Schober, **W303**
GA-3285	**MATa** of GA-2961	this study, **W303**
GA-3362	**MATalpha,** rif1::TRP1, NUP49-GFP (URA FOA)	orig. from J. Lingner, **FYBL1-23D**
GA-3399	**MATa,** TelVII::URA3, lys2::HMLEI::ADE2, hta1-S129* hta2-S129*, (Cross of GA-3285 and GA-1053)	this study, **W303**
GA-3467	**MATa,** TelVII::URA3, lys2::HMLEI::ADE2, hta1-S129* hta2-S129*,(Cross of GA-3285 and GA-1053	this study, **W303**
GA-3400	**MATa/alpha,** est1::HgmRes, EST1, in GA-196	this laboratory, H. Schober, **W303**
GA-3653	**MATa/alpha,** hta1-S129*/hta2-S129*, cross between GA-2961 and GA-3285	this study, **W303**
GA-3701	**MATa/alpha,** est1::HIS/EST1 in GA-3653	this study, **W303**
GA-4089	**MATa,** LEU2-GAL10-FLP1 cir° in GA-180	orig. lev 178, Marcand, et al 1999, **W303**
GA-4090	**MATa,** telVII adh4::FRT-URA3-FRT3-tel in GA-4089	orig. lev 187, Marcand, et al 1999, **W303**
GA-4091	**MATa,** telVII adh4::FRT-URA3-[tel270]-FRT3-tel in GA-4089	orig. lev 189, Marcand, et al 1999, **W303**
GA-4092	**MATa,** telVII adh4::FRT-URA3-[tel270]x2-FRT3-tel in GA-4089	orig. lev 222, Marcand, et al 1999, **W303**
GA-4093	**MATa,** telVII adh4::FRT-URA3-[tel270]x3-FRT3-tel in GA-4089	orig. lev 220, Marcand, et al 1999, **W303**
GA-4112	**MATalpha,** hta1-S129*/hta2-S-129* NUP49.GFP::URA, -lacO and LexA binding sites (TRP1) at ARS609 -lac I-GFP (HIS3) at his3-15, from a cross between GA-1561 and GA-3285	this study, **W303**
GA-4159	**MATalpha,** ku70::KanMX in GA4112	this study, **W303**
GA-4169	**MATalpha,** sir4::KanMX in GA4112	this study, **W303**
GA-4225	**MATa,** hta1-S129*/hta2-S-129* in GA-1917	this study, **W303**
GA-4226	**MATalpha,** isogenic wt for GA-4225, HTA1, HTA2	this study, **W303**

Supplemental Table 4.1: Yeast strains used in this study

4.8.2 Supplemental Figures

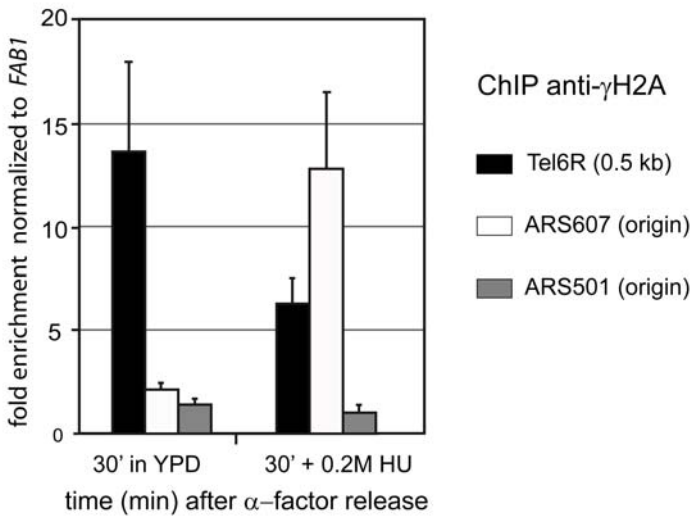

Supplemental Figure 4.1: γH2A levels at telomeres are very high

ChIP was performed on WT cultures (GA-180) after α-factor arrest and release into YPAD +/- 0.2M HU as described in Figure 4.1c. qPCR monitors were Tel6R at 0.5kb, *ARS607*, and the late firing origin *ARS501*. Data was normalized to enrichment obtained for *FAB1*.

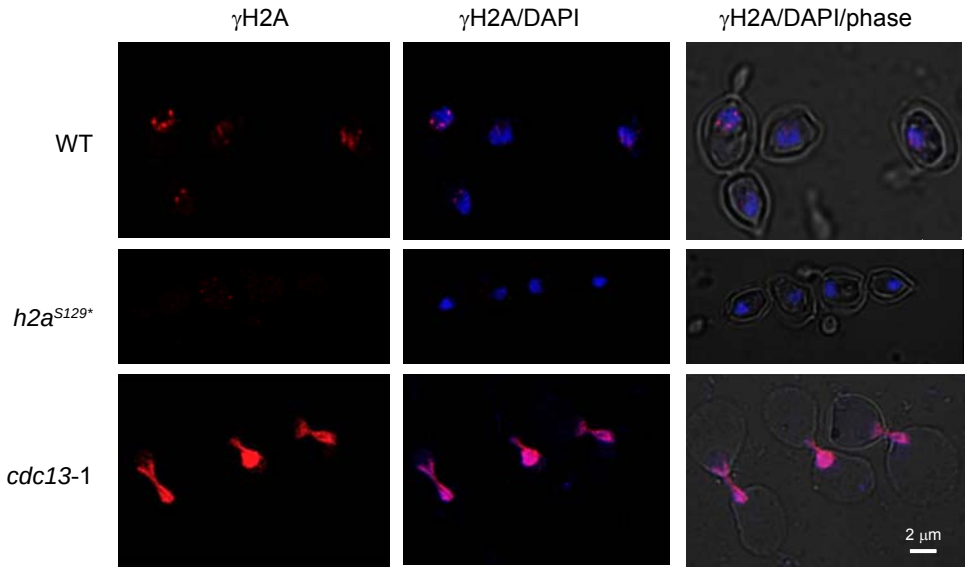

Supplemental Figure 4.2: γH2A levels increase dramatically after telomere uncapping

WT (GA-196) and *h2a*^{S129*} (GA-3653) mutant strains were grown exponentially at 30°C, whereas the *cdc13*-1 mutant strain (GA-172) was grown exponentially at 23°C and shifted for 2 h to 30°C. Cells were fixed for immunofluorescence and stained with monoclonal mouse anti-γH2A SG1-25J14 (1:20) and goat anti-mouse Alexa 488 (1:200). Images were acquired on an LSM510 Zeiss confocal microscope. Bars indicate 2μm.

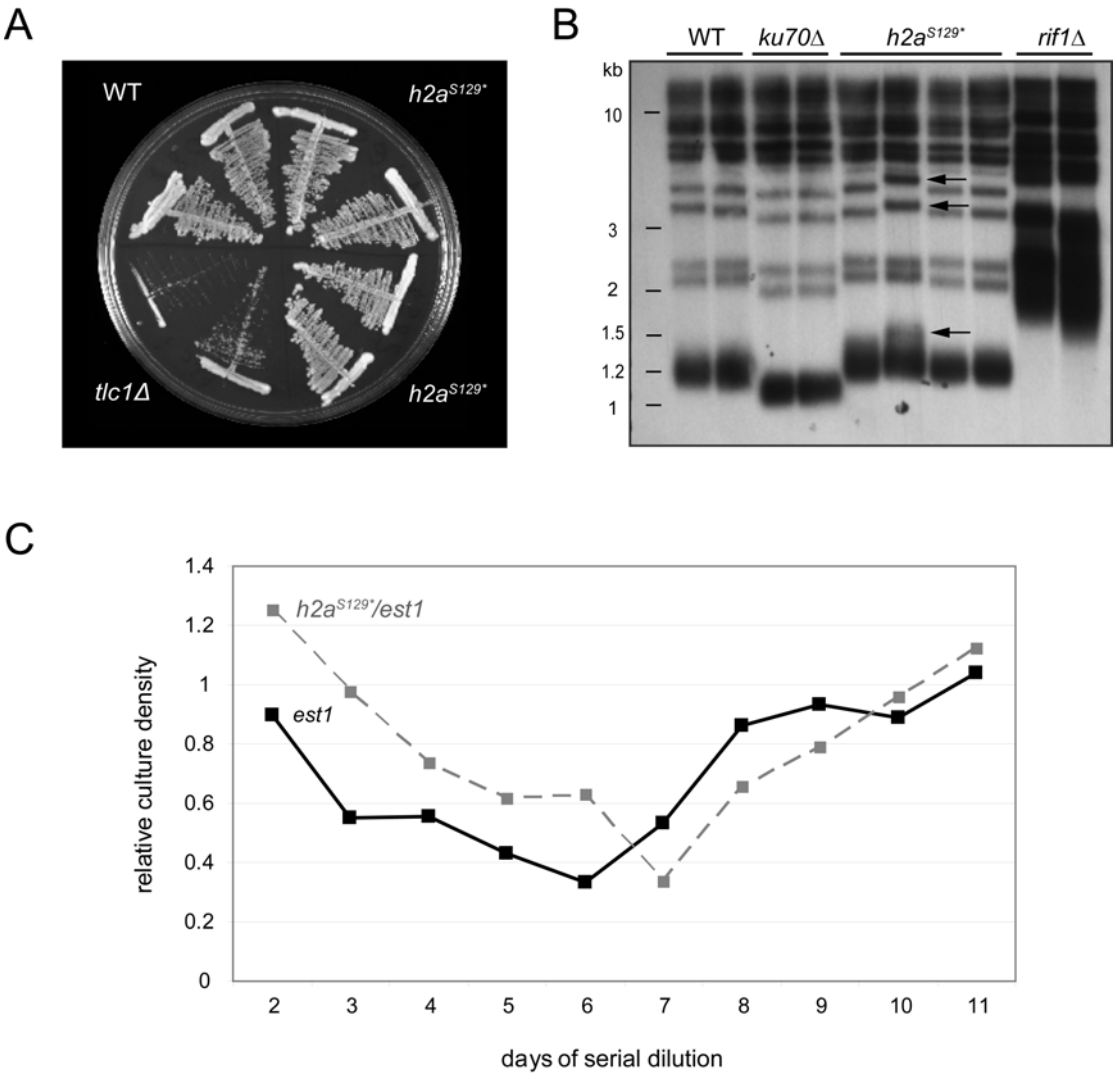

Supplemental Figure 4.3: Loss of γH2A does not provoke senescence, telomere shortening, or survivor appearance in a telomerase-deficient strain

A: *h2a*^{S129*} mutant cells are not senescent.
GA-3701 was sporulated and spores grown on a plate for 2 days. Senescence of four of the *h2a*^{S129*} spores was determined by re-streaking single colonies thrice after growing for 2 days. Similar treatments are shown for WT (GA-180) and *tlc1* deletion strains.
B: Telomeric distal TG-repeat length is normal in *h2a*^{S129*} mutant cells.
Genomic DNAs from WT (GA-180), *yku70* (GA-1949), *h2a*^{S129*} (GA-2961 and GA-3285), and *rif1* (GA-3362) mutant strains were digested with *Xho*I, run on a 1.5% agarose gel, and probed with a 300-bp $TG_{1\text{-}3}$ fragment as described (Hediger et al., 2006).
C: *h2a*^{S129*} mutant cells can generate survivors in the absence of *EST1*.
Spores bearing the *est1* mutation as well as spores WT for *EST1* of GA-3467 (*HTA1, HTA2*) and GA-3701 (*h2a*^{S129*}) were grown in YPAD and cell density was counted every 24h. Cells were diluted each day to 5×10^5 cells/ml. The relative culture density between *est1/EST1* (GA-3467) and *est1 h2a*^{S129*}*/EST1 h2a*^{S129*}.(GA-3701) is shown here. The increase after 6-7 days reflects the appearance of survivors that maintain telomere length by recombination in the absence of telomerase. The slight kinetic delay of the *h2a*^{S129*} strain may reflect its slower growth rate (Downs et al., 2000).

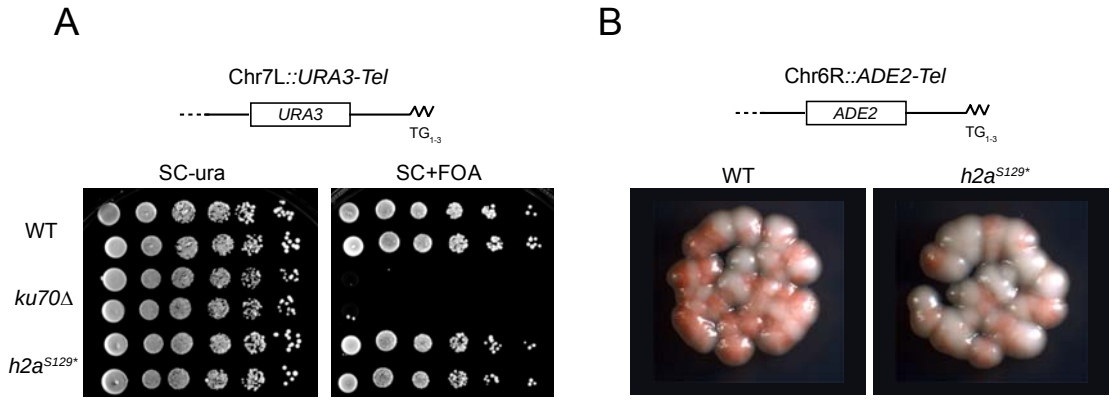

Supplemental Figure 4.4. Absence of γH2A affects telomeric silencing

A: Telomeric silencing was assayed for repression of the *URA3* gene at Tel7L by selection for resistance to 5-FOA. WT (GA-1053), *ku70* (GA-1054), and $h2a^{S129*}$ (GA-3399/GA-3400) mutant strains, having an *URA3* gene integrated at the *ADH4* locus at Tel7L, were plated in 10-fold serial dilutions on SD-ura plates and on SC+FOA plates (containing 0.1% 5-fluoro-orotic acid).
B: Telomeric silencing assayed for repression of the *ADE2* gene integrated at a truncated Tel6R downstream of *YFRO55W*. *ADE2* silencing assay for WT (GA-4226) and $h2a^{S129*}$ (GA-4225) mutant strains reveals the degree of telomeric position effect, where white shows the de-repressed state.

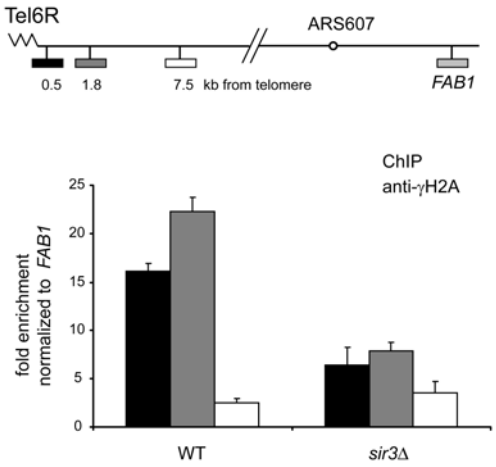

Supplemental Figure 4.5. Telomeric γH2A is reduced in the absence of SIR-complex spreading

γH2A-ChIP was performed on exponentially growing WT (GA-180) and *sir3* mutant (GA-278) cells. qPCR used probes at 0.5, 1.8, and 7.5 kb from the Tel6R TG-repeat. The mean of two experiments, normalized to *FAB1*, is shown.

4.8.3 References for the Supplemental Material:

Cobb, J.A., L. Bjergbaek, K. Shimada, C. Frei, and S.M. Gasser. 2003. DNA polymerase stabilization at stalled replication forks requires Mec1 and the RecQ helicase Sgs1. *Embo J*. 22:4325-36.

Downs, J.A., N.F. Lowndes, and S.P. Jackson. 2000. A role for Saccharomyces cerevisiae histone H2A in DNA repair. *Nature*. 408:1001-4.

Hayashi, A., H. Ogawa, K. Kohno, S.M. Gasser, and Y. Hiraoka. 1998. Meiotic behaviours of chromosomes and microtubules in budding yeast: relocalization of centromeres and telomeres during meiotic prophase. *Genes Cells*. 3:587-601.

Hediger, F., A.S. Berthiau, G. van Houwe, E. Gilson, and S.M. Gasser. 2006. Subtelomeric factors antagonize telomere anchoring and Tel1-independent telomere length regulation. *Embo J*. 25:857-67.

Lee, S.E., J.K. Moore, A. Holmes, K. Umezu, R.D. Kolodner, and J.E. Haber. 1998. Saccharomyces Ku70, mre11/rad50 and RPA proteins regulate adaptation to G2/M arrest after DNA damage. *Cell*. 94:399-409.

Maillet, L., F. Gaden, V. Brevet, G. Fourel, S.G. Martin, K. Dubrana, S.M. Gasser, and E. Gilson. 2001. Ku-deficient yeast strains exhibit alternative states of silencing competence. *EMBO Rep*. 2:203-10.

Perrod, S., M.M. Cockell, T. Laroche, H. Renauld, A.L. Ducrest, C. Bonnard, and S.M. Gasser. 2001. A cytosolic NAD-dependent deacetylase, Hst2p, can modulate nucleolar and telomeric silencing in yeast. *Embo J*. 20:197-209.

Stone, E.M., M.J. Swanson, A.M. Romeo, J.B. Hicks, and R. Sternglanz. 1991. The SIR1 gene of Saccharomyces cerevisiae and its role as an extragenic suppressor of several mating-defective mutants. *Mol Cell Biol*. 11:2253-62.

Taddei, A., F. Hediger, F.R. Neumann, C. Bauer, and S.M. Gasser. 2004b. Separation of silencing from perinuclear anchoring functions in yeast Ku80, Sir4 and Esc1 proteins. *Embo J*. 23:1301-12.

Thomas, B.J., and R. Rothstein. 1989. Elevated recombination rates in transcriptionally active DNA. *Cell*. 56:619-30.

Wood, J.S., and L.H. Hartwell. 1982. A dependent pathway of gene functions leading to chromosome segregation in Saccharomyces cerevisiae. *J Cell Biol*. 94:718-26.